

THE EFFECT OF RECESSED SPRINKLER INSTALLATION  
ON SPRINKLER ACTIVATION TIME AND PREDICTION

by

Daniel Madrzykowski

Thesis submitted to the Faculty of the Graduate School  
of The University of Maryland in partial fulfillment  
of the requirements for the degree of  
Master of Science  
1993

Advisory Committee:

Associate Professor Frederick W. Mowrer, Advisor  
Professor James G. Quintiere  
Assistant Professor James A. Milke

## ABSTRACT

Title of Thesis: THE EFFECT OF RECESSED SPRINKLER INSTALLATION  
ON SPRINKLER ACTIVATION TIME AND PREDICTION

Name of degree candidate: Daniel Madrzykowski

Degree and Year: Master of Science, 1993

Thesis directed by: Associate Professor Frederick W. Mowrer  
Department of Fire Protection Engineering

The objectives of this study were to analyze the effects of recessed sprinkler installation on sprinkler activation time and evaluate the ability of sprinkler activation models to predict activation time. Full scale compartment fire tests were used to obtain activation times for four different types of sprinklers. The tests were conducted in an 18.9 m by 9.1 m by 2.35 m high compartment using floor based fires with constant heat release rates of 115, 155, 215, 290 and 520 kW. Non-dimensional sprinkler radial positions,  $r/H$ , of 0.64 and 1.28 were evaluated. In addition to sprinkler activation times, ceiling jet temperature, velocity and radiation measurements were made. Comparisons of activation times were made between sprinklers in a fully exposed pendent position versus those in a 25 mm recessed position. The 95% confidence limits for the test data were developed and a thermal tenability analysis was made to determine if the difference in response times was significant with respect to life safety. This analysis suggests that recessed installation does not have an adverse effect on life safety for the conditions tested. Several sprinkler activation models were compared to the test data. A modified sprinkler activation algorithm was developed that includes hot gas layer effects to the ceiling jet once the ceiling jet is fully developed.

## DEDICATION

To my loving wife and family for their patience and support

## ACKNOWLEDGEMENTS

Appreciation is extended to Mr. Donald G. Bathurst and Mr. David W. Stroup of the General Services Administration for their interest in fire protection engineering research and their support of this project. Appreciation is also extended to the personnel of the National Institute of Standards and Technology's Building and Fire Research Laboratory (BFRL), Mr. Robert L. Vettori, Mr. Jay A. McElroy, Mr. Gerald A. Haynes, for their assistance in conducting the large scale fire tests and Mr. Charles E. Arnold for his assistance with the FPEtool source code modification. I would especially like to thank Dr. David D. Evans and Mr. William D. Walton of BFRL who provided motivation, encouragement and advice toward the successful completion of this project.

## Table of Contents

<u>Section</u>	<u>Page</u>
List of Tables .....	v
List of Figures .....	vi
Problem Definition .....	1
Chapter I Overview .....	4
Theoretical Development .....	4
RTI Application .....	12
Current Methods of Classifying Sprinkler Activation Performance .....	14
Chapter II Review of Sprinkler Activation Models .....	17
DETECT-QS .....	18
LAVENT .....	20
FPEtool .....	21
Chapter III Large Scale Sprinkler Activation Tests .....	23
Experimental Design .....	23
Experimental Approach .....	26
Experimental Results .....	26
Chapter IV Analysis and Discussion .....	30
DETECT-QS Comparison .....	35
LAVENT Comparison .....	37
FPEtool Comparison .....	40
FPEtool Modification .....	43
Recommendation for Sprinkler Activation Model Usage .....	43
Summary .....	47
Appendix A Example Sprinkler Activation Model Inputs and Outputs .....	49
References .....	150

## List of Tables

<u>Number</u>	<u>Page</u>
1. Instrumentation List. ....	67
2. Test Matrix. ....	68
3. Average Heat Flux. ....	68
4. Sprinkler Activation Times, Tests 1-3. ....	69
5. Sprinkler Activation Times, Tests 4-6. ....	69
6. Comparison of Average Activation Times, Tests 1-3 vs. Tests 4-6. ....	69
7. Sprinkler Activation Times, Tests 7-9. ....	70
8. Sprinkler Activation Times, Tests 10-12. ....	70
9. Comparison of Average Activation Times, Tests 7-9 vs. Tests 10-12. ....	70
10. Sprinkler Activation Times, Tests 13-15. ....	71
11. Sprinkler Activation Times, Tests 16-17. ....	71
12. Comparison of Average Activation Times, Tests 13-15 vs. Tests 16-18. ....	71
13. Sprinkler Activation Times, Tests 19-21. ....	72
14. Sprinkler Activation Times, Tests 22-24. ....	72
15. Comparison of Average Activation Times, Tests 19-21 vs. Tests 22-24. ....	72
16. Sprinkler Activation Times, Tests 25-27. ....	73
17. Sprinkler Activation Times, Tests 28-30. ....	73
18. Comparison of Average Activation Times, Tests 25-27 vs. Tests 28-30. ....	73
19. Sprinkler Activation Times, Tests 31-33. ....	74
20. Sprinkler Activation Times, Tests 34-36. ....	74
21. Comparison of Average Activation Times, Tests 31-33 vs. Tests 34-36. ....	74
22. Comparison of Average RTIs, Tests 1-3 vs. Tests 4-6. ....	75
23. Comparison of Average RTIs, Tests 7-9 vs. Tests 10-12. ....	75
24. Comparison of Average RTIs, Tests 13-15 vs. Tests 16-18. ....	75
25. Comparison of Average RTIs, Tests 19-21 vs. Tests 22-24. ....	76
26. Comparison of Average RTIs, Tests 25-27 vs. Tests 28-30. ....	76
27. Comparison of Average RTIs, Tests 31-33 vs. Tests 34-36. ....	76
28. Comparison of Plunge Test vs. Average Experimental RTIs ....	77
29. Comparison of Experimental vs. Predicted Activation Times for Tests 1-3. ...	78
30. Comparison of Experimental vs. Predicted Activation Times for Tests 7-9. ...	78
31. Comparison of Experimental vs. Predicted Activation Times for Tests 13-15. ....	79
32. Comparison of Experimental vs. Predicted Activation Times for Tests 19-21. ....	79
33. Comparison of Experimental vs. Predicted Activation Times for Tests 25-27. ....	80
34. Comparison of Experimental vs. Predicted Activation Times for Tests 31-33. ....	80
35. Sprinkler Activation Time Comparison, QR bulb. ....	81
36. Sprinkler Activation Time Comparison, QR link. ....	81
37. Sprinkler Activation Time Comparison, SS bulb. ....	82
38. Sprinkler Activation Time Comparison, SS link. ....	82

## List of Figures

<u>Number</u>	<u>Page</u>
1. Schematic of pendent, recessed and concealed sprinklers with ceiling jet. ....	83
2. First-order response, ramp change. ....	84
3. Ramp test, determination of time constant ....	85
4. First-order response, step change. ....	86
5. Schematic of sensitivity test oven (Elevation) ....	87
6. Schematic of sensitivity test oven (Plan View). ....	88
7. Schematic of room heat test configuration. ....	89
8. Schematic of DETACT-QS inputs. ....	90
9. Schematic of LAVENT inputs. ....	91
10. Schematic of Fire Simulator inputs. ....	92
11. Schematic of sprinkler activation test configuration. ....	93
12. Schematic of sprinkler activation test instrumentation configuration (plan view). ....	94
13. Schematic of sprinkler array with sprinklers in pendent position. ....	95
14. Schematic of sprinkler array with sprinklers in recessed position. ....	96
15. Average ceiling jet temperature increase: 520 kW, 3 m case. ....	97
16. Average ceiling jet velocity: 520 kW, 3 m case. ....	98
17. Average ceiling jet temperature increase: 290 kW, 3 m case. ....	99
18. Average ceiling jet velocity: 290 kW, 3 m case. ....	100
19. Average ceiling jet temperature increase: 290 kW, 1.5 m case. ....	101
20. Average ceiling jet velocity: 290 kW, 1.5 m case. ....	102
21. Average ceiling jet temperature increase: 215 kW, 1.5 m case. ....	103
22. Average ceiling jet velocity: 215 kW, 1.5 m case. ....	104
23. Average ceiling jet temperature increase: 155 kW, 1.5 m case. ....	105
24. Average ceiling jet velocity: 155 kW, 1.5 m case. ....	106
25. Average ceiling jet temperature increase: 115 kW, 1.5 m case. ....	107
26. Average ceiling jet velocity: 115 kW, 1.5 m case. ....	108
27. Pendent vs recessed activation times at $r = 3$ m, QR bulb. ....	109
28. Pendent vs recessed activation times at $r = 3$ m, QR link. ....	110
29. Pendent vs recessed activation times at $r = 3$ m, SS bulb. ....	111
30. Pendent vs recessed activation times at $r = 3$ m, SS link. ....	112
31. Pendent vs recessed activation times at $r = 1.5$ m, QR bulb. ....	113
32. Pendent vs recessed activation times at $r = 1.5$ m, QR link. ....	114
33. Pendent vs recessed activation times at $r = 1.5$ m, SS bulb. ....	115
34. Pendent vs recessed activation times at $r = 1.5$ m, SS link. ....	116
35. Actual vs predicted activation times at $r = 3$ m, QR bulb. ....	117
36. Actual vs predicted activation times at $r = 3$ m, QR link. ....	118
37. Actual vs predicted activation times at $r = 3$ m, SS bulb. ....	119
38. Actual vs predicted activation times at $r = 3$ m, SS link. ....	120
39. Actual vs predicted activation times at $r = 1.5$ m, QR bulb. ....	121
40. Actual vs predicted activation times at $r = 1.5$ m, QR link. ....	122
41. Actual vs predicted activation times at $r = 1.5$ m, SS bulb. ....	123

42. Actual vs predicted activation times at $r = 1.5$ m, SS link. ....	124
43. Ceiling jet temperature comparison at $r = 3$ m, 520 kW. ....	125
44. Ceiling jet velocity comparison at $r = 3$ m, 520 kW. ....	126
45. Ceiling jet temperature comparison at $r = 3$ m, 290 kW. ....	127
46. Ceiling jet velocity comparison at $r = 3$ m, 290 kW. ....	128
47. Ceiling jet temperature comparison at $r = 1.5$ m, 290 kW. ....	129
48. Ceiling jet velocity comparison at $r = 1.5$ m, 290 kW. ....	130
49. Ceiling jet temperature comparison at $r = 1.5$ m, 215 kW. ....	131
50. Ceiling jet velocity comparison at $r = 1.5$ m, 215 kW. ....	132
51. Ceiling jet temperature comparison at $r = 1.5$ m, 155 kW. ....	133
52. Ceiling jet velocity comparison at $r = 1.5$ m, 155 kW. ....	134
53. Ceiling jet temperature comparison at $r = 1.5$ m, 115 kW. ....	135
54. Ceiling jet velocity comparison at $r = 1.5$ m, 115 kW. ....	136
55. FPEtool Ceiling jet temperature comparison at $r = 3$ m, 520 kW. ....	137
56. FPEtool Ceiling jet velocity comparison at $r = 3$ m, 520 kW. ....	138
57. FPEtool Ceiling jet temperature comparison at $r = 3$ m, 290 kW. ....	139
58. FPEtool Ceiling jet velocity comparison at $r = 3$ m, 290 kW. ....	140
59. FPEtool Ceiling jet temperature comparison at $r = 1.5$ m, 290 kW. ....	141
60. FPEtool Ceiling jet velocity comparison at $r = 1.5$ m, 290 kW. ....	142
61. FPEtool Ceiling jet temperature comparison at $r = 1.5$ m, 215 kW. ....	143
62. FPEtool Ceiling jet velocity comparison at $r = 1.5$ m, 215 kW. ....	144
63. FPEtool Ceiling jet temperature comparison at $r = 1.5$ m, 155 kW. ....	145
64. FPEtool Ceiling jet velocity comparison at $r = 1.5$ m, 155 kW. ....	146
65. FPEtool Ceiling jet temperature comparison at $r = 1.5$ m, 115 kW. ....	147
66. FPEtool Ceiling jet velocity comparison at $r = 1.5$ m, 115 kW. ....	148
67. First-order response model sensitivity to gas temperature. ....	149



## Problem Definition

Fire protection engineering is evolving from consensus based design practices to performance based analyses. Computer models have become primary tools enabling fire protection engineers to analyze fire protection problems. Friedman has recently surveyed 62 computer models for fire and smoke[1]. Five of those models were designed specifically to predict the actuation of thermal fire detectors: DETACT-QS[2], DETACT-T2[3], LAVENT[4], TDISX[5], AND PALDET[6]. Other models, including FPEtool[7], HAZARD I[8], RADISM[9], and SPLASH[10], contain thermal fire detector actuation subroutines, some of which are based on the stand-algorithms.

These activation models are being used by fire protection engineers in the design and evaluation of fire suppression systems. These models have evolved from direct application of engineering correlations to models that consider additional effects such as heat loss to the compartment, the hot gas layer, and the position of the sprinkler link below the ceiling.

One of the input parameters needed for the thermal detector activation models is the Response Time Index (RTI) of the detector[11]. The RTI is a relative measure of a detector's thermal sensitivity. One test used to determine the RTI of a thermally sensitive device is the sensitivity oven or "plunge test"[12]. In the plunge test a sprinkler is tested in the pendent position with the thermally sensitive element fully exposed to the hot gas flow. Hence, the activation models which use RTIs calculated from plunge test

data do not consider the potential effects of a recessed installation on sprinkler activation.

In the past, the mission of sprinklers was primarily property protection. Sprinkler technology has evolved to the point that certain automatic sprinklers are now designed to maintain tenable conditions in the room of fire origin[13]. Studies[14-18] have demonstrated that new sprinkler technology such as Quick Response Sprinklers (QRS) can substantially improve life safety in occupancies such as offices, hotels, hospitals and residences. As a result of this improved sprinkler technology, NFPA 101, the Life Safety Code[19], has added mandatory automatic sprinkler requirements for health care, hotel, apartment, lodging and rooming, and existing high rise apartments and hotels. Hence the use of sprinklers in such spaces has increased and will continue to do so.

In an effort to make ceilings in sprinklered commercial and residential buildings more aesthetically pleasing and to maintain maximum clearance heights, some sprinklers may be recessed into the ceiling or recessed and concealed with decorative temperature activated plates. Current thermal detector activation models do not account for the effects of recessing the sprinklers into the ceiling, or covering the sprinkler with a plate (Figure 1). Recessing or covering the sprinklers could increase the activation time, adversely affecting the protection provided.

As Mowrer [20] points out, there are "three distinct time lags associated with building fires: a transport time lag, a detection (activation) time lag and a suppression time lag."

He continues, "the general goal of fire mitigation strategies is to minimize the net effect of the three time lags...". The transport time lag is not considered by current sprinkler activation models. The activation time lag depends on the sprinkler's environment and the sprinkler's response characteristics. The suppression time lag will not be addressed in this study because for wet-pipe sprinkler systems typically used in business and residential occupancies this lag is virtually zero. The question addressed here is how a recessed configuration affects the environment at the sprinkler and consequently the response time of the sprinkler.

This study includes: 1) a review of current methods for classifying sprinkler activation performance, 2) a review of public domain, personal computer based, single compartment thermal detector activation models, 3) an analysis of large scale fire experiments performed as part of this study in an effort to quantify the impact of recessed sprinkler installation on sprinkler activation time, 4) an analysis of predicted vs. experimental activation times utilizing the reviewed thermal detector activation models and 5) a recommendation for improving a ceiling jet algorithm. This paper will focus on the activation of automatic sprinklers, so references to thermally sensitive elements should be considered in the context of automatic sprinklers.

## **Chapter I Overview**

Current sprinkler activation models do not consider the effect of recessed installation on sprinkler activation time. This study will provide an analysis to determine if such a feature is necessary. In order to evaluate the effect of recessed sprinkler installation on sprinkler activation time, a series of large scale sprinkler activation tests has been performed. The tests compare activation times of sprinklers in a fully exposed pendent position with activation times of similar sprinklers in a recessed pendent position for several fire sizes. RTIs for the sprinklers used in the tests were determined from the large scale test data and compared with the RTIs measured in the sensitivity oven or plunge test. The data from the large scale tests were then used to evaluate the predictions of several sprinkler activation models. A modification to one of the sprinkler activation models is proposed.

### **Theoretical Development**

An accurate prediction of sprinkler activation time can be made if the response of the sprinkler's thermally sensitive element to a given change in its environmental condition is known. However, "because of inertia, no instrument (or anything else for that matter) responds instantly or with perfect fidelity to a change in its environment[21]." In the case of sprinklers the inertia is the resistance to temperature change and is characterized by the specific heat capacity and thermal conductivity of the element and the film coefficient for the element. The change in environment caused by a fire is characterized by an

increase in temperature and flow around the thermally sensitive element. Therefore, sprinkler response is primarily a function of the physical properties of the thermally sensitive element and the physical and dynamic properties of its environment.

Assuming that heat is transferred to the thermally sensitive element only by convection, and assuming that no heat is lost from the element, a simple heat balance can be written for the element subjected to a time dependent temperature change. Small internal resistance to heat flow is also assumed, so that the temperature of the element can be considered to be uniform.

$$mc\left(\frac{dT_e}{dt}\right) = h_c A(T_g - T_e) \quad (1)$$

where:  $m$  = mass of element (kg)  
 $c$  = specific heat of element (kJ/kg K)  
 $h_c$  = convective heat transfer coefficient (kW/m<sup>2</sup> K)  
 $A$  = surface area of element (m<sup>2</sup>)  
 $T_e$  = temperature of element (K)  
 $T_g$  = temperature of gas (K)  
 $t$  = time (s)

This equation shows that the rate of heat storage in the element is equal to the heat transfer rate to the element. Separating the variables in equation 1 yields:

$$\frac{dt}{(mc/hA)} = \frac{dT_e}{T_g - T_e} \quad (2)$$

The quantity in parentheses has dimensions of time and is referred to as the time constant,  $\tau$ .

$$\tau = \frac{mc}{hA} = \frac{\text{thermal capacitance of element}}{\text{thermal conductance of film}} \quad (3)$$

Substituting  $\tau$  into equation 2 and solving for  $T_e$  gives a first-order, first degree, linear, differential equation which has a general solution of:

$$T_e = Ce^{\frac{-t}{\tau}} + \frac{1}{\tau} e^{\frac{-t}{\tau}} \int_0^t T_g e^{\frac{t}{\tau}} dt \quad (4)$$

where  $C$  is an integration constant determined by the boundary conditions.

Equation 4 can be solved analytically for three types of temperature boundary conditions:

- Ramp Change
- Step Change
- Periodic Change (Oscillating)

Since the case of sprinkler activation is normally considered as an increasing temperature change only the ramp and step changes will be considered here.

In the linear ramp change case the temperature of the environment and the temperature of the thermal element are equal at  $t = 0$ ,  $T_o = T_e$ . At  $t > 0$ , the temperature of the environment (gas) increases linearly such that the gas temperature is given by:

$$T_g = T_o + Rt \quad (5)$$

where:

$R$  = Rate of temperature increase (K/s)

The temperature of the element  $T_e$  lags the temperature of the gas. When  $t \gg \tau$  the exponential terms in equation 4 approach zero and the relationship between the temperature difference and the time constant can be shown as:

$$T_g - T_e = R\tau \quad (6)$$

For the ramp case, the time constant can be defined as the time lag between the environment temperature and the thermal element temperature at long times. Hence, the temperature difference at a given time increases with an increase in time constant as shown in Figure 2.

A sprinkler sensitivity test utilizing the ramp change temperature increase has been investigated at the Fire Research Station (FRS)[22]. The test is conducted in a heated, constant mass flow wind tunnel. The test procedure consists of heating the sprinkler for 5 minutes at 30 °C. Then the air temperature in the wind tunnel is increased at a linear rate. The activation time and the air temperature at the time of activation are recorded. Each sprinkler is tested with a series of rates of rise ranging from 2 to 30 °C/min. The sprinkler's time constant and effective activation temperature are then derived from the test results as shown in Figure 3.

In the step change case the temperature of the test environment,  $T_g$ , is higher than the ambient temperature,  $T_o$ , and the temperature of the thermal element,  $T_e$ , is equal to the ambient temperature at  $t = 0$ . At  $t > 0$ , the thermal element is inserted or "plunged" into the test environment. The temperature of the element increases until it reaches

equilibrium with the test environment. Evaluating equation 4 for  $T_e$  with these boundary conditions yields:

$$T_e = T_o e^{-t/\tau} + T_g - T_g e^{-t/\tau} \quad (7)$$

Expressing equation 7 in terms of the temperature difference yields:

$$(T_g - T_e) = (T_g - T_o) e^{-t/\tau} \quad (8)$$

From this equation the time constant for the step change case can be defined as the time required to reduce the temperature difference between the test environment and the thermal element by  $1-1/e$  or 63.2%. The temperature difference between  $T_g$  and  $T_e$  at a given time increases with an increased time constant as shown in Figure 4.

Based on a step change temperature increase, Heskestad and Smith [23] developed a sprinkler sensitivity test, the "plunge test". Utilizing a heated wind tunnel as shown in Figure 5 and 6, a sprinkler is tested by plunging it into the hot air flow of known constant temperature and velocity.

Rearranging equation 1 in terms of the temperature rise over the initial element and gas temperatures,  $T_o$  gives equation 9.

$$\frac{d(\Delta T_e)}{dt} = \frac{1}{\tau} (\Delta T_g - \Delta T_e) \quad (9)$$

$$\begin{aligned} \text{where: } \Delta T_e &= T_e - T_o \\ \Delta T_g &= T_g - T_o \\ \tau &= mc/h_c A \end{aligned}$$



For a known and constant gas flow and a sprinkler with known physical properties, the gas temperature, the activation temperature, the element mass, and the element's surface area are all constants. The element specific heat is assumed constant. Therefore, for a known rate of element temperature change, the only variable in equation 9 is the convective heat transfer coefficient,  $h_c$ . The convective heat transfer coefficient is a function of the thermal conductivity of the gas,  $k$ , the Reynolds number,  $Re$ , and the characteristic length of the element,  $L$ . The Reynolds number is given by:

$$Re = \frac{uL}{\nu} \quad (10)$$

where:  $u$  = gas velocity (m/s)  
 $\nu$  = kinematic viscosity of the gas ( $m^2/s$ )

Consequently, the "time constant" is not constant for different flow conditions.

Heskestad and Smith [11] continued their analysis by examining the non-dimensional heat transfer coefficient, the Nusselt number ( $Nu$ ).

$$Nu = h_c \frac{L}{k} \quad (11)$$

where:  $k$  = thermal conductivity of gas at film temperature (W/m K)

Empirical data on the convective heating and cooling of cylindrical and spherical objects representative of sprinkler elements in gas flows with Reynolds numbers representative of those expected in a fire environment exhibited the following relationship:

$$Nu = C(Re)^{1/2} \quad (12)$$

where  $C$  is a constant characteristic of the element geometry. Combining equations 10 through 12 and solving for  $h_c$  gives:

$$h_c = C \left( \frac{k}{\nu^{1/2}} \right) u^{1/2} L^{-1/2} \quad (13)$$

While both  $k$  and  $\nu$  are sensitive to temperature, Heskestad and Smith found from tabulated air data that  $k/\nu^{1/2}$  is nearly independent of temperature. Since  $C$  and  $L$  are constants it follows from equation 13 that for a given thermal element:

$$h \propto u^{1/2} \quad (14)$$

Therefore the time constant,  $\tau$ , is proportional to the inverse square root of the gas velocity past the element. Hence, if  $\tau_o$  is the time constant at a given gas velocity,  $u_o$ , the time constant at an arbitrary velocity,  $u$ , can be determined from:

$$\tau = \tau_o \sqrt{\frac{u_o}{u}} \quad (15)$$

Equation 15 also suggests that the product  $\tau\sqrt{u}$  is constant. Heskestad and Smith called this product the Response Time Index (RTI).

$$RTI = \tau \sqrt{u} \quad (16)$$

Heskestad and Smith's[23] experiments found this condition to be true in the "plunge test" for velocities above 2.5 m/s and temperatures below 383 °C. At velocities below 2.5 m/s and at temperatures above 382 °C, the RTIs tended to increase. The higher RTI values at velocities below 2.5 m/s were attributed to radiant heat loss from the

thermal element. The reason that the RTI increased at temperatures above 382 °C was not clearly understood.

The time constant can be determined for a sprinkler utilizing plunge test data in the following manner;

$$\tau = \frac{-t_r}{\ln(1 - \frac{\Delta T_{ea}}{\Delta T_g})} \quad (17)$$

where:  $t_r$  = activation time of sprinkler in plunge test  
 $T_{ea}$  = activation temp. of sprinkler  
 $\Delta T_{ea} = T_{ea} - T_o$   
 $\Delta T_g = T_g - T_o$   
 $T_g$  = gas temperature in plunge test

Multiplying the time constant by the square root of the gas velocity used in the plunge test yields the RTI as shown in equation 16.

The development of the RTI concept assumes that heat transfer effects due to conduction and radiation are negligible. Convective heat transfer effects from the hot gas flow across the sprinkler are assumed to dominate. If these assumptions hold, then any effect on the RTI due to recessed installation would be based on the change of the heat transfer coefficient, i.e. due to a change in gas velocity seen by the element. This is true provided that the gas temperature seen by the element was not significantly different from that seen by the element when installed in the pendent position. This issue will be addressed by the large scale experiments.

## RTI Application

The RTI is a relative measure which is used to categorize sprinkler heads. The smaller the RTI value the more thermally responsive the sprinkler is, i.e. the faster it will activate in a given environment. Standard response sprinklers have an RTI range of 100 to 400  $s^{1/2} m^{1/2}$ . Fast response sprinklers have RTIs in the range of 28 to 50  $s^{1/2} m^{1/2}$  [24].

The thermal sensitivity, characterized by the RTI, is one of the critical parameters affecting the activation time of a sprinkler. However, Bryan[25] points out there are many variables beside the thermal sensitivity of the device which effect the operation of an installed sprinkler including: the height of the sprinkler above the floor, distance of the sprinkler from the ceiling, the surface configuration of the ceiling and location of the sprinkler relative to the fire.

The geometry considerations mentioned above are important because they affect the temperature and velocity of the gas flow around the thermally sensitive element. In the context of a room fire scenario this gas flow is referred to as the ceiling jet. As a fire develops, the hot products of combustion form a buoyant thermal plume which rises and in most cases impinges on the ceiling. If the ceiling is smooth and horizontal, the hot gases will move radially outward from the impingement area. As the gas flow moves across the ceiling it becomes cooler and slower. At any given point away from the fire plume, this movement of gas or ceiling jet has a vertical velocity gradient and a temperature gradient below the ceiling. The temperature gradient would initially show

the temperature at the ceiling to be just above ambient, while within 1% of the distance between the ceiling and the fuel below the ceiling, the ceiling jet temperature would be at its maximum temperature [26] and below that point the temperature would decrease as you moved further below the ceiling until ambient temperatures were reached. The velocity gradient behaves in a similar fashion, as shown qualitatively in Figure 1. Hence placing obstructions on the ceiling to disturb the ceiling jet flow or positioning the thermally sensitive element out of the flow would have the effect of cooling and slowing down the gas flow around the sprinkler, adversely affecting the element's heat transfer coefficient.

From a modeling perspective, RTI, geometry and fire specification are the primary inputs. Current sprinkler activation models[2,3,7,8] assume a pendent type sprinkler mounted under a smooth ceiling and located in the ceiling jet at the point of maximum temperature and velocity. Only one sprinkler activation model, LAVENT[4], allows consideration of sprinklers located outside the maximum temperature and velocity position.

In practice, sprinkler installations are not always pendent heads located below smooth ceilings. In order to enhance appearance, sprinklers have been recessed into the ceiling or recessed and covered with decorative temperature activated plates (Figure 1). Current thermal detector activation models do not account for the effects of recessing or covering the sprinkler.

## **Current Methods of Classifying Sprinkler Activation Performance**

The National Fire Protection Association's Standard for the Installation of Sprinkler Systems[27] specifies that only "listed" components may be used in a sprinkler system. In the United States, Underwriters Laboratories (UL) is one of the primary listing laboratories for fire protection equipment, including automatic sprinklers. To be listed for commercial use by UL, automatic sprinklers must pass the applicable tests specified in the Standard for Automatic Sprinklers for Fire Protection Service, UL 199[12]. This study will be limited to sprinklers with an "ordinary" activation temperature classification (57-77 °C).

The standard contains at least thirty performance tests which a sprinkler must pass. Three of those tests deal with automatic sprinkler activation performance: 1)operating temperature (bath) test, 2)oven heat test, and 3)room heat test. The basic formats of the tests will be outlined below, however the reader is referred to UL 199 for further details.

The operating temperature (bath) test utilizes a water bath for sprinklers having an operating temperature of 79 °C or lower. The sprinklers are completely immersed and the water bath temperature is increased to within 11 °C of the sprinklers temperature rating. The rate of temperature increase is then controlled at 0.5 °C or less per minute until the device operates or the bath temperature exceeds the temperature rating of the

device by 11 °C. The time and temperature of operation are recorded. If the sprinkler requires internal pressure to operate, it is tested with a pressure of  $31 \pm 3.4$  kPa.

The sensitivity tests determine a relative response time for use in comparing one sprinkler with another sprinkler. The oven heat test is based on the theoretical and experimental work of Heskestad and Smith[11,23] discussed previously. In the oven heat test (Figures 5 and 6) the sprinkler is installed on a test mount, conditioned to an initial temperature of  $24 \pm 1$  °C, and pressurized with air to  $28 \pm 7$  kPa. The mounting plate is attached to the oven and the sprinkler is plunged into a hot air flow of 135 °C at a velocity of  $2.54 \pm 0.01$  m/s and the time to activation is recorded. If the sprinkler operates in 14 seconds or less it is considered a Quick Response (QR) sprinkler. Standard response sprinklers must operate in 100 seconds or less. The thermally sensitive elements of the sprinklers are fully exposed to the hot air flow even if the sprinkler may in practice be installed in a concealed or recessed fixture.

To account for a sprinkler's activation performance in its installed configuration, a full scale fire test, called the "room heat test" (Figure 7) is conducted. In the room heat test, the sprinklers are installed in their intended position at the ceiling, ie. concealed, recessed, or pendent. The test room for a QR sprinkler is 4.6 m x 4.6 m x 2.4 m high. A natural gas fire of approximately 140 kW is ignited in one corner of the room. The QR sprinkler is to be installed on the ceiling 5.1 m from the corner with the burner. The sprinkler inlet waterway is filled with water at  $21 \pm 1.6$  °C (to account for conduction effects) and pressurized to  $31 \pm 3.4$  kPa. The test may begin when the

ambient temperature in the test room is  $31 \pm 1$  °C. The time from ignition to sprinkler operation is recorded. For a sprinkler to be listed as QR it must activate in 75 seconds or less.



## Chapter II Review of Sprinkler Activation Models

The majority of the compartment fire models used routinely by practicing fire protection engineers in the U.S. are classified as zone models. These models divide a compartment into two primary zones, a hot gas upper zone and a cool gas lower zone. The fire is assumed to be a point source and the fire plume acts as a pump for moving mass from the lower layer into the upper layer. Examples of this type of model include: ASET-B[28], FPEtool[7], and LAVENT[4].

There are also multiple room zone models, such as HAZARD I[8] which also fit into this category. The primary concern of this study deals with sprinkler activation in the room of fire origin. Smoke flow into the other spaces is not an issue addressed by this study. The sprinkler activation sub-model in HAZARD I is based on the DETACT-QS [2] correlation.

Another class of models which can be used to evaluate sprinkler activation are field models. Field models can divide the compartment of interest into thousands of zones or control volumes to provide a detailed look at the physical phenomena occurring in a compartment. This includes thermal gradients, gas velocities and flow fields. In most cases, sufficient information is not available to identify a space, its fuel load and the ambient conditions to utilize the precision of the field models. Field models are not included in this review because as Nelson states " field models involve a level of

complexity and difficulty that precludes their frequent use in the day-to-day practice of fire protection engineering[29]."

DETECT-QS, LAVENT and FPEtool represent a cross section of the types of sprinkler activation algorithms available. For this study, sprinkler activation times were predicted using these three models.

### **DETECT-QS**

DETECT-QS is based on the experimental work of Alpert[26]. Alpert burned several well characterized fuel packages under a smooth, unconfined ceiling and measured the temperature and velocity profiles of the near-ceiling flow to characterize the ceiling jet as it moves radially outward from the fire plume. He developed steady-state correlations for temperature and velocity of the ceiling jet based on heat release rate of the fire, ceiling height and radial distance of the detector from the fire plume axis. The temperature correlations are divided into two categories based on the position of the sprinkler relative to the centerline of the fire; 1) radial positions less than or equal to 18 percent of the fuel to ceiling height and 2) radial positions greater than 18 percent of the fuel to ceiling height. The velocity correlations are also divided into two categories based on the position of the sprinkler relative to the centerline of the fire; 1) radial positions less than or equal to 15 percent of the fuel to ceiling height and 2) radial positions greater than 15 percent of the fuel to ceiling height.

The first category ( $r \leq 0.18H$ ,  $r \leq 0.15H$ ) represents the area where the fire plume impinges on the ceiling. The correlation equations for maximum temperature and velocity at the sprinkler are given as:

$$T_{\max} - T_o = \frac{16.9 \dot{Q}^{2/3}}{H^{5/3}} \quad (18)$$

where:  $T_{\max}$  = maximum gas temp. at the sprinkler ( $^{\circ}\text{C}$ )

$\dot{Q}$  = total heat release rate (kW)

$H$  = distance between ceiling and fuel (m)

$T_o$  = initial gas temperature ( $^{\circ}\text{C}$ )

$$v = 0.946 \left( \frac{\dot{Q}}{H} \right)^{1/3} \quad (19)$$

where:  $v$  = gas velocity at the sprinkler (m/s)

The second category ( $r > 0.18H$ ,  $r > 0.15H$ ) represents the steady-state conditions of the ceiling jet region. The equations for maximum temperature and velocity at the sprinkler are given as:

$$T_{\max} - T_o = \frac{5.38 (\dot{Q}/r)^{2/3}}{H} \quad (20)$$

$$v = 0.197 \dot{Q}^{1/3} \left( \frac{H^{1/2}}{r^{5/6}} \right) \quad (21)$$

Utilizing these correlations with the work of Heskestad and Smith[11,23] on convection heat transfer and sprinkler activation yields the information necessary to calculate the activation time of a heat detector or sprinkler located at the ceiling.

Evans and Stroup[2] developed the computer programs, DETACT-T2, based on the ceiling jet correlations of Heskestad and Delichatsios[30] and DETACT-QS, based on Alpert's ceiling jet correlations[26], to calculate sprinkler activation time. DETACT-T2 calculates sprinkler activation for fires with heat release rates that develop with the square of time. DETACT-QS allows any user specified fire. DETACT-QS will be discussed since it is the more general of the two correlations.

DETACT-QS assumes the fire and the heat detector or sprinkler are located under an unconfined smooth ceiling. This means that any heating of the thermally sensitive element will be based only on the temperature and velocity of the ceiling jet and no account is made for the effects of a hot gas layer. The fire is assumed to be a quasi-steady point source. Required inputs to the model (Figure 8) include:

- fire heat release rate history,  $\dot{Q}$
- fire (fuel) to ceiling height,  $H$
- radial distance to sprinkler,  $r$
- room temperature,  $T_o$
- sprinkler activation temperature,  $T_{act}$
- sprinkler response time index, RTI

## LAVENT

Link-Actuated VENTS or LAVENT by Davis and Cooper[4] was developed based on the work of Cooper[31]. LAVENT was developed to predict the activation of sprinklers and thermally sensitive link actuated ceiling vents in compartment fires. LAVENT takes into account the effect of the upper hot gas layer on the ceiling jet, as well as heat loss

to the ceiling and the distance between the ceiling and the sprinkler link. The list of required inputs is more extensive (Figure 9) than for DETACT-QS:

- room geometry,  $L, W, H$
- thermal properties of ceiling materials,  $k\rho c$
- fire heat release rate history,  $\dot{Q}$
- fire area,  $A_F$
- fire (fuel) height,  $h_F$
- radial distance to sprinkler,  $r$
- distance of sprinkler link below ceiling,  $d$
- sprinkler activation temperature,  $T_{act}$
- sprinkler response time index, RTI
- ceiling vent areas

### FPEtool

In the Fire Simulator sub-model of FPEtool[7], the sprinkler activation algorithm considers the effect of the hot gas layer on the ceiling jet. This algorithm is based on Evans[32] equivalent virtual source, which is used in conjunction with Alpert's correlations[26].

Alpert's correlations assume that the fire plume entrains air which is at room temperature (lower layer temperature). Evans' equivalent virtual source addresses the case where a hot gas layer has developed in a compartment prior to sprinkler activation. With a hot gas layer in the compartment the fire plume no longer entrains air only from the cool lower layer. Instead some portion of the gas entrained by the plume comes from the hot gas layer. This in turn increases the temperature and velocity of the ceiling jet.

The equivalent virtual source calculations yield an adjusted heat release rate and an adjusted distance from fire to ceiling to account for the effects of entraining hot gas into the plume. These adjusted values can then be used as input values to Alpert's correlations.

Fire Simulator considers heat loss to the walls and ceilings and it allows flow into or out of the compartment. It cannot specify the location of the sprinkler below the ceiling.

The required inputs for Fire Simulator are (Figure 10):

- room geometry,  $L, W, H$
- thermal properties of walls and ceilings,  $k\rho c$
- fire heat release rate history,  $\dot{Q}$
- fire (fuel) height,  $h_F$
- wall vents
- Inlet/Exhaust air flow
- radial distance to sprinkler,  $R$
- activation temperature,  $T_{act}$
- sprinkler response time index, RTI

### **Chapter III Large Scale Sprinkler Activation Tests**

Sprinkler activation tests were conducted with both quick response and standard response sprinklers using glass bulb and solder link thermal elements. A range of quasi-steady state heat release rate fires were used to activate the sprinklers. The sprinklers were tested in a fully exposed pendent position and in a 25 mm recessed position. The test area was instrumented with thermocouples and bi-directional pressure probes in order to characterize the ceiling jet.

#### **Experimental Design**

The tests were conducted in a space 18.9 m x 9.1 m with a ceiling height of 2.35 m. During the experiments the room was closed, but not sealed, and no mechanical ventilation was operating. This provided a quiescent test environment. The ceiling of the compartment was composed of 12mm thick gypsum board with concrete block walls. The area of the ceiling above the fire was covered with 12 mm thick calcium silicate board.

The fire source for all of the tests was a gaseous propane diffusion flame. The burner was an open top cylinder, 0.6 m in diameter and 0.1 m high. The shell of the burner was filled with pea gravel and covered with expanded metal. The burner was positioned on the floor. A 6 mm tube with a constricted tip was mounted on the top edge of the

burner to provide a pilot light for ignition. It took approximately 5 seconds for fire development after ignition.

The heat release rates of the fires were calculated based on the fuel flow rate. The propane flow rate was measured and controlled with variable area flowmeters. During the test, the pressure and temperature of the propane gas were also measured. The flow rate was then corrected based on the specific gravity and temperature of the gas. The change in pressure in the gas supply line was negligible. The fuel flow was also measured with a linear mass flow transducer which was located downstream of the variable area flowmeters (Figure 11). This provided a second measurement of the fuel flow rate.

The sprinkler array had positions for four sprinkler specimens. The sprinklers were installed either with an escutcheon plate in their fully exposed pendent position (Figure 13) or installed with a recessed cup fixture and recessed into the ceiling 25 mm (Figure 14). The recessed cup fixture is made of steel and fits over the threaded portion of the sprinkler head. The cup portion of the fixture, where the thermally sensitive portion of the sprinkler is located has an opening approximately 50 mm in diameter. The cup has three slotted vents on its top face (when in its installed position), each slot is approximately 27 mm long and 4 mm wide. The vents were open to the quiescent interstitial space above the ceiling as would be the normal installation practice for these types of fixtures.



Sprinkler activation times were recorded with electric timers controlled by air pressure switches. Each sprinkler had a dedicated air line and accompanying air pressure switch. Before the start of the test, the air lines were pressurized to approximately 135 kPa. When a sprinkler head activated during the test the pressure in the air line was released, the pressure switch tripped at approximately 35 kPa and the timer stopped, indicating the sprinkler activation time.

In addition to sprinkler activation time, temperature and pressure measurements of the ceiling jet were made. The ceiling jet velocity could then be calculated from the thermocouple and bi-directional pressure probe readings. A plan view of the test area and the instrumentation arrangement is shown in Figure 12. A complete list of the instrumentation and locations is given in Table 1.

In order to monitor the sprinkler element temperature, thermocouples were attached to the sprinklers using the elements as the thermocouple bead. Only the solder link type sprinklers could be instrumented in this fashion. A test was conducted with an instrumented QR solder link sprinkler vs. a non-instrumented QR link to determine if the thermocouple would have an effect on the response time. The difference in activation time was less than 2 percent with the instrumented link activating first. Therefore, the effect, was considered negligible.

A total heat flux sensor and a radiometer were installed next to the sprinkler array. The faces of the sensors were mounted perpendicular to the ceiling, with the centerlines of

the sensors 25 mm below the ceiling and aimed toward the centerline of the thermal plume.

Temperature, pressure and heat flux measurements were made and recorded at approximately 2 second intervals using a computerized data acquisition system.

### **Experimental Approach**

A series of steady-state fires ranging in heat release rate (HRR) from 115 kW to 520 kW was used during the course of this study to evaluate the response of sprinklers in both the pendent and recessed positions. Two radial positions from the fire's vertical centerline were used, 1.5 m and 3 m. The complete test matrix is given in Table 2. In each configuration three tests were run and the results from each set of tests were averaged together for analysis.

### **Experimental Results**

A pair of graphs are provided for each HRR and burner location tested. The instrument array is located at the centerline of the sprinkler array. The first graph of each set (Figures 15, 17, 19, 21, 23, 25) shows the average measured temperature increase and the temperature gradient from 12 mm beneath the ceiling to 152 mm beneath the ceiling. The second graph of each pair (Figures 16, 18, 20, 22, 24, 26) is a plot of the average ceiling jet velocity measured 76 mm below the ceiling.

Figure 15 shows the temperature profile of the ceiling jet, from the 520 kW tests, as having a range of approximately 30 °C between 15 and 30 seconds after ignition. During this period, the average rate of temperature increase was 1 °C/s. Between 35 and 40 s, the hot gas layer has developed and is beginning to increase the temperature of the ceiling jet and decrease the temperature difference across the ceiling jet. For this particular case the hot gas layer effect on the ceiling jet temperatures appears as a pronounced temperature gradient, exhibiting a temperature increase rate of approximately 6 °C/s. Figure 16 reveals that the average velocity of 1.7 m/s remains constant during the test, however the magnitude of the fluctuations appear to increase as the hot gas layer develops.

During the 520 kW tests, the visible flames impinged on the ceiling and fanned out radially. Radiant heat flux, measured adjacent to the sprinkler's positions, averaged 1.23 kW/m<sup>2</sup>.

Similar ceiling jet temperature trends can be seen in the remainder of the test cases, although the temperature gradient due to layer development is not always as pronounced as it is in the 520 kW case. Ceiling jet temperature increases ranged from a high of 190 °C for the 520 kW, 3 m test case (Figure 15) to a low of 75 °C for the 115 kW, 1.5 m test case (Figure 25). The ceiling jet velocities ranged from an average high of 2.2 m/s for the 290 kW, 1.5 m case (Figure 22) to an average low of 1.1 m/s for the

115 kW, 1.5 m case (Figure 26). In Figures 18, 20, 22, 24 and 26 the average velocity can be seen to decrease as the hot gas layer develops. This phenomena will be discussed in Chapter IV.

Average radiant heat flux values at the sprinkler position for each test are given in Table 3. The values ranged from a high of  $1.27 \text{ kW/m}^2$  for the 290 kW,  $r = 1.5 \text{ m}$  case, to a low of  $0.22 \text{ kW/m}^2$  for the 115 kW case.

The sprinkler activation time results, the average activation times, and the comparison of the average activation times for the sprinklers installed under the ceiling versus the recessed sprinklers are shown in Tables 4 through 21.

The tables of sprinkler activation times listed above provide a measure of the repeatability of the experiments. The average activation time and the second standard deviation [33] are provided on the bottom line of each of the sprinkler activation time tables. The second standard deviation ( $2\sigma$ ) represents the upper and lower bound for the 95% confidence limits. In other words, assuming that the sprinkler activation times fit a normal distribution, the probability of obtaining an activation time outside of this range is about 5% [34]. The QR bulb sprinkler had a second standard deviation as a percentage of the average activation time as low as  $\pm 2.4\%$  (115 kW case) and as high as  $\pm 38.9\%$  (290 kW, 1.5 m) in the pendent position. The QR link sprinkler had  $2\sigma$  values as low as  $\pm 9.1\%$  (290 kW, 3 m) and as high as  $\pm 65.0\%$  (155 kW). The second standard deviation ranges for the SS bulb and SS link in terms of percentage were lows

of  $\pm 7.7\%$  (155 kW),  $\pm 1.5\%$  (155 kW) and highs of  $\pm 21.4\%$  (290 kW, 1.5 m) and  $\pm 30.4\%$  (290 kW, 1.5 m) respectively.

The comparison tables show the change in average activation time, where a positive value is indicative of an increase in activation time. These tables indicate that the general trend was an increase in average activation time due to recessing the sprinkler, although in three out of the six test scenarios, the SS link sprinkler showed a slight decrease in average activation time when installed in the recessed position.

The difference in the temperature increase, between the instrumented fully exposed pendent sprinkler links and the recessed sprinkler links, was typically 5 to 10 °C, with the exposed sprinkler having the higher temperature. After an initial delay of a few seconds or less, the recessed link would increase in temperature at a rate similar to that of the exposed sprinkler link.

RTI's were calculated using the sprinkler activation times, and the measured ceiling jet temperatures and velocities from the large scale tests as input to equations 16 and 17. The temperatures and velocities were averaged from time of ignition to the time of each sprinkler activation. The measurements taken 76 mm below the ceiling were used as characteristic ceiling jet values for the calculations. The average RTI's are given and compared in Tables 22 through 27.

## Chapter IV Analysis and Discussion

The data from Tables 4 through 21 are summarized and presented in Figures 27 through 34. These graphs show the average activation times for both the pendent and recessed installation for each sprinkler type at each HRR. The 95% confidence limits are presented and can be seen to overlap to some degree in all of the cases. Although the average recessed activation time was generally longer than the average pendent activation time, the difference may not be significant. A "test of significance" can be performed by determining whether or not the confidence interval for the recessed case includes the mean of the pendent case[34]. Using that criteria, 5 out of the 24 test cases are "significantly" different on a statistical basis. The test cases yielding a "significant difference" are SS bulb, 520 kW; QR bulb, 215 kW; QR link 115 kW, SS bulb, 115 kW, and SS link, 115 kW. With the exception of the 115 kW cases, the margin of "significance" is less than a few seconds.

Another way of analyzing the significance of the increased activation times is on an application basis, in this case life safety. Temperatures in the range of 65 to 100 °C at face level (1.5 m) have been used in previous life safety analyses as a thermal tenability limit [8]. The 65 °C criteria will be used in this analysis to evaluate whether the measured delays in activation due to a recessed installation would have an adverse effect on the safety of individuals in the fire area.

Temperature data for the 115, 155, 215 and 290 kW cases, where  $r = 1.5$  m, exhibit temperatures, at 1.5 m above the floor and 3 m from the fire centerline, to be less than 65 °C through the entire test periods. The test period being defined as the time required to activate all of the sprinkler heads in a given test. The measurement location considers a conservative temperature limit (lower tenability limit) for a person located in the room but not intimate with the fire. At that location, the temperature never exceeded 58 °C in any of the 4 test cases listed above. Therefore on a temperature basis, the conditions in the room remain tenable, hence the recessed installations did not have an adverse impact on life safety for these cases.

In the  $r = 3$  m cases, the maximum temperature at 1.5 m above the floor and 3 m from the fire centerline exceeds the 65 °C tenability limit during the test period. For the 290 kW case, the thermal tenability limit is reached at approximately 175 seconds. However, the QR sprinklers, both pendent or recessed installations, activated at least 60 seconds prior to the onset of the 65 °C threshold. The SS sprinklers, both pendent and recessed, do not activate until after the 65 °C tenability benchmark was reached (Tables 7 and 8). For this test condition, the type of sprinkler has an impact on tenability, but the installation configuration does not.

The most severe fire case, 520 kW, produced the 65 °C tenability limit at 1.5 m above the floor at approximately 90 seconds after ignition, all of the sprinklers except the SS bulb activated prior to 90 seconds (Tables 4 and 5). The SS bulb had a maximum pendent activation time of 89 seconds and a maximum recessed activation time of 96

seconds. The SS bulb sprinkler in this scenario is the only case where untenable thermal conditions occurred and there was a "significant difference" between the average pendent and recessed activation times. Given that the untenable conditions in the room would only have lasted six seconds based on the slowest sprinkler activation, it can be seen that the "significant" difference did not have a significant impact on life safety in the room.

Figures 27 through 34 showed shorter activation times and time ranges for each of the sprinkler types as the HRR increased. Therefore, if the fire was growing, the activation time and scatter of activation times should also be reduced, thus minimizing any delay that a recessed installation might cause.

The RTI is one of the required inputs for a thermal element activation model. In addition to having the plunge test based RTI for these sprinklers, the RTI was calculated from the full scale test data by considering the time averaged temperature increase and velocity at the time of sprinkler activation. These full scale RTIs will be used as a check for theoretical and practical agreement with the RTI concept and the sprinkler activation models respectively.

The RTIs obtained by the standard heat sensitivity oven method or plunge test for the four sprinklers used in the study are as follows: QR bulb,  $42.1 \text{ m}^{1/2}\text{s}^{1/2}$ , QR link,  $34.1 \text{ m}^{1/2}\text{s}^{1/2}$ , SS bulb,  $234.8 \text{ m}^{1/2}\text{s}^{1/2}$ , and SS link,  $129.8 \text{ m}^{1/2}\text{s}^{1/2}$ . Table 28 summarizes the large scale experiment RTI averages from Tables 22 through 27, and compares them to the average plunge test RTIs. It can be seen that the time averaged full scale RTIs are



not representative of those developed in the plunge test. Qualitatively, some of the discrepancies can be accounted for. For example, in the 520 kW and the 290 kW at  $r = 1.5$  m cases, the pendent position RTIs for the QR sprinklers are smaller than the plunge test RTIs and the recessed position RTIs are closer to the plunge test value. These two cases had the highest radiative flux exposure. Therefore, when the recess blocked the radiative flux to the thermal element, the RTIs became more representative of the plunge test values. This also suggests that there is sufficient hot gas flow around the thermal element such that the convective heat transfer coefficient is not adversely or significantly changed. These two cases also had the highest ceiling jet velocities, which were closest to the standard plunge test velocity of 2.5 m/s.

Conversely, for the 290 kW at 3 m and the 115 kW cases, where the ceiling jet velocity is less than half of the velocity used in the plunge test and there are little if any radiation effects, the QR sprinklers yielded large experimental RTI values. In some cases the RTI values are 3 to 4 times higher than plunge test values.

Tables 22 through 27 compare the "pendent RTIs" with the "recessed RTIs". This comparison shows that the recess installation affects each type of sprinkler differently. While some of the discrepancies can be explained by the arguments given above, others can not.

Given the wide variety of parameters affecting the response of a sprinkler in addition to the location of the element; type of sprinkler, mass of thermal element, thermal inertia

of element, absorptivity, reflectivity, emissivity and conductivity of element, and exposure conditions it is not practical to develop factors which modify the RTI value to account for installation position. If the physical values were available for each sprinkler and the physical characteristics of the "design fire" were known, then a theoretical model could be developed for that specific case. This is an impractical design approach. The current approach, which is a generalized method that does not strictly depend on sprinkler type, i.e. glass bulb or link, QR or standard response, or the configuration of the fire is a more practical design approach. However, it is important to know what the accuracy and the limits of the current methods are. Therefore the models, DETACT-QS, LAVENT and FPEtool will be compared with the full scale experimental results to determine the level of agreement between actual activation times and experimental results.

Instead of choosing a fixed criteria across the board for evaluating the level of agreement between experiment and model, the 95% confidence limits of the data will be utilized for each case. The models should not be expected to predict results better than the experiment can reproduce them. While an uncertainty analysis can be conducted for some portions of the experiment, i.e. accuracy in gas flow meter and potential thermocouple error, other tolerances of the experimental system are relatively unknown. Unknown variables would include the tolerances for the thermal elements in the sprinklers and the exact heat of combustion of propane from one tank to another. Therefore replicate tests were performed and the uncertainty of the system as a whole was considered.

The comparison is based on the full scale, pendent case test results. Utilizing DETACT-QS, LAVENT and FPEtool the experimental scenario was modeled for quasi-steady heat release rates of 115, 155, 215 and 290 kW for  $r/h = 0.64$  ( $r = 1.5$  m case) and 290 and 520 kW for  $r/h = 1.28$  ( $r = 3$  m case). The RTIs used in these models were RTI values determined from the standard sensitivity oven test. A summary of the predicted response times compared to the actual response times is given for each RTI in Tables 29 through 34. The input fires go from a zero HRR to the steady-state HRR in 5 seconds in all of the modelled cases.

### **DETACT-QS Comparison**

The output from DETACT-QS provides the following information: minimum heat release rate required to activate detector, the ceiling jet temperature, the element temperature and the activation time. A sample DETACT-QS output is included in Appendix A. In the comparison of DETACT-QS predictions with experimental data, these output parameters will be used to the extent possible to explain the agreement or lack thereof between the model and the large scale test. The DETACT programs do not provide a velocity output, therefore the velocity used in the comparisons is calculated from equation 21.

The activation time comparisons for the tests conducted at  $r = 3$  m are shown in Figures 35 through 38. The average test activation times for each type of sprinkler are compared

with the predicted pendent activation time based on the plunge test RTI. The activation times used in these graphs are from Tables 29 and 30.

In general, DETACT yields conservative predictions, i.e. it predicts longer activation times than actually required. As the HRR rate decreases or as the RTI increases, the difference between the DETACT prediction and the actual activation time increases.

The same trends are seen for the  $r = 1.5$  m tests. The activation time comparisons are given in Figures 39-42 and on Tables 31-34. Reviewing Figures 39 through 42 it can be seen that DETACT provides the best agreement for the 290 kW, 1.5 m case (tests 13-15). The steady-state ceiling jet temperature increase of 80 °C predicted by DETACT is very close to the average measured ceiling jet temperature, at 76 mm below the ceiling, reached during the initial 35 seconds after ignition as shown in Figure 47. After 35 seconds the average ceiling jet temperature increases due to hot layer effects. Therefore DETACT provides the best agreement for the QR devices which activated prior to the development of the hot upper layer. As the hot gas layer increases the temperature of the ceiling jet, a condition DETACT does not account for, DETACT's predictive accuracy diminishes rapidly. DETACT's prediction of ceiling jet velocity for the 290 kW, 1.5 m case is very close to the other models' predictions, although approximately 33% less than the measured average velocity at 76 mm below the ceiling as shown in Figure 48.

There are many cases where DETACT predicts "no activation", when in fact the sprinklers do activate. These would be considered DETACT's worst cases of agreement. For instance, the 115 kW, 1.5 m case (tests 31-33), DETACT reached a maximum, steady-state ceiling jet temperature of 64 °C. The ambient temperature used in the DETACT model was 21 °C, therefore the maximum temperature increase for the 115 kW, 1.5 m case is 43 °C. The measured average ceiling jet temperature increase at 76 mm below the ceiling (Figure 53) ranged from approximately 45 °C at 50 seconds to 65 °C at 250 seconds after ignition. Higher temperatures developed over time due to hot gas layer buildup in the compartment, which enabled sprinkler activation. Again, DETACT does not account for this phenomena, so the predicted ceiling jet temperatures from DETACT never reached activation temperature. Figure 54 shows that DETACT does a good agreement between the predicted velocity and the measured velocity for this test case.

### **LAVENT Comparison**

Figures 35 through 42 show that LAVENT does not always provide conservative sprinkler activation predictions. In general as the HRR decreases LAVENT tends to underpredict the activation time. The temperature increase comparison figures (Figures 43, 45, 47, 49, 51, 53) show that LAVENT predicts higher temperatures than given by the temperature data. When the hot gas layer is fully developed and contributing to the temperature of the ceiling jet, the difference between LAVENT and the measured ceiling jet temperatures decreases.

LAVENT demonstrates the best agreement between the predicted and actual activation times for the 215 kW case, with the exception of the QR link. Figure 49 shows that LAVENT, for times greater than 20 seconds after ignition, calculates a ceiling jet temperature that is approximately 20 °C higher than measured. However, the measured temperature of the hot gas layer enhanced ceiling jet increases until it converges with the LAVENT calculation at approximately 100 seconds. Velocity comparisons for the same case yield good agreement for the first 40 seconds after ignition. Then the measured values decrease while the LAVENT values show a slight increase.

A decrease in velocity is not surprising when the hot gas layer is well developed in a compartment. The fire plume's rise to the ceiling is due to a buoyancy force. The buoyancy force is created by a difference in density between a convecting fluid and an ambient fluid. Morton, Taylor, Turner [35] show the relationship of the density deficit to temperature as:

$$\frac{\rho_o - \rho}{\rho_1} = \beta(T - T_o) \quad (22)$$

where  $\rho_o$  and  $\rho$  are the densities of the ambient and of the plume fluids respectively. The reference density is defined as  $\rho_1 = \rho(o)$ .  $\beta$  is the expansion coefficient. From equation 22 it can be seen that if the temperature differential between the fluid in the convecting plume and the ambient surroundings is reduced, the density defect or buoyant force is also reduced. This can be seen in terms of velocity by applying the conservation of momentum and assuming a steady source in a uniform ambient field with a point source.

$$\frac{d}{dx} (r^2 v^2) = r^2 g \frac{\rho_o - \rho}{\rho_1} \quad (23)$$

This equation equates the squared change in radius,  $r$ , and vertical velocity,  $v$ , relative to changes in elevation to the product of the radius squared times the gravitational acceleration,  $g$ , times the density defect. By substituting equation 22 into equation 23 and assuming a boundary condition of  $\rho_o = \rho_1$ , the velocity can be solved for as shown below:

$$v = \frac{5}{6\alpha} [0.9 \alpha (T - T_o)]^{1/3} x^{-1/3} \quad (24)$$

where  $\alpha$  is an entrainment constant and  $x$  is the height above the source. Equation 24 clearly shows that the velocity is dependent on temperature differential and height above the source. Velocity decreases by either a decrease in the temperature differential and/or an increase in height above the source. Since the height is fixed in our experimental case the only variable is the temperature differential. As the smoke layer in the compartment heats up and becomes thicker the temperature differential between the plume and the upper layer decreases and hence the velocity of the plume, which is the source for the ceiling jet, decreases.

Given that it is buoyant force which drives the hot gases to the ceiling and in turn provides the momentum for the ceiling jet, it should be noted that the ceiling jet still has a vertical buoyant force which would force the hot gases to rise if given an opening in the ceiling, such as a recessed sprinkler cup. Based on the ceiling jet and upper layer temperatures from the large scale tests, it appears that gases flowing through an opening

in the ceiling would have a vertical velocity with the same order of magnitude as the horizontal ceiling jet velocity. Perhaps this accounts for the similar temperature increase rates of the exposed and recessed sprinkler links after the ceiling jet is developed.

LAVENT exhibits its worst predictions for the 115 kW case (Figures 39 - 42), the same as DETACT's worst case. However, the reasons are completely different. DETACT failed on the conservative side predicting no activations. LAVENT failed by predicting early activations. Looking at Figures 53 and 54, it appears that LAVENT's predicted ceiling jet temperature begins and remains hotter than the measured temperature. Approximately 2 minutes after ignition it can be seen that the difference in temperature is 10 °C or less. Referring back to the concept of a time constant (Figure 4) we can see that after 2 or 3 time constants the response of the elements becomes very sensitive to temperature. As a result a few degrees temperature difference can have a significant impact on the time of activation.

### **FPEtool Comparison**

A FPEtool Fire Simulator case, representative of cases used for this comparison is provided in Appendix A. In the input, the heat of combustion and radiant energy fraction for propane are used, the ceiling and wall materials are specified, and the maximum energy loss is given as 85%. The only modifications made to this input set between cases involved changing the HRR curve and the sprinkler description and location to the fire.



The output from Fire Simulator provides the following information relative to thermal element response: link (element) temperature, ceiling jet temperature, ceiling jet velocity and activation time. These output parameters will be compared with the test measurements.

Reviewing Figures 35 through 42 again, FPEtool exhibits its best agreement with the 290 kW,  $r = 1.5$  m case and yields conservative predictions for all for the cases except the 290 kW,  $r = 3$  m, and 115 kW test cases. Looking at Figure 47, it can be seen that FPEtool seems to average the measured temperature over the period of the test. By referring to the other ceiling jet temperature figures (Figures 43, 45, 49, 51, 53) the alignment of the models can be seen, i.e. DETACT is always has the lowest ceiling jet temperature prediction, LAVENT always has the hottest temperature prediction and FPEtool is always in the middle. Based on the fact that DETACT only considers unconfined ceilings it is easy to understand why it always predicts the lowest temperature. The difference between LAVENT and FPEtool, and why both of these models predict higher temperatures than DETACT prior to the development of the hot upper gas layer, was not evident.

FPEtool version 3.00 has an empirical coefficient which reduces the predicted temperature of the ceiling jet. When the coefficient was deleted from the equation, the resulting ceiling jet temperatures were similar to those of LAVENT. While the use of the coefficient provided reasonable sprinkler activation predictions, it did not appear to be modeling the ceiling jet. In theory, the ceiling jet begins as predicted by Alpert's

correlations. The temperature and velocity should remain as predicted by Alpert until they reach the boundaries of a confined area. Then the upper portion of the compartment begins to fill with hot gas. Depending on the size of the compartment and the relative size of the fire, the effects from the smoke filling could have an immediate impact on the ceiling jet or in the case of a large space not have any significant impact for some time. Based on the temperature data from the large scale activation tests it appears that the ceiling jet temperature reaches a quasi-steady state condition prior to being affected by the development of the hot gas layer. In the case of the 520 kW fire the time period is approximately 30 seconds until there is a noticeable change in the rate of temperature increase. In the case of the 115 kW fire this increase does not take place until approximately 100 s after ignition. This data shows that the ceiling jet is not effected by the hot upper gas layer until the layer is developed and has dropped below the level of the fully developed ceiling jet thus forcing the jet to entrain hot gas. One of the reasons that FPEtool predicts higher temperatures immediately is because the virtual source which enhances the ceiling jet temperature is invoked before the hot gas layer is even formed.

A second reason for the higher predictions is the use of the total HRR in the virtual source. The basis of the sprinkler activation routine in FPEtool are the same equations which comprise DETACT. These equations require the use of total HRR. Evan's virtual source algorithm should only consider the convective input to the layer, therefore it requires only the convective portion of the heat release rate. FPEtool version 3.00 considers only the total HRR.

### **FPEtool Modification**

The FPEtool sprinkler activation subroutine was modified to apply the virtual source only after the upper layer has dropped below the fully developed ceiling jet or 88 % of the distance from the ceiling to the fuel based on Alpert's lower boundary for a fully developed ceiling jet [26]. Also when the virtual source is used, it will only utilize the convective portion of the HRR.

The temperature and velocity predictions as a result of the modification are given in Figures 55 through 66. FPEtool now has good agreement with DETACT predictions and the data early in the ceiling jet growth period and then takes a step increase when the upper layer descends to 88% of the height between the ceiling and the fuel surface. This predicted increase follows the data in most cases. Another result of this change is a predicted decrease in ceiling jet velocity. While it qualitatively follows the trend of the data, it is still based on an algorithm that appears to be underpredicting the velocity. Fortunately the lumped mass convective heat transfer equation is not as sensitive to velocity as it is to temperature. Tables 35 through 38 compare the actual activation times with predictions of DETACT, FPEtool 3.00 and the modified version.

### **Recommendation for Sprinkler Activation Model Usage**

After comparing the predictions of the four models to experimental data we see that the models agree within the 95% percent confidence limits of the data or provide

conservative results for the majority of cases. However, there are two notable test cases where the models fail to provide acceptable agreement with the experimental data, the 290 kW,  $r = 3$  m case and the 115 kW case. LAVENT, FPEtool and FPEtool modified underpredict the activation time because they are overpredicting the ceiling jet temperature (Figures 57 and 65). This could still be an issue of misapplying the effects of the hot gas layer or perhaps the heat transfer to the ceiling is incorrect. Data is not available to determine the source or combination of sources which are responsible for this error in the models.

In order to have confidence in applying the sprinkler activation models properly, the results of this study provide the basis for a recommendation. After a design fire and the  $r/H$  are chosen, check the maximum temperature increase provided by Alpert's correlations (equations 18 and 20) for the case under investigation. If the temperature increase is equal to or less than the increase required to activate the sprinkler, then based on the results of this limited study, an accurate prediction cannot be made. While it may be obvious that DETACT would not provide a good prediction in such a case, it is not so obvious that LAVENT and FPEtool would not provide a good prediction. For both of the cases where underprediction of the sprinkler activation time was outside the 95% confidence limit, DETACT's prediction was just at or below the temperature increase required for activation.

Remembering that the time constant is the core of these activation models will help demonstrate the sensitivity of the thermal response model and of the sprinkler to small

changes in temperature. Figure 67 shows the sensitivity of a sprinkler with an activation temperature of 74 °C. An ambient temperature of 25 °C was assumed and the sprinkler's theoretical thermal response to three different steady gas temperatures is shown. The 135 °C gas temperature is representative of the temperature used in the plunge test. Notice that the sprinkler reaches activation temperature during a period of rapid temperature increase. If the sprinkler's environment changed, causing a slightly lower ( $< 5$  °C) ambient temperature or a lower gas temperature the effect on the time to sprinkler activation would be minimal. The same is true for the 110 °C curve which is representative of the temperature in the first 30 seconds of the 290 kW, 1.5 m case. However, the activation time of the same sprinkler exposed to a 75 °C gas temperature, which is representative of the average ceiling jet temperature for the 115 kW case, would change significantly if the temperature of the ceiling jet was reduced by 1 or 2 °C. The plunge test gas and ambient sample temperatures are chosen so that the activation always occurs in the rapid temperature increase region, in an exposure time region which is less than  $\tau$ . The thermal element of the sprinkler is not very sensitive to small fluctuations in temperature in this situation. After exposure times greater than  $3 \tau$ , where the sprinkler's element temperature is approaching the gas temperature asymptotically the element is very sensitive to small difference changes in temperature.

If the chosen design fire in a 25 °C compartment provided a temperature increase per equation 21 of 47 °C, DETACT will not predict an activation. If a hot gas layer can form in the compartment, LAVENT and FPEtool will provide an activation time. However given the potential for error when trying to predict sprinkler activation times

in this asymptotic response region, it would be poor engineering judgement to base life safety decisions on the use of a sprinkler activation model with such a design fire.

In summary, if the predicted ceiling jet temperature, without layer effects, is higher than the activation temperature then relatively accurate predictions of response time are possible. If the ceiling jet temperature is at or below the activation temperature, then accurate predictions of response time are less likely.

## Summary

1. For conditions evaluated in this test series, the activation delay due to a recessed sprinkler head installation was negligible for fires with the potential of providing untenable conditions in the test area.
2. The general trend of the data shows slight increases in activation time for recessed sprinklers exposed to low heat release rate fires. However, the change in activation time is not uniform among the sprinkler types, therefore a constant modifying the RTI to account for the increased activation time is not practical.
3. The ability of several models to predict sprinkler activation times was checked against activation times made during large scale fire tests in a compartment. A criteria for "good" agreement between the models and the data was defined in the range of the 95% confidence limits of the data. None of the models provided accurate predictions for all of the cases. Prediction of the ceiling jet conditions was compared to the measured conditions to determine the cause of the cases with poor predictions.
4. An alternative sprinkler algorithm is proposed for the FIRE SIMULATOR program in FPEtool. The current routine utilized a virtual source for the hot layer effect based on total heat release rate. The virtual source was applied immediately even before a hot layer could form. Even though the entire

equation was then multiplied by a empirical factor to cool the resulting ceiling jet prediction, the predicted ceiling jet was still hotter than the measured ceiling jet in the early stages of the fire development, a critical time for sprinkler link heating, especially for QR heads. The proposed algorithm utilizes Alpert's correlations until the hot gas layer has dropped to 88% of H, thus dropping below the bottom edge of the ceiling jet. At that time the virtual source is invoked. While Alpert's correlations are based on the total HRR, the virtual source is based on the convective portion of the HRR.

5. All of the models underpredict velocity. Since velocity is a square root relation to the RTI, the underprediction is usually of minimal effect. However, the ceiling jet velocity was seen to decrease as the hot upper gas layer developed. The proposed algorithm was the only model to follow the trend although the time of occurrence of the velocity reduction differs between the model and the test.
6. Sprinkler response is difficult to predict accurately when the sprinkler is exposed to gas temperatures near the sprinklers activation temperature. The utility of the design fire can be checked with Alpert's equations (DETECT-QS) to determine if the models, which include secondary effects, are being applied properly.



## Appendix A Example Sprinkler Activation Model Inputs and Outputs

# DETECT-QS

290 kW, 1.5 M, SSB, RTI=234.8      03-01-1993

Fire to	Detector	Room	Device	RTI
ceiling	axial dist.	temp.	rating	
m	m	C	C	(metric)
2.25	1.5	21.1	68	234.8

Minimum heat release rate necessary to activate the  
detector at the location described is    130 kW

Time(Sec)	RHR(kW)	Jet (C)	Head/det (C)
0	0	21	21
10	290	101	24
20	290	101	28
30	290	101	31
40	290	101	35
50	290	101	38
60	290	101	41
70	290	101	44
80	290	101	47
90	290	101	50
100	290	101	52
110	290	101	55
120	290	101	57
130	290	101	59
140	290	101	61
150	290	101	63
160	290	101	65
170	290	101	67

---- Detector activation at 177.5 seconds ----

# LAVENT

```

CEILING HEIGHT = 2.4 M
ROOM LENGTH = 18.9 M
ROOM WIDTH = 9.1 M
CURTAIN LENGTH = 0.0 M
CURTAIN HEIGHT = 0.0 M
MATERIAL = calcium silicate
CEILING CONDUCTIVITY = .120E+00 W/M K
CEILING DENSITY = .740E+03 KG/M3
CEILING HEAT CAPACITY = .143E+04 J/M K
CEILING THICKNESS = .250E-01 M
FIRE HEIGHT = 0.1 M
FIRE DIAMETER = 0.6 M

LINK NO = 1 RADIUS = 3.0 M DIST CEILING = 0.03 M
RTI = 42.10 SQRT(MS) FUSION TEMPERATURE FOR LINK = 341.15
LINK NO = 2 RADIUS = 3.0 M DIST CEILING = 0.03 M
RTI = 57.90 SQRT(MS) FUSION TEMPERATURE FOR LINK = 341.15
LINK NO = 3 RADIUS = 3.0 M DIST CEILING = 0.03 M
RTI = 34.10 SQRT(MS) FUSION TEMPERATURE FOR LINK = 347.15
LINK NO = 4 RADIUS = 3.0 M DIST CEILING = 0.03 M
RTI = 74.80 SQRT(MS) FUSION TEMPERATURE FOR LINK = 347.15
LINK NO = 5 RADIUS = 3.0 M DIST CEILING = 0.03 M
RTI = 234.80 SQRT(MS) FUSION TEMPERATURE FOR LINK = 341.15
LINK NO = 6 RADIUS = 3.0 M DIST CEILING = 0.03 M
RTI = 251.90 SQRT(MS) FUSION TEMPERATURE FOR LINK = 341.15
LINK NO = 7 RADIUS = 3.0 M DIST CEILING = 0.03 M
RTI = 129.80 SQRT(MS) FUSION TEMPERATURE FOR LINK = 347.15
LINK NO = 8 RADIUS = 3.0 M DIST CEILING = 0.03 M
RTI = 205.50 SQRT(MS) FUSION TEMPERATURE FOR LINK = 347.15
LINK NO = 9 RADIUS = 3.0 M DIST CEILING = 0.08 M
RTI = 400.00 SQRT(MS) FUSION TEMPERATURE FOR LINK = 600.00
VENT = 1 VENT AREA = 0.0 M2 LINK CONTROLLING VENT = 8
VENT = 2 VENT AREA = 0.0 M2 LINK CONTROLLING VENT = 8
TIME (S)= 0.0000 LVR TEMP (K)= 295.1 LVR HT (M) = 2.35 LVR MASS (KG)=0.000E+00
FIRE OUTPUT (W) = 0.0000E+00 VENT AREA (M2) = 0.00
LINK = 1 LINK TEMP (K) = 295.15 JET VELOCITY (M/S) = 0.000 JET TEMP (K) = 295.1
LINK = 2 LINK TEMP (K) = 295.15 JET VELOCITY (M/S) = 0.000 JET TEMP (K) = 295.1
LINK = 3 LINK TEMP (K) = 295.15 JET VELOCITY (M/S) = 0.000 JET TEMP (K) = 295.1
LINK = 4 LINK TEMP (K) = 295.15 JET VELOCITY (M/S) = 0.000 JET TEMP (K) = 295.1
LINK = 5 LINK TEMP (K) = 295.15 JET VELOCITY (M/S) = 0.000 JET TEMP (K) = 295.1
LINK = 6 LINK TEMP (K) = 295.15 JET VELOCITY (M/S) = 0.000 JET TEMP (K) = 295.1
LINK = 7 LINK TEMP (K) = 295.15 JET VELOCITY (M/S) = 0.000 JET TEMP (K) = 295.1
LINK = 8 LINK TEMP (K) = 295.15 JET VELOCITY (M/S) = 0.000 JET TEMP (K) = 295.1
LINK = 9 LINK TEMP (K) = 295.15 JET VELOCITY (M/S) = 0.000 JET TEMP (K) = 295.1
R (M) = 0.00 TSL (K) = 295.1 QB (W/M2) = 0.000E+00 QT (W/M2) = 0.000E+00
R (M) = 1.97 TSL (K) = 295.1 QB (W/M2) = 0.000E+00 QT (W/M2) = 0.000E+00
R (M) = 3.93 TSL (K) = 295.1 QB (W/M2) = 0.000E+00 QT (W/M2) = 0.000E+00
R (M) = 5.90 TSL (K) = 295.1 QB (W/M2) = 0.000E+00 QT (W/M2) = 0.000E+00
R (M) = 7.86 TSL (K) = 295.1 QB (W/M2) = 0.000E+00 QT (W/M2) = 0.000E+00
R (M) = 9.83 TSL (K) = 295.1 QB (W/M2) = 0.000E+00 QT (W/M2) = 0.000E+00
TIME (S)= 10.0000 LVR TEMP (K)= 349.2 LVR HT (M) = 2.26 LVR MASS (KG)=0.160E+02
FIRE OUTPUT (W) = 0.2900E+06 VENT AREA (M2) = 0.00
LINK = 1 LINK TEMP (K) = 303.18 JET VELOCITY (M/S) = 0.701 JET TEMP (K) = 357.1
LINK = 2 LINK TEMP (K) = 301.10 JET VELOCITY (M/S) = 0.701 JET TEMP (K) = 357.1
LINK = 3 LINK TEMP (K) = 304.89 JET VELOCITY (M/S) = 0.701 JET TEMP (K) = 357.1
LINK = 4 LINK TEMP (K) = 299.82 JET VELOCITY (M/S) = 0.701 JET TEMP (K) = 357.1
LINK = 5 LINK TEMP (K) = 296.68 JET VELOCITY (M/S) = 0.701 JET TEMP (K) = 357.1
LINK = 6 LINK TEMP (K) = 296.58 JET VELOCITY (M/S) = 0.701 JET TEMP (K) = 357.1
LINK = 7 LINK TEMP (K) = 297.89 JET VELOCITY (M/S) = 0.701 JET TEMP (K) = 357.1
LINK = 8 LINK TEMP (K) = 296.89 JET VELOCITY (M/S) = 0.701 JET TEMP (K) = 357.1
LINK = 9 LINK TEMP (K) = 296.45 JET VELOCITY (M/S) = 0.729 JET TEMP (K) = 381.2
R (M) = 0.00 TSL (K) = 353.2 QB (W/M2) = 0.634E+04 QT (W/M2) = 0.167E-13
R (M) = 1.97 TSL (K) = 307.3 QB (W/M2) = 0.145E+04 QT (W/M2) = 0.167E-13

```

R (M) = 3.93 TSL (K) = 299.7 QB (W/M2) = 0.554E+03 QT (W/M2) = 0.167E-13  
 R (M) = 5.90 TSL (K) = 297.7 QB (W/M2) = 0.308E+03 QT (W/M2) = 0.167E-13  
 R (M) = 7.86 TSL (K) = 296.8 QB (W/M2) = 0.206E+03 QT (W/M2) = 0.167E-13  
 R (M) = 9.83 TSL (K) = 295.3 QB (W/M2) = 0.169E+02 QT (W/M2) = 0.167E-13  
 TIME (S)= 20.0000 LVR TEMP (K)= 355.4 LVR HT (M) = 2.16 LVR MASS (KG)=0.329E+02  
 FIRE OUTPUT (W) = 0.2900E+06 VENT AREA (M2) = 0.00  
 LINK = 1 LINK TEMP (K) = 313.45 JET VELOCITY (M/S) = 0.699 JET TEMP (K) = 362.5  
 LINK = 2 LINK TEMP (K) = 309.05 JET VELOCITY (M/S) = 0.699 JET TEMP (K) = 362.5  
 LINK = 3 LINK TEMP (K) = 316.92 JET VELOCITY (M/S) = 0.699 JET TEMP (K) = 362.5  
 LINK = 4 LINK TEMP (K) = 306.20 JET VELOCITY (M/S) = 0.699 JET TEMP (K) = 362.5  
 LINK = 5 LINK TEMP (K) = 298.90 JET VELOCITY (M/S) = 0.699 JET TEMP (K) = 362.5  
 LINK = 6 LINK TEMP (K) = 298.65 JET VELOCITY (M/S) = 0.699 JET TEMP (K) = 362.5  
 LINK = 7 LINK TEMP (K) = 301.77 JET VELOCITY (M/S) = 0.699 JET TEMP (K) = 362.5  
 LINK = 8 LINK TEMP (K) = 299.42 JET VELOCITY (M/S) = 0.699 JET TEMP (K) = 362.5  
 LINK = 9 LINK TEMP (K) = 298.31 JET VELOCITY (M/S) = 0.727 JET TEMP (K) = 387.2  
 R (M) = 0.00 TSL (K) = 374.5 QB (W/M2) = 0.543E+04 QT (W/M2) = 0.167E-13  
 R (M) = 1.97 TSL (K) = 313.7 QB (W/M2) = 0.139E+04 QT (W/M2) = 0.167E-13  
 R (M) = 3.93 TSL (K) = 302.3 QB (W/M2) = 0.550E+03 QT (W/M2) = 0.167E-13  
 R (M) = 5.90 TSL (K) = 299.2 QB (W/M2) = 0.311E+03 QT (W/M2) = 0.167E-13  
 R (M) = 7.86 TSL (K) = 297.8 QB (W/M2) = 0.210E+03 QT (W/M2) = 0.167E-13  
 R (M) = 9.83 TSL (K) = 295.4 QB (W/M2) = 0.165E+02 QT (W/M2) = 0.167E-13  
 TIME (S)= 30.0000 LVR TEMP (K)= 358.4 LVR HT (M) = 2.06 LVR MASS (KG)=0.487E+02  
 FIRE OUTPUT (W) = 0.2900E+06 VENT AREA (M2) = 0.00  
 LINK = 1 LINK TEMP (K) = 322.61 JET VELOCITY (M/S) = 0.706 JET TEMP (K) = 365.7  
 LINK = 2 LINK TEMP (K) = 316.48 JET VELOCITY (M/S) = 0.706 JET TEMP (K) = 365.7  
 LINK = 3 LINK TEMP (K) = 327.23 JET VELOCITY (M/S) = 0.706 JET TEMP (K) = 365.7  
 LINK = 4 LINK TEMP (K) = 312.35 JET VELOCITY (M/S) = 0.706 JET TEMP (K) = 365.7  
 LINK = 5 LINK TEMP (K) = 301.19 JET VELOCITY (M/S) = 0.706 JET TEMP (K) = 365.7  
 LINK = 6 LINK TEMP (K) = 300.80 JET VELOCITY (M/S) = 0.706 JET TEMP (K) = 365.7  
 LINK = 7 LINK TEMP (K) = 305.67 JET VELOCITY (M/S) = 0.706 JET TEMP (K) = 365.7  
 LINK = 8 LINK TEMP (K) = 302.00 JET VELOCITY (M/S) = 0.706 JET TEMP (K) = 365.7  
 LINK = 9 LINK TEMP (K) = 300.22 JET VELOCITY (M/S) = 0.734 JET TEMP (K) = 390.5  
 R (M) = 0.00 TSL (K) = 387.2 QB (W/M2) = 0.493E+04 QT (W/M2) = 0.167E-13  
 R (M) = 1.97 TSL (K) = 318.1 QB (W/M2) = 0.135E+04 QT (W/M2) = 0.167E-13  
 R (M) = 3.93 TSL (K) = 304.2 QB (W/M2) = 0.548E+03 QT (W/M2) = 0.167E-13  
 R (M) = 5.90 TSL (K) = 300.2 QB (W/M2) = 0.312E+03 QT (W/M2) = 0.167E-13  
 R (M) = 7.86 TSL (K) = 298.6 QB (W/M2) = 0.212E+03 QT (W/M2) = 0.167E-13  
 R (M) = 9.83 TSL (K) = 295.4 QB (W/M2) = 0.162E+02 QT (W/M2) = 0.167E-13  
 TIME (S)= 40.0000 LVR TEMP (K)= 360.7 LVR HT (M) = 1.97 LVR MASS (KG)=0.636E+02  
 FIRE OUTPUT (W) = 0.2900E+06 VENT AREA (M2) = 0.00  
 LINK = 1 LINK TEMP (K) = 330.69 JET VELOCITY (M/S) = 0.715 JET TEMP (K) = 368.3  
 LINK = 2 LINK TEMP (K) = 323.34 JET VELOCITY (M/S) = 0.715 JET TEMP (K) = 368.3  
 LINK = 3 LINK TEMP (K) = 335.97 JET VELOCITY (M/S) = 0.715 JET TEMP (K) = 368.3  
 LINK = 4 LINK TEMP (K) = 318.18 JET VELOCITY (M/S) = 0.715 JET TEMP (K) = 368.3  
 LINK = 5 LINK TEMP (K) = 303.51 JET VELOCITY (M/S) = 0.715 JET TEMP (K) = 368.3  
 LINK = 6 LINK TEMP (K) = 302.98 JET VELOCITY (M/S) = 0.715 JET TEMP (K) = 368.3  
 LINK = 7 LINK TEMP (K) = 309.53 JET VELOCITY (M/S) = 0.715 JET TEMP (K) = 368.3  
 LINK = 8 LINK TEMP (K) = 304.62 JET VELOCITY (M/S) = 0.715 JET TEMP (K) = 368.3  
 LINK = 9 LINK TEMP (K) = 302.17 JET VELOCITY (M/S) = 0.743 JET TEMP (K) = 393.3  
 R (M) = 0.00 TSL (K) = 396.5 QB (W/M2) = 0.460E+04 QT (W/M2) = -0.143E-10  
 R (M) = 1.97 TSL (K) = 321.5 QB (W/M2) = 0.132E+04 QT (W/M2) = -0.231E-11  
 R (M) = 3.93 TSL (K) = 305.7 QB (W/M2) = 0.545E+03 QT (W/M2) = -0.308E-12  
 R (M) = 5.90 TSL (K) = 301.1 QB (W/M2) = 0.313E+03 QT (W/M2) = 0.167E-13  
 R (M) = 7.86 TSL (K) = 299.2 QB (W/M2) = 0.214E+03 QT (W/M2) = 0.167E-13  
 R (M) = 9.83 TSL (K) = 295.5 QB (W/M2) = 0.159E+02 QT (W/M2) = 0.167E-13  
 TIME (S)= 50.0000 LVR TEMP (K)= 362.8 LVR HT (M) = 1.89 LVR MASS (KG)=0.776E+02  
 FIRE OUTPUT (W) = 0.2900E+06 VENT AREA (M2) = 0.00  
 LINK = 1 LINK TEMP (K) = 337.78 JET VELOCITY (M/S) = 0.724 JET TEMP (K) = 370.7  
 LINK = 2 LINK TEMP (K) = 329.64 JET VELOCITY (M/S) = 0.724 JET TEMP (K) = 370.7  
 LINK = 3 LINK TEMP (K) = 343.37 JET VELOCITY (M/S) = 0.724 JET TEMP (K) = 370.7  
 LINK = 4 LINK TEMP (K) = 323.69 JET VELOCITY (M/S) = 0.724 JET TEMP (K) = 370.7  
 LINK = 5 LINK TEMP (K) = 305.85 JET VELOCITY (M/S) = 0.724 JET TEMP (K) = 370.7  
 LINK = 6 LINK TEMP (K) = 305.18 JET VELOCITY (M/S) = 0.724 JET TEMP (K) = 370.7  
 LINK = 7 LINK TEMP (K) = 313.33 JET VELOCITY (M/S) = 0.724 JET TEMP (K) = 370.7  
 LINK = 8 LINK TEMP (K) = 307.24 JET VELOCITY (M/S) = 0.724 JET TEMP (K) = 370.7  
 LINK = 9 LINK TEMP (K) = 304.15 JET VELOCITY (M/S) = 0.753 JET TEMP (K) = 395.8  
 R (M) = 0.00 TSL (K) = 403.9 QB (W/M2) = 0.435E+04 QT (W/M2) = -0.110E-08

R (M) = 1.97 TSL (K) = 324.5 QB (W/M2) = 0.130E+04 QT (W/M2) = -0.207E-09  
 R (M) = 3.93 TSL (K) = 307.0 QB (W/M2) = 0.544E+03 QT (W/M2) = -0.610E-10  
 R (M) = 5.90 TSL (K) = 301.9 QB (W/M2) = 0.315E+03 QT (W/M2) = -0.331E-10  
 R (M) = 7.86 TSL (K) = 299.7 QB (W/M2) = 0.216E+03 QT (W/M2) = -0.216E-10  
 R (M) = 9.83 TSL (K) = 295.5 QB (W/M2) = 0.157E+02 QT (W/M2) = -0.166E-11  
 TIME (S)= 60.0000 LVR TEMP (K)= 364.6 LVR HT (M) = 1.81 LVR MASS (KG)=0.907E+02  
 FIRE OUTPUT (W) = 0.2900E+06 VENT AREA (M2) = 0.00  
 LINK = 1 LINK TEMP (K) = 344.03 JET VELOCITY (M/S) = 0.733 JET TEMP (K) = 372.9  
 LINK = 2 LINK TEMP (K) = 335.42 JET VELOCITY (M/S) = 0.733 JET TEMP (K) = 372.9  
 LINK = 3 LINK TEMP (K) = 349.68 JET VELOCITY (M/S) = 0.733 JET TEMP (K) = 372.9  
 LINK = 4 LINK TEMP (K) = 328.88 JET VELOCITY (M/S) = 0.733 JET TEMP (K) = 372.9  
 LINK = 5 LINK TEMP (K) = 308.21 JET VELOCITY (M/S) = 0.733 JET TEMP (K) = 372.9  
 LINK = 6 LINK TEMP (K) = 307.40 JET VELOCITY (M/S) = 0.733 JET TEMP (K) = 372.9  
 LINK = 7 LINK TEMP (K) = 317.05 JET VELOCITY (M/S) = 0.733 JET TEMP (K) = 372.9  
 LINK = 8 LINK TEMP (K) = 309.87 JET VELOCITY (M/S) = 0.733 JET TEMP (K) = 372.9  
 LINK = 9 LINK TEMP (K) = 306.15 JET VELOCITY (M/S) = 0.762 JET TEMP (K) = 398.2  
 TIME LINK 1 OPENS EQUALS 56.0000 (S)  
 TIME LINK 3 OPENS EQUALS 56.0000 (S)  
 R (M) = 0.00 TSL (K) = 410.0 QB (W/M2) = 0.415E+04 QT (W/M2) = -0.323E-07  
 R (M) = 1.97 TSL (K) = 327.0 QB (W/M2) = 0.129E+04 QT (W/M2) = -0.523E-08  
 R (M) = 3.93 TSL (K) = 308.2 QB (W/M2) = 0.543E+03 QT (W/M2) = -0.191E-08  
 R (M) = 5.90 TSL (K) = 302.6 QB (W/M2) = 0.317E+03 QT (W/M2) = -0.104E-08  
 R (M) = 7.86 TSL (K) = 300.2 QB (W/M2) = 0.218E+03 QT (W/M2) = -0.689E-09  
 R (M) = 9.83 TSL (K) = 295.5 QB (W/M2) = 0.155E+02 QT (W/M2) = -0.594E-10  
 TIME (S)= 70.0000 LVR TEMP (K)= 366.4 LVR HT (M) = 1.73 LVR MASS (KG)=0.103E+03  
 FIRE OUTPUT (W) = 0.2900E+06 VENT AREA (M2) = 0.00  
 LINK = 1 LINK TEMP (K) = 349.55 JET VELOCITY (M/S) = 0.741 JET TEMP (K) = 374.9  
 LINK = 2 LINK TEMP (K) = 340.73 JET VELOCITY (M/S) = 0.741 JET TEMP (K) = 374.9  
 LINK = 3 LINK TEMP (K) = 355.08 JET VELOCITY (M/S) = 0.741 JET TEMP (K) = 374.9  
 LINK = 4 LINK TEMP (K) = 333.76 JET VELOCITY (M/S) = 0.741 JET TEMP (K) = 374.9  
 LINK = 5 LINK TEMP (K) = 310.57 JET VELOCITY (M/S) = 0.741 JET TEMP (K) = 374.9  
 LINK = 6 LINK TEMP (K) = 309.63 JET VELOCITY (M/S) = 0.741 JET TEMP (K) = 374.9  
 LINK = 7 LINK TEMP (K) = 320.69 JET VELOCITY (M/S) = 0.741 JET TEMP (K) = 374.9  
 LINK = 8 LINK TEMP (K) = 312.49 JET VELOCITY (M/S) = 0.741 JET TEMP (K) = 374.9  
 LINK = 9 LINK TEMP (K) = 308.16 JET VELOCITY (M/S) = 0.771 JET TEMP (K) = 400.5  
 TIME LINK 1 OPENS EQUALS 56.0000 (S)  
 TIME LINK 3 OPENS EQUALS 56.0000 (S)  
 R (M) = 0.00 TSL (K) = 415.3 QB (W/M2) = 0.399E+04 QT (W/M2) = -0.477E-06  
 R (M) = 1.97 TSL (K) = 329.4 QB (W/M2) = 0.127E+04 QT (W/M2) = -0.942E-07  
 R (M) = 3.93 TSL (K) = 309.3 QB (W/M2) = 0.544E+03 QT (W/M2) = -0.299E-07  
 R (M) = 5.90 TSL (K) = 303.3 QB (W/M2) = 0.319E+03 QT (W/M2) = -0.163E-07  
 R (M) = 7.86 TSL (K) = 300.7 QB (W/M2) = 0.220E+03 QT (W/M2) = -0.108E-07  
 R (M) = 9.83 TSL (K) = 295.6 QB (W/M2) = 0.153E+02 QT (W/M2) = -0.935E-09  
 TIME (S)= 80.0000 LVR TEMP (K)= 368.1 LVR HT (M) = 1.65 LVR MASS (KG)=0.115E+03  
 FIRE OUTPUT (W) = 0.2900E+06 VENT AREA (M2) = 0.00  
 LINK = 1 LINK TEMP (K) = 354.45 JET VELOCITY (M/S) = 0.750 JET TEMP (K) = 376.9  
 LINK = 2 LINK TEMP (K) = 345.61 JET VELOCITY (M/S) = 0.750 JET TEMP (K) = 376.9  
 LINK = 3 LINK TEMP (K) = 359.75 JET VELOCITY (M/S) = 0.750 JET TEMP (K) = 376.9  
 LINK = 4 LINK TEMP (K) = 338.36 JET VELOCITY (M/S) = 0.750 JET TEMP (K) = 376.9  
 LINK = 5 LINK TEMP (K) = 312.93 JET VELOCITY (M/S) = 0.750 JET TEMP (K) = 376.9  
 LINK = 6 LINK TEMP (K) = 311.86 JET VELOCITY (M/S) = 0.750 JET TEMP (K) = 376.9  
 LINK = 7 LINK TEMP (K) = 324.25 JET VELOCITY (M/S) = 0.750 JET TEMP (K) = 376.9  
 LINK = 8 LINK TEMP (K) = 315.10 JET VELOCITY (M/S) = 0.750 JET TEMP (K) = 376.9  
 LINK = 9 LINK TEMP (K) = 310.20 JET VELOCITY (M/S) = 0.780 JET TEMP (K) = 402.6  
 TIME LINK 1 OPENS EQUALS 56.0000 (S)  
 TIME LINK 2 OPENS EQUALS 72.0000 (S)  
 TIME LINK 3 OPENS EQUALS 56.0000 (S)  
 R (M) = 0.00 TSL (K) = 420.0 QB (W/M2) = 0.385E+04 QT (W/M2) = -0.423E-05  
 R (M) = 1.97 TSL (K) = 331.5 QB (W/M2) = 0.126E+04 QT (W/M2) = -0.754E-06  
 R (M) = 3.93 TSL (K) = 310.3 QB (W/M2) = 0.544E+03 QT (W/M2) = -0.279E-06  
 R (M) = 5.90 TSL (K) = 303.9 QB (W/M2) = 0.321E+03 QT (W/M2) = -0.153E-06  
 R (M) = 7.86 TSL (K) = 301.2 QB (W/M2) = 0.222E+03 QT (W/M2) = -0.101E-06  
 R (M) = 9.83 TSL (K) = 295.6 QB (W/M2) = 0.152E+02 QT (W/M2) = -0.869E-08  
 TIME (S)= 90.0000 LVR TEMP (K)= 369.7 LVR HT (M) = 1.58 LVR MASS (KG)=0.126E+03  
 FIRE OUTPUT (W) = 0.2900E+06 VENT AREA (M2) = 0.00  
 LINK = 1 LINK TEMP (K) = 358.81 JET VELOCITY (M/S) = 0.758 JET TEMP (K) = 378.8  
 LINK = 2 LINK TEMP (K) = 350.10 JET VELOCITY (M/S) = 0.758 JET TEMP (K) = 378.8

LINK = 3 LINK TEMP (K) = 363.83 JET VELOCITY (M/S) = 0.758 JET TEMP (K) = 378.8  
 LINK = 4 LINK TEMP (K) = 342.69 JET VELOCITY (M/S) = 0.758 JET TEMP (K) = 378.8  
 LINK = 5 LINK TEMP (K) = 315.28 JET VELOCITY (M/S) = 0.758 JET TEMP (K) = 378.8  
 LINK = 6 LINK TEMP (K) = 314.10 JET VELOCITY (M/S) = 0.758 JET TEMP (K) = 378.8  
 LINK = 7 LINK TEMP (K) = 327.72 JET VELOCITY (M/S) = 0.758 JET TEMP (K) = 378.8  
 LINK = 8 LINK TEMP (K) = 317.70 JET VELOCITY (M/S) = 0.758 JET TEMP (K) = 378.8  
 LINK = 9 LINK TEMP (K) = 312.24 JET VELOCITY (M/S) = 0.788 JET TEMP (K) = 404.8  
 TIME LINK 1 OPENS EQUALS 56.0000 (S)  
 TIME LINK 2 OPENS EQUALS 72.0000 (S)  
 TIME LINK 3 OPENS EQUALS 56.0000 (S)  
 R (M) = 0.00 TSL (K) = 424.2 QB (W/M2) = 0.373E+04 QT (W/M2) = -0.254E-04  
 R (M) = 1.97 TSL (K) = 333.5 QB (W/M2) = 0.125E+04 QT (W/M2) = -0.521E-05  
 R (M) = 3.93 TSL (K) = 311.3 QB (W/M2) = 0.545E+03 QT (W/M2) = -0.175E-05  
 R (M) = 5.90 TSL (K) = 304.5 QB (W/M2) = 0.323E+03 QT (W/M2) = -0.959E-06  
 R (M) = 7.86 TSL (K) = 301.6 QB (W/M2) = 0.225E+03 QT (W/M2) = -0.637E-06  
 R (M) = 9.83 TSL (K) = 295.6 QB (W/M2) = 0.150E+02 QT (W/M2) = -0.542E-07  
 TIME (S)= 100.0000 LTR TEMP (K)= 371.3 LTR HT (M) = 1.52 LTR MASS (KG)=0.136E+03  
 FIRE OUTPUT (W) = 0.2900E+06 VENT AREA (M2) = 0.00  
 LINK = 1 LINK TEMP (K) = 362.73 JET VELOCITY (M/S) = 0.766 JET TEMP (K) = 380.6  
 LINK = 2 LINK TEMP (K) = 354.24 JET VELOCITY (M/S) = 0.766 JET TEMP (K) = 380.6  
 LINK = 3 LINK TEMP (K) = 367.42 JET VELOCITY (M/S) = 0.766 JET TEMP (K) = 380.6  
 LINK = 4 LINK TEMP (K) = 346.77 JET VELOCITY (M/S) = 0.766 JET TEMP (K) = 380.6  
 LINK = 5 LINK TEMP (K) = 317.63 JET VELOCITY (M/S) = 0.766 JET TEMP (K) = 380.6  
 LINK = 6 LINK TEMP (K) = 316.33 JET VELOCITY (M/S) = 0.766 JET TEMP (K) = 380.6  
 LINK = 7 LINK TEMP (K) = 331.10 JET VELOCITY (M/S) = 0.766 JET TEMP (K) = 380.6  
 LINK = 8 LINK TEMP (K) = 320.28 JET VELOCITY (M/S) = 0.766 JET TEMP (K) = 380.6  
 LINK = 9 LINK TEMP (K) = 314.30 JET VELOCITY (M/S) = 0.797 JET TEMP (K) = 406.8  
 TIME LINK 1 OPENS EQUALS 56.0000 (S)  
 TIME LINK 2 OPENS EQUALS 72.0000 (S)  
 TIME LINK 3 OPENS EQUALS 56.0000 (S)  
 R (M) = 0.00 TSL (K) = 428.0 QB (W/M2) = 0.363E+04 QT (W/M2) = -0.113E-03  
 R (M) = 1.97 TSL (K) = 335.4 QB (W/M2) = 0.124E+04 QT (W/M2) = -0.216E-04  
 R (M) = 3.93 TSL (K) = 312.2 QB (W/M2) = 0.546E+03 QT (W/M2) = -0.809E-05  
 R (M) = 5.90 TSL (K) = 305.1 QB (W/M2) = 0.326E+03 QT (W/M2) = -0.445E-05  
 R (M) = 7.86 TSL (K) = 302.0 QB (W/M2) = 0.227E+03 QT (W/M2) = -0.296E-05  
 R (M) = 9.83 TSL (K) = 295.6 QB (W/M2) = 0.149E+02 QT (W/M2) = -0.250E-06  
 TIME (S)= 110.0000 LTR TEMP (K)= 372.9 LTR HT (M) = 1.45 LTR MASS (KG)=0.146E+03  
 FIRE OUTPUT (W) = 0.2900E+06 VENT AREA (M2) = 0.00  
 LINK = 1 LINK TEMP (K) = 366.25 JET VELOCITY (M/S) = 0.774 JET TEMP (K) = 382.3  
 LINK = 2 LINK TEMP (K) = 358.07 JET VELOCITY (M/S) = 0.774 JET TEMP (K) = 382.3  
 LINK = 3 LINK TEMP (K) = 370.61 JET VELOCITY (M/S) = 0.774 JET TEMP (K) = 382.3  
 LINK = 4 LINK TEMP (K) = 350.61 JET VELOCITY (M/S) = 0.774 JET TEMP (K) = 382.3  
 LINK = 5 LINK TEMP (K) = 319.98 JET VELOCITY (M/S) = 0.774 JET TEMP (K) = 382.3  
 LINK = 6 LINK TEMP (K) = 318.56 JET VELOCITY (M/S) = 0.774 JET TEMP (K) = 382.3  
 LINK = 7 LINK TEMP (K) = 334.39 JET VELOCITY (M/S) = 0.774 JET TEMP (K) = 382.3  
 LINK = 8 LINK TEMP (K) = 322.83 JET VELOCITY (M/S) = 0.774 JET TEMP (K) = 382.3  
 LINK = 9 LINK TEMP (K) = 316.37 JET VELOCITY (M/S) = 0.805 JET TEMP (K) = 408.7  
 TIME LINK 1 OPENS EQUALS 56.0000 (S)  
 TIME LINK 2 OPENS EQUALS 72.0000 (S)  
 TIME LINK 3 OPENS EQUALS 56.0000 (S)  
 TIME LINK 4 OPENS EQUALS 100.9968 (S)  
 R (M) = 0.00 TSL (K) = 431.4 QB (W/M2) = 0.351E+04 QT (W/M2) = -0.399E-03  
 R (M) = 1.97 TSL (K) = 337.1 QB (W/M2) = 0.123E+04 QT (W/M2) = -0.849E-04  
 R (M) = 3.93 TSL (K) = 313.0 QB (W/M2) = 0.547E+03 QT (W/M2) = -0.295E-04  
 R (M) = 5.90 TSL (K) = 305.6 QB (W/M2) = 0.328E+03 QT (W/M2) = -0.163E-04  
 R (M) = 7.86 TSL (K) = 302.4 QB (W/M2) = 0.229E+03 QT (W/M2) = -0.108E-04  
 R (M) = 9.83 TSL (K) = 295.7 QB (W/M2) = 0.148E+02 QT (W/M2) = -0.909E-06  
 TIME (S)= 120.0000 LTR TEMP (K)= 374.4 LTR HT (M) = 1.39 LTR MASS (KG)=0.156E+03  
 FIRE OUTPUT (W) = 0.2900E+06 VENT AREA (M2) = 0.00  
 LINK = 1 LINK TEMP (K) = 369.44 JET VELOCITY (M/S) = 0.782 JET TEMP (K) = 383.9  
 LINK = 2 LINK TEMP (K) = 361.60 JET VELOCITY (M/S) = 0.782 JET TEMP (K) = 383.9  
 LINK = 3 LINK TEMP (K) = 373.45 JET VELOCITY (M/S) = 0.782 JET TEMP (K) = 383.9  
 LINK = 4 LINK TEMP (K) = 354.22 JET VELOCITY (M/S) = 0.782 JET TEMP (K) = 383.9  
 LINK = 5 LINK TEMP (K) = 322.30 JET VELOCITY (M/S) = 0.782 JET TEMP (K) = 383.9  
 LINK = 6 LINK TEMP (K) = 320.78 JET VELOCITY (M/S) = 0.782 JET TEMP (K) = 383.9  
 LINK = 7 LINK TEMP (K) = 337.59 JET VELOCITY (M/S) = 0.782 JET TEMP (K) = 383.9  
 LINK = 8 LINK TEMP (K) = 325.36 JET VELOCITY (M/S) = 0.782 JET TEMP (K) = 383.9

LINK = 9 LINK TEMP (K) = 318.44 JET VELOCITY (M/S) = 0.813 JET TEMP (K) = 410.5  
 TIME LINK 1 OPENS EQUALS 56.0000 (S)  
 TIME LINK 2 OPENS EQUALS 72.0000 (S)  
 TIME LINK 3 OPENS EQUALS 56.0000 (S)  
 TIME LINK 4 OPENS EQUALS 100.9968 (S)  
 R (M) = 0.00 TSL (K) = 434.3 QB (W/M2) = 0.341E+04 QT (W/M2) = -0.117E-02  
 R (M) = 1.97 TSL (K) = 338.8 QB (W/M2) = 0.122E+04 QT (W/M2) = -0.237E-03  
 R (M) = 3.93 TSL (K) = 313.9 QB (W/M2) = 0.548E+03 QT (W/M2) = -0.895E-04  
 R (M) = 5.90 TSL (K) = 306.2 QB (W/M2) = 0.330E+03 QT (W/M2) = -0.494E-04  
 R (M) = 7.86 TSL (K) = 302.8 QB (W/M2) = 0.231E+03 QT (W/M2) = -0.329E-04  
 R (M) = 9.83 TSL (K) = 295.7 QB (W/M2) = 0.147E+02 QT (W/M2) = -0.274E-05  
 TIME (S)= 130.0000 LYR TEMP (K)= 375.9 LYR HT (M) = 1.33 LYR MASS (KG)=0.165E+03  
 FIRE OUTPUT (W) = 0.2900E+06 VENT AREA (M2) = 0.00  
 LINK = 1 LINK TEMP (K) = 372.33 JET VELOCITY (M/S) = 0.789 JET TEMP (K) = 385.4  
 LINK = 2 LINK TEMP (K) = 364.88 JET VELOCITY (M/S) = 0.789 JET TEMP (K) = 385.4  
 LINK = 3 LINK TEMP (K) = 376.03 JET VELOCITY (M/S) = 0.789 JET TEMP (K) = 385.4  
 LINK = 4 LINK TEMP (K) = 357.62 JET VELOCITY (M/S) = 0.789 JET TEMP (K) = 385.4  
 LINK = 5 LINK TEMP (K) = 324.61 JET VELOCITY (M/S) = 0.789 JET TEMP (K) = 385.4  
 LINK = 6 LINK TEMP (K) = 322.99 JET VELOCITY (M/S) = 0.789 JET TEMP (K) = 385.4  
 LINK = 7 LINK TEMP (K) = 340.69 JET VELOCITY (M/S) = 0.789 JET TEMP (K) = 385.4  
 LINK = 8 LINK TEMP (K) = 327.87 JET VELOCITY (M/S) = 0.789 JET TEMP (K) = 385.4  
 LINK = 9 LINK TEMP (K) = 320.52 JET VELOCITY (M/S) = 0.821 JET TEMP (K) = 412.3  
 TIME LINK 1 OPENS EQUALS 56.0000 (S)  
 TIME LINK 2 OPENS EQUALS 72.0000 (S)  
 TIME LINK 3 OPENS EQUALS 56.0000 (S)  
 TIME LINK 4 OPENS EQUALS 100.9968 (S)  
 R (M) = 0.00 TSL (K) = 437.0 QB (W/M2) = 0.333E+04 QT (W/M2) = -0.297E-02  
 R (M) = 1.97 TSL (K) = 340.4 QB (W/M2) = 0.121E+04 QT (W/M2) = -0.614E-03  
 R (M) = 3.93 TSL (K) = 314.7 QB (W/M2) = 0.549E+03 QT (W/M2) = -0.233E-03  
 R (M) = 5.90 TSL (K) = 306.7 QB (W/M2) = 0.332E+03 QT (W/M2) = -0.129E-03  
 R (M) = 7.86 TSL (K) = 303.1 QB (W/M2) = 0.233E+03 QT (W/M2) = -0.860E-04  
 R (M) = 9.83 TSL (K) = 295.7 QB (W/M2) = 0.146E+02 QT (W/M2) = -0.710E-05  
 TIME (S)= 140.0000 LYR TEMP (K)= 377.4 LYR HT (M) = 1.27 LYR MASS (KG)=0.174E+03  
 FIRE OUTPUT (W) = 0.2900E+06 VENT AREA (M2) = 0.00  
 LINK = 1 LINK TEMP (K) = 374.98 JET VELOCITY (M/S) = 0.796 JET TEMP (K) = 387.0  
 LINK = 2 LINK TEMP (K) = 367.92 JET VELOCITY (M/S) = 0.796 JET TEMP (K) = 387.0  
 LINK = 3 LINK TEMP (K) = 378.38 JET VELOCITY (M/S) = 0.796 JET TEMP (K) = 387.0  
 LINK = 4 LINK TEMP (K) = 360.83 JET VELOCITY (M/S) = 0.796 JET TEMP (K) = 387.0  
 LINK = 5 LINK TEMP (K) = 326.90 JET VELOCITY (M/S) = 0.796 JET TEMP (K) = 387.0  
 LINK = 6 LINK TEMP (K) = 325.19 JET VELOCITY (M/S) = 0.796 JET TEMP (K) = 387.0  
 LINK = 7 LINK TEMP (K) = 343.71 JET VELOCITY (M/S) = 0.796 JET TEMP (K) = 387.0  
 LINK = 8 LINK TEMP (K) = 330.34 JET VELOCITY (M/S) = 0.796 JET TEMP (K) = 387.0  
 LINK = 9 LINK TEMP (K) = 322.60 JET VELOCITY (M/S) = 0.829 JET TEMP (K) = 414.1  
 TIME LINK 1 OPENS EQUALS 56.0000 (S)  
 TIME LINK 2 OPENS EQUALS 72.0000 (S)  
 TIME LINK 3 OPENS EQUALS 56.0000 (S)  
 TIME LINK 4 OPENS EQUALS 100.9968 (S)  
 R (M) = 0.00 TSL (K) = 439.6 QB (W/M2) = 0.326E+04 QT (W/M2) = -0.669E-02  
 R (M) = 1.97 TSL (K) = 341.9 QB (W/M2) = 0.121E+04 QT (W/M2) = -0.141E-02  
 R (M) = 3.93 TSL (K) = 315.4 QB (W/M2) = 0.550E+03 QT (W/M2) = -0.538E-03  
 R (M) = 5.90 TSL (K) = 307.2 QB (W/M2) = 0.334E+03 QT (W/M2) = -0.298E-03  
 R (M) = 7.86 TSL (K) = 303.5 QB (W/M2) = 0.235E+03 QT (W/M2) = -0.199E-03  
 R (M) = 9.83 TSL (K) = 295.7 QB (W/M2) = 0.145E+02 QT (W/M2) = -0.163E-04  
 TIME (S)= 150.0000 LYR TEMP (K)= 378.8 LYR HT (M) = 1.22 LYR MASS (KG)=0.182E+03  
 FIRE OUTPUT (W) = 0.2900E+06 VENT AREA (M2) = 0.00  
 LINK = 1 LINK TEMP (K) = 377.44 JET VELOCITY (M/S) = 0.803 JET TEMP (K) = 388.5  
 LINK = 2 LINK TEMP (K) = 370.77 JET VELOCITY (M/S) = 0.803 JET TEMP (K) = 388.5  
 LINK = 3 LINK TEMP (K) = 380.55 JET VELOCITY (M/S) = 0.803 JET TEMP (K) = 388.5  
 LINK = 4 LINK TEMP (K) = 363.87 JET VELOCITY (M/S) = 0.803 JET TEMP (K) = 388.5  
 LINK = 5 LINK TEMP (K) = 329.18 JET VELOCITY (M/S) = 0.803 JET TEMP (K) = 388.5  
 LINK = 6 LINK TEMP (K) = 327.37 JET VELOCITY (M/S) = 0.803 JET TEMP (K) = 388.5  
 LINK = 7 LINK TEMP (K) = 346.65 JET VELOCITY (M/S) = 0.803 JET TEMP (K) = 388.5  
 LINK = 8 LINK TEMP (K) = 332.79 JET VELOCITY (M/S) = 0.803 JET TEMP (K) = 388.5  
 LINK = 9 LINK TEMP (K) = 324.69 JET VELOCITY (M/S) = 0.836 JET TEMP (K) = 415.9  
 TIME LINK 1 OPENS EQUALS 56.0000 (S)  
 TIME LINK 2 OPENS EQUALS 72.0000 (S)  
 TIME LINK 3 OPENS EQUALS 56.0000 (S)

TIME LINK 4 OPENS EQUALS 100.9968 (S)  
 R (M) = 0.00 TSL (K) = 442.1 QB (W/M2) = 0.320E+04 QT (W/M2) = -0.137E-01  
 R (M) = 1.97 TSL (K) = 343.3 QB (W/M2) = 0.120E+04 QT (W/M2) = -0.308E-02  
 R (M) = 3.93 TSL (K) = 316.2 QB (W/M2) = 0.551E+03 QT (W/M2) = -0.112E-02  
 R (M) = 5.90 TSL (K) = 307.6 QB (W/M2) = 0.336E+03 QT (W/M2) = -0.623E-03  
 R (M) = 7.86 TSL (K) = 303.8 QB (W/M2) = 0.237E+03 QT (W/M2) = -0.417E-03  
 R (M) = 9.83 TSL (K) = 295.7 QB (W/M2) = 0.144E+02 QT (W/M2) = -0.339E-04  
 TIME (S)= 160.0000 LTR TEMP (K)= 380.2 LTR HT (M) = 1.16 LTR MASS (KG)=0.190E+03  
 FIRE OUTPUT (W) = 0.2900E+06 VENT AREA (M2) = 0.00  
 LINK = 1 LINK TEMP (K) = 379.72 JET VELOCITY (M/S) = 0.810 JET TEMP (K) = 390.1  
 LINK = 2 LINK TEMP (K) = 373.43 JET VELOCITY (M/S) = 0.810 JET TEMP (K) = 390.1  
 LINK = 3 LINK TEMP (K) = 382.59 JET VELOCITY (M/S) = 0.810 JET TEMP (K) = 390.1  
 LINK = 4 LINK TEMP (K) = 366.75 JET VELOCITY (M/S) = 0.810 JET TEMP (K) = 390.1  
 LINK = 5 LINK TEMP (K) = 331.44 JET VELOCITY (M/S) = 0.810 JET TEMP (K) = 390.1  
 LINK = 6 LINK TEMP (K) = 329.54 JET VELOCITY (M/S) = 0.810 JET TEMP (K) = 390.1  
 LINK = 7 LINK TEMP (K) = 349.50 JET VELOCITY (M/S) = 0.810 JET TEMP (K) = 390.1  
 LINK = 8 LINK TEMP (K) = 335.20 JET VELOCITY (M/S) = 0.810 JET TEMP (K) = 390.1  
 LINK = 9 LINK TEMP (K) = 326.77 JET VELOCITY (M/S) = 0.843 JET TEMP (K) = 417.7  
 TIME LINK 1 OPENS EQUALS 56.0000 (S)  
 TIME LINK 2 OPENS EQUALS 72.0000 (S)  
 TIME LINK 3 OPENS EQUALS 56.0000 (S)  
 TIME LINK 4 OPENS EQUALS 100.9968 (S)  
 TIME LINK 7 OPENS EQUALS 152.0000 (S)  
 R (M) = 0.00 TSL (K) = 444.5 QB (W/M2) = 0.315E+04 QT (W/M2) = -0.258E-01  
 R (M) = 1.97 TSL (K) = 344.7 QB (W/M2) = 0.120E+04 QT (W/M2) = -0.563E-02  
 R (M) = 3.93 TSL (K) = 316.9 QB (W/M2) = 0.553E+03 QT (W/M2) = -0.216E-02  
 R (M) = 5.90 TSL (K) = 308.1 QB (W/M2) = 0.338E+03 QT (W/M2) = -0.120E-02  
 R (M) = 7.86 TSL (K) = 304.2 QB (W/M2) = 0.239E+03 QT (W/M2) = -0.802E-03  
 R (M) = 9.83 TSL (K) = 295.7 QB (W/M2) = 0.143E+02 QT (W/M2) = -0.647E-04  
 TIME (S)= 170.0000 LTR TEMP (K)= 381.6 LTR HT (M) = 1.11 LTR MASS (KG)=0.197E+03  
 FIRE OUTPUT (W) = 0.2900E+06 VENT AREA (M2) = 0.00  
 LINK = 1 LINK TEMP (K) = 381.87 JET VELOCITY (M/S) = 0.816 JET TEMP (K) = 391.6  
 LINK = 2 LINK TEMP (K) = 375.95 JET VELOCITY (M/S) = 0.816 JET TEMP (K) = 391.6  
 LINK = 3 LINK TEMP (K) = 384.51 JET VELOCITY (M/S) = 0.816 JET TEMP (K) = 391.6  
 LINK = 4 LINK TEMP (K) = 369.49 JET VELOCITY (M/S) = 0.816 JET TEMP (K) = 391.6  
 LINK = 5 LINK TEMP (K) = 333.67 JET VELOCITY (M/S) = 0.816 JET TEMP (K) = 391.6  
 LINK = 6 LINK TEMP (K) = 331.69 JET VELOCITY (M/S) = 0.816 JET TEMP (K) = 391.6  
 LINK = 7 LINK TEMP (K) = 352.27 JET VELOCITY (M/S) = 0.816 JET TEMP (K) = 391.6  
 LINK = 8 LINK TEMP (K) = 337.59 JET VELOCITY (M/S) = 0.816 JET TEMP (K) = 391.6  
 LINK = 9 LINK TEMP (K) = 328.86 JET VELOCITY (M/S) = 0.849 JET TEMP (K) = 419.5  
 TIME LINK 1 OPENS EQUALS 56.0000 (S)  
 TIME LINK 2 OPENS EQUALS 72.0000 (S)  
 TIME LINK 3 OPENS EQUALS 56.0000 (S)  
 TIME LINK 4 OPENS EQUALS 100.9968 (S)  
 TIME LINK 7 OPENS EQUALS 152.0000 (S)  
 R (M) = 0.00 TSL (K) = 446.8 QB (W/M2) = 0.311E+04 QT (W/M2) = -0.438E-01  
 R (M) = 1.97 TSL (K) = 346.1 QB (W/M2) = 0.119E+04 QT (W/M2) = -0.101E-01  
 R (M) = 3.93 TSL (K) = 317.6 QB (W/M2) = 0.555E+03 QT (W/M2) = -0.387E-02  
 R (M) = 5.90 TSL (K) = 308.6 QB (W/M2) = 0.340E+03 QT (W/M2) = -0.215E-02  
 R (M) = 7.86 TSL (K) = 304.5 QB (W/M2) = 0.241E+03 QT (W/M2) = -0.144E-02  
 R (M) = 9.83 TSL (K) = 295.8 QB (W/M2) = 0.142E+02 QT (W/M2) = -0.115E-03  
 TIME (S)= 180.0000 LTR TEMP (K)= 383.0 LTR HT (M) = 1.06 LTR MASS (KG)=0.204E+03  
 FIRE OUTPUT (W) = 0.2900E+06 VENT AREA (M2) = 0.00  
 LINK = 1 LINK TEMP (K) = 383.90 JET VELOCITY (M/S) = 0.822 JET TEMP (K) = 393.1  
 LINK = 2 LINK TEMP (K) = 378.32 JET VELOCITY (M/S) = 0.822 JET TEMP (K) = 393.1  
 LINK = 3 LINK TEMP (K) = 386.35 JET VELOCITY (M/S) = 0.822 JET TEMP (K) = 393.1  
 LINK = 4 LINK TEMP (K) = 372.09 JET VELOCITY (M/S) = 0.822 JET TEMP (K) = 393.1  
 LINK = 5 LINK TEMP (K) = 335.89 JET VELOCITY (M/S) = 0.822 JET TEMP (K) = 393.1  
 LINK = 6 LINK TEMP (K) = 333.83 JET VELOCITY (M/S) = 0.822 JET TEMP (K) = 393.1  
 LINK = 7 LINK TEMP (K) = 354.97 JET VELOCITY (M/S) = 0.822 JET TEMP (K) = 393.1  
 LINK = 8 LINK TEMP (K) = 339.95 JET VELOCITY (M/S) = 0.822 JET TEMP (K) = 393.1  
 LINK = 9 LINK TEMP (K) = 330.95 JET VELOCITY (M/S) = 0.855 JET TEMP (K) = 421.2  
 TIME LINK 1 OPENS EQUALS 56.0000 (S)  
 TIME LINK 2 OPENS EQUALS 72.0000 (S)  
 TIME LINK 3 OPENS EQUALS 56.0000 (S)  
 TIME LINK 4 OPENS EQUALS 100.9968 (S)  
 TIME LINK 7 OPENS EQUALS 152.0000 (S)



R (M) = 0.00 TSL (K) = 449.1 QB (W/M2) = 0.308E+04 QT (W/M2) = -0.732E-01  
 R (M) = 1.97 TSL (K) = 347.4 QB (W/M2) = 0.119E+04 QT (W/M2) = -0.170E-01  
 R (M) = 3.93 TSL (K) = 318.3 QB (W/M2) = 0.556E+03 QT (W/M2) = -0.655E-02  
 R (M) = 5.90 TSL (K) = 309.0 QB (W/M2) = 0.343E+03 QT (W/M2) = -0.365E-02  
 R (M) = 7.86 TSL (K) = 304.9 QB (W/M2) = 0.243E+03 QT (W/M2) = -0.244E-02  
 R (M) = 9.83 TSL (K) = 295.8 QB (W/M2) = 0.141E+02 QT (W/M2) = -0.194E-03  
 TIME (S)= 190.0000 LVR TEMP (K)= 384.3 LVR HT (M) = 1.01 LVR MASS (KG)=0.211E+03  
 FIRE OUTPUT (W) = 0.2900E+06 VENT AREA (M2) = 0.00  
 LINK = 1 LINK TEMP (K) = 385.84 JET VELOCITY (M/S) = 0.827 JET TEMP (K) = 394.6  
 LINK = 2 LINK TEMP (K) = 380.58 JET VELOCITY (M/S) = 0.827 JET TEMP (K) = 394.6  
 LINK = 3 LINK TEMP (K) = 388.12 JET VELOCITY (M/S) = 0.827 JET TEMP (K) = 394.6  
 LINK = 4 LINK TEMP (K) = 374.59 JET VELOCITY (M/S) = 0.827 JET TEMP (K) = 394.6  
 LINK = 5 LINK TEMP (K) = 338.09 JET VELOCITY (M/S) = 0.827 JET TEMP (K) = 394.6  
 LINK = 6 LINK TEMP (K) = 335.96 JET VELOCITY (M/S) = 0.827 JET TEMP (K) = 394.6  
 LINK = 7 LINK TEMP (K) = 357.60 JET VELOCITY (M/S) = 0.827 JET TEMP (K) = 394.6  
 LINK = 8 LINK TEMP (K) = 342.28 JET VELOCITY (M/S) = 0.827 JET TEMP (K) = 394.6  
 LINK = 9 LINK TEMP (K) = 333.03 JET VELOCITY (M/S) = 0.861 JET TEMP (K) = 423.0  
 TIME LINK 1 OPENS EQUALS 56.0000 (S)  
 TIME LINK 2 OPENS EQUALS 72.0000 (S)  
 TIME LINK 3 OPENS EQUALS 56.0000 (S)  
 TIME LINK 4 OPENS EQUALS 100.9968 (S)  
 TIME LINK 7 OPENS EQUALS 152.0000 (S)  
 R (M) = 0.00 TSL (K) = 451.4 QB (W/M2) = 0.304E+04 QT (W/M2) = -0.120E+00  
 R (M) = 1.97 TSL (K) = 348.6 QB (W/M2) = 0.119E+04 QT (W/M2) = -0.273E-01  
 R (M) = 3.93 TSL (K) = 319.0 QB (W/M2) = 0.558E+03 QT (W/M2) = -0.105E-01  
 R (M) = 5.90 TSL (K) = 309.5 QB (W/M2) = 0.345E+03 QT (W/M2) = -0.588E-02  
 R (M) = 7.86 TSL (K) = 305.2 QB (W/M2) = 0.245E+03 QT (W/M2) = -0.394E-02  
 R (M) = 9.83 TSL (K) = 295.8 QB (W/M2) = 0.140E+02 QT (W/M2) = -0.313E-03  
 TIME (S)= 200.0000 LVR TEMP (K)= 385.7 LVR HT (M) = 0.97 LVR MASS (KG)=0.217E+03  
 FIRE OUTPUT (W) = 0.2900E+06 VENT AREA (M2) = 0.00  
 LINK = 1 LINK TEMP (K) = 387.71 JET VELOCITY (M/S) = 0.832 JET TEMP (K) = 396.1  
 LINK = 2 LINK TEMP (K) = 382.74 JET VELOCITY (M/S) = 0.832 JET TEMP (K) = 396.1  
 LINK = 3 LINK TEMP (K) = 389.83 JET VELOCITY (M/S) = 0.832 JET TEMP (K) = 396.1  
 LINK = 4 LINK TEMP (K) = 376.97 JET VELOCITY (M/S) = 0.832 JET TEMP (K) = 396.1  
 LINK = 5 LINK TEMP (K) = 340.27 JET VELOCITY (M/S) = 0.832 JET TEMP (K) = 396.1  
 LINK = 6 LINK TEMP (K) = 338.07 JET VELOCITY (M/S) = 0.832 JET TEMP (K) = 396.1  
 LINK = 7 LINK TEMP (K) = 360.16 JET VELOCITY (M/S) = 0.832 JET TEMP (K) = 396.1  
 LINK = 8 LINK TEMP (K) = 344.58 JET VELOCITY (M/S) = 0.832 JET TEMP (K) = 396.1  
 LINK = 9 LINK TEMP (K) = 335.12 JET VELOCITY (M/S) = 0.866 JET TEMP (K) = 424.8  
 TIME LINK 1 OPENS EQUALS 56.0000 (S)  
 TIME LINK 2 OPENS EQUALS 72.0000 (S)  
 TIME LINK 3 OPENS EQUALS 56.0000 (S)  
 TIME LINK 4 OPENS EQUALS 100.9968 (S)  
 TIME LINK 7 OPENS EQUALS 152.0000 (S)  
 R (M) = 0.00 TSL (K) = 453.6 QB (W/M2) = 0.301E+04 QT (W/M2) = -0.182E+00  
 R (M) = 1.97 TSL (K) = 349.9 QB (W/M2) = 0.118E+04 QT (W/M2) = -0.419E-01  
 R (M) = 3.93 TSL (K) = 319.7 QB (W/M2) = 0.560E+03 QT (W/M2) = -0.162E-01  
 R (M) = 5.90 TSL (K) = 309.9 QB (W/M2) = 0.347E+03 QT (W/M2) = -0.907E-02  
 R (M) = 7.86 TSL (K) = 305.5 QB (W/M2) = 0.247E+03 QT (W/M2) = -0.608E-02  
 R (M) = 9.83 TSL (K) = 295.8 QB (W/M2) = 0.139E+02 QT (W/M2) = -0.473E-03  
 TIME (S)= 210.0000 LVR TEMP (K)= 387.1 LVR HT (M) = 0.92 LVR MASS (KG)=0.224E+03  
 FIRE OUTPUT (W) = 0.2900E+06 VENT AREA (M2) = 0.00  
 LINK = 1 LINK TEMP (K) = 389.50 JET VELOCITY (M/S) = 0.837 JET TEMP (K) = 397.7  
 LINK = 2 LINK TEMP (K) = 384.81 JET VELOCITY (M/S) = 0.837 JET TEMP (K) = 397.7  
 LINK = 3 LINK TEMP (K) = 391.50 JET VELOCITY (M/S) = 0.837 JET TEMP (K) = 397.7  
 LINK = 4 LINK TEMP (K) = 379.27 JET VELOCITY (M/S) = 0.837 JET TEMP (K) = 397.7  
 LINK = 5 LINK TEMP (K) = 342.43 JET VELOCITY (M/S) = 0.837 JET TEMP (K) = 397.7  
 LINK = 6 LINK TEMP (K) = 340.17 JET VELOCITY (M/S) = 0.837 JET TEMP (K) = 397.7  
 LINK = 7 LINK TEMP (K) = 362.66 JET VELOCITY (M/S) = 0.837 JET TEMP (K) = 397.7  
 LINK = 8 LINK TEMP (K) = 346.86 JET VELOCITY (M/S) = 0.837 JET TEMP (K) = 397.7  
 LINK = 9 LINK TEMP (K) = 337.21 JET VELOCITY (M/S) = 0.871 JET TEMP (K) = 426.6  
 TIME LINK 1 OPENS EQUALS 56.0000 (S)  
 TIME LINK 2 OPENS EQUALS 72.0000 (S)  
 TIME LINK 3 OPENS EQUALS 56.0000 (S)  
 TIME LINK 4 OPENS EQUALS 100.9968 (S)  
 TIME LINK 5 OPENS EQUALS 205.0909 (S)  
 TIME LINK 7 OPENS EQUALS 152.0000 (S)

R (M) = 0.00 TSL (K) = 455.8 QB (W/M2) = 0.299E+04 QT (W/M2) = -0.268E+00  
 R (M) = 1.97 TSL (K) = 351.1 QB (W/M2) = 0.118E+04 QT (W/M2) = -0.637E-01  
 R (M) = 3.93 TSL (K) = 320.3 QB (W/M2) = 0.561E+03 QT (W/M2) = -0.241E-01  
 R (M) = 5.90 TSL (K) = 310.4 QB (W/M2) = 0.349E+03 QT (W/M2) = -0.135E-01  
 R (M) = 7.86 TSL (K) = 305.9 QB (W/M2) = 0.249E+03 QT (W/M2) = -0.905E-02  
 R (M) = 9.83 TSL (K) = 295.8 QB (W/M2) = 0.138E+02 QT (W/M2) = -0.683E-03  
 TIME (S)= 220.0000 LVR TEMP (K)= 388.4 LVR HT (M) = 0.88 LVR MASS (KG)=0.229E+03  
 FIRE OUTPUT (W) = 0.2900E+06 VENT AREA (M2) = 0.00  
 LINK = 1 LINK TEMP (K) = 391.25 JET VELOCITY (M/S) = 0.842 JET TEMP (K) = 399.2  
 LINK = 2 LINK TEMP (K) = 386.80 JET VELOCITY (M/S) = 0.842 JET TEMP (K) = 399.2  
 LINK = 3 LINK TEMP (K) = 393.13 JET VELOCITY (M/S) = 0.842 JET TEMP (K) = 399.2  
 LINK = 4 LINK TEMP (K) = 381.47 JET VELOCITY (M/S) = 0.842 JET TEMP (K) = 399.2  
 LINK = 5 LINK TEMP (K) = 344.58 JET VELOCITY (M/S) = 0.842 JET TEMP (K) = 399.2  
 LINK = 6 LINK TEMP (K) = 342.25 JET VELOCITY (M/S) = 0.842 JET TEMP (K) = 399.2  
 LINK = 7 LINK TEMP (K) = 365.10 JET VELOCITY (M/S) = 0.842 JET TEMP (K) = 399.2  
 LINK = 8 LINK TEMP (K) = 349.11 JET VELOCITY (M/S) = 0.842 JET TEMP (K) = 399.2  
 LINK = 9 LINK TEMP (K) = 339.29 JET VELOCITY (M/S) = 0.876 JET TEMP (K) = 428.4  
 TIME LINK 1 OPENS EQUALS 56.0000 (S)  
 TIME LINK 2 OPENS EQUALS 72.0000 (S)  
 TIME LINK 3 OPENS EQUALS 56.0000 (S)  
 TIME LINK 4 OPENS EQUALS 100.9968 (S)  
 TIME LINK 5 OPENS EQUALS 205.0909 (S)  
 TIME LINK 6 OPENS EQUALS 214.7270 (S)  
 TIME LINK 7 OPENS EQUALS 152.0000 (S)  
 TIME LINK 8 OPENS EQUALS 211.4545 (S)  
 R (M) = 0.00 TSL (K) = 458.0 QB (W/M2) = 0.297E+04 QT (W/M2) = -0.380E+00  
 R (M) = 1.97 TSL (K) = 352.3 QB (W/M2) = 0.118E+04 QT (W/M2) = -0.912E-01  
 R (M) = 3.93 TSL (K) = 321.0 QB (W/M2) = 0.563E+03 QT (W/M2) = -0.347E-01  
 R (M) = 5.90 TSL (K) = 310.8 QB (W/M2) = 0.351E+03 QT (W/M2) = -0.194E-01  
 R (M) = 7.86 TSL (K) = 306.2 QB (W/M2) = 0.251E+03 QT (W/M2) = -0.130E-01  
 R (M) = 9.83 TSL (K) = 295.8 QB (W/M2) = 0.138E+02 QT (W/M2) = -0.977E-03  
 TIME (S)= 230.0000 LVR TEMP (K)= 389.8 LVR HT (M) = 0.84 LVR MASS (KG)=0.235E+03  
 FIRE OUTPUT (W) = 0.2900E+06 VENT AREA (M2) = 0.00  
 LINK = 1 LINK TEMP (K) = 392.95 JET VELOCITY (M/S) = 0.846 JET TEMP (K) = 400.7  
 LINK = 2 LINK TEMP (K) = 388.73 JET VELOCITY (M/S) = 0.846 JET TEMP (K) = 400.7  
 LINK = 3 LINK TEMP (K) = 394.74 JET VELOCITY (M/S) = 0.846 JET TEMP (K) = 400.7  
 LINK = 4 LINK TEMP (K) = 383.61 JET VELOCITY (M/S) = 0.846 JET TEMP (K) = 400.7  
 LINK = 5 LINK TEMP (K) = 346.70 JET VELOCITY (M/S) = 0.846 JET TEMP (K) = 400.7  
 LINK = 6 LINK TEMP (K) = 344.31 JET VELOCITY (M/S) = 0.846 JET TEMP (K) = 400.7  
 LINK = 7 LINK TEMP (K) = 367.48 JET VELOCITY (M/S) = 0.846 JET TEMP (K) = 400.7  
 LINK = 8 LINK TEMP (K) = 351.33 JET VELOCITY (M/S) = 0.846 JET TEMP (K) = 400.7  
 LINK = 9 LINK TEMP (K) = 341.38 JET VELOCITY (M/S) = 0.880 JET TEMP (K) = 430.2  
 TIME LINK 1 OPENS EQUALS 56.0000 (S)  
 TIME LINK 2 OPENS EQUALS 72.0000 (S)  
 TIME LINK 3 OPENS EQUALS 56.0000 (S)  
 TIME LINK 4 OPENS EQUALS 100.9968 (S)  
 TIME LINK 5 OPENS EQUALS 205.0909 (S)  
 TIME LINK 6 OPENS EQUALS 214.7270 (S)  
 TIME LINK 7 OPENS EQUALS 152.0000 (S)  
 TIME LINK 8 OPENS EQUALS 211.4545 (S)  
 R (M) = 0.00 TSL (K) = 460.2 QB (W/M2) = 0.296E+04 QT (W/M2) = -0.525E+00  
 R (M) = 1.97 TSL (K) = 353.4 QB (W/M2) = 0.118E+04 QT (W/M2) = -0.124E+00  
 R (M) = 3.93 TSL (K) = 321.6 QB (W/M2) = 0.565E+03 QT (W/M2) = -0.484E-01  
 R (M) = 5.90 TSL (K) = 311.2 QB (W/M2) = 0.353E+03 QT (W/M2) = -0.271E-01  
 R (M) = 7.86 TSL (K) = 306.5 QB (W/M2) = 0.253E+03 QT (W/M2) = -0.182E-01  
 R (M) = 9.83 TSL (K) = 295.8 QB (W/M2) = 0.137E+02 QT (W/M2) = -0.137E-02  
 TIME (S)= 240.0000 LVR TEMP (K)= 391.1 LVR HT (M) = 0.80 LVR MASS (KG)=0.240E+03  
 FIRE OUTPUT (W) = 0.2900E+06 VENT AREA (M2) = 0.00  
 LINK = 1 LINK TEMP (K) = 394.62 JET VELOCITY (M/S) = 0.850 JET TEMP (K) = 402.2  
 LINK = 2 LINK TEMP (K) = 390.60 JET VELOCITY (M/S) = 0.850 JET TEMP (K) = 402.2  
 LINK = 3 LINK TEMP (K) = 396.33 JET VELOCITY (M/S) = 0.850 JET TEMP (K) = 402.2  
 LINK = 4 LINK TEMP (K) = 385.67 JET VELOCITY (M/S) = 0.850 JET TEMP (K) = 402.2  
 LINK = 5 LINK TEMP (K) = 348.80 JET VELOCITY (M/S) = 0.850 JET TEMP (K) = 402.2  
 LINK = 6 LINK TEMP (K) = 346.36 JET VELOCITY (M/S) = 0.850 JET TEMP (K) = 402.2  
 LINK = 7 LINK TEMP (K) = 369.80 JET VELOCITY (M/S) = 0.850 JET TEMP (K) = 402.2  
 LINK = 8 LINK TEMP (K) = 353.52 JET VELOCITY (M/S) = 0.850 JET TEMP (K) = 402.2  
 LINK = 9 LINK TEMP (K) = 343.46 JET VELOCITY (M/S) = 0.884 JET TEMP (K) = 432.0

TIME LINK 1 OPENS EQUALS 56.0000 (S)  
 TIME LINK 2 OPENS EQUALS 72.0000 (S)  
 TIME LINK 3 OPENS EQUALS 56.0000 (S)  
 TIME LINK 4 OPENS EQUALS 100.9968 (S)  
 TIME LINK 5 OPENS EQUALS 205.0909 (S)  
 TIME LINK 6 OPENS EQUALS 214.7270 (S)  
 TIME LINK 7 OPENS EQUALS 152.0000 (S)  
 TIME LINK 8 OPENS EQUALS 211.4545 (S)  
 R (M) = 0.00 TSL (K) = 462.5 QB (W/M2) = 0.295E+04 QT (W/M2) = -0.708E+00  
 R (M) = 1.97 TSL (K) = 354.6 QB (W/M2) = 0.118E+04 QT (W/M2) = -0.169E+00  
 R (M) = 3.93 TSL (K) = 322.3 QB (W/M2) = 0.567E+03 QT (W/M2) = -0.660E-01  
 R (M) = 5.90 TSL (K) = 311.6 QB (W/M2) = 0.356E+03 QT (W/M2) = -0.370E-01  
 R (M) = 7.86 TSL (K) = 306.8 QB (W/M2) = 0.255E+03 QT (W/M2) = -0.249E-01  
 R (M) = 9.83 TSL (K) = 295.9 QB (W/M2) = 0.136E+02 QT (W/M2) = -0.190E-02  
 TIME (S)= 250.0000 Lyr TEMP (K)= 392.5 Lyr HT (M) = 0.77 Lyr MASS (KG)=0.245E+03  
 FIRE OUTPUT (W) = 0.2900E+06 VENT AREA (M2) = 0.00  
 LINK = 1 LINK TEMP (K) = 396.26 JET VELOCITY (M/S) = 0.853 JET TEMP (K) = 403.7  
 LINK = 2 LINK TEMP (K) = 392.42 JET VELOCITY (M/S) = 0.853 JET TEMP (K) = 403.7  
 LINK = 3 LINK TEMP (K) = 397.91 JET VELOCITY (M/S) = 0.853 JET TEMP (K) = 403.7  
 LINK = 4 LINK TEMP (K) = 387.68 JET VELOCITY (M/S) = 0.853 JET TEMP (K) = 403.7  
 LINK = 5 LINK TEMP (K) = 350.89 JET VELOCITY (M/S) = 0.853 JET TEMP (K) = 403.7  
 LINK = 6 LINK TEMP (K) = 348.40 JET VELOCITY (M/S) = 0.853 JET TEMP (K) = 403.7  
 LINK = 7 LINK TEMP (K) = 372.08 JET VELOCITY (M/S) = 0.853 JET TEMP (K) = 403.7  
 LINK = 8 LINK TEMP (K) = 355.69 JET VELOCITY (M/S) = 0.853 JET TEMP (K) = 403.7  
 LINK = 9 LINK TEMP (K) = 345.54 JET VELOCITY (M/S) = 0.888 JET TEMP (K) = 433.8  
 TIME LINK 1 OPENS EQUALS 56.0000 (S)  
 TIME LINK 2 OPENS EQUALS 72.0000 (S)  
 TIME LINK 3 OPENS EQUALS 56.0000 (S)  
 TIME LINK 4 OPENS EQUALS 100.9968 (S)  
 TIME LINK 5 OPENS EQUALS 205.0909 (S)  
 TIME LINK 6 OPENS EQUALS 214.7270 (S)  
 TIME LINK 7 OPENS EQUALS 152.0000 (S)  
 TIME LINK 8 OPENS EQUALS 211.4545 (S)  
 R (M) = 0.00 TSL (K) = 464.7 QB (W/M2) = 0.294E+04 QT (W/M2) = -0.935E+00  
 R (M) = 1.97 TSL (K) = 355.7 QB (W/M2) = 0.117E+04 QT (W/M2) = -0.225E+00  
 R (M) = 3.93 TSL (K) = 322.9 QB (W/M2) = 0.569E+03 QT (W/M2) = -0.879E-01  
 R (M) = 5.90 TSL (K) = 312.1 QB (W/M2) = 0.358E+03 QT (W/M2) = -0.494E-01  
 R (M) = 7.86 TSL (K) = 307.1 QB (W/M2) = 0.257E+03 QT (W/M2) = -0.332E-01  
 R (M) = 9.83 TSL (K) = 295.9 QB (W/M2) = 0.135E+02 QT (W/M2) = -0.255E-02  
 TIME (S)= 260.0000 Lyr TEMP (K)= 393.8 Lyr HT (M) = 0.73 Lyr MASS (KG)=0.250E+03  
 FIRE OUTPUT (W) = 0.2900E+06 VENT AREA (M2) = 0.00  
 LINK = 1 LINK TEMP (K) = 397.88 JET VELOCITY (M/S) = 0.856 JET TEMP (K) = 405.2  
 LINK = 2 LINK TEMP (K) = 394.20 JET VELOCITY (M/S) = 0.856 JET TEMP (K) = 405.2  
 LINK = 3 LINK TEMP (K) = 399.47 JET VELOCITY (M/S) = 0.856 JET TEMP (K) = 405.2  
 LINK = 4 LINK TEMP (K) = 389.63 JET VELOCITY (M/S) = 0.856 JET TEMP (K) = 405.2  
 LINK = 5 LINK TEMP (K) = 352.96 JET VELOCITY (M/S) = 0.856 JET TEMP (K) = 405.2  
 LINK = 6 LINK TEMP (K) = 350.42 JET VELOCITY (M/S) = 0.856 JET TEMP (K) = 405.2  
 LINK = 7 LINK TEMP (K) = 374.30 JET VELOCITY (M/S) = 0.856 JET TEMP (K) = 405.2  
 LINK = 8 LINK TEMP (K) = 357.84 JET VELOCITY (M/S) = 0.856 JET TEMP (K) = 405.2  
 LINK = 9 LINK TEMP (K) = 347.62 JET VELOCITY (M/S) = 0.891 JET TEMP (K) = 435.7  
 TIME LINK 1 OPENS EQUALS 56.0000 (S)  
 TIME LINK 2 OPENS EQUALS 72.0000 (S)  
 TIME LINK 3 OPENS EQUALS 56.0000 (S)  
 TIME LINK 4 OPENS EQUALS 100.9968 (S)  
 TIME LINK 5 OPENS EQUALS 205.0909 (S)  
 TIME LINK 6 OPENS EQUALS 214.7270 (S)  
 TIME LINK 7 OPENS EQUALS 152.0000 (S)  
 TIME LINK 8 OPENS EQUALS 211.4545 (S)  
 R (M) = 0.00 TSL (K) = 466.9 QB (W/M2) = 0.294E+04 QT (W/M2) = -0.119E+01  
 R (M) = 1.97 TSL (K) = 356.8 QB (W/M2) = 0.117E+04 QT (W/M2) = -0.293E+00  
 R (M) = 3.93 TSL (K) = 323.5 QB (W/M2) = 0.571E+03 QT (W/M2) = -0.115E+00  
 R (M) = 5.90 TSL (K) = 312.5 QB (W/M2) = 0.360E+03 QT (W/M2) = -0.646E-01  
 R (M) = 7.86 TSL (K) = 307.4 QB (W/M2) = 0.259E+03 QT (W/M2) = -0.435E-01  
 R (M) = 9.83 TSL (K) = 295.9 QB (W/M2) = 0.135E+02 QT (W/M2) = -0.326E-02  
 TIME (S)= 270.0000 Lyr TEMP (K)= 395.2 Lyr HT (M) = 0.70 Lyr MASS (KG)=0.254E+03  
 FIRE OUTPUT (W) = 0.2900E+06 VENT AREA (M2) = 0.00  
 LINK = 1 LINK TEMP (K) = 399.48 JET VELOCITY (M/S) = 0.859 JET TEMP (K) = 406.7

LINK = 2 LINK TEMP (K) = 395.94 JET VELOCITY (M/S) = 0.859 JET TEMP (K) = 406.7  
 LINK = 3 LINK TEMP (K) = 401.02 JET VELOCITY (M/S) = 0.859 JET TEMP (K) = 406.7  
 LINK = 4 LINK TEMP (K) = 391.53 JET VELOCITY (M/S) = 0.859 JET TEMP (K) = 406.7  
 LINK = 5 LINK TEMP (K) = 355.01 JET VELOCITY (M/S) = 0.859 JET TEMP (K) = 406.7  
 LINK = 6 LINK TEMP (K) = 352.42 JET VELOCITY (M/S) = 0.859 JET TEMP (K) = 406.7  
 LINK = 7 LINK TEMP (K) = 376.48 JET VELOCITY (M/S) = 0.859 JET TEMP (K) = 406.7  
 LINK = 8 LINK TEMP (K) = 359.96 JET VELOCITY (M/S) = 0.859 JET TEMP (K) = 406.7  
 LINK = 9 LINK TEMP (K) = 349.70 JET VELOCITY (M/S) = 0.894 JET TEMP (K) = 437.5  
 TIME LINK 1 OPENS EQUALS 56.0000 (S)  
 TIME LINK 2 OPENS EQUALS 72.0000 (S)  
 TIME LINK 3 OPENS EQUALS 56.0000 (S)  
 TIME LINK 4 OPENS EQUALS 100.9968 (S)  
 TIME LINK 5 OPENS EQUALS 205.0909 (S)  
 TIME LINK 6 OPENS EQUALS 214.7270 (S)  
 TIME LINK 7 OPENS EQUALS 152.0000 (S)  
 TIME LINK 8 OPENS EQUALS 211.4545 (S)  
 R (M) = 0.00 TSL (K) = 469.1 QB (W/M2) = 0.293E+04 QT (W/M2) = -0.154E+01  
 R (M) = 1.97 TSL (K) = 357.9 QB (W/M2) = 0.117E+04 QT (W/M2) = -0.376E+00  
 R (M) = 3.93 TSL (K) = 324.1 QB (W/M2) = 0.573E+03 QT (W/M2) = -0.148E+00  
 R (M) = 5.90 TSL (K) = 312.9 QB (W/M2) = 0.362E+03 QT (W/M2) = -0.830E-01  
 R (M) = 7.86 TSL (K) = 307.7 QB (W/M2) = 0.261E+03 QT (W/M2) = -0.559E-01  
 R (M) = 9.83 TSL (K) = 295.9 QB (W/M2) = 0.134E+02 QT (W/M2) = -0.407E-02  
 TIME (S) = 280.0000 LVR TEMP (K) = 396.5 LVR HT (M) = 0.66 LVR MASS (KG) = 0.258E+03  
 FIRE OUTPUT (W) = 0.2900E+06 VENT AREA (M2) = 0.00  
 LINK = 1 LINK TEMP (K) = 401.07 JET VELOCITY (M/S) = 0.862 JET TEMP (K) = 408.2  
 LINK = 2 LINK TEMP (K) = 397.65 JET VELOCITY (M/S) = 0.862 JET TEMP (K) = 408.2  
 LINK = 3 LINK TEMP (K) = 402.57 JET VELOCITY (M/S) = 0.862 JET TEMP (K) = 408.2  
 LINK = 4 LINK TEMP (K) = 393.39 JET VELOCITY (M/S) = 0.862 JET TEMP (K) = 408.2  
 LINK = 5 LINK TEMP (K) = 357.04 JET VELOCITY (M/S) = 0.862 JET TEMP (K) = 408.2  
 LINK = 6 LINK TEMP (K) = 354.41 JET VELOCITY (M/S) = 0.862 JET TEMP (K) = 408.2  
 LINK = 7 LINK TEMP (K) = 378.62 JET VELOCITY (M/S) = 0.862 JET TEMP (K) = 408.2  
 LINK = 8 LINK TEMP (K) = 362.06 JET VELOCITY (M/S) = 0.862 JET TEMP (K) = 408.2  
 LINK = 9 LINK TEMP (K) = 351.77 JET VELOCITY (M/S) = 0.897 JET TEMP (K) = 439.3  
 TIME LINK 1 OPENS EQUALS 56.0000 (S)  
 TIME LINK 2 OPENS EQUALS 72.0000 (S)  
 TIME LINK 3 OPENS EQUALS 56.0000 (S)  
 TIME LINK 4 OPENS EQUALS 100.9968 (S)  
 TIME LINK 5 OPENS EQUALS 205.0909 (S)  
 TIME LINK 6 OPENS EQUALS 214.7270 (S)  
 TIME LINK 7 OPENS EQUALS 152.0000 (S)  
 TIME LINK 8 OPENS EQUALS 211.4545 (S)  
 R (M) = 0.00 TSL (K) = 471.4 QB (W/M2) = 0.293E+04 QT (W/M2) = -0.193E+01  
 R (M) = 1.97 TSL (K) = 358.9 QB (W/M2) = 0.117E+04 QT (W/M2) = -0.474E+00  
 R (M) = 3.93 TSL (K) = 324.7 QB (W/M2) = 0.575E+03 QT (W/M2) = -0.186E+00  
 R (M) = 5.90 TSL (K) = 313.3 QB (W/M2) = 0.364E+03 QT (W/M2) = -0.105E+00  
 R (M) = 7.86 TSL (K) = 308.0 QB (W/M2) = 0.263E+03 QT (W/M2) = -0.707E-01  
 R (M) = 9.83 TSL (K) = 295.9 QB (W/M2) = 0.133E+02 QT (W/M2) = -0.527E-02  
 TIME (S) = 290.0000 LVR TEMP (K) = 397.9 LVR HT (M) = 0.63 LVR MASS (KG) = 0.262E+03  
 FIRE OUTPUT (W) = 0.2900E+06 VENT AREA (M2) = 0.00  
 LINK = 1 LINK TEMP (K) = 402.64 JET VELOCITY (M/S) = 0.864 JET TEMP (K) = 409.7  
 LINK = 2 LINK TEMP (K) = 399.33 JET VELOCITY (M/S) = 0.864 JET TEMP (K) = 409.7  
 LINK = 3 LINK TEMP (K) = 404.11 JET VELOCITY (M/S) = 0.864 JET TEMP (K) = 409.7  
 LINK = 4 LINK TEMP (K) = 395.22 JET VELOCITY (M/S) = 0.864 JET TEMP (K) = 409.7  
 LINK = 5 LINK TEMP (K) = 359.06 JET VELOCITY (M/S) = 0.864 JET TEMP (K) = 409.7  
 LINK = 6 LINK TEMP (K) = 356.39 JET VELOCITY (M/S) = 0.864 JET TEMP (K) = 409.7  
 LINK = 7 LINK TEMP (K) = 380.72 JET VELOCITY (M/S) = 0.864 JET TEMP (K) = 409.7  
 LINK = 8 LINK TEMP (K) = 364.13 JET VELOCITY (M/S) = 0.864 JET TEMP (K) = 409.7  
 LINK = 9 LINK TEMP (K) = 353.85 JET VELOCITY (M/S) = 0.900 JET TEMP (K) = 441.2  
 TIME LINK 1 OPENS EQUALS 56.0000 (S)  
 TIME LINK 2 OPENS EQUALS 72.0000 (S)  
 TIME LINK 3 OPENS EQUALS 56.0000 (S)  
 TIME LINK 4 OPENS EQUALS 100.9968 (S)  
 TIME LINK 5 OPENS EQUALS 205.0909 (S)  
 TIME LINK 6 OPENS EQUALS 214.7270 (S)  
 TIME LINK 7 OPENS EQUALS 152.0000 (S)  
 TIME LINK 8 OPENS EQUALS 211.4545 (S)  
 R (M) = 0.00 TSL (K) = 473.6 QB (W/M2) = 0.293E+04 QT (W/M2) = -0.238E+01

R (M) = 1.97 TSL (K) = 360.0 QB (W/M2) = 0.117E+04 QT (W/M2) = -0.589E+00  
 R (M) = 3.93 TSL (K) = 325.3 QB (W/M2) = 0.577E+03 QT (W/M2) = -0.232E+00  
 R (M) = 5.90 TSL (K) = 313.7 QB (W/M2) = 0.366E+03 QT (W/M2) = -0.131E+00  
 R (M) = 7.86 TSL (K) = 308.3 QB (W/M2) = 0.265E+03 QT (W/M2) = -0.882E-01  
 R (M) = 9.83 TSL (K) = 295.9 QB (W/M2) = 0.133E+02 QT (W/M2) = -0.648E-02  
 TIME (S) = 300.0000 LTR TEMP (K) = 399.2 LTR HT (M) = 0.60 LTR MASS (KG) = 0.266E+03  
 FIRE OUTPUT (W) = 0.2900E+06 VENT AREA (M2) = 0.00  
 LINK = 1 LINK TEMP (K) = 404.21 JET VELOCITY (M/S) = 0.866 JET TEMP (K) = 411.3  
 LINK = 2 LINK TEMP (K) = 401.00 JET VELOCITY (M/S) = 0.866 JET TEMP (K) = 411.3  
 LINK = 3 LINK TEMP (K) = 405.64 JET VELOCITY (M/S) = 0.866 JET TEMP (K) = 411.3  
 LINK = 4 LINK TEMP (K) = 397.01 JET VELOCITY (M/S) = 0.866 JET TEMP (K) = 411.3  
 LINK = 5 LINK TEMP (K) = 361.06 JET VELOCITY (M/S) = 0.866 JET TEMP (K) = 411.3  
 LINK = 6 LINK TEMP (K) = 358.35 JET VELOCITY (M/S) = 0.866 JET TEMP (K) = 411.3  
 LINK = 7 LINK TEMP (K) = 382.78 JET VELOCITY (M/S) = 0.866 JET TEMP (K) = 411.3  
 LINK = 8 LINK TEMP (K) = 366.19 JET VELOCITY (M/S) = 0.866 JET TEMP (K) = 411.3  
 LINK = 9 LINK TEMP (K) = 355.91 JET VELOCITY (M/S) = 0.902 JET TEMP (K) = 443.0  
 TIME LINK 1 OPENS EQUALS 56.0000 (S)  
 TIME LINK 2 OPENS EQUALS 72.0000 (S)  
 TIME LINK 3 OPENS EQUALS 56.0000 (S)  
 TIME LINK 4 OPENS EQUALS 100.9968 (S)  
 TIME LINK 5 OPENS EQUALS 205.0909 (S)  
 TIME LINK 6 OPENS EQUALS 214.7270 (S)  
 TIME LINK 7 OPENS EQUALS 152.0000 (S)  
 TIME LINK 8 OPENS EQUALS 211.4545 (S)  
 R (M) = 0.00 TSL (K) = 475.9 QB (W/M2) = 0.295E+04 QT (W/M2) = -0.286E+01  
 R (M) = 1.97 TSL (K) = 361.0 QB (W/M2) = 0.117E+04 QT (W/M2) = -0.723E+00  
 R (M) = 3.93 TSL (K) = 325.9 QB (W/M2) = 0.579E+03 QT (W/M2) = -0.285E+00  
 R (M) = 5.90 TSL (K) = 314.1 QB (W/M2) = 0.368E+03 QT (W/M2) = -0.161E+00  
 R (M) = 7.86 TSL (K) = 308.6 QB (W/M2) = 0.266E+03 QT (W/M2) = -0.109E+00  
 R (M) = 9.83 TSL (K) = 295.9 QB (W/M2) = 0.132E+02 QT (W/M2) = -0.787E-02

# FPETool Fire Simulator

## FIRE SIMULATOR

[VER 3.00]

Input data used for run of: 08-03-1993 10:39:44  
 Data file used: 290.IN as of 08/03/93 10:39:22  
 Run title: Bldg 530, 290 kW, r = 1.5 m, SS bulb, RTI=234.8  
 LOTUS file name: 290\_15.WKS  
 Heat of combustion: 19990.53 BTU/lb 46450.00 KJ/Kg  
 Specific extinction coefficient: .10  
 Flashover temperature: 1112.00 F 600.00 C  
 Oxygen starvation threshold: 10.00 % by volume  
 Radiant energy fraction (from flame): .27  
 Maximum pre flashover energy loss: .85  
 Sprinkler/Heat detector description:  
   Radial distance 4.92 ft 1.50 m  
   RTI: 425.30 (ft-Sec)^.5 234.80 (m-Sec)^.5  
   Sprinkler rating: 154.40 F 68.00 C  
   Sprinkler is not sidewall mounted  
 There is no Smoke detector defined  
 There is no initial inside opening defined  
  
 Spacial dimensions of room:  
   Room height: 7.71 ft 2.35 m  
   Room floor area: 1851.29 ft^2 171.99 m^2  
   Room wall perimeter: 183.73 ft 56.00 m  
   Room is rectangular: 62.01 ft by 29.86 ft 18.90 m by 9.10 m  
  
 Description of ceiling materials:  
   100% CALCIUM SILICATE BOARD 0.984 in 25.000 mm  
  
 Description of wall materials:  
   100% CONCRETE BLOCK 0.984 in 25.000 mm  
 There is no HVAC defined  
 Fire height: 0.33 ft 0.10 m  
 290 kW, 500 s  
 Fire description was manually entered as follows:  
   TIME (Sec) FIRE (kW)

A halt flag is set for Sprinkler activation

TIME	-----TEMP-----		-----LAYER-----		-----FIRE-----	
sec	F	C	ft	m	kW	BTU/sec
0.0	70.0	21.1	7.7	2.3	0.1	0.1
Link temperature = 70.0 F 21.1 C						
Ceiling Jet Temperature (at link) = 70.8 F 21.6 C						
Ceiling Jet Velocity (at link) = 0.31 ft/sec 0.09 m/sec						
Vision distance (smoke layer) = 3000.00 m 9842.52 ft						
Smoke gases : Oxygen = 21.0 % : CO = 0.0000 : CO2 = 0.0000 %						
10.0	153.3	67.4	7.4	2.3	290.0	275.1
Link temperature = 76.2 F 24.6 C						
Ceiling Jet Temperature (at link) = 238.0 F 114.4 C						
Ceiling Jet Velocity (at link) = 4.51 ft/sec 1.37 m/sec						
Vision distance (smoke layer) = 9.77 m 32.04 ft						
Smoke gases : Oxygen = 19.9 % : CO = 0.0001 : CO2 = 0.5221 %						
20.0	157.8	69.9	7.1	2.2	290.0	275.1
Link temperature = 84.2 F 29.0 C						
Ceiling Jet Temperature (at link) = 241.4 F 116.3 C						
Ceiling Jet Velocity (at link) = 4.50 ft/sec 1.37 m/sec						
Vision distance (smoke layer) = 8.43 m 27.65 ft						
Smoke gases : Oxygen = 19.8 % : CO = 0.0001 : CO2 = 0.5878 %						
30.0	161.3	71.8	6.9	2.1	290.0	275.1
Link temperature = 91.9 F 33.3 C						

Ceiling Jet Temperature (at link) = 243.6 F 117.6 C  
 Ceiling Jet Velocity (at link) = 4.51 ft/sec 1.37 m/sec  
 Vision distance (smoke layer) = 7.92 m 25.98 ft  
 Smoke gases : Oxygen = 19.8 % : CO = 0.0002 : CO2 = 0.6209 %

40.0 164.3 73.5 6.6 2.0 290.0 275.1  
 Link temperature = 99.3 F 37.4 C  
 Ceiling Jet Temperature (at link) = 245.6 F 118.7 C  
 Ceiling Jet Velocity (at link) = 4.51 ft/sec 1.38 m/sec  
 Vision distance (smoke layer) = 7.57 m 24.85 ft  
 Smoke gases : Oxygen = 19.7 % : CO = 0.0002 : CO2 = 0.6478 %

50.0 166.9 74.9 6.3 1.9 290.0 275.1  
 Link temperature = 106.5 F 41.4 C  
 Ceiling Jet Temperature (at link) = 247.4 F 119.7 C  
 Ceiling Jet Velocity (at link) = 4.52 ft/sec 1.38 m/sec  
 Vision distance (smoke layer) = 7.29 m 23.92 ft  
 Smoke gases : Oxygen = 19.6 % : CO = 0.0002 : CO2 = 0.6726 %

60.0 169.2 76.2 6.1 1.9 290.0 275.1  
 Link temperature = 113.4 F 45.2 C  
 Ceiling Jet Temperature (at link) = 249.2 F 120.7 C  
 Ceiling Jet Velocity (at link) = 4.52 ft/sec 1.38 m/sec  
 Vision distance (smoke layer) = 7.05 m 23.12 ft  
 Smoke gases : Oxygen = 19.6 % : CO = 0.0002 : CO2 = 0.6964 %

70.0 171.4 77.4 5.9 1.8 290.0 275.1  
 Link temperature = 120.1 F 48.9 C  
 Ceiling Jet Temperature (at link) = 250.9 F 121.6 C  
 Ceiling Jet Velocity (at link) = 4.53 ft/sec 1.38 m/sec  
 Vision distance (smoke layer) = 6.82 m 22.38 ft  
 Smoke gases : Oxygen = 19.6 % : CO = 0.0002 : CO2 = 0.7197 %

80.0 173.4 78.5 5.7 1.7 290.0 275.1  
 Link temperature = 126.5 F 52.5 C  
 Ceiling Jet Temperature (at link) = 252.6 F 122.6 C  
 Ceiling Jet Velocity (at link) = 4.53 ft/sec 1.38 m/sec  
 Vision distance (smoke layer) = 6.62 m 21.71 ft  
 Smoke gases : Oxygen = 19.5 % : CO = 0.0003 : CO2 = 0.7429 %

90.0 175.2 79.6 5.5 1.7 290.0 275.1  
 Link temperature = 132.7 F 56.0 C  
 Ceiling Jet Temperature (at link) = 254.3 F 123.5 C  
 Ceiling Jet Velocity (at link) = 4.53 ft/sec 1.38 m/sec  
 Vision distance (smoke layer) = 6.42 m 21.08 ft  
 Smoke gases : Oxygen = 19.5 % : CO = 0.0003 : CO2 = 0.7659 %

100.0 177.0 80.6 5.3 1.6 290.0 275.1  
 Link temperature = 138.7 F 59.3 C  
 Ceiling Jet Temperature (at link) = 256.0 F 124.5 C  
 Ceiling Jet Velocity (at link) = 4.54 ft/sec 1.38 m/sec  
 Vision distance (smoke layer) = 6.24 m 20.49 ft  
 Smoke gases : Oxygen = 19.4 % : CO = 0.0003 : CO2 = 0.7890 %

110.0 178.7 81.5 5.1 1.6 290.0 275.1  
 Link temperature = 144.5 F 62.5 C  
 Ceiling Jet Temperature (at link) = 257.7 F 125.4 C  
 Ceiling Jet Velocity (at link) = 4.54 ft/sec 1.38 m/sec  
 Vision distance (smoke layer) = 6.07 m 19.93 ft  
 Smoke gases : Oxygen = 19.4 % : CO = 0.0003 : CO2 = 0.8120 %

\*\*\*\*\* HAZARD WARNING \*\*\*\*\*

At 118 seconds the vision dropped to 19.5 ft 5.94m

118.0 180.0 82.2 5.0 1.5 290.0 275.1  
 Link temperature = 149.0 F 65.0 C

Ceiling Jet Temperature (at link) = 259.1 F 126.2 C  
 Ceiling Jet Velocity (at link) = 4.54 ft/sec 1.39 m/sec  
 Vision distance (smoke layer) = 5.94 m 19.50 ft  
 Smoke gases : Oxygen = 19.3 % : CO = 0.0003 : CO2 = 0.8305 %

120.0 180.3 82.4 5.0 1.5 290.0 275.1  
 Link temperature = 150.1 F 65.6 C  
 Ceiling Jet Temperature (at link) = 259.4 F 126.3 C  
 Ceiling Jet Velocity (at link) = 4.55 ft/sec 1.39 m/sec  
 Vision distance (smoke layer) = 5.91 m 19.40 ft  
 Smoke gases : Oxygen = 19.3 % : CO = 0.0003 : CO2 = 0.8352 %

Sprinkler/Heat detector  
 activated at 129 seconds.

129.0 181.7 83.1 4.8 1.5 290.0 275.1  
 Vision distance (smoke layer) = 5.78 m 18.95 ft  
 Smoke gases : Oxygen = 19.3 % : CO = 0.0003 : CO2 = 0.8560 %

129.0 181.7 83.1 4.8 1.5 290.0 275.1  
 Vision distance (smoke layer) = 5.78 m 18.95 ft  
 Smoke gases : Oxygen = 19.3 % : CO = 0.0003 : CO2 = 0.8583 %

130.0 181.8 83.2 4.8 1.5 290.0 275.1  
 Vision distance (smoke layer) = 5.76 m 18.90 ft  
 Smoke gases : Oxygen = 19.3 % : CO = 0.0003 : CO2 = 0.8583 %

140.0 183.3 84.0 4.7 1.4 290.0 275.1  
 Vision distance (smoke layer) = 5.62 m 18.42 ft  
 Smoke gases : Oxygen = 19.2 % : CO = 0.0003 : CO2 = 0.8816 %

150.0 184.7 84.8 4.5 1.4 290.0 275.1  
 Vision distance (smoke layer) = 5.48 m 17.97 ft  
 Smoke gases : Oxygen = 19.2 % : CO = 0.0003 : CO2 = 0.9049 %

160.0 186.0 85.6 4.4 1.3 290.0 275.1  
 Vision distance (smoke layer) = 5.35 m 17.54 ft  
 Smoke gases : Oxygen = 19.1 % : CO = 0.0003 : CO2 = 0.9283 %

170.0 187.4 86.3 4.2 1.3 290.0 275.1  
 Vision distance (smoke layer) = 5.22 m 17.12 ft  
 Smoke gases : Oxygen = 19.1 % : CO = 0.0004 : CO2 = 0.9519 %

180.0 188.6 87.0 4.1 1.3 290.0 275.1  
 Vision distance (smoke layer) = 5.10 m 16.73 ft  
 Smoke gases : Oxygen = 19.0 % : CO = 0.0004 : CO2 = 0.9755 %

190.0 189.8 87.7 4.0 1.2 290.0 275.1  
 Vision distance (smoke layer) = 4.98 m 16.35 ft  
 Smoke gases : Oxygen = 19.0 % : CO = 0.0004 : CO2 = 0.9991 %

200.0 191.0 88.4 3.9 1.2 290.0 275.1  
 Vision distance (smoke layer) = 4.87 m 15.99 ft  
 Smoke gases : Oxygen = 18.9 % : CO = 0.0004 : CO2 = 1.0229 %

210.0 192.2 89.0 3.8 1.2 290.0 275.1  
 Vision distance (smoke layer) = 4.77 m 15.64 ft  
 Smoke gases : Oxygen = 18.9 % : CO = 0.0004 : CO2 = 1.0468 %

220.0 193.3 89.6 3.7 1.1 290.0 275.1  
 Vision distance (smoke layer) = 4.67 m 15.31 ft  
 Smoke gases : Oxygen = 18.9 % : CO = 0.0004 : CO2 = 1.0707 %

\*\*\*\*\* HAZARD WARNING \*\*\*\*\*

At 230 seconds the vision dropped to 15.0 ft 4.57 m



230.0	194.4	90.2	3.6	1.1	290.0	275.1
Vision distance (smoke layer) =			4.57 m	14.99 ft		
Smoke gases : Oxygen = 18.8 % : CO = 0.0004 : CO2 = 1.0948 %						
230.0	194.4	90.2	3.6	1.1	290.0	275.1
Vision distance (smoke layer) =			4.57 m	14.99 ft		
Smoke gases : Oxygen = 18.8 % : CO = 0.0004 : CO2 = 1.0948 %						
240.0	195.6	90.9	3.5	1.1	290.0	275.1
Vision distance (smoke layer) =			4.47 m	14.68 ft		
Smoke gases : Oxygen = 18.8 % : CO = 0.0004 : CO2 = 1.1187 %						
250.0	196.8	91.5	3.4	1.0	290.0	275.1
Vision distance (smoke layer) =			4.39 m	14.39 ft		
Smoke gases : Oxygen = 18.7 % : CO = 0.0004 : CO2 = 1.1426 %						
260.0	198.1	92.3	3.3	1.0	290.0	275.1
Vision distance (smoke layer) =			4.30 m	14.11 ft		
Smoke gases : Oxygen = 18.7 % : CO = 0.0005 : CO2 = 1.1665 %						
270.0	199.4	93.0	3.2	1.0	290.0	275.1
Vision distance (smoke layer) =			4.22 m	13.84 ft		
Smoke gases : Oxygen = 18.6 % : CO = 0.0005 : CO2 = 1.1903 %						
280.0	200.8	93.8	3.1	1.0	290.0	275.1
Vision distance (smoke layer) =			4.14 m	13.59 ft		
Smoke gases : Oxygen = 18.6 % : CO = 0.0005 : CO2 = 1.2140 %						
290.0	202.3	94.6	3.1	0.9	290.0	275.1
Vision distance (smoke layer) =			4.07 m	13.34 ft		
Smoke gases : Oxygen = 18.5 % : CO = 0.0005 : CO2 = 1.2377 %						
300.0	203.8	95.5	3.0	0.9	290.0	275.1
Vision distance (smoke layer) =			3.99 m	13.10 ft		
Smoke gases : Oxygen = 18.5 % : CO = 0.0005 : CO2 = 1.2614 %						
310.0	205.4	96.3	2.9	0.9	290.0	275.1
Vision distance (smoke layer) =			3.92 m	12.87 ft		
Smoke gases : Oxygen = 18.4 % : CO = 0.0005 : CO2 = 1.2851 %						
320.0	207.0	97.2	2.8	0.9	290.0	275.1
Vision distance (smoke layer) =			3.86 m	12.65 ft		
Smoke gases : Oxygen = 18.4 % : CO = 0.0005 : CO2 = 1.3088 %						
330.0	208.6	98.1	2.8	0.8	290.0	275.1
Vision distance (smoke layer) =			3.79 m	12.44 ft		
Smoke gases : Oxygen = 18.3 % : CO = 0.0005 : CO2 = 1.3325 %						
340.0	210.3	99.0	2.7	0.8	290.0	275.1
Vision distance (smoke layer) =			3.73 m	12.24 ft		
Smoke gases : Oxygen = 18.3 % : CO = 0.0005 : CO2 = 1.3562 %						
350.0	212.0	100.0	2.6	0.8	290.0	275.1
Vision distance (smoke layer) =			3.67 m	12.04 ft		
Smoke gases : Oxygen = 18.2 % : CO = 0.0005 : CO2 = 1.3799 %						
360.0	213.7	101.0	2.6	0.8	290.0	275.1
Vision distance (smoke layer) =			3.61 m	11.85 ft		
Smoke gases : Oxygen = 18.2 % : CO = 0.0006 : CO2 = 1.4037 %						
370.0	215.5	101.9	2.5	0.8	290.0	275.1
Vision distance (smoke layer) =			3.56 m	11.67 ft		
Smoke gases : Oxygen = 18.1 % : CO = 0.0006 : CO2 = 1.4274 %						
380.0	217.3	102.9	2.5	0.7	290.0	275.1
Vision distance (smoke layer) =			3.50 m	11.49 ft		
Smoke gases : Oxygen = 18.1 % : CO = 0.0006 : CO2 = 1.4512 %						

390.0	219.1	103.9	2.4	0.7	290.0	275.1
Vision distance (smoke layer) =			3.45 m		11.32 ft	
Smoke gases : Oxygen = 18.0 % : CO = 0.0006 : CO2 = 1.4750 %						
400.0	220.9	105.0	2.3	0.7	290.0	275.1
Vision distance (smoke layer) =			3.40 m		11.15 ft	
Smoke gases : Oxygen = 18.0 % : CO = 0.0006 : CO2 = 1.4988 %						
410.0	222.8	106.0	2.3	0.7	290.0	275.1
Vision distance (smoke layer) =			3.35 m		10.99 ft	
Smoke gases : Oxygen = 17.9 % : CO = 0.0006 : CO2 = 1.5226 %						
420.0	224.7	107.1	2.2	0.7	290.0	275.1
Vision distance (smoke layer) =			3.30 m		10.83 ft	
Smoke gases : Oxygen = 17.9 % : CO = 0.0006 : CO2 = 1.5465 %						
430.0	226.6	108.1	2.2	0.7	290.0	275.1
Vision distance (smoke layer) =			3.25 m		10.68 ft	
Smoke gases : Oxygen = 17.9 % : CO = 0.0006 : CO2 = 1.5704 %						
440.0	228.6	109.2	2.1	0.6	290.0	275.1
Vision distance (smoke layer) =			3.21 m		10.53 ft	
Smoke gases : Oxygen = 17.8 % : CO = 0.0006 : CO2 = 1.5943 %						
450.0	230.6	110.3	2.1	0.6	290.0	275.1
Vision distance (smoke layer) =			3.17 m		10.39 ft	
Smoke gases : Oxygen = 17.8 % : CO = 0.0007 : CO2 = 1.6183 %						
460.0	232.5	111.4	2.0	0.6	290.0	275.1
Vision distance (smoke layer) =			3.12 m		10.25 ft	
Smoke gases : Oxygen = 17.7 % : CO = 0.0007 : CO2 = 1.6423 %						
470.0	234.5	112.5	2.0	0.6	290.0	275.1
Vision distance (smoke layer) =			3.08 m		10.11 ft	
Smoke gases : Oxygen = 17.7 % : CO = 0.0007 : CO2 = 1.6663 %						
480.0	236.6	113.7	1.9	0.6	290.0	275.1
Vision distance (smoke layer) =			3.04 m		9.98 ft	
Smoke gases : Oxygen = 17.6 % : CO = 0.0007 : CO2 = 1.6904 %						
490.0	238.6	114.8	1.9	0.6	290.0	275.1
Vision distance (smoke layer) =			3.00 m		9.85 ft	
Smoke gases : Oxygen = 17.6 % : CO = 0.0007 : CO2 = 1.7145 %						
500.0	240.7	115.9	1.8	0.6	290.0	275.1
Vision distance (smoke layer) =			2.97 m		9.73 ft	
Smoke gases : Oxygen = 17.5 % : CO = 0.0007 : CO2 = 1.7386 %						

-----END OF INPUT FIRE-----

Table 1. Instrumentation List.

Sensor	Distance from Sprinkler Array (m)	Distance below Ceiling (mm)
Thermocouple	1.0	12
Thermocouple	1.0	25
Thermocouple	1.0	76
Bi-Directional Probe	1.0	76
Thermocouple	1.0	152
Thermocouple	1.0	305
Thermocouple	1.0	610
Thermocouple	1.0	914
Thermocouple	1.0	1,220
QRS Link	0.0	32 pendent/-6 recessed
SS Link	0.0	32 pendent/-6 recessed
Radiometer	0.0	25
Total Heat Flux	0.0	25
Thermocouple	0.05	12
Thermocouple	0.05	25
Thermocouple	0.05	76
Bi-Directional Probe	0.05	76
Thermocouple	0.05	102
Thermocouple	0.05	127
Thermocouple	0.05	152
Thermocouple	0.05	305
Thermocouple	0.05	610
Thermocouple	0.05	914
Thermocouple	0.05	1,220
Thermocouple	1.5/3.0	Located directly over burner

Table 2. Test Matrix.

Test Number	Heat Release Rate (kW)	Sprinkler Position	Distance between Sprinklers and Burner (m)
1-3	520	Pendent	3
4-6	520	Recessed	3
7-9	290	Pendent	3
10-12	290	Recessed	3
13-15	290	Pendent	1.5
16-18	290	Recessed	1.5
19-21	215	Pendent	1.5
22-24	215	Recessed	1.5
25-27	155	Pendent	1.5
28-30	155	Recessed	1.5
31-33	115	Pendent	1.5
34-36	115	Recessed	1.5

Table 3. Average Heat Flux.

Heat Release Rate (kW)	Distance between Sprinklers and Burner (m)	Radiant Heat Flux (kW/m <sup>2</sup> )
520	3	1.23
290	3	0.53
290	1.5	1.27
215	1.5	0.90
155	1.5	0.38
115	1.5	0.23

Table 4. Sprinkler Activation Times, Tests 1-3.

Sprinkler Activation Times (s) HRR = 520 kW, R = 3m, Pendent				
Test No.	QR/Bulb	QR/Link	SS/Bulb	SS/Link
1	19.9	28.6	85.2	67.7
2	23.6	25.9	79.3	73.8
3	26.0	30	89.0	75.8
Avg. $\pm 2\sigma$	23.2 $\pm$ 6.2	28.2 $\pm$ 4.6	80.2 $\pm$ 9.8	72.4 $\pm$ 8.4

Table 5. Sprinkler Activation Times, Tests 4-6.

Sprinkler Activation Times (s) HRR = 520 kW, R = 3m, 25mm recess				
Test No.	QR/Bulb	QR/Link	SS/Bulb	SS/Link
4	38.1	39	95.9	71.4
5	26.2	30.3	93.8	73.9
6	33.7	30	89.8	60.1
Avg. $\pm 2\sigma$	32.7 $\pm$ 12.0	33.1 $\pm$ 10.2	93.2 $\pm$ 6.2	68.5 $\pm$ 14.8

Table 6. Comparison of Average Activation Times, Tests 1-3 vs. Tests 4-6.

Change in Activation Time Due to 25 mm Recess [time (s) / %]			
QR/Bulb	QR/Link	SS/Bulb	SS/Link
9.5/41	4.9/17	13.0/16	-3.9/-5

Table 7. Sprinkler Activation Times, Tests 7-9.

Sprinkler Activation Times (s) HRR = 290 kW, R = 3m, Pendent				
Test No.	QR/Bulb	QR/Link	SS/Bulb	SS/Link
7	76.9	115.2	214.6	200.5
8	94.0	105.4	187.8	212.2
9	82.2	108.4	204.1	189.8
Avg. $\pm 2\sigma$	84.4 $\pm$ 17.5	109.7 $\pm$ 10.0	202.2 $\pm$ 27.0	200.8 $\pm$ 22.4

Table 8. Sprinkler Activation Times, Tests 10-12.

Sprinkler Activation Times (s) HRR = 290 kW, R = 3m, 25mm recess				
Test No.	QR/Bulb	QR/Link	SS/Bulb	SS/Link
10	97.3	110.3	214.0	198.5
11	73.0	102.6	229.8	182.7
12	88.3	120.8	208.8	190.3
Avg. $\pm 2\sigma$	86.2 $\pm$ 24.6	111.2 $\pm$ 18.3	217.5 $\pm$ 22.3	190.5 $\pm$ 16.0

Table 9. Comparison of Average Activation Times, Tests 7-9 vs. Tests 10-12.

Change in Activation Time Due to 25 mm Recess [time (s) / %]			
QR/Bulb	QR/Link	SS/Bulb	SS/Link
1.8/2	1.5/1	15.3/7	-10.3/-5

Table 10. Sprinkler Activation Times, Tests 13-15.

Sprinkler Activation Times (s) HRR = 290 kW, R = 1.5 m, Pendent				
Test No.	QR/Bulb	QR/Link	SS/Bulb	SS/Link
13	28.0	43.1	92.4	95.1
14	20.7	27.1	81.7	72.3
15	30.7	27	98.9	75.7
Avg. $\pm 2\sigma$	26.5 $\pm$ 10.3	32.4 $\pm$ 18.5	91.0 $\pm$ 19.5	81.0 $\pm$ 24.6

Table 11. Sprinkler Activation Times, Tests 16-17.

Sprinkler Activation Times (s) HRR = 290 kW, R = 1.5 m, 25 mm recess				
Test No.	QR/Bulb	QR/Link	SS/Bulb	SS/Link
16	39.1	45.9	108.1	75.8
17	34.2	32.7	98.7	63.7
18	29.7	36.8	102.6	81.1
Avg. $\pm 2\sigma$	34.3 $\pm$ 9.4	38.5 $\pm$ 13.5	103.1 $\pm$ 9.4	73.5 $\pm$ 17.8

Table 12. Comparison of Average Activation Times, Tests 13-15 vs. Tests 16-18.

Change in Activation Time Due to 25 mm Recess [time (s) / %]			
QR/Bulb	QR/Link	SS/Bulb	SS/Link
7.8/29	6.1/19	12.1/13	-7.5/-9

Table 13. Sprinkler Activation Times, Tests 19-21.

Sprinkler Activation Times (s) HRR = 215 kW, R = 1.5m, Pendent				
Test No.	QR/Bulb	QR/Link	SS/Bulb	SS/Link
19	29.2	47.1	113.4	94.3
20	32.3	46.7	111.2	87.6
21	31.0	33.8	97.6	81.8
Avg. $\pm 2\sigma$	30.8 $\pm$ 3.1	42.5 $\pm$ 15.1	107.4 $\pm$ 17.1	87.9 $\pm$ 12.5

Table 14. Sprinkler Activation Times, Tests 22-24.

Sprinkler Activation Times (s) HRR = 215 kW, R = 1.5m, 25mm Recess				
Test No.	QR/Bulb	QR/Link	SS/Bulb	SS/Link
22	36.6	41.2	123.4	101.7
23	35.7	43.1	118.4	87.7
24	35.2	60.4	112.9	92.2
Avg. $\pm 2\sigma$	35.8 $\pm$ 1.4	48.2 $\pm$ 21.2	118.2 $\pm$ 10.5	93.9 $\pm$ 14.3

Table 15. Comparison of Average Activation Times, Tests 19-21 vs. Tests 22-24.

Change in Activation Time Due to 25 mm Recess [time (s) / %]			
QR/Bulb	QR/Link	SS/Bulb	SS/Link
5/16	5.7/13	10.8/10	6/7



Table 16. Sprinkler Activation Times, Tests 25-27.

Sprinkler Activation Times (s) HRR = 155 kW, R = 1.5m, Pendent				
Test No.	QR/Bulb	QR/Link	SS/Bulb	SS/Link
25	52.1	96.5	160.1	149.7
26	47.8	50.5	157.2	147.5
27	37.2	66.8	148.6	147.9
Avg. $\pm 2\sigma$	45.7 $\pm$ 15.3	71.3 $\pm$ 46.3	155.3 $\pm$ 12.0	148.4 $\pm$ 2.3

Table 17. Sprinkler Activation Times, Tests 28-30.

Sprinkler Activation Times (s) HRR = 155 kW, R = 1.5m, 25mm Recess				
Test No.	QR/Bulb	QR/Link	SS/Bulb	SS/Link
28	63.2	108.4	194.3	166.9
29	49.5	81.7	165.7	139.0
30	81.8	92.4	181.5	141.8
Avg. $\pm 2\sigma$	64.8 $\pm$ 32.4	94.2 $\pm$ 26.9	180.5 $\pm$ 28.7	149.2 $\pm$ 30.8

Table 18. Comparison of Average Activation Times, Tests 25-27 vs. Tests 28-30.

Change in Activation Time Due to 25 mm Recess [time (s) / %]			
QR/Bulb	QR/Link	SS/Bulb	SS/Link
19.1/42	22.9/32	25.2/14	1/00

Table 19. Sprinkler Activation Times, Tests 31-33.

Sprinkler Activation Times (s) HRR = 115 kW, R = 1.5m, Pendent				
Test No.	QR/Bulb	QR/Link	SS/Bulb	SS/Link
31	167.5	252.0	329.6	326.5
32	163.7	183.6	313.2	264.0
33	166.8	180.4	278.0	315.3
Avg. $\pm 2\sigma$	166.0 $\pm$ 4.0	205.3 $\pm$ 95.2	306.9 $\pm$ 52.7	301.9 $\pm$ 66.6

Table 20. Sprinkler Activation Times, Tests 34-36.

Sprinkler Activation Times (s) HRR = 115 kW, R = 1.5m, 25mm Recess				
Test No.	QR/Bulb	QR/Link	SS/Bulb	SS/Link
34	183.6	310.5	475.7	455.9
35	225.0	335.1	403.0	409.2
36	280.8	307.9	412.2	353.1
Avg. $\pm 2\sigma$	229.8 $\pm$ 97.6	317.8 $\pm$ 30.0	430.3 $\pm$ 79.2	406.1 $\pm$ 103.3

Table 21. Comparison of Average Activation Times, Tests 31-33 vs. Tests 34-36.

Change in Activation Time Due to 25 mm Recess [time (s) / %]			
QR/Bulb	QR/Link	SS/Bulb	SS/Link
63.8/38	112.5/55	123.4/40	104.2/35

Table 22. Comparison of Average RTIs, Tests 1-3 vs. Tests 4-6.

Comparison of Average RTIs, Tests 1-3 vs. Tests 4-6 (m <sup>1/2</sup> s <sup>1/2</sup> )				
Test No.	QR/Bulb	QR/Link	SS/Bulb	SS/Link
1-3	24.6	28.6	226.7	151.3
4-6	44.4	36.0	268.0	143.1
Percent Difference	81	26	18	-6

Table 23. Comparison of Average RTIs, Tests 7-9 vs. Tests 10-12.

Comparison of Average RTIs, Tests 7-9 vs. Tests 10-12 (m <sup>1/2</sup> s <sup>1/2</sup> )				
Test No.	QR/Bulb	QR/Link	SS/Bulb	SS/Link
7-9	57.9	74.8	251.9	205.5
10-12	69.9	89.9	297.8	206.3
Percent Difference	21	20	18	0

Table 24. Comparison of Average RTIs, Tests 13-15 vs. Tests 16-18.

Comparison of Average RTIs, Tests 13-15 vs. Tests 16-18 (m <sup>1/2</sup> s <sup>1/2</sup> )				
Test No.	QR/Bulb	QR/Link	SS/Bulb	SS/Link
13-15	25.8	25.4	181.4	129.3
16-18	36.7	35.0	217.3	111.6
Percent Difference	42	38	20	-14

Table 25. Comparison of Average RTIs, Tests 19-21 vs. Tests 22-24.

Comparison of Average RTIs, Tests 19-21 vs. Tests 22-24 (m <sup>1/2</sup> s <sup>1/2</sup> )				
Test No.	QR/Bulb	QR/Link	SS/Bulb	SS/Link
19-21	25.5	32.4	183.0	110.3
22-24	33.3	42.2	196.5	113.8
Percent Difference	31	30	7	3

Table 26. Comparison of Average RTIs, Tests 25-27 vs. Tests 28-30.

Comparison of Average RTIs, Tests 25-27 vs. Tests 28-30 (m <sup>1/2</sup> s <sup>1/2</sup> )				
Test No.	QR/Bulb	QR/Link	SS/Bulb	SS/Link
25-27	11.4	40.3	164.1	114.0
28-30	41.6	58.5	212.6	123.6
Percent Difference	265	45	30	8

Table 27. Comparison of Average RTIs, Tests 31-33 vs. Tests 34-36.

Comparison of Average RTIs, Tests 31-33 vs. Tests 34-36 (m <sup>1/2</sup> s <sup>1/2</sup> )				
Test No.	QR/Bulb	QR/Link	SS/Bulb	SS/Link
31-33	58.1	52.2	214.6	144.8
34-36	113.4	121.7	300.0	193.2
Percent Difference	78	133	40	33

Table 28. Comparison of Plunge Test vs. Average Experimental RTIs.

RTI Comparison - Plunge Test vs Experimental							
Type	Plunge Test RTIs	Experimental RTIs *					
		520 kW 3 m	290 kW 3 m	290 kW 1.5 m	215 kW 1.5 m	155 kW 1.5 m	115 kW
QR Bulb	42.1	24.6 (44.4)	57.9 (69.9)	25.8 (36.7)	25.5 (33.3)	11.4 (41.6)	58.1 (113.4)
QR Link	34.1	28.6 (36.0)	74.8 (89.9)	25.4 (35.0)	32.4 (42.2)	40.3 (58.5)	52.2 (121.7)
SS Bulb	234.8	226.7 (268.0)	251.9 (297.8)	181.4 (217.3)	183.0 (196.5)	164.1 (212.6)	214.6 (300.0)
SS Link	129.8	151.3 (143.1)	205.5 (206.3)	129.3 (111.6)	110.3 (113.8)	114.0 (123.6)	144.8 (193.2)

\* The first RTI in each block represents the fully exposed pendent case. The second RTI, in parentheses, represents the recessed case.

Table 29. Comparison of Experimental vs. Predicted Activation Times for Tests 1-3.

Comparison of Experimental vs. Predicted Activation Times for Tests 1-3 HRR = 520 kW, r = 3 m					
Sprinkler Type/ Element Type*	Plunge Test RTI ( $m^{1/2} s^{1/2}$ )	Full Scale Activation Time, Pendent Position (s)	Predicted Activation Times (s)		
			DETECT	LAVENT	FPEtool
QR/Bulb	42.1	23.2	46.0	30.0	33
QR/Link	34.1	28.2	46.4	28.6	32
SS/Bulb	234.8	80.2	241.4	116.0	135
SS/Link	129.8	72.4	167.5	83.4	94

\* Activation temperature of the bulb type sprinklers is 68°C.  
Activation temperature of the link type sprinklers is 74°C.

Table 30. Comparison of Experimental vs. Predicted Activation Times for Tests 7-9.

Comparison of Experimental vs. Predicted Activation Times for Tests 7-9 HRR = 290 kW, r = 3 m					
Sprinkler Type/ Element Type*	Plunge Test RTI ( $m^{1/2} s^{1/2}$ )	Full Scale Activation Time, Pendent Position (s)	Predicted Activation Times (s)		
			DETECT	LAVENT	FPEtool
QR/Bulb	42.1	84.7	129.7	56.0	57
QR/Link	34.1	109.7	NA	56.0	59
SS/Bulb	234.8	202.2	708.2	205.1	245
SS/Link	129.8	200.8	NA	152.0	186

\* Activation temperature of the bulb type sprinklers is 68°C.  
Activation temperature of the link type sprinklers is 74°C.

Table 31. Comparison of Experimental vs. Predicted Activation Times for Tests 13-15.

Comparison of Experimental vs. Predicted Activation Times for Tests 13-15 HRR = 290 kW, r = 1.5 m					
Sprinkler Type/ Element Type*	Plunge Test RTI (m <sup>1/2</sup> s <sup>1/2</sup> )	Full Scale Activation Time, Pendent Position (s)	Predicted Activation Times (s)		
			DETECT	LAVENT	FPEtool
QR/Bulb	42.1	26.5	34.5	21.6	28
QR/Link	34.1	32.4	34.3	20.8	27
SS/Bulb	234.8	91.0	177.5	90.0	129
SS/Link	129.8	81.0	121.4	62.5	88

- \* Activation temperature of the bulb type sprinklers is 68°C.  
Activation temperature of the link type sprinklers is 74°C.

Table 32. Comparison of Experimental vs. Predicted Activation Times for Tests 19-21.

Comparison of Experimental vs. Predicted Activation Times for Tests 19-21 HRR = 215 kW, r = 1.5 m					
Sprinkler Type/ Element Type*	Plunge Test RTI (m <sup>1/2</sup> s <sup>1/2</sup> )	Full Scale Activation Time, Pendent Position (s)	Predicted Activation Times (s)		
			DETECT	LAVENT	FPEtool
QR/Bulb	42.1	30.8	50.1	28.9	38
QR/Link	34.1	42.5	52.9	28.0	38
SS/Bulb	234.8	107.4	264.4	122.8	177
SS/Link	129.8	87.9	192.3	86.4	125

- \* Activation temperature of the bulb type sprinklers is 68°C.  
Activation temperature of the link type sprinklers is 74°C.

Table 33. Comparison of Experimental vs. Predicted Activation Times for Tests 25-27.

Comparison of Experimental vs. Predicted Activation Times for Tests 25-27 HRR = 155 kW, r = 1.5 m					
Sprinkler Type/ Element Type	Plunge Test RTI ( $m^{1/2} s^{1/2}$ )	Full Scale Activation Time, Pendent Position (s)	Predicted Activation Times (s)		
			DETECT	LAVENT	FPEtool
QR/Bulb	42.1	45.7	90.2	41.8	58
QR/Link	34.1	71.3	NA	42.5	62
SS/Bulb	234.8	155.3	488.1	173.8	260
SS/Link	129.8	148.4	NA	127.3	194

- Activation temperature of the bulb type sprinklers is 68°C.  
Activation temperature of the link type sprinklers is 74°C.

Table 34. Comparison of Experimental vs. Predicted Activation Times for Tests 31-33.

Comparison of Experimental vs. Predicted Activation Times for Tests 31-33 HRR = 115 kW, r = 1.5 m					
Sprinkler Type/ Element Type	Plunge Test RTI ( $m^{1/2} s^{1/2}$ )	Full Scale Activation Time, Pendent Position (s)	Predicted Activation Times (s)		
			DETECT	LAVENT	FPEtool
QR/Bulb	42.1	166.0	NA	63.9	97
QR/Link	34.1	205.3	NA	70.0	140
SS/Bulb	234.8	306.9	NA	245.6	388
SS/Link	129.8	301.9	NA	190.0	328

- Activation temperature of the bulb type sprinklers is 68°C.  
Activation temperature of the link type sprinklers is 74°C.



Table 35. Sprinkler Activation Time Comparison, QR bulb.

QR Bulb Sprinkler Activation Comparison					
Heat Release Rate (kW)	Distance between Sprinkler and Burner (m)	Full Scale Activation Time, Pendent Position (s)	Predicted Activation Times (s)		
			DETECT	FPEtool 3.00	FPEtool Modified
520	3	23.2	46	33	33
290	3	84.4	129.7	57	55
290	1.5	26.5	34.5	28	33
215	1.5	30.8	50.1	38	43
155	1.5	45.7	90	58	62
115	1.5	166	NA	97	95

Table 36. Sprinkler Activation Time Comparison, QR link.

QR Link Sprinkler Activation Comparison					
Heat Release Rate (kW)	Distance between Sprinkler and Burner (m)	Full Scale Activation Time, Pendent Position (s)	Predicted Activation Times (s)		
			DETECT	FPEtool 3.00	FPEtool Modified
520	3	28.2	46.4	32	32
290	3	109.7	NA	59	54
290	1.5	32.4	34.3	27	33
215	1.5	42.5	52.9	38	43
155	1.5	71.3	NA	62	64
115	1.5	205.3	NA	140	111

Table 37. Sprinkler Activation Time Comparison, SS bulb.

SS Bulb Sprinkler Activation Comparison					
Heat Release Rate (kW)	Distance between Sprinkler and Burner (m)	Full Scale Activation Time, Pendent Position (s)	Predicted Activation Times (s)		
			DETECT	FPEtool 3.00	FPEtool Modified
520	3	80.2	241.4	135	108
290	3	202.2	708.2	245	195
290	1.5	91	177.5	129	120
215	1.5	107.4	264.4	177	164
155	1.5	155.3	488.1	260	238
115	1.5	306.9	NA	388	351

Table 38. Sprinkler Activation Time Comparison, SS link.

SS Link Sprinkler Activation Comparison					
Heat Release Rate (kW)	Distance between Sprinkler and Burner (m)	Full Scale Activation Time, Pendent Position (s)	Predicted Activation Times (s)		
			DETECT	FPEtool 3.00	FPEtool Modified
520	3	72.4	167.5	94	77
290	3	200.8	NA	186	140
290	1.5	81	121.4	88	84
215	1.5	87.9	192.3	125	117
155	1.5	148.4	NA	194	176
115	1.5	301.9	NA	328	279

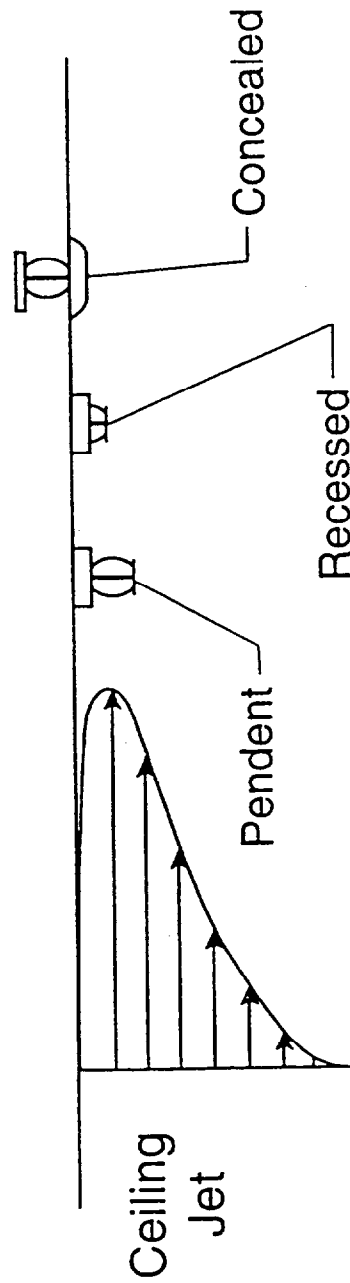


Figure 1. Schematic of pendant, recessed and concealed sprinklers with ceiling jet.

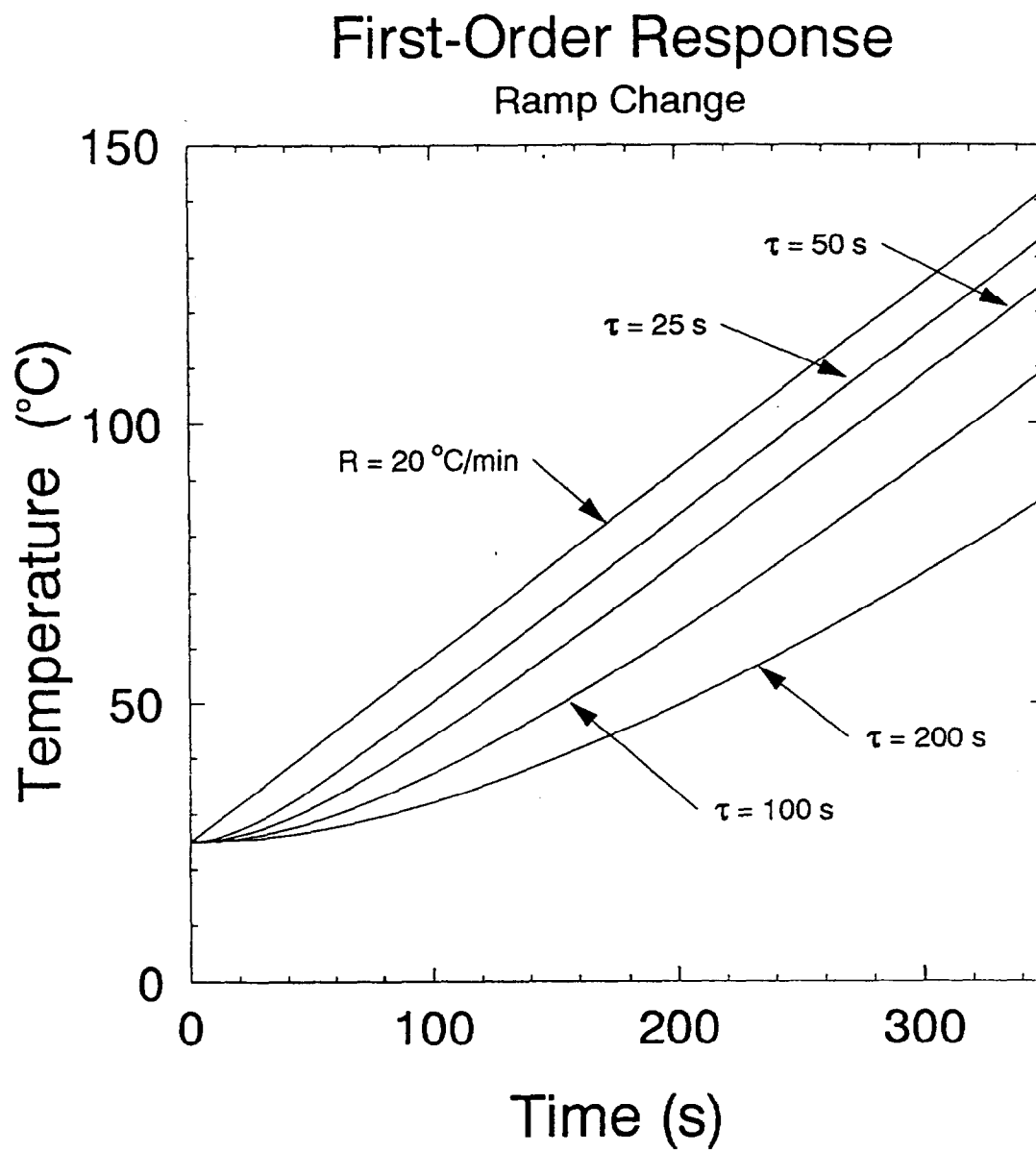


Figure 2. First-order response, ramp change.

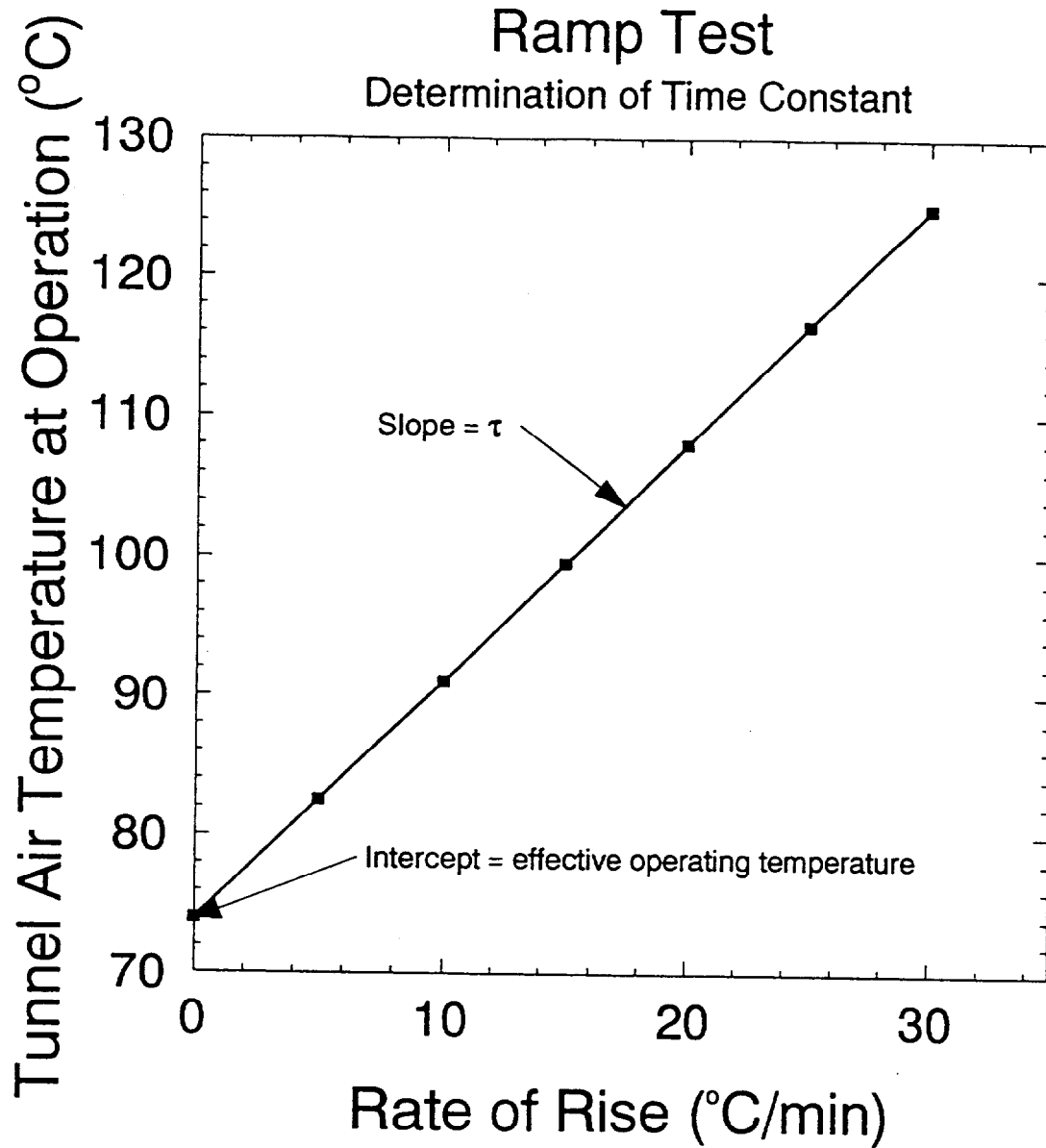


Figure 3. Ramp test, determination of time constant.

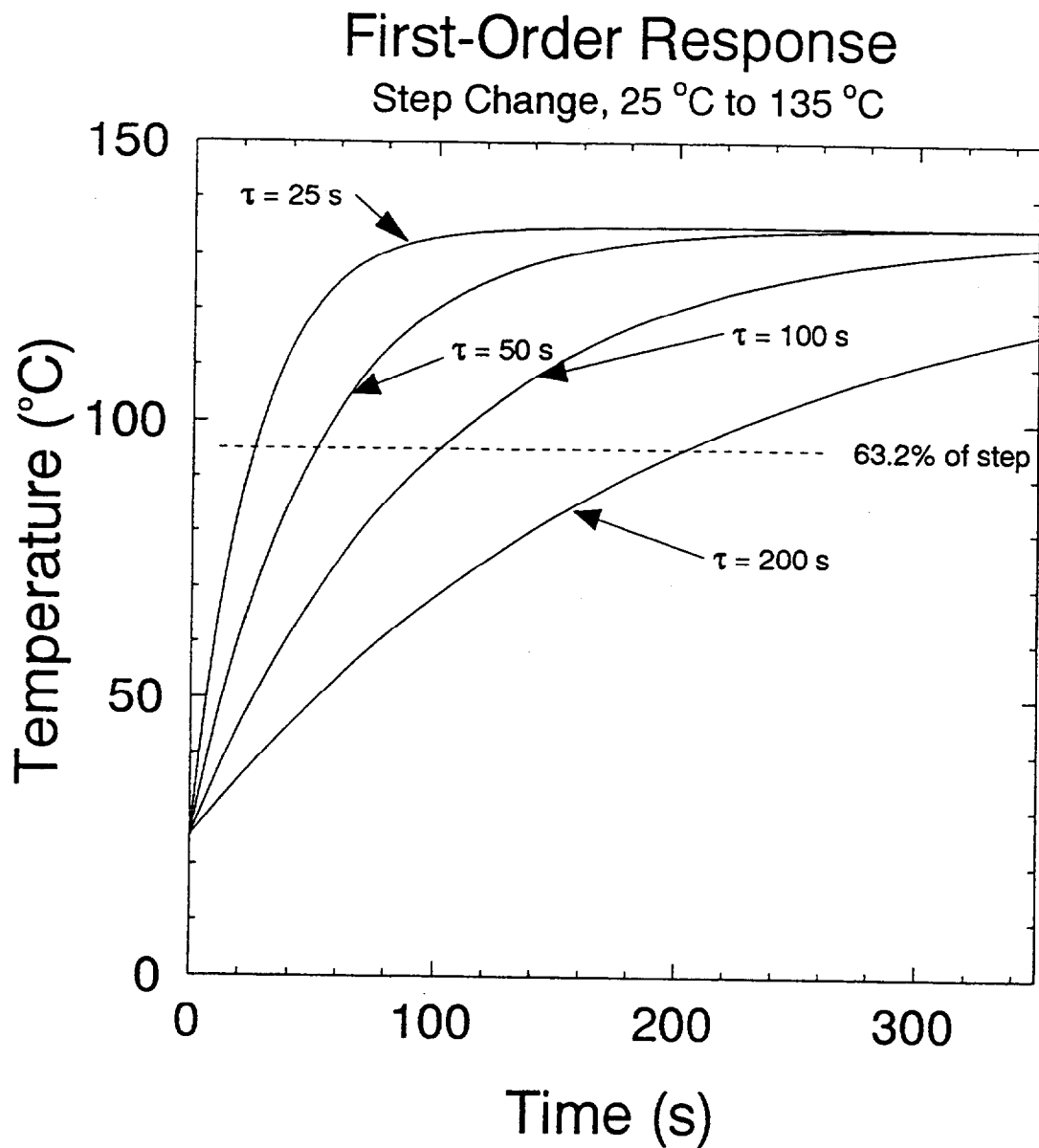


Figure 4. First-order response, step change.

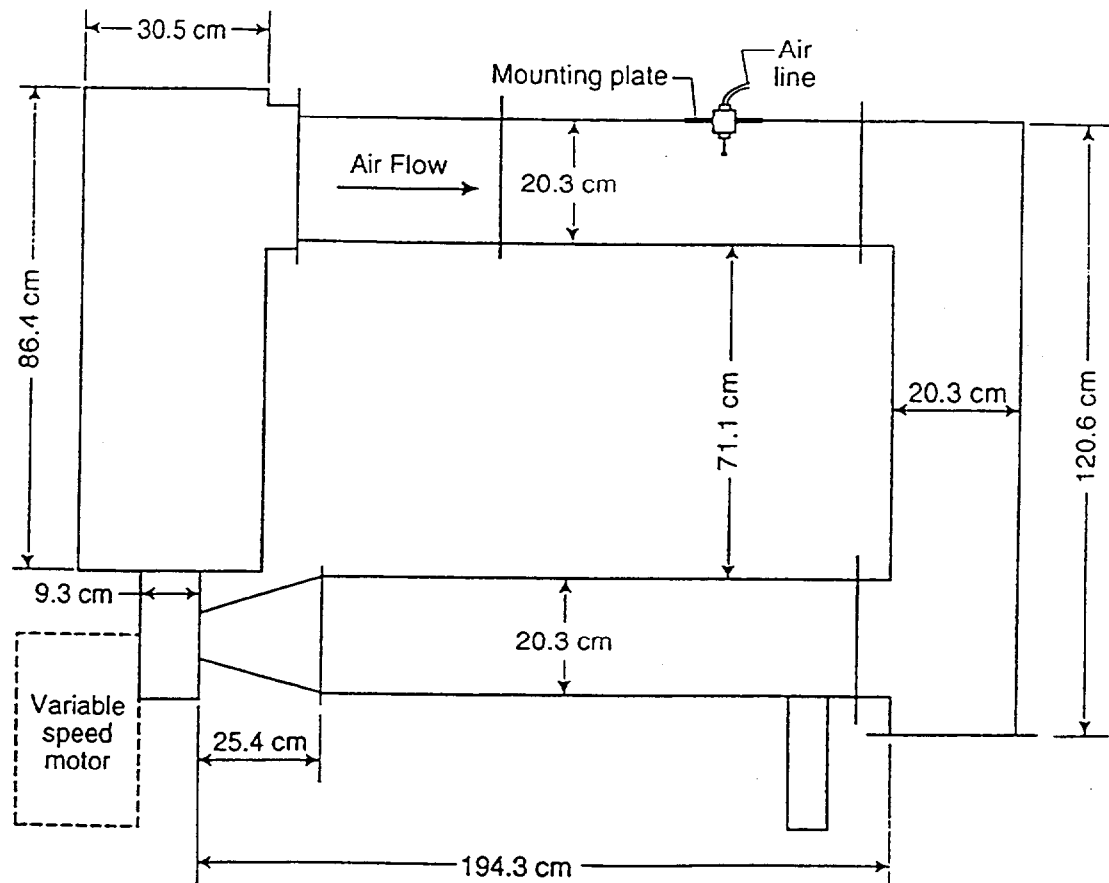


Figure 5. Schematic of sensitivity test oven (Elevation).

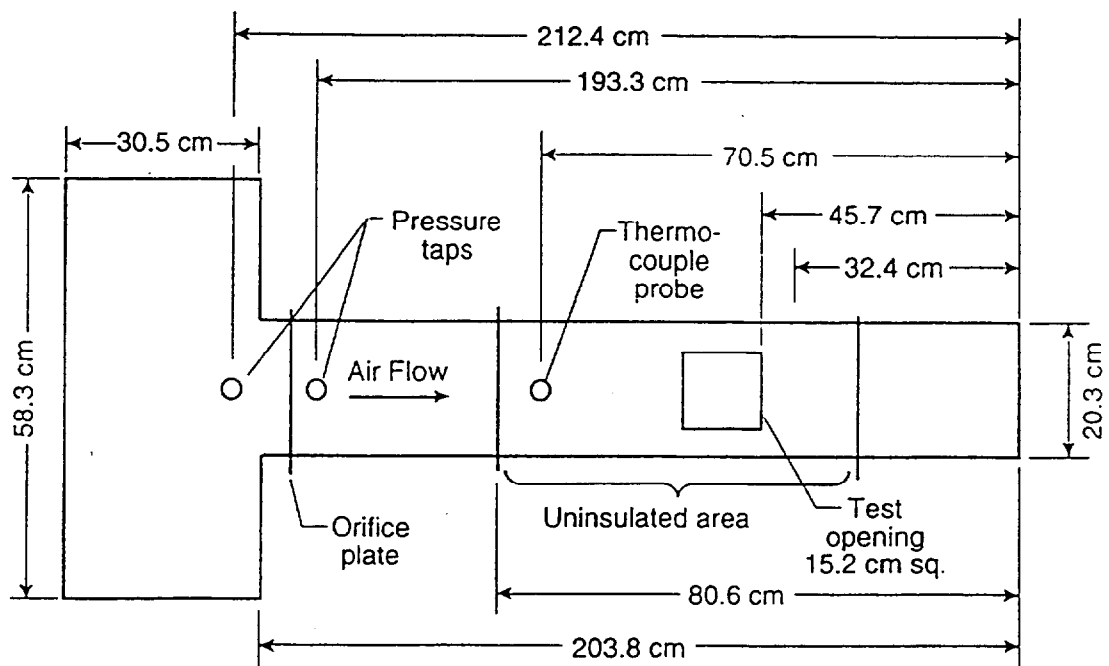


Figure 6. Schematic of sensitivity test oven (Plan View).



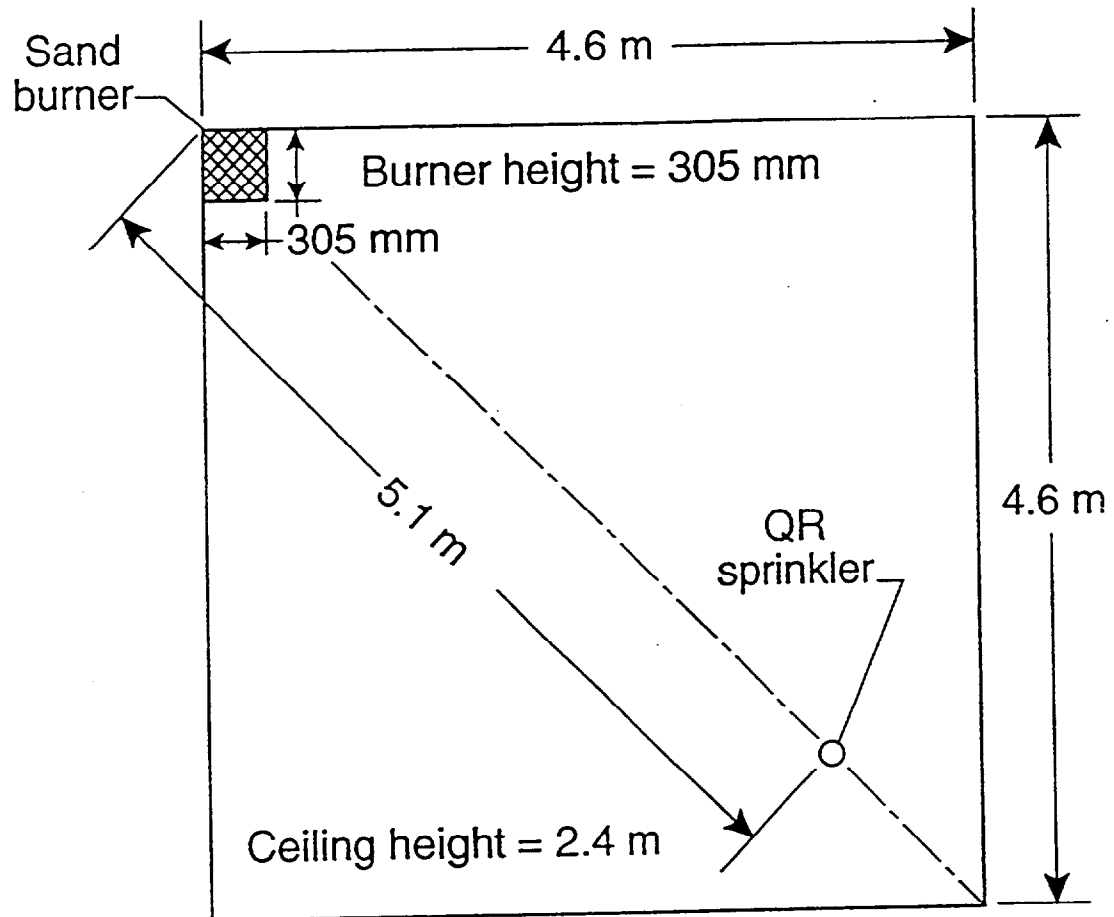


Figure 7. Schematic of room heat test configuration.

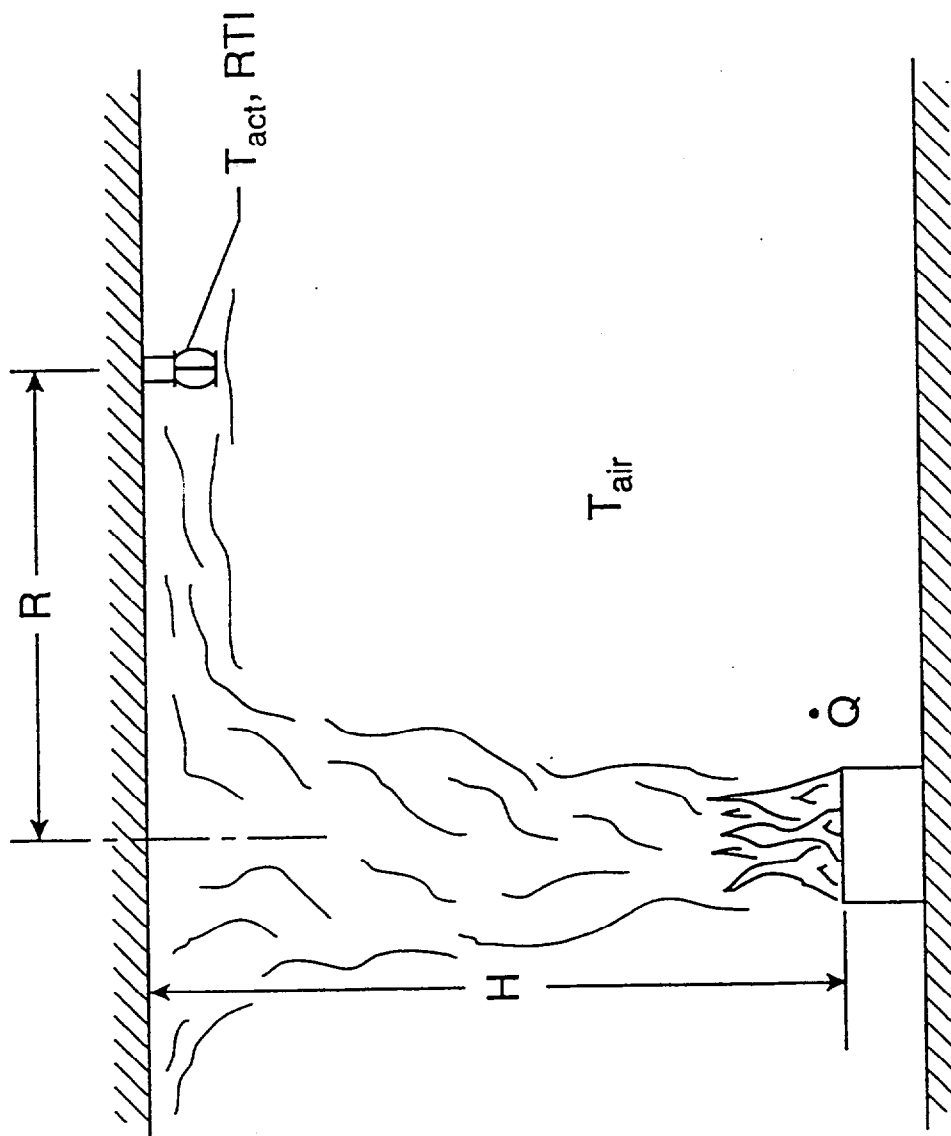


Figure 8. Schematic of DETACT-QS inputs.

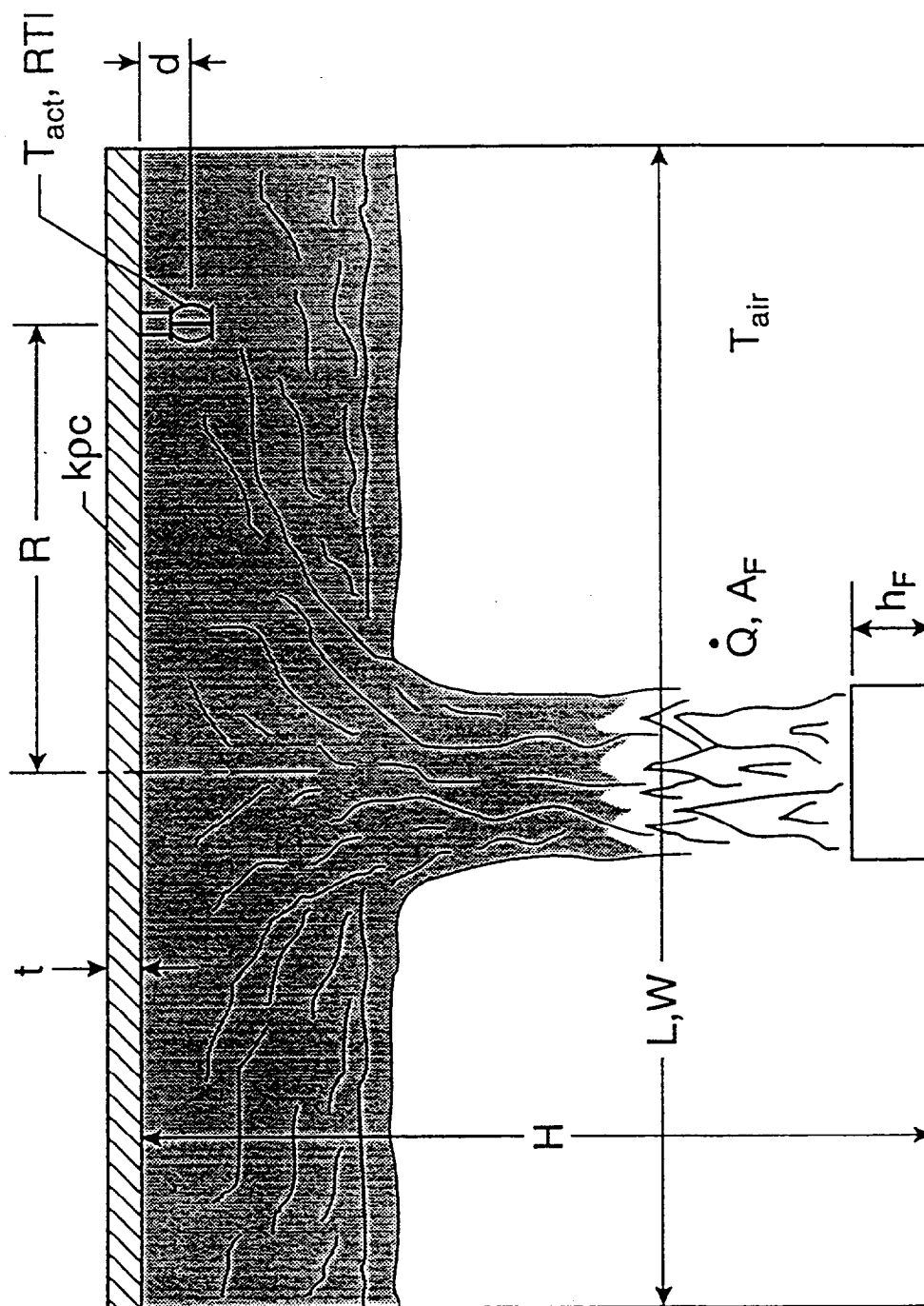


Figure 9. Schematic of LAVENT inputs.

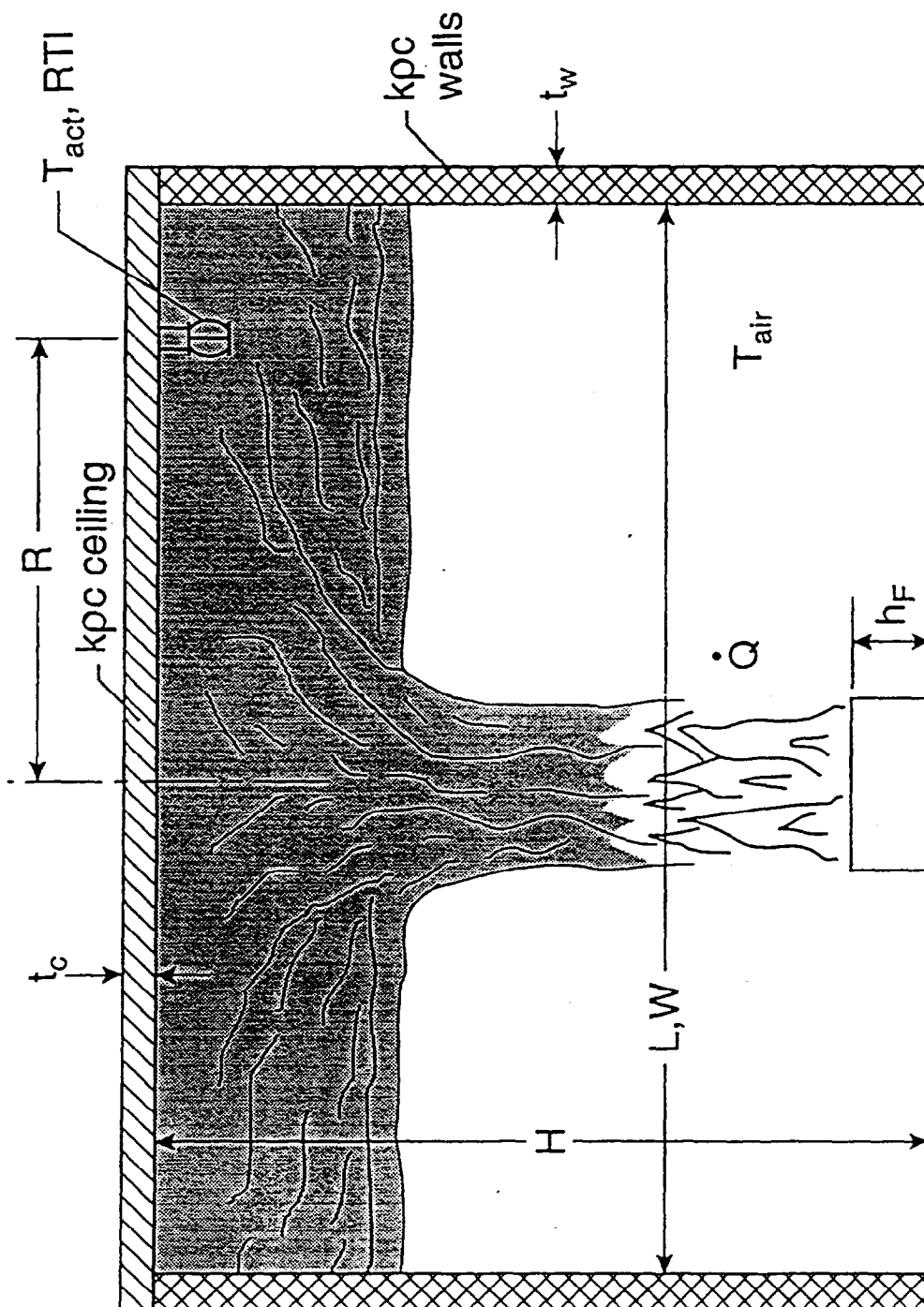


Figure 10. Schematic of Fire Simulator inputs.

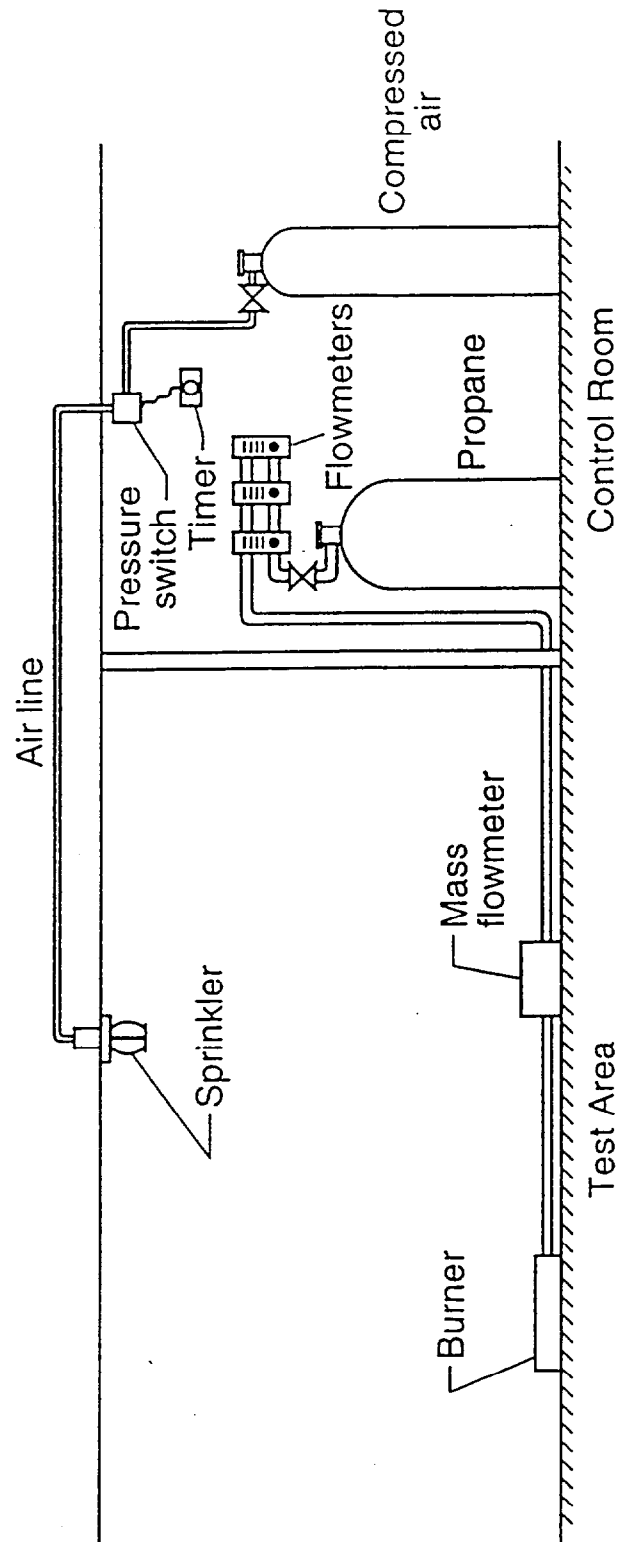


Figure 11. Schematic of sprinkler activation test configuration.

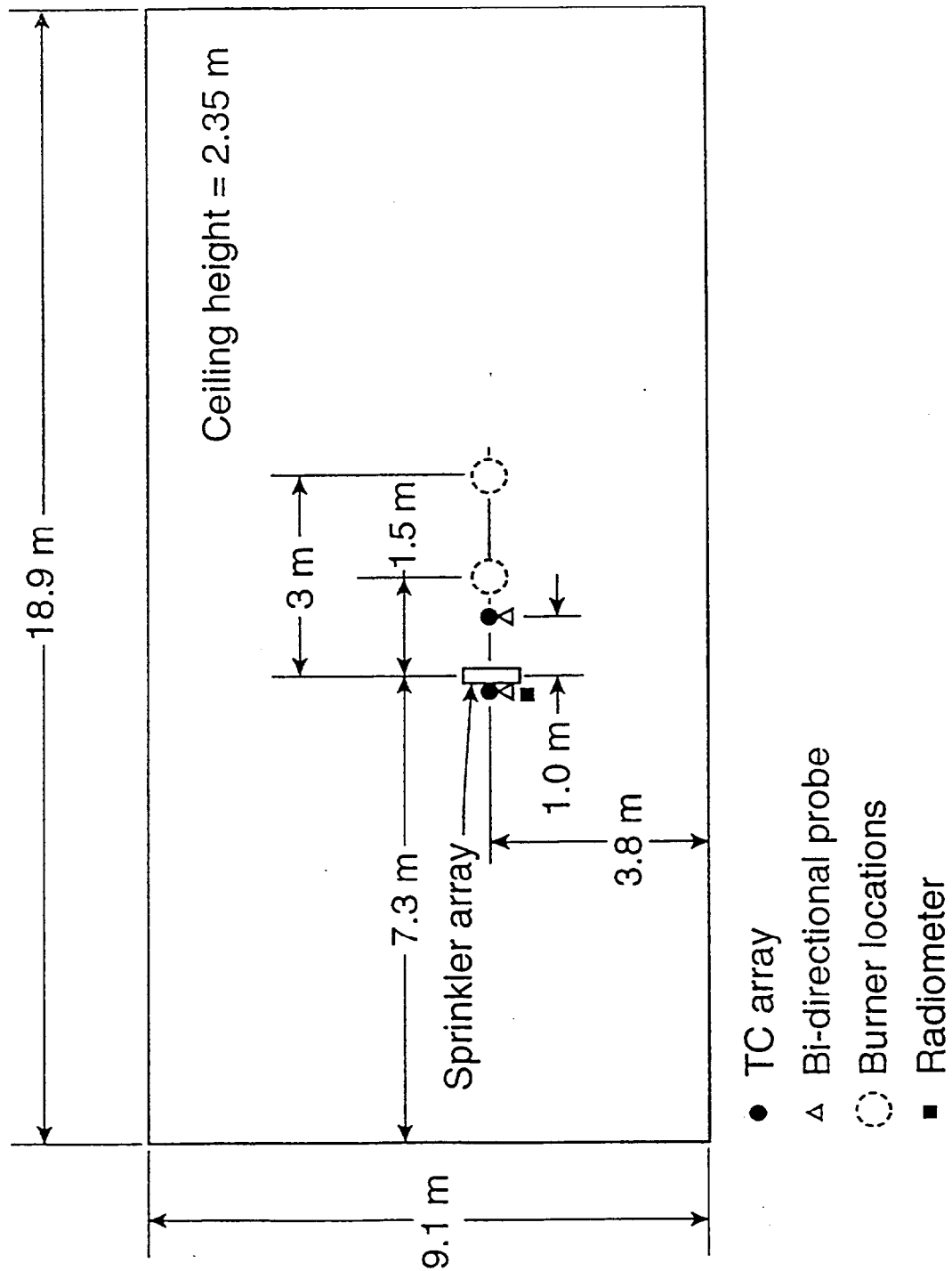


Figure 12. Schematic of sprinkler activation test instrumentation configuration (plan view).

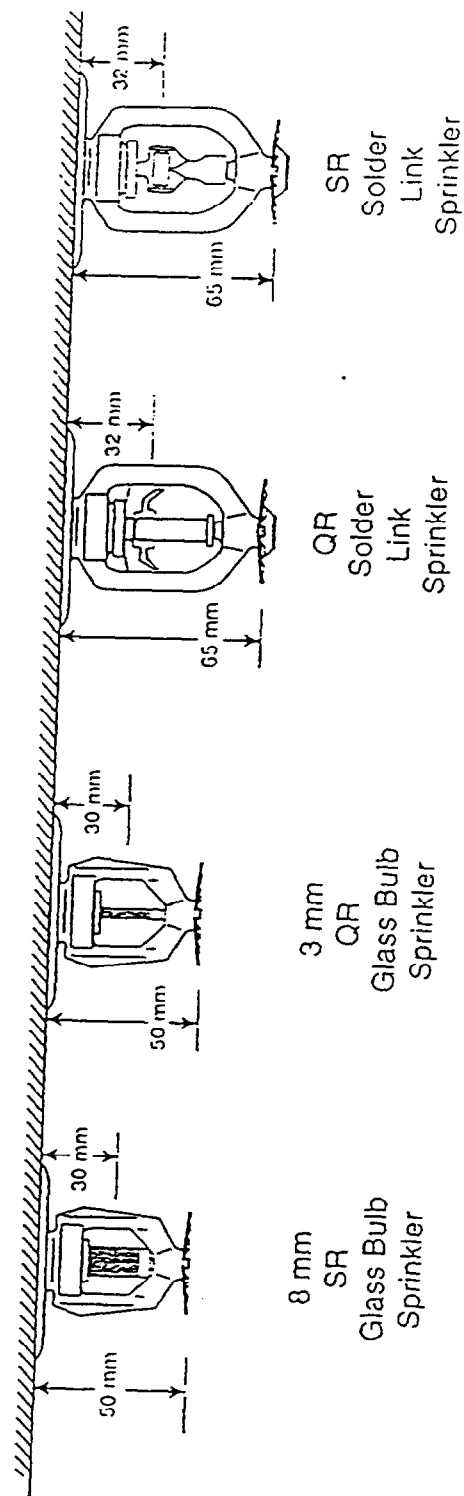


Figure 13. Schematic of sprinkler array with sprinklers in pendent position.

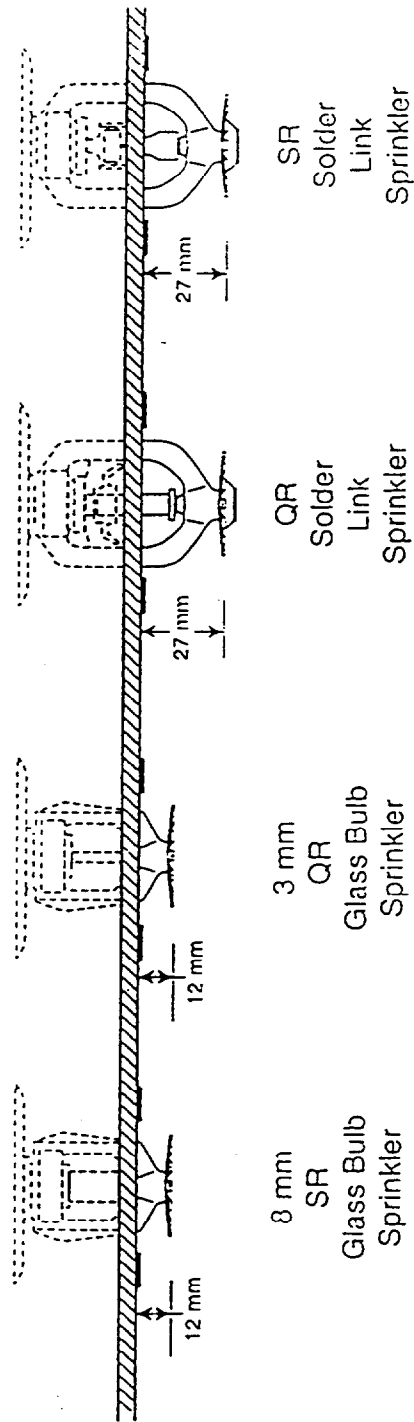


Figure 14. Schematic of sprinkler array with sprinklers in recessed position.



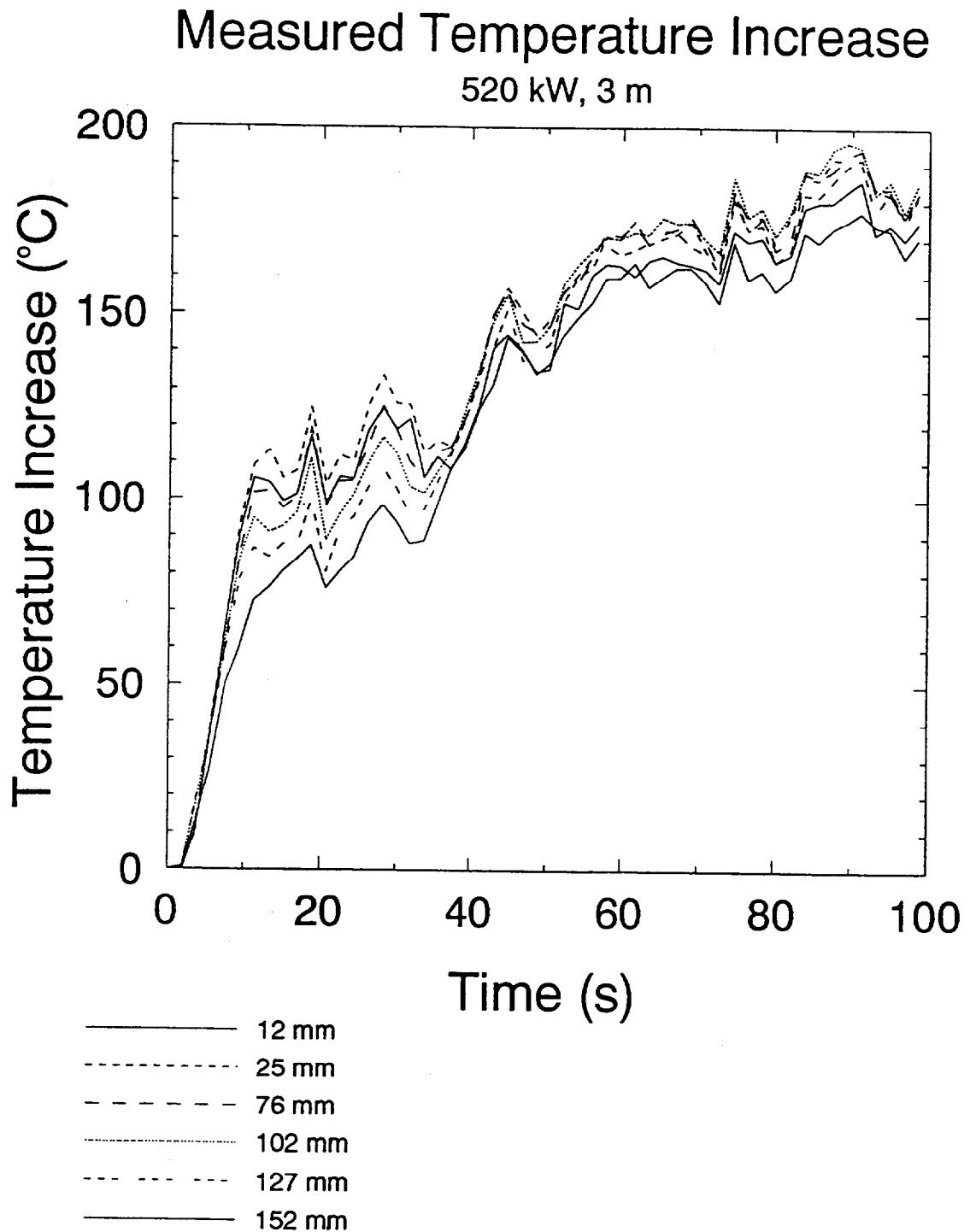


Figure 15. Average ceiling jet temperature increase: 520 kW, 3 m case.

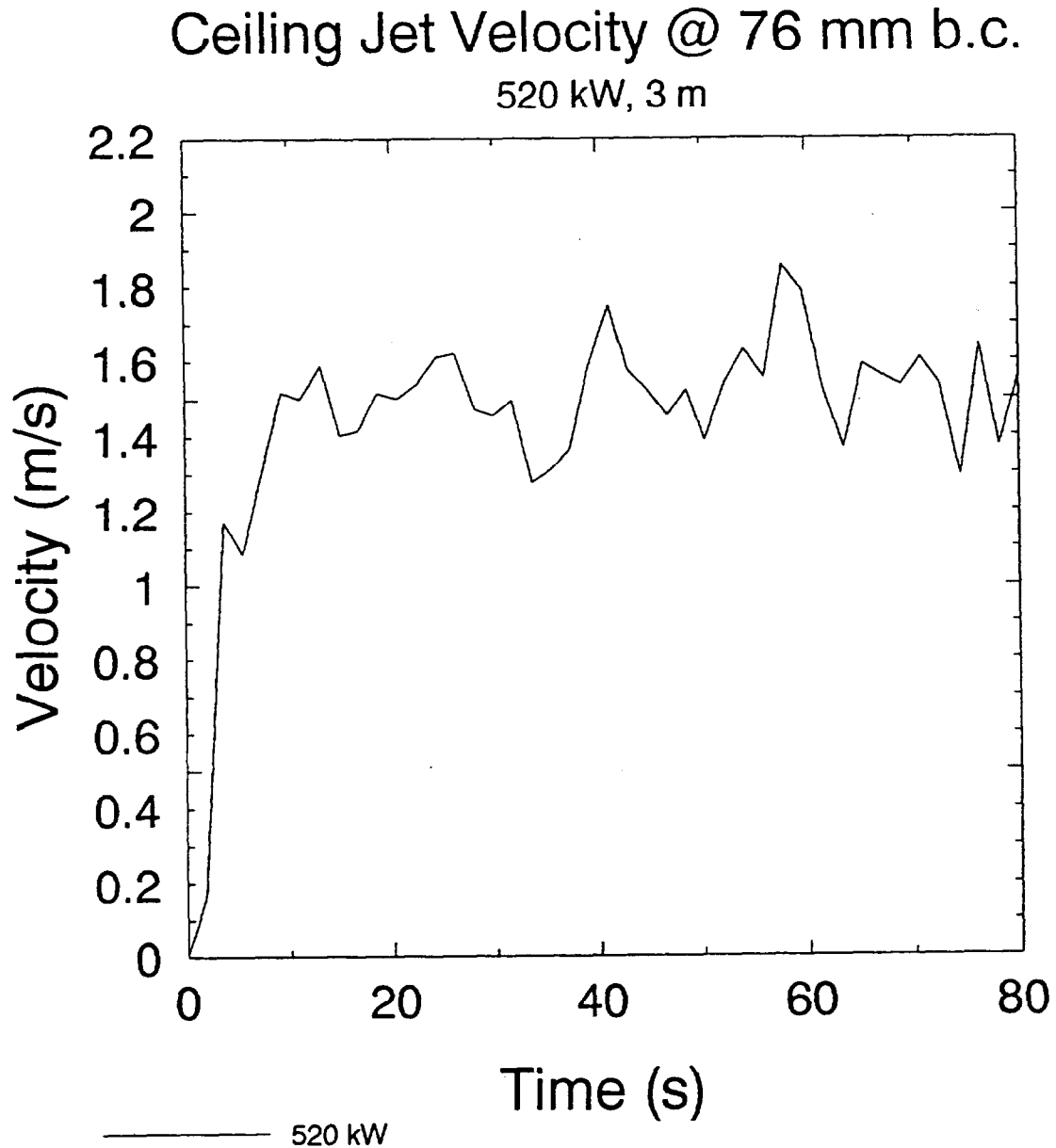


Figure 16. Average ceiling jet velocity: 520 kW, 3 m case.

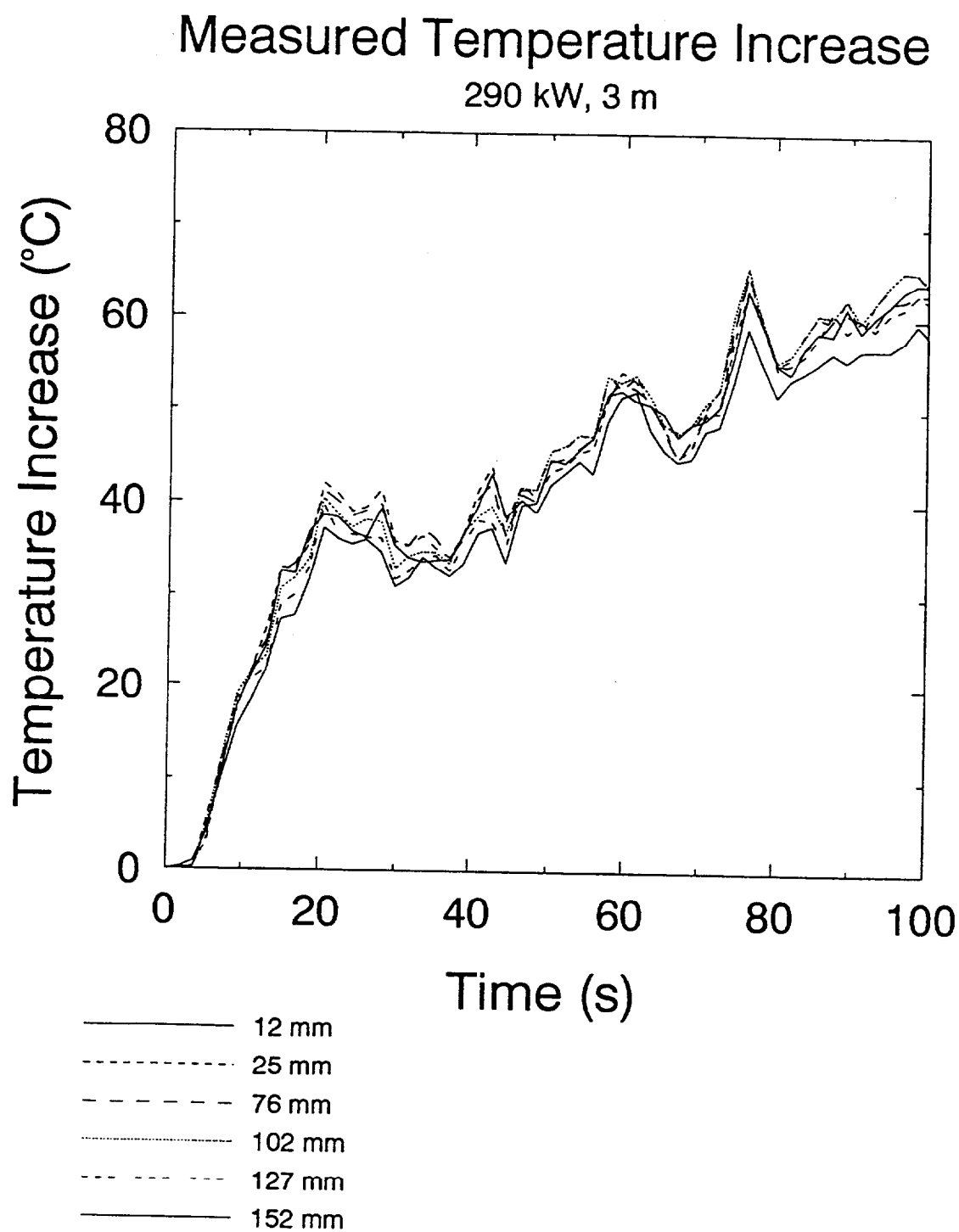


Figure 17. Average ceiling jet temperature increase: 290 kW, 3 m case.

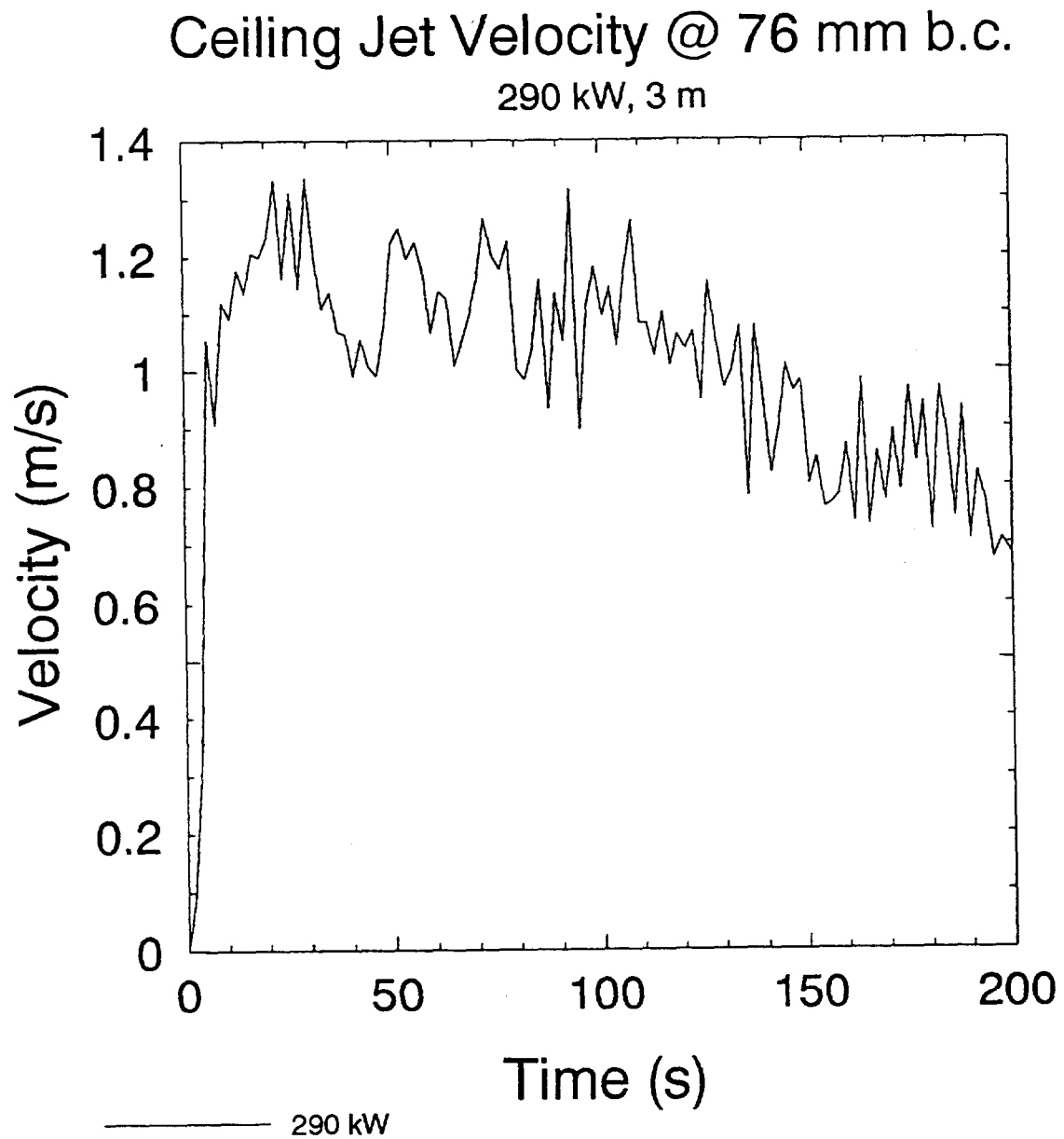


Figure 18. Average ceiling jet velocity: 290 kW, 3 m case.

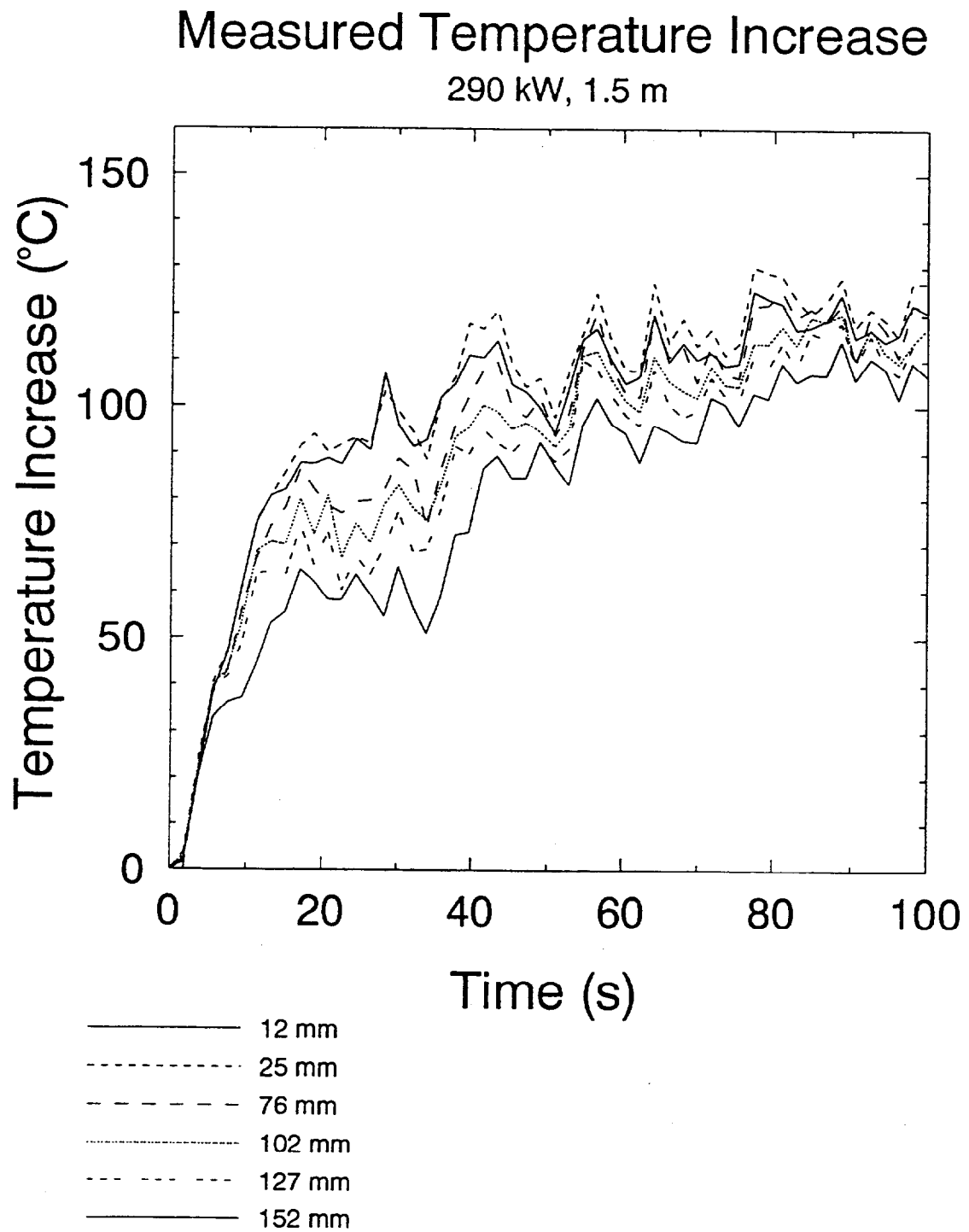


Figure 19. Average ceiling jet temperature increase: 290 kW, 1.5 m case.

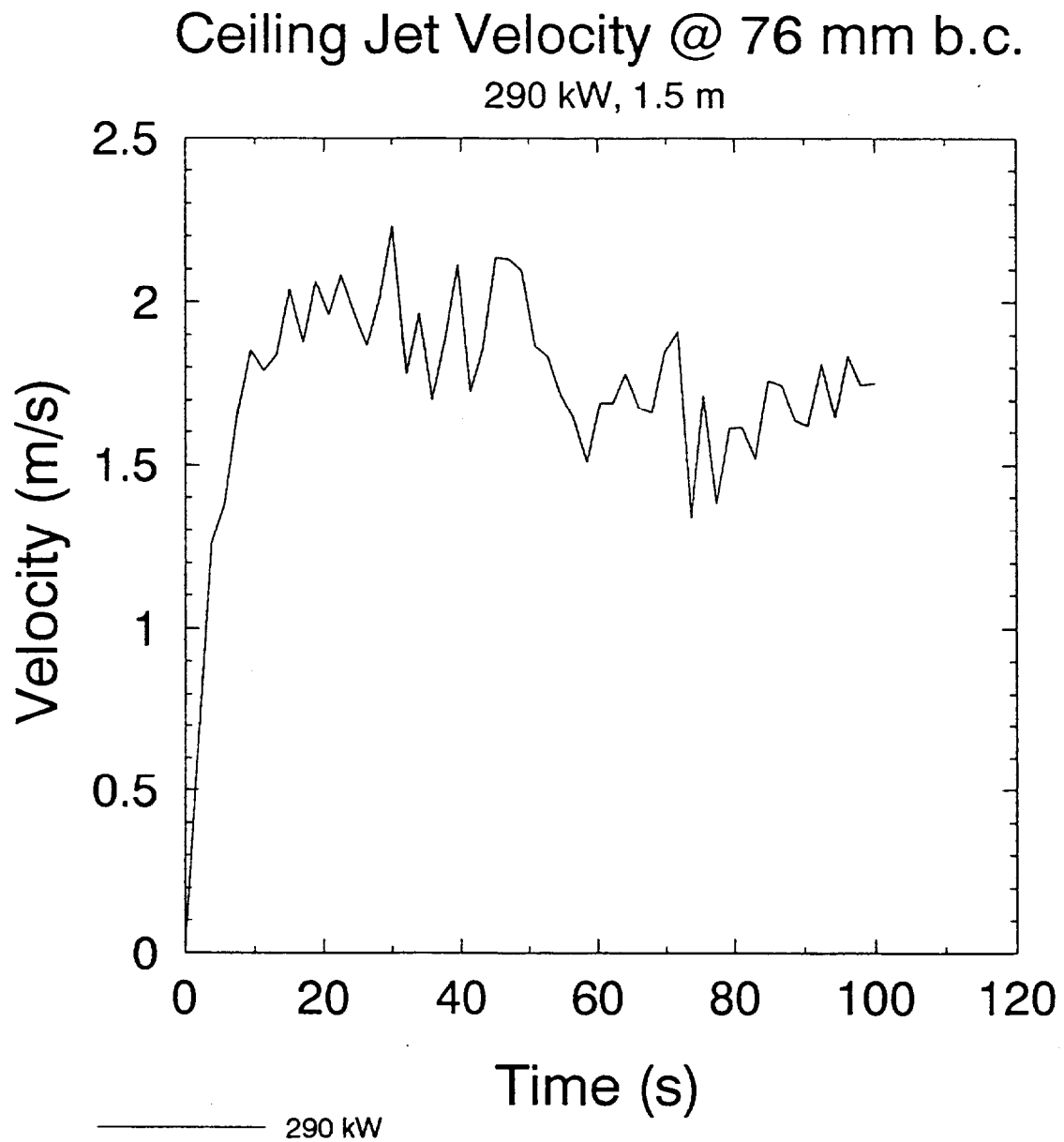


Figure 20. Average ceiling jet velocity: 290 kW, 1.5 m case.

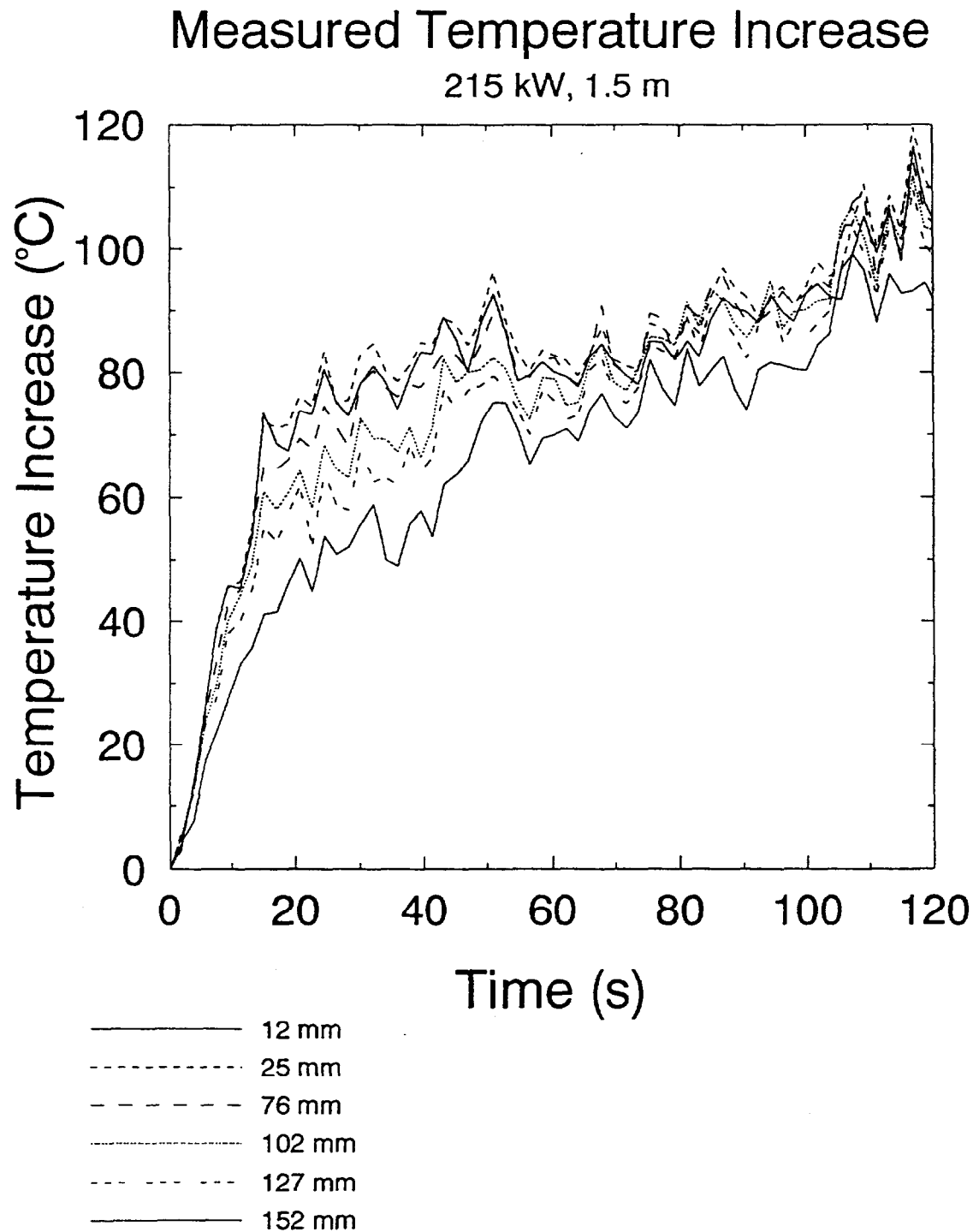


Figure 21. Average ceiling jet temperature increase: 215 kW, 1.5 m case.

Ceiling Jet Velocity @ 76 mm b.c.  
215 kW, 1.5 m

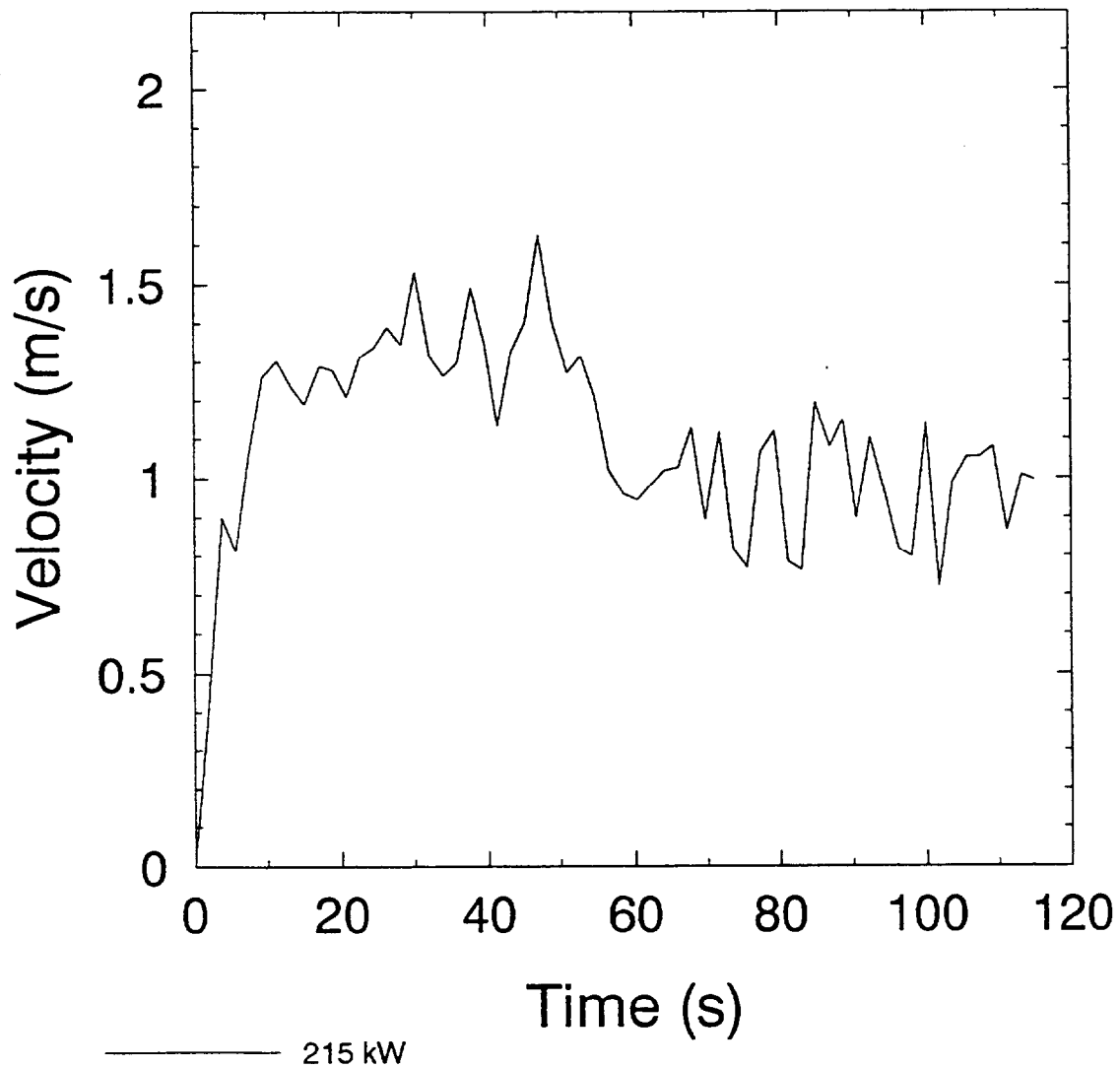


Figure 22. Average ceiling jet velocity: 215 kW, 1.5 m case.



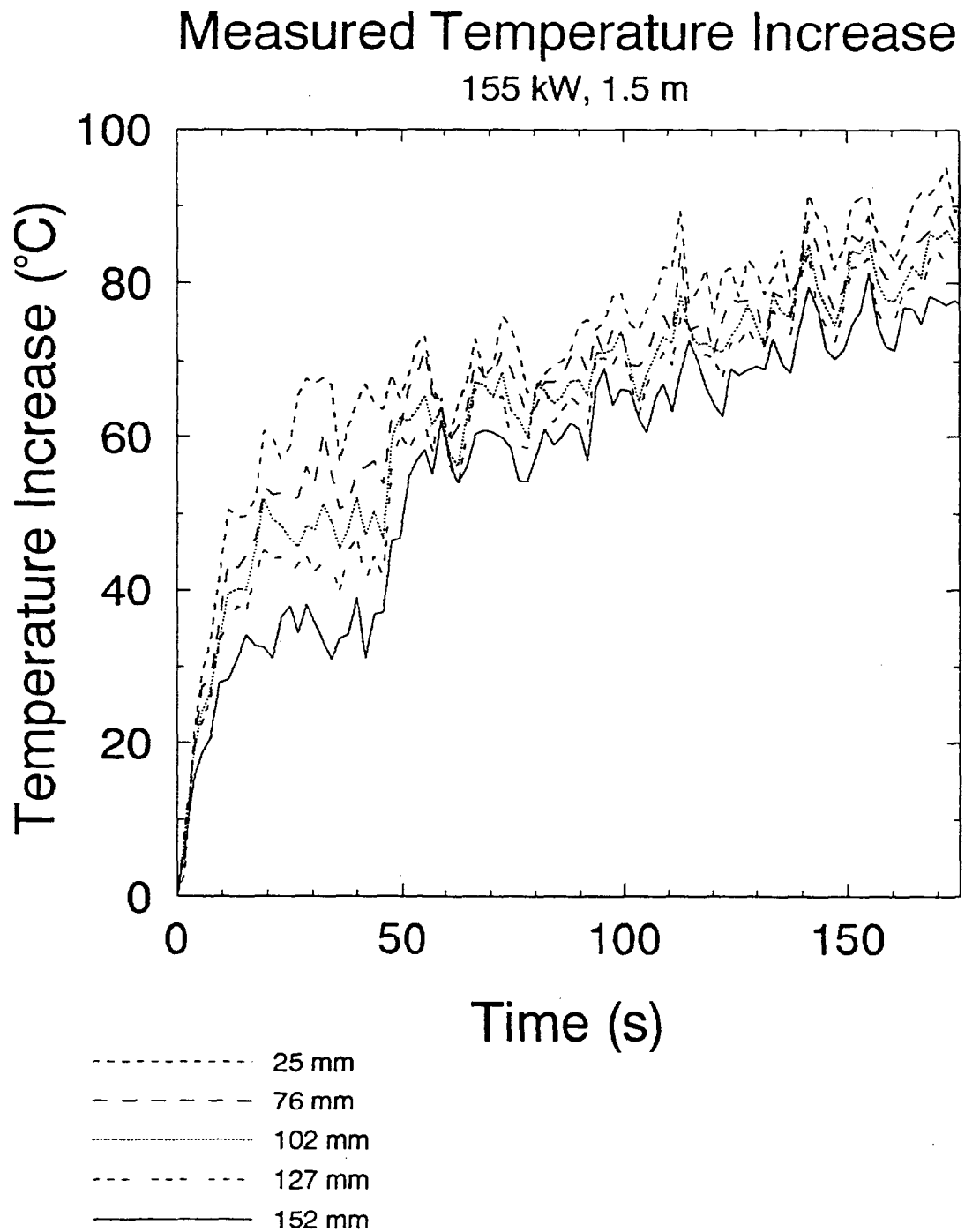


Figure 23. Average ceiling jet temperature increase: 155 kW, 1.5 m case.

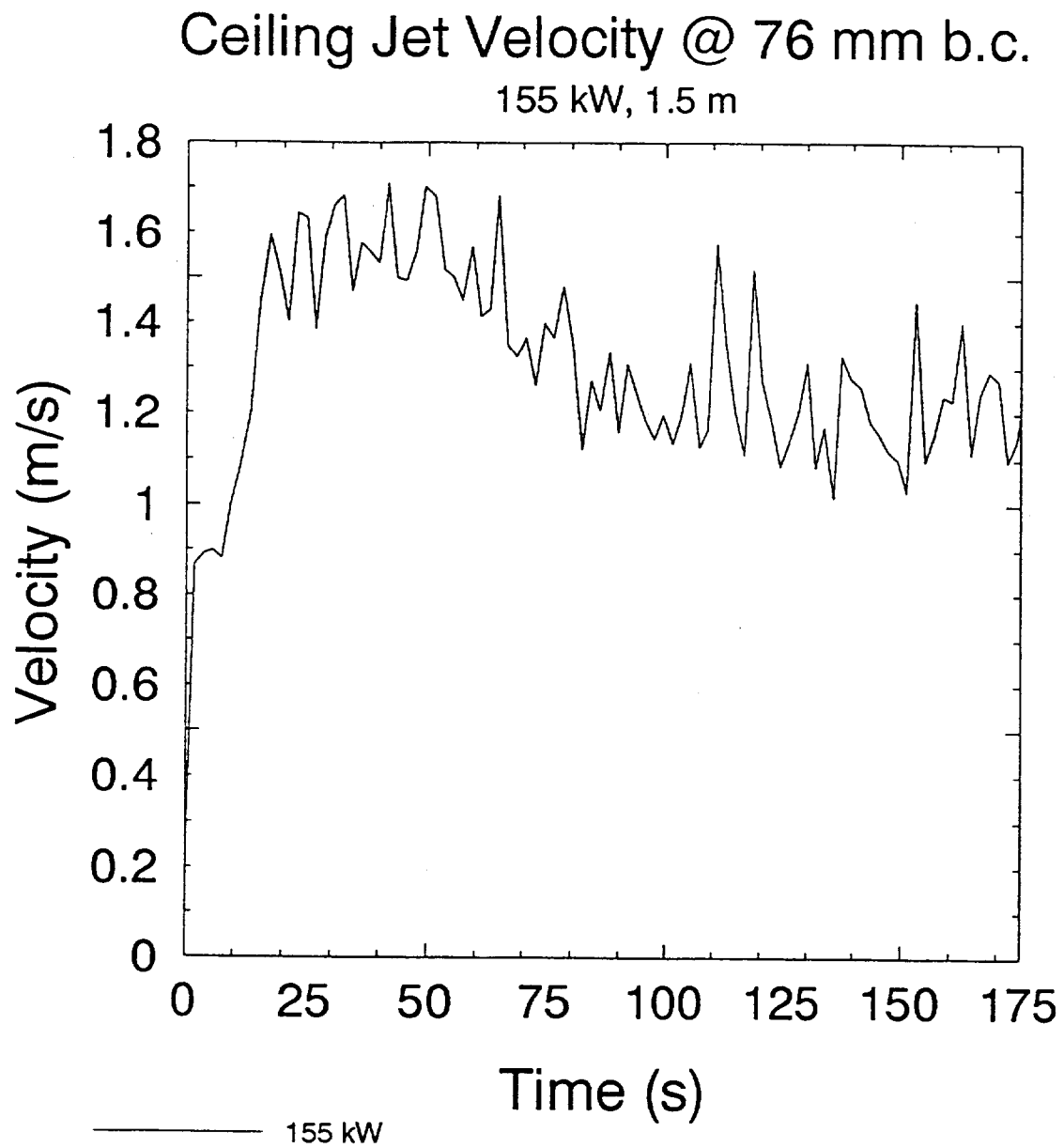


Figure 24. Average ceiling jet velocity: 155 kW, 1.5 m case.

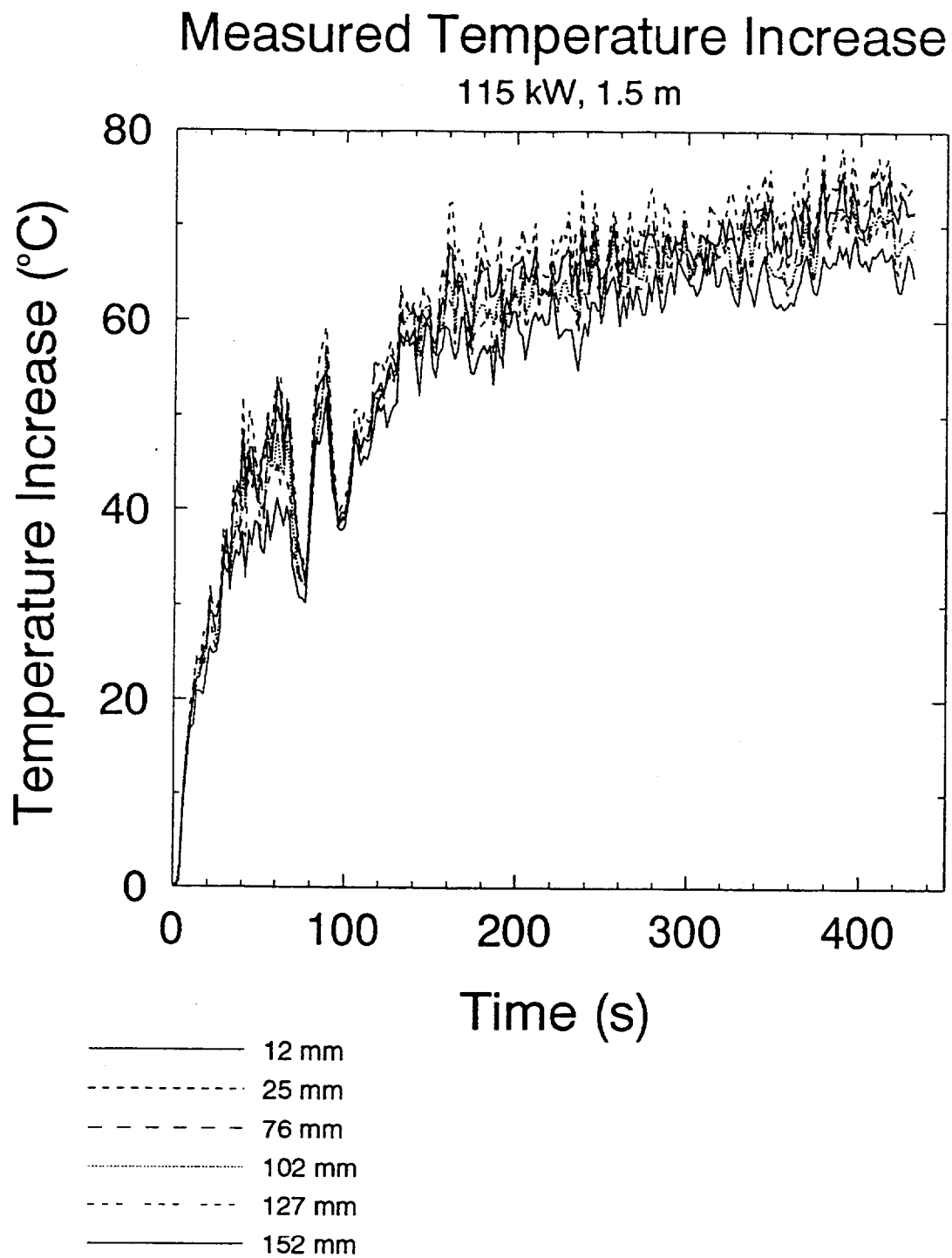


Figure 25. Average ceiling jet temperature increase: 115 kW, 1.5 m case.

## Ceiling Jet Velocity @ 76 mm b.c.

115 kW, 1.5 m

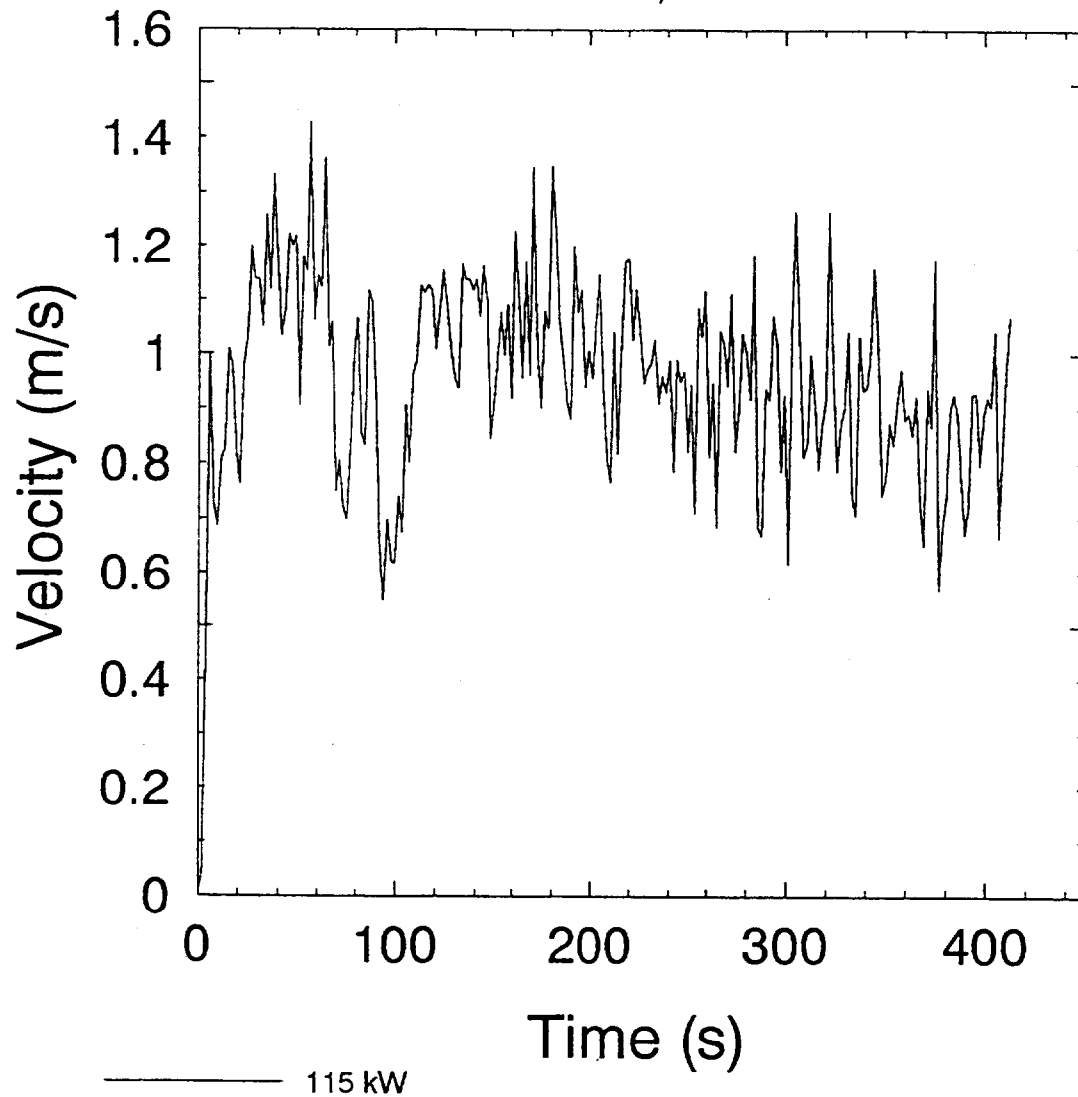


Figure 26. Average ceiling jet velocity: 115 kW, 1.5 m case.

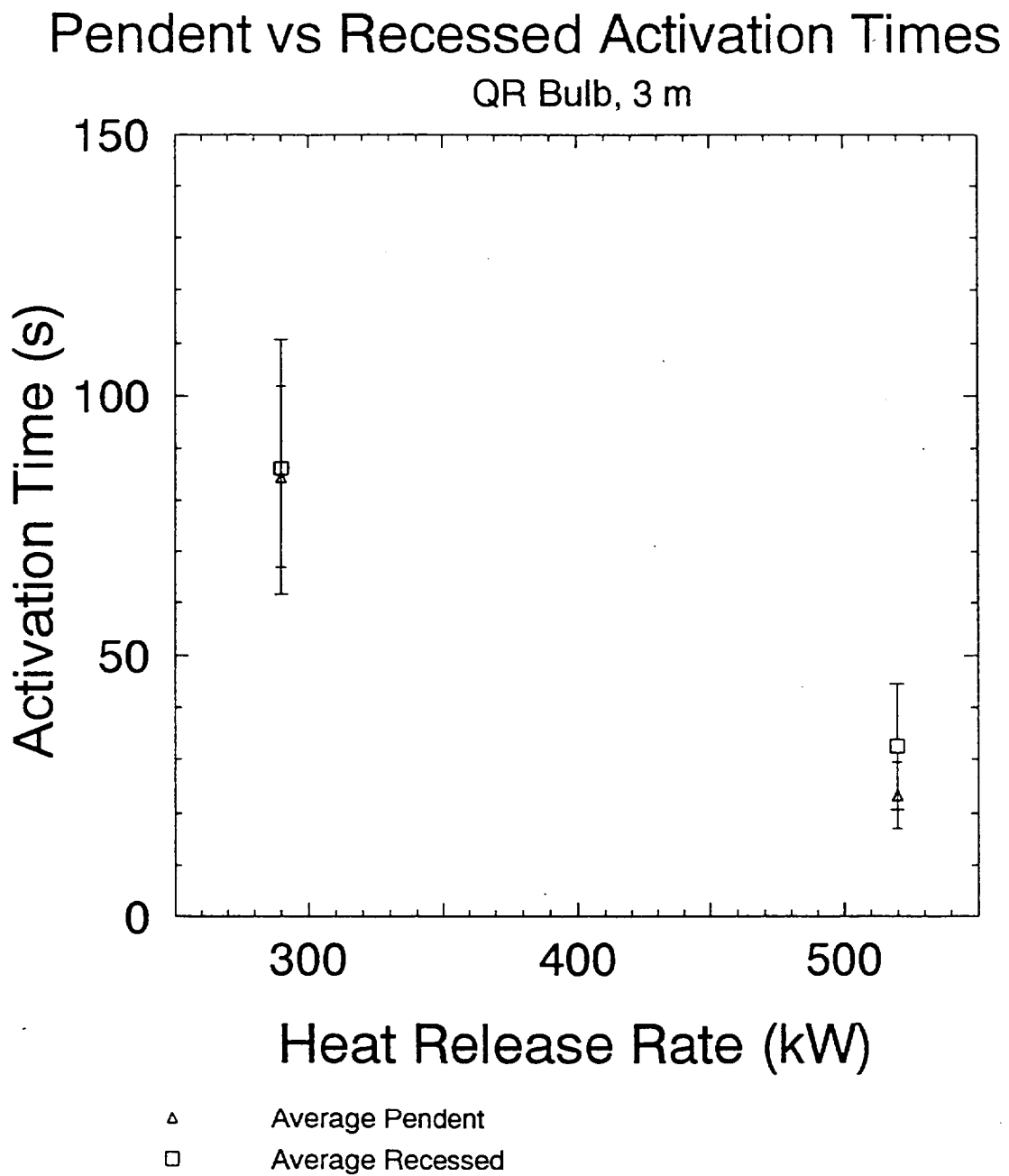


Figure 27. Pendent vs recessed activation times at  $r = 3$  m, QR bulb.

## Pendent vs Recessed Activation Times

QR Link, 3 m

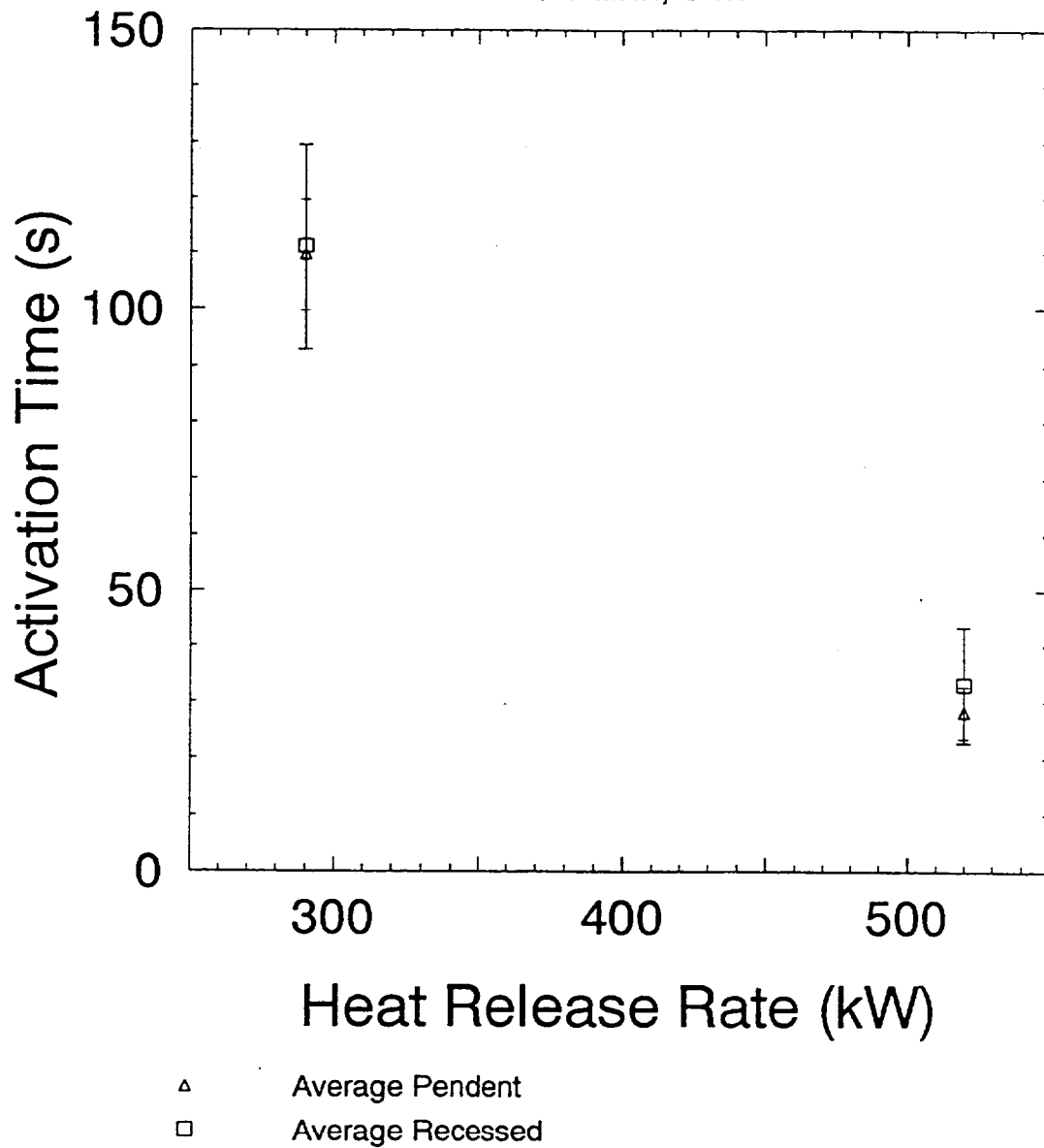


Figure 28. Pendent vs recessed activation times at  $r = 3$  m, QR link.

## Pendent vs Recessed Activation Times

SS Bulb, 3 m

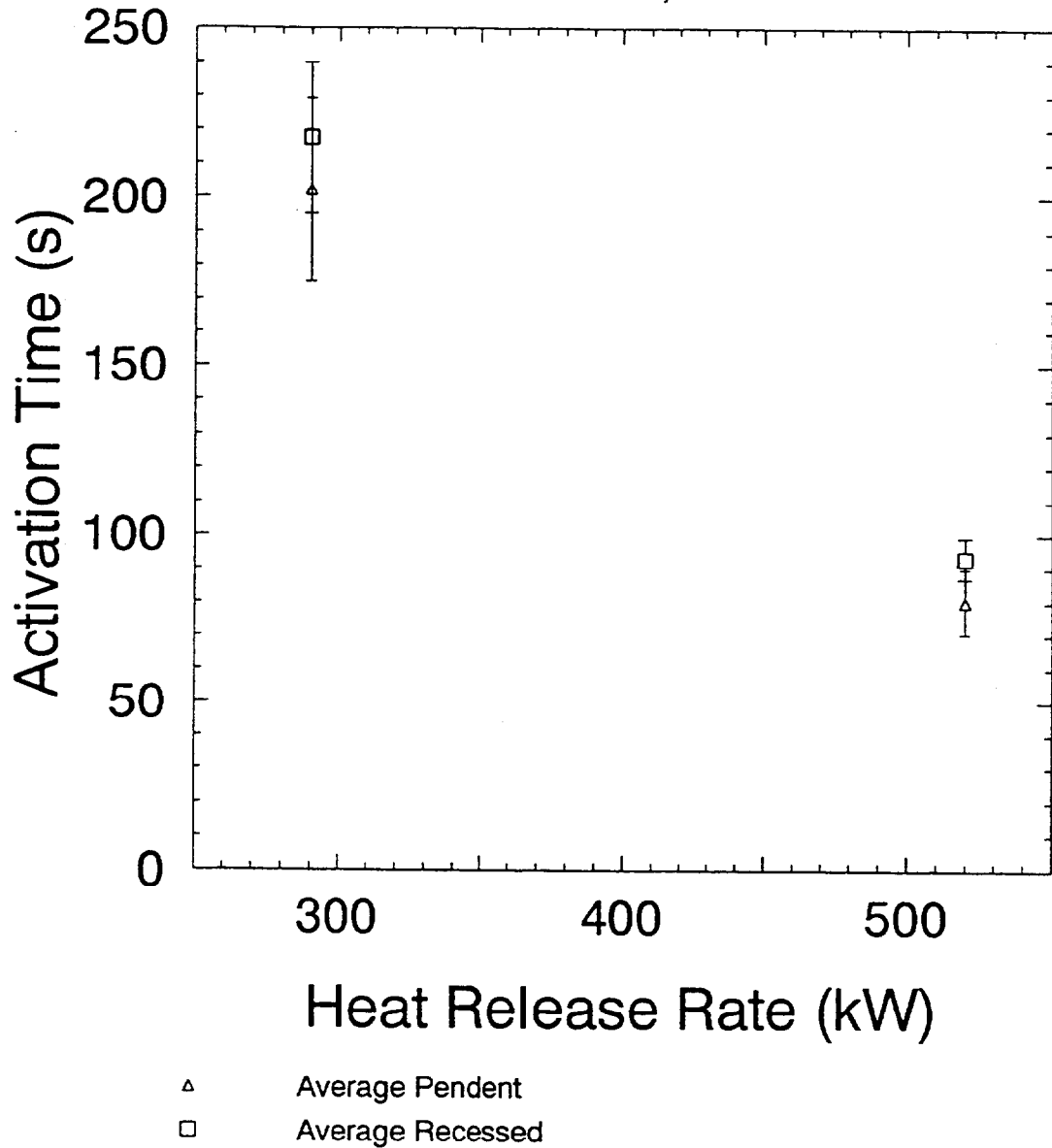


Figure 29. Pendent vs recessed activation times at  $r = 3$  m, SS bulb.

## Pendent vs Recessed Activation Times

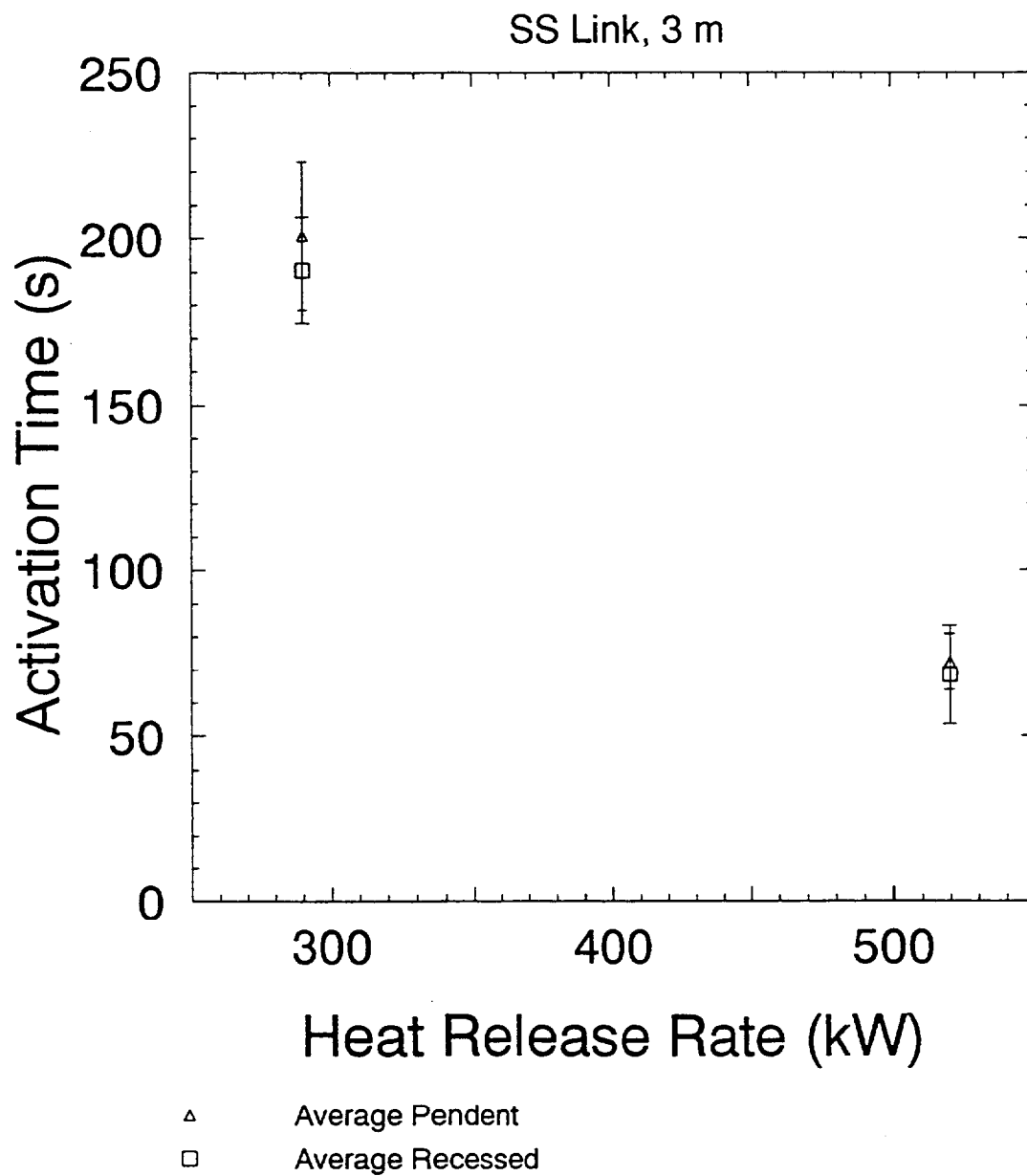


Figure 30. Pendent vs recessed activation times at  $r = 3$  m, SS link.



## Pendent vs Recessed Activation Times

QR Bulb, 1.5 m

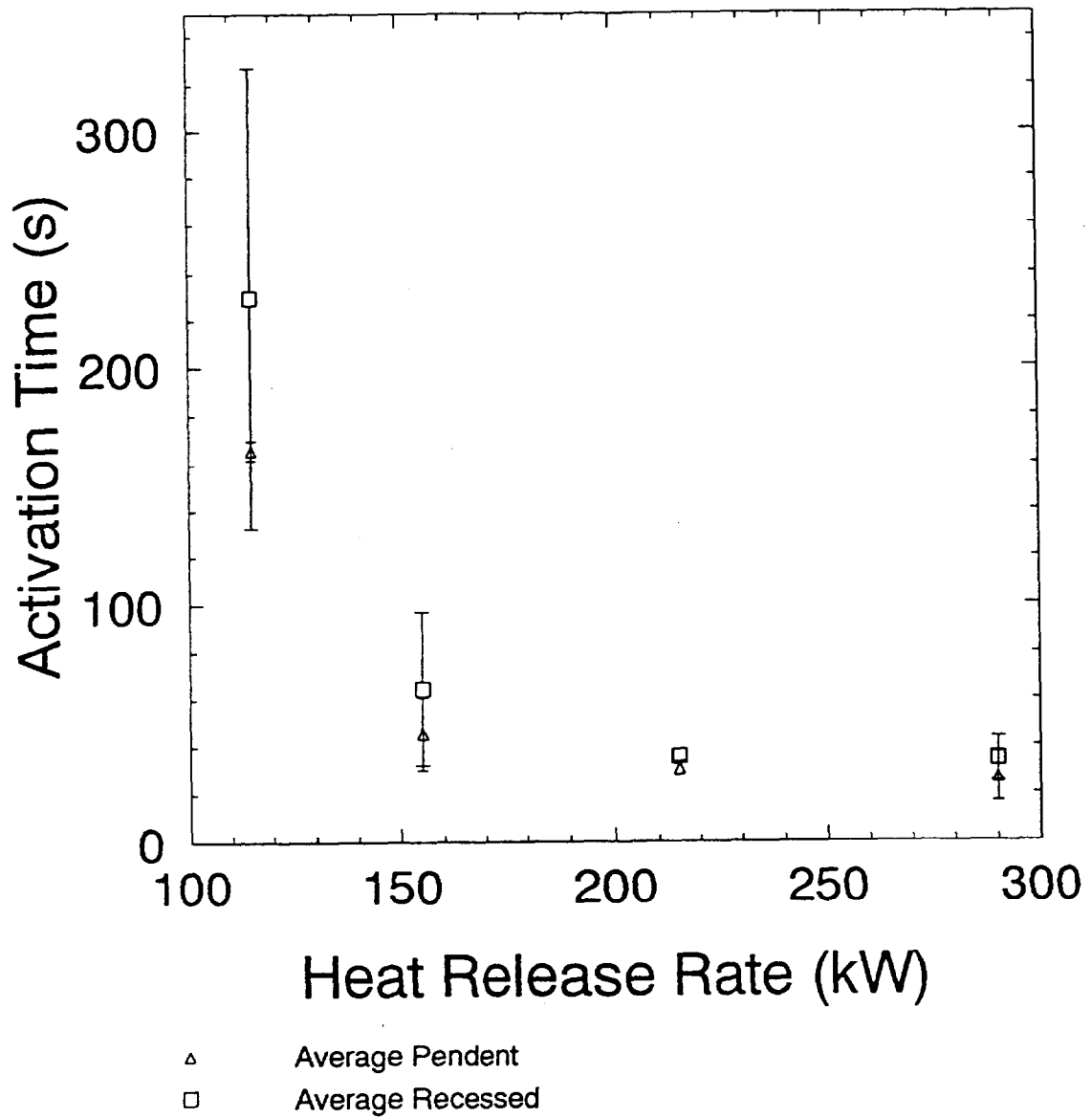


Figure 31. Pendent vs recessed activation times at  $r = 1.5$  m, QR bulb.

# Pendent vs Recessed Activation Times

QR Link, 1.5 m

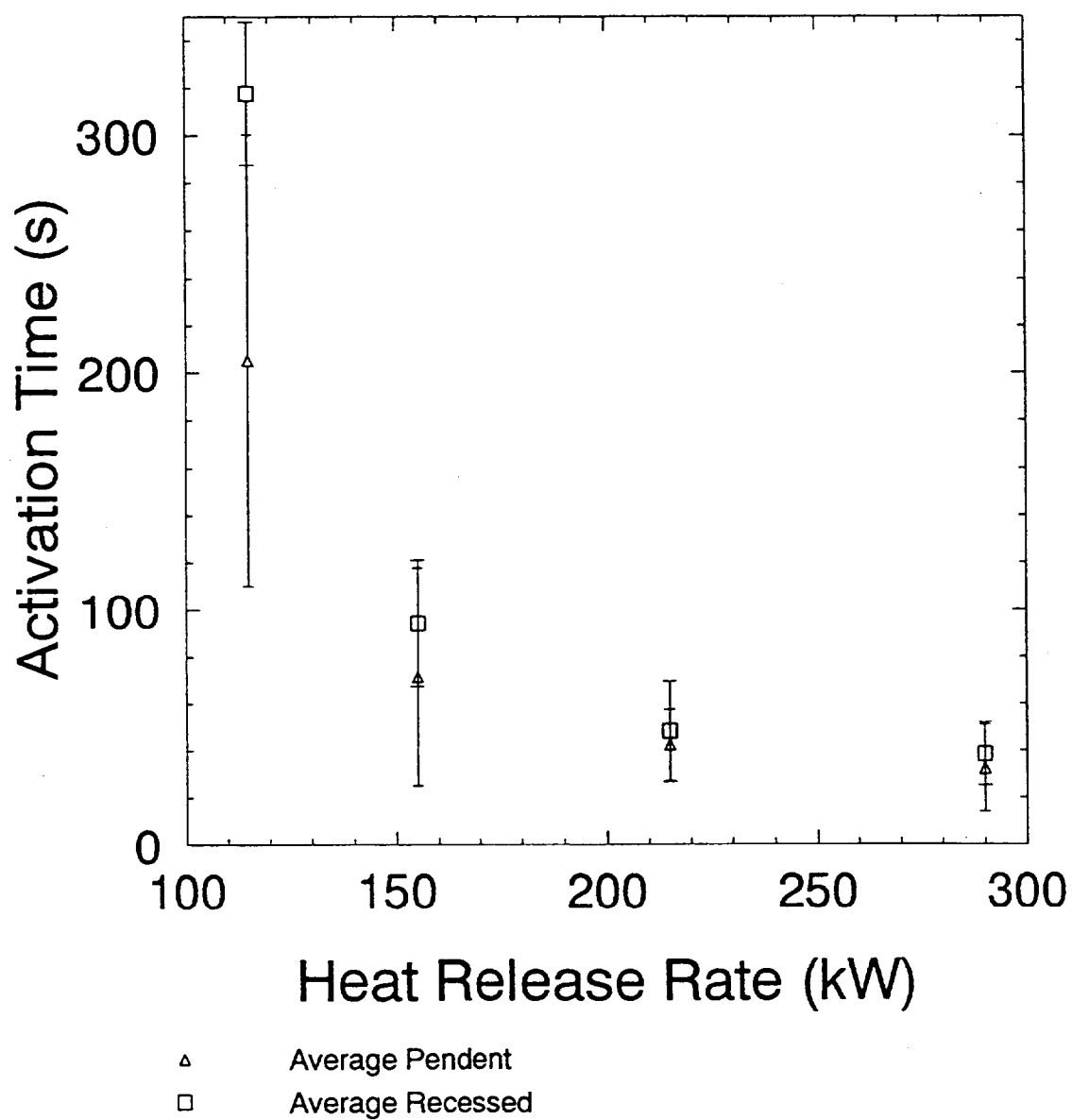


Figure 32. Pendent vs recessed activation times at  $r = 1.5$  m, QR link.

## Pendent vs Recessed Activation Times

SS Bulb, 1.5 m

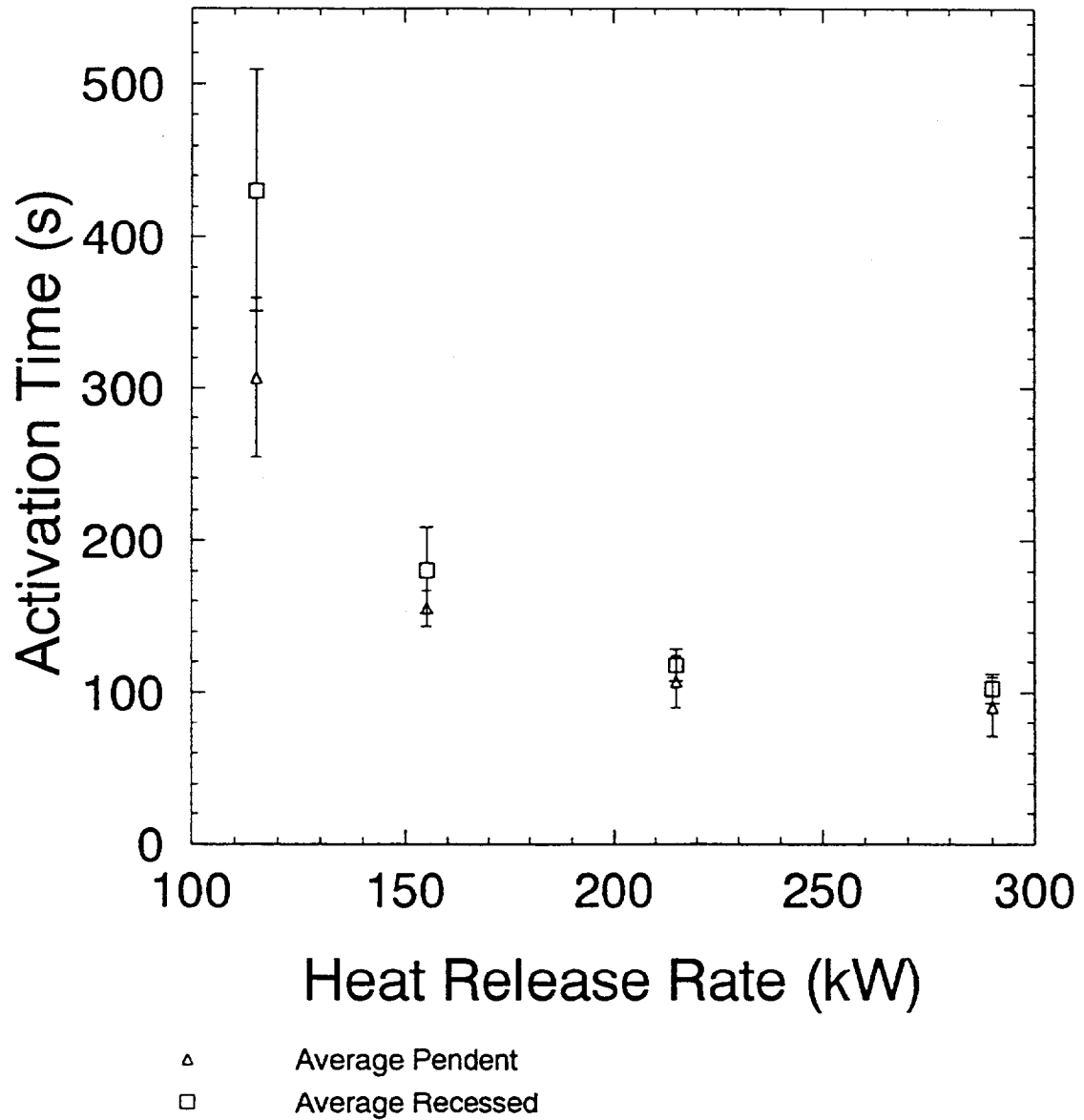


Figure 33. Pendent vs recessed activation times at  $r = 1.5$  m, SS bulb.

## Pendent vs Recessed Activation Times

SS Link, 1.5 m

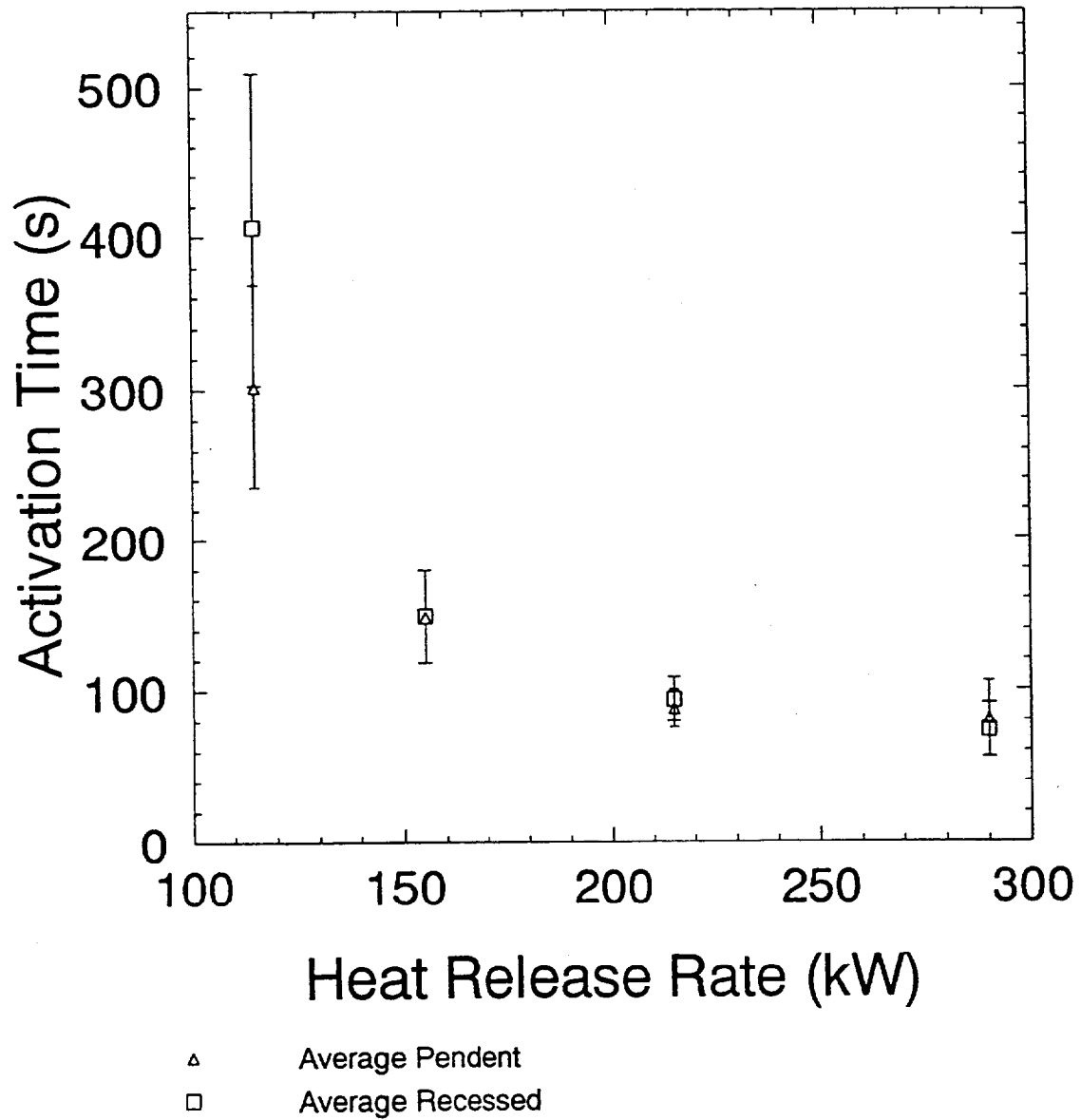


Figure 34. Pendent vs recessed activation times at  $r = 1.5$  m, SS link.

## Pendent vs Predicted Activation Times

QR Bulb, 3 m

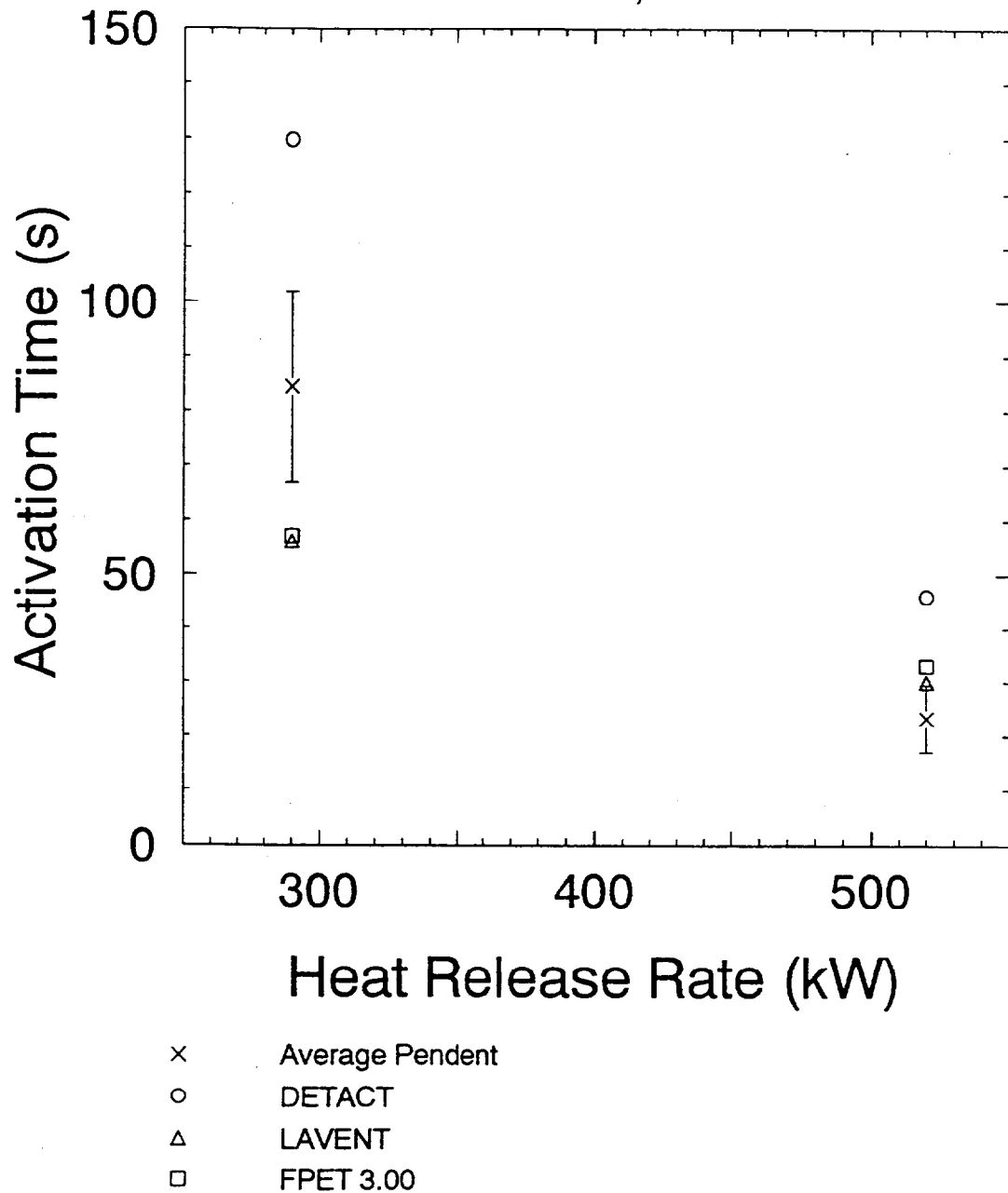


Figure 35. Actual vs predicted activation times at  $r = 3$  m, QR bulb.

# Pendent vs Predicted Activation Times

QR Link, 3 m

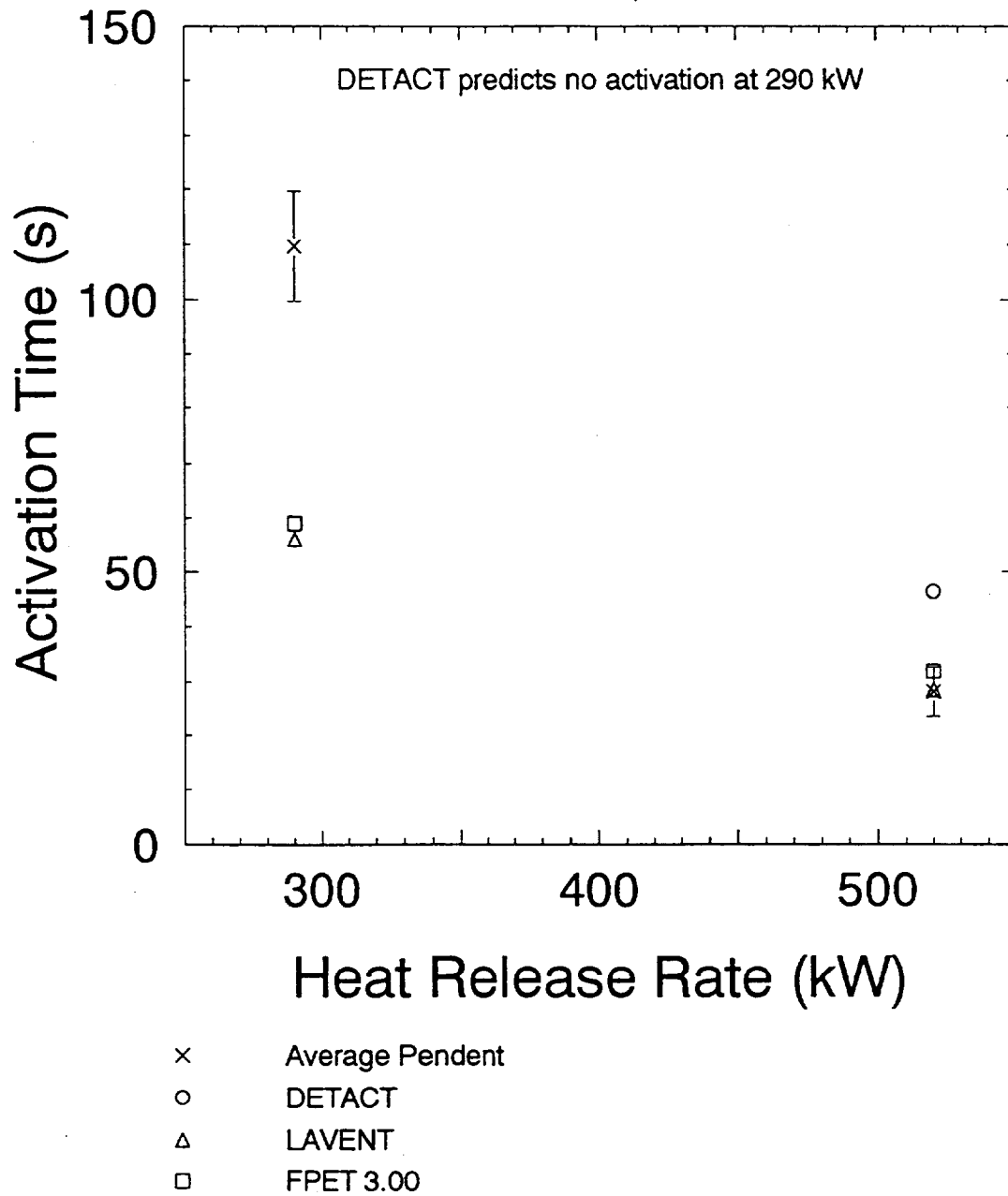
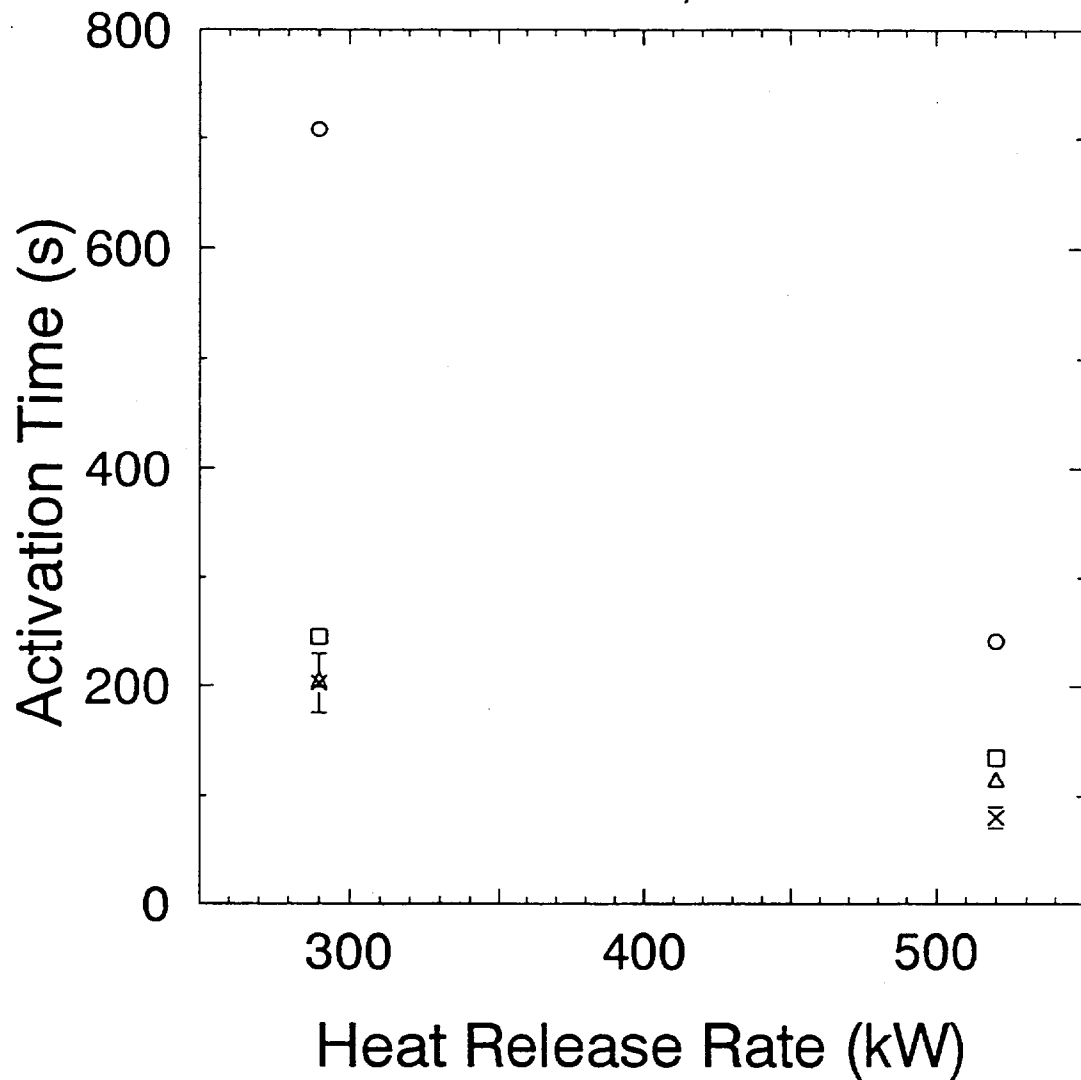


Figure 36. Actual vs predicted activation times at  $r = 3$  m, QR link.

## Pendent vs Predicted Activation Times

SS Bulb, 3 m

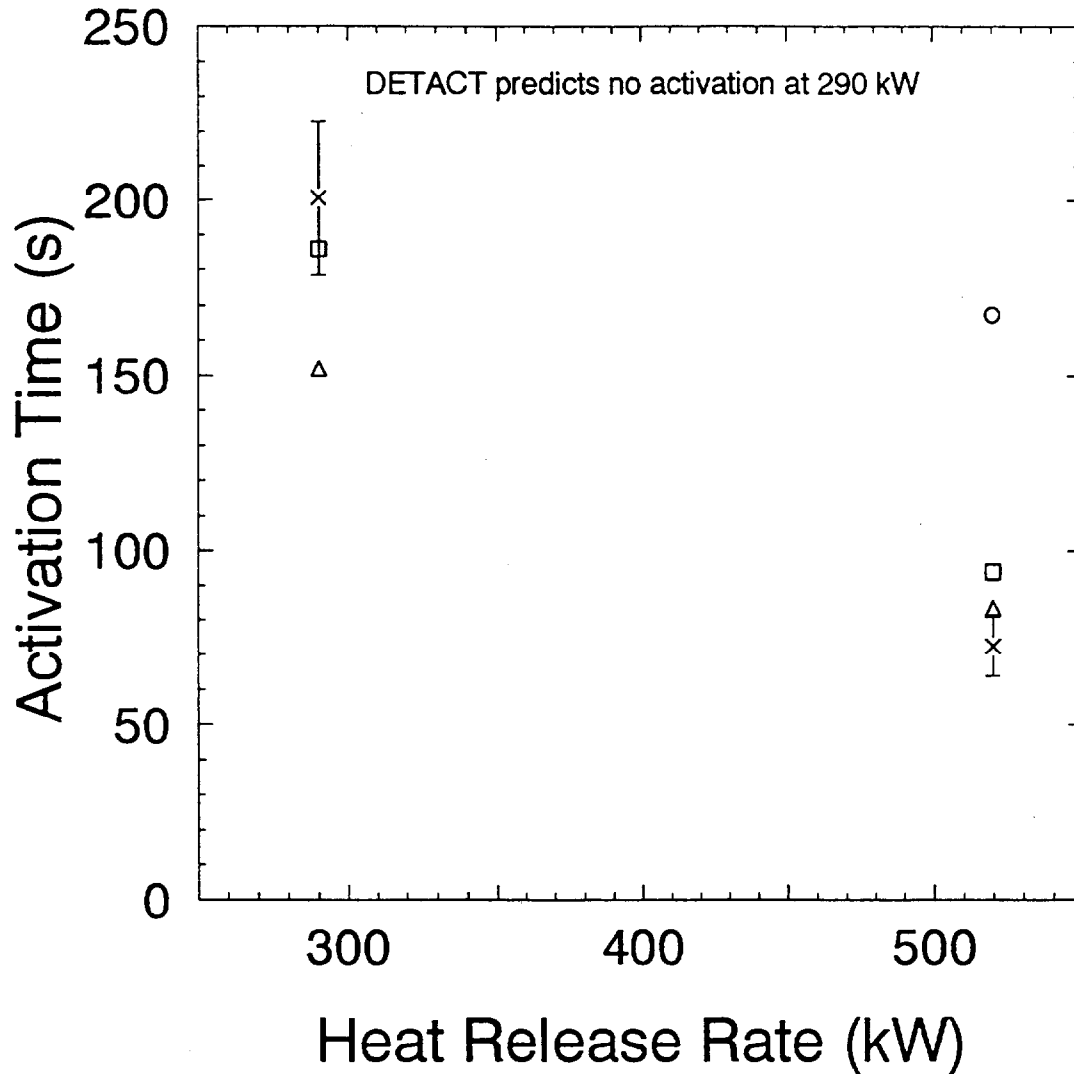


- × Average Pendent
- DETACT
- △ LAVENT
- FPET 3.00

Figure 37. Actual vs predicted activation times at  $r = 3$  m, SS bulb.

# Pendent vs Predicted Activation Times

SS Link, 3 m



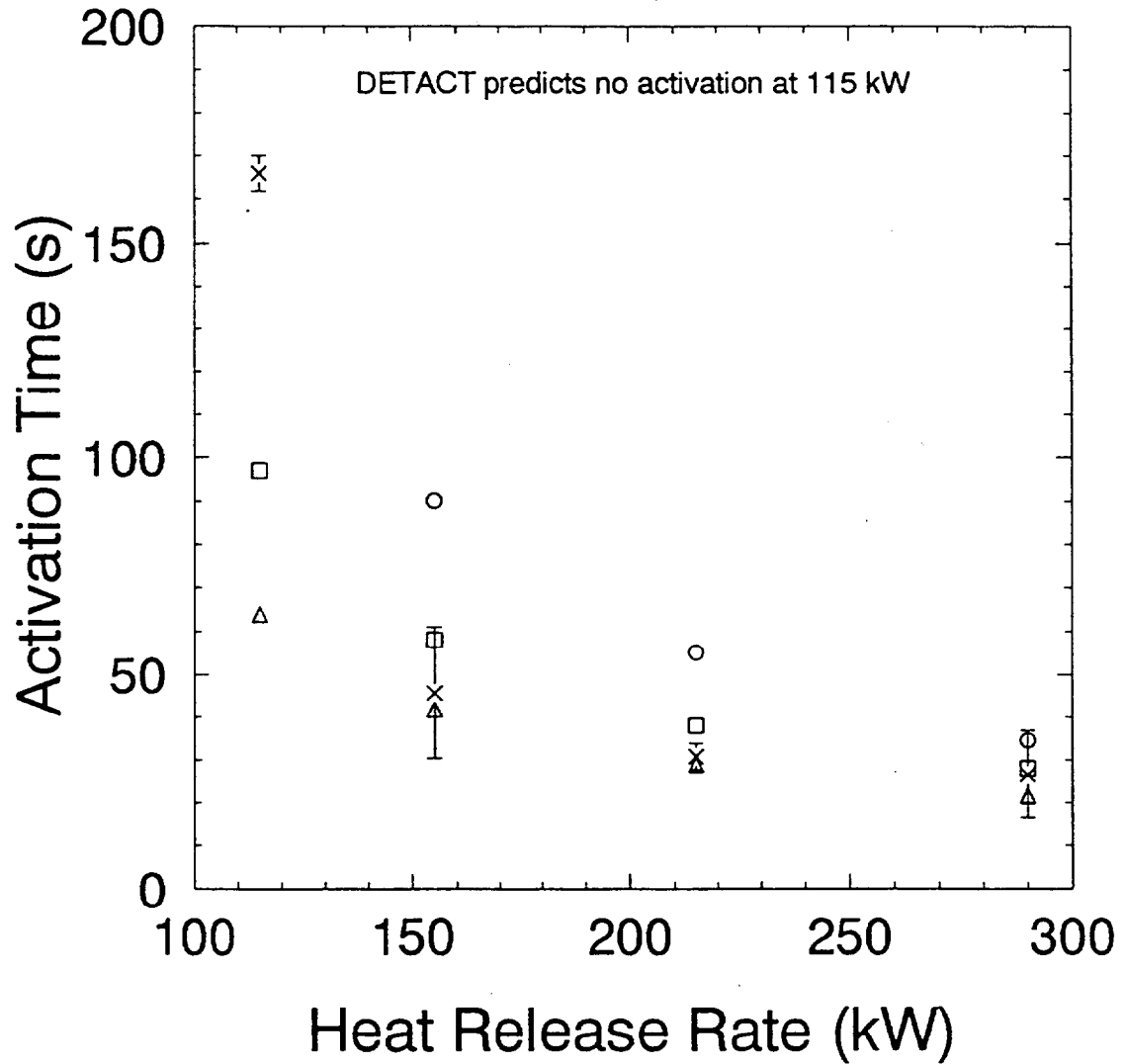
- × Average Pendent
- DETACT
- △ LAVENT
- FPET 3.00

Figure 38. Actual vs predicted activation times at  $r = 3$  m, SS link



## Pendent vs Predicted Activation Times

QR Bulb, 1.5 m

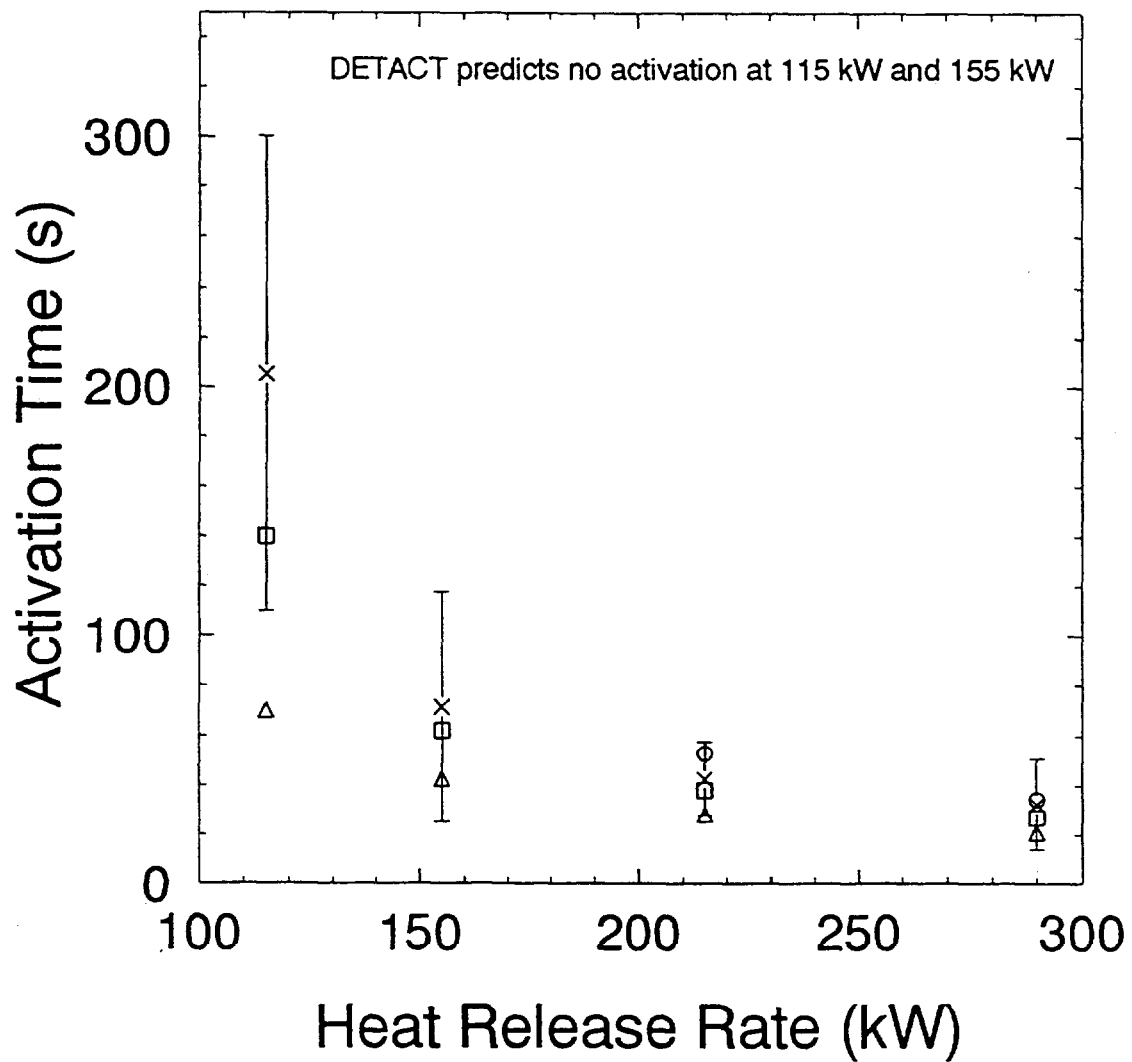


- × Average Pendent
- DETACT
- △ LAVENT
- FPET 3.00

Figure 39. Actual vs predicted activation times at  $r = 1.5$  m, QR bulb.

# Pendent vs Predicted Activation Times

QR Link, 1.5 m

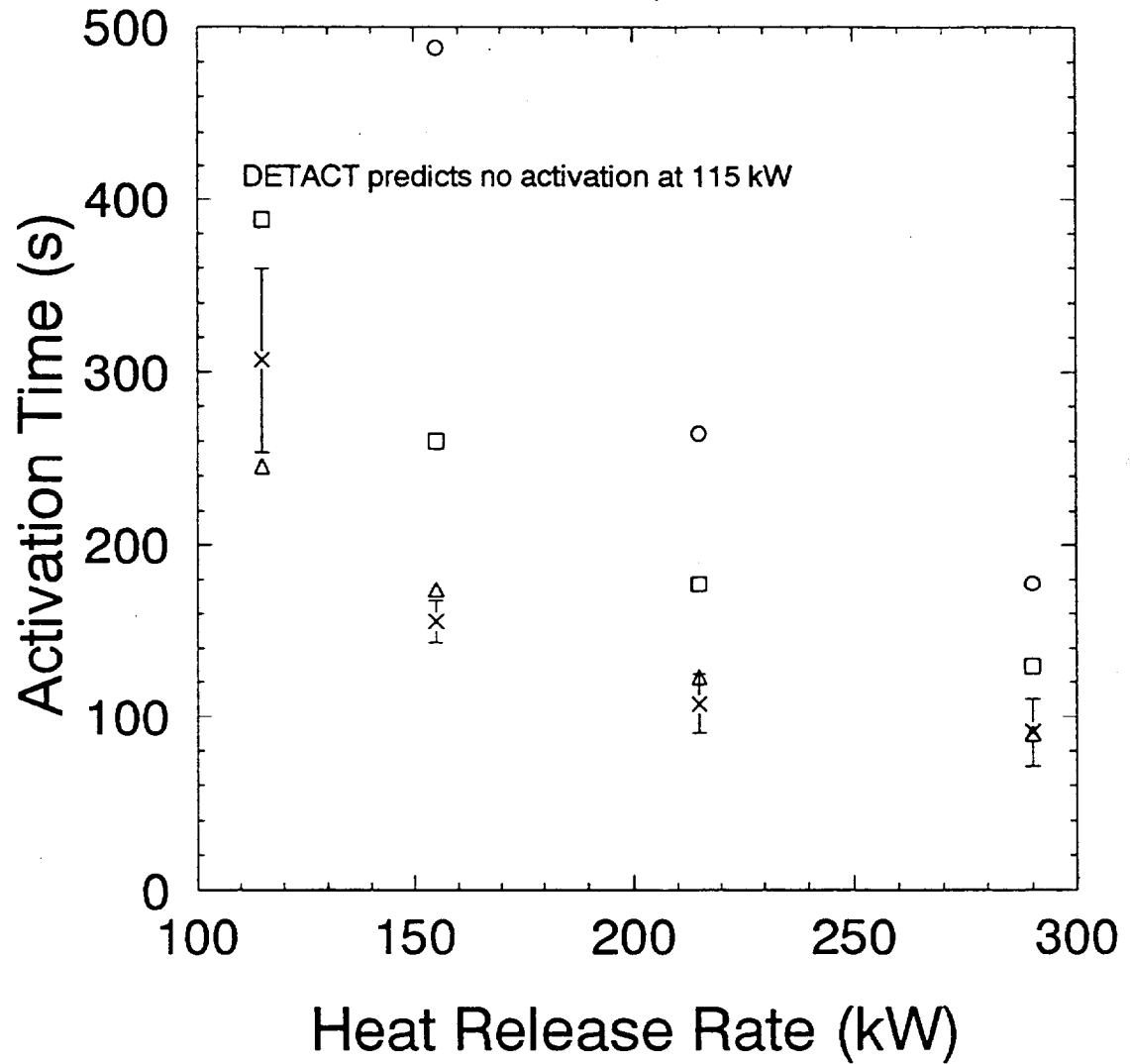


- x Average Pendent
- o DETACT
- Δ LAVENT
- FPET 3.00

Figure 40. Actual vs predicted activation times at  $r = 1.5$  m, QR link.

## Pendent vs Predicted Activation Times

SS Bulb, 1.5 m

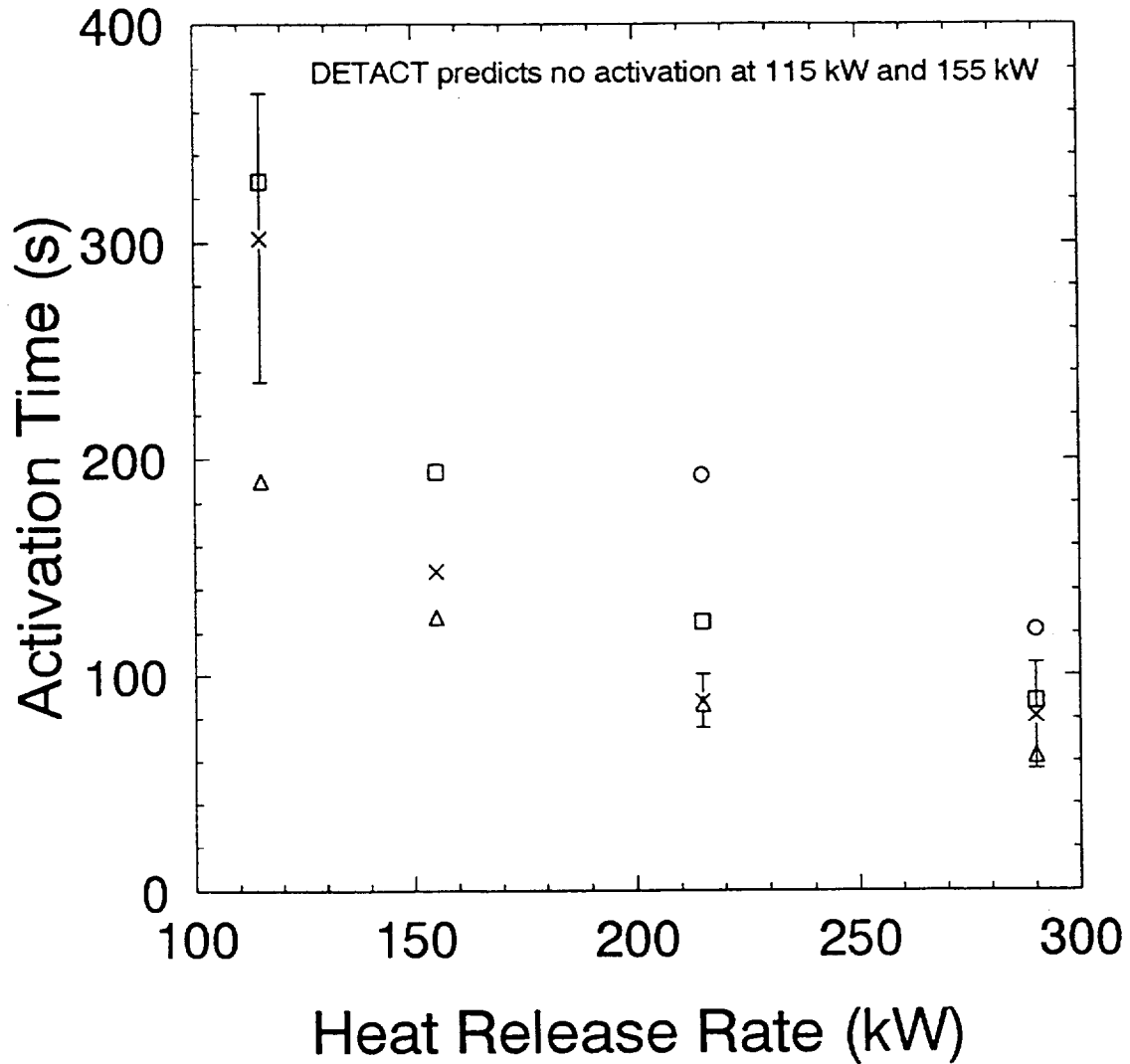


- × Average Pendent
- DETACT
- △ LAVENT
- FPET 3.00

Figure 41. Actual vs predicted activation times at  $r = 1.5$  m, SS bulb.

# Pendent vs Predicted Activation Times

SS Link, 1.5 m



- × Average Pendent
- DETACT
- Δ LAVENT
- FPET 3.00

Figure 42. Actual vs predicted activation times at  $r = 1.5$  m, SS link.

## C. J. Temperature Increase Comparison

520 kW, 3 m

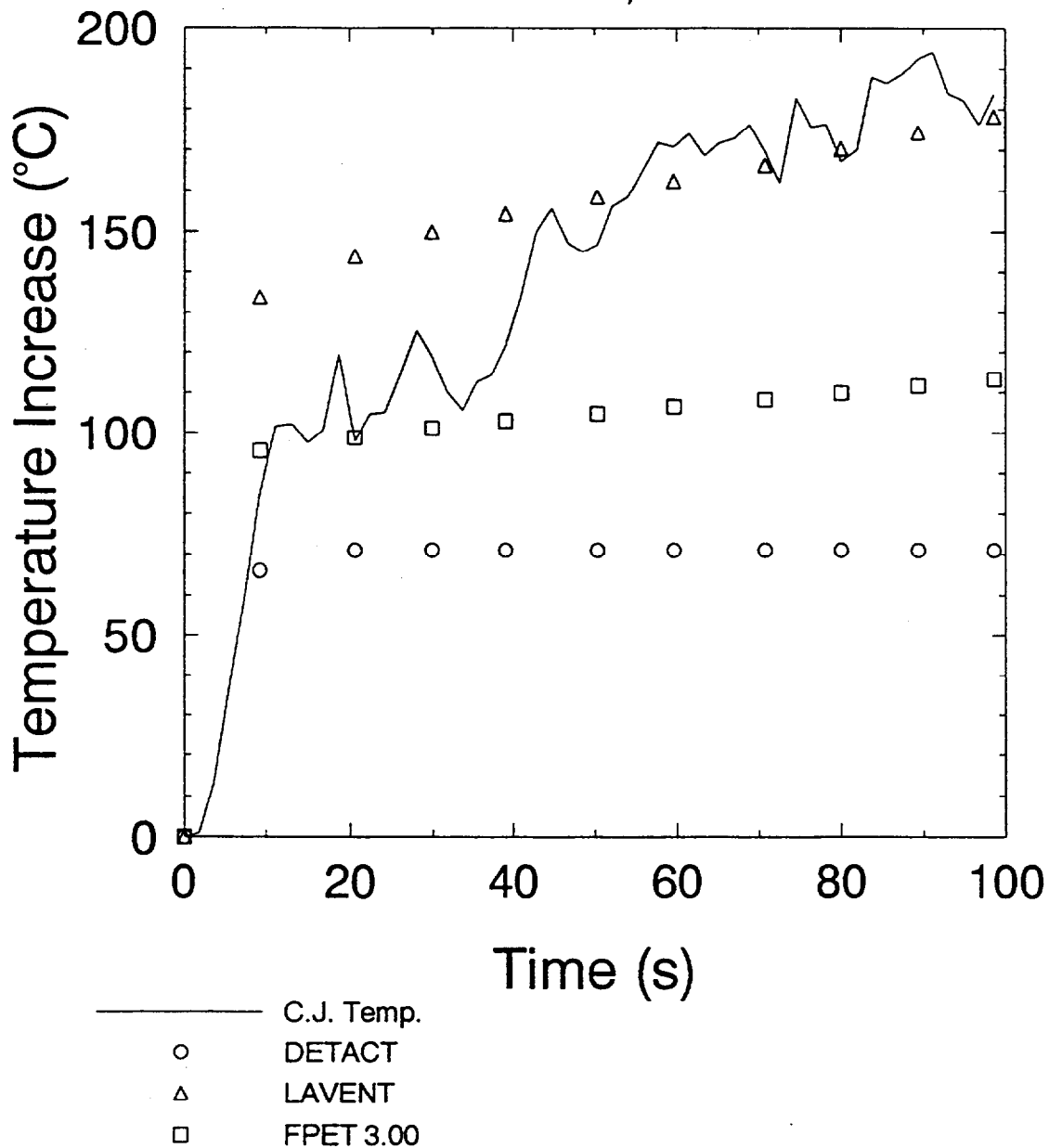


Figure 43. Ceiling jet temperature comparison at  $r = 3$  m, 520 kW.

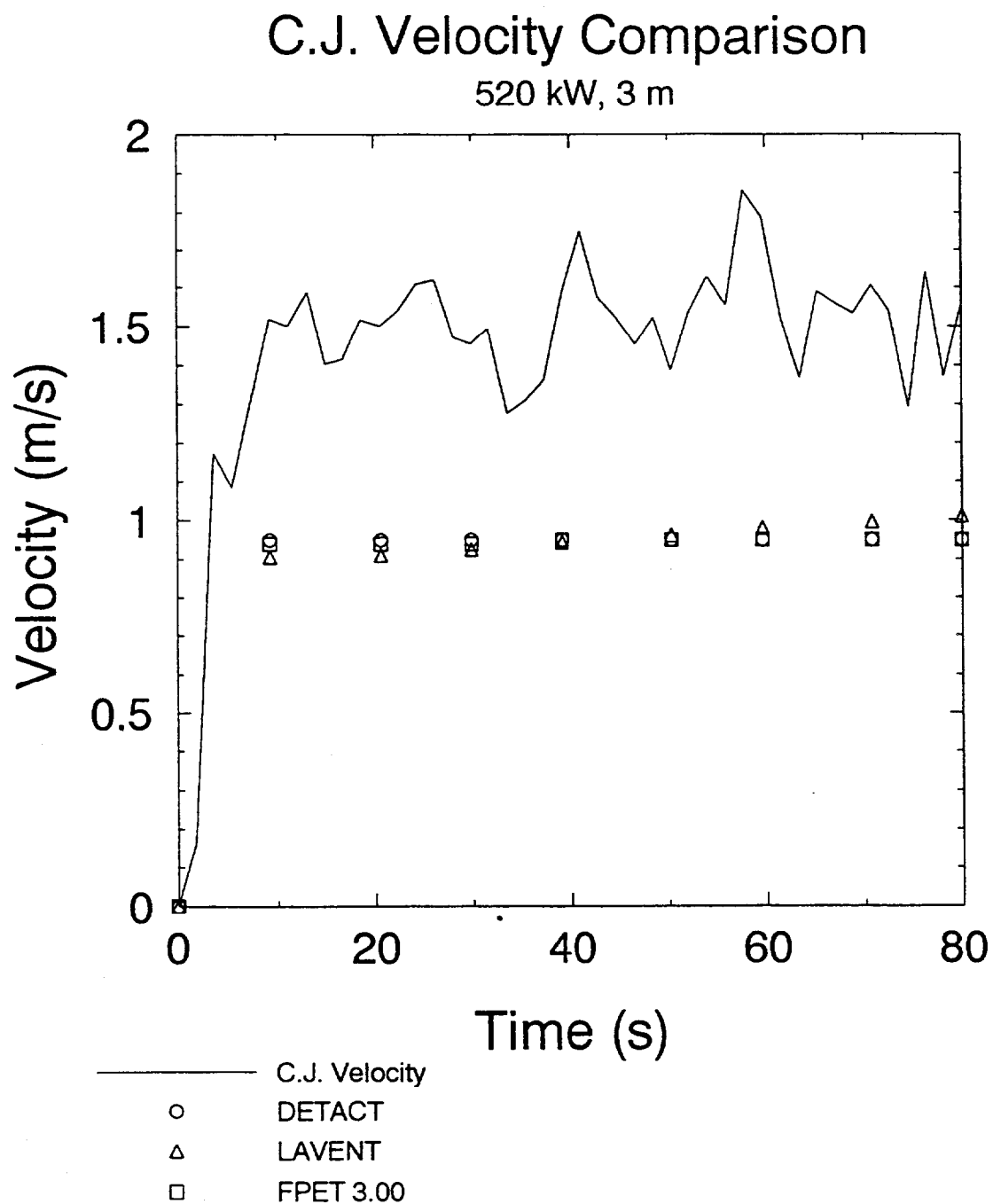


Figure 44. Ceiling jet velocity comparison at  $r = 3$  m, 520 kW.

## C. J. Temperature Increase Comparison

290 kW, 3 m

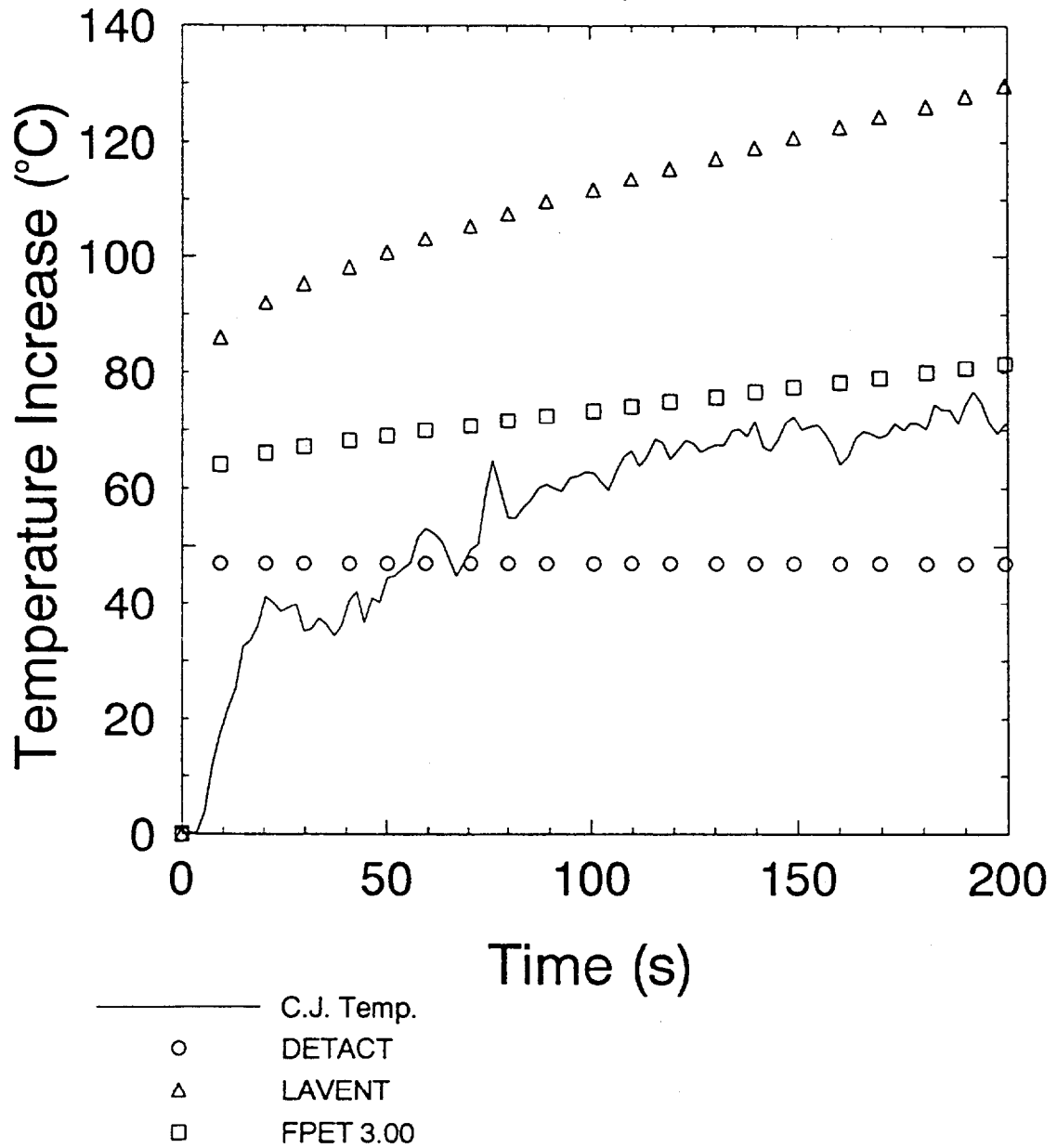


Figure 45. Ceiling jet temperature comparison at  $r = 3$  m, 290 kW.

## C.J. Velocity Comparison

290 kW, 3 m

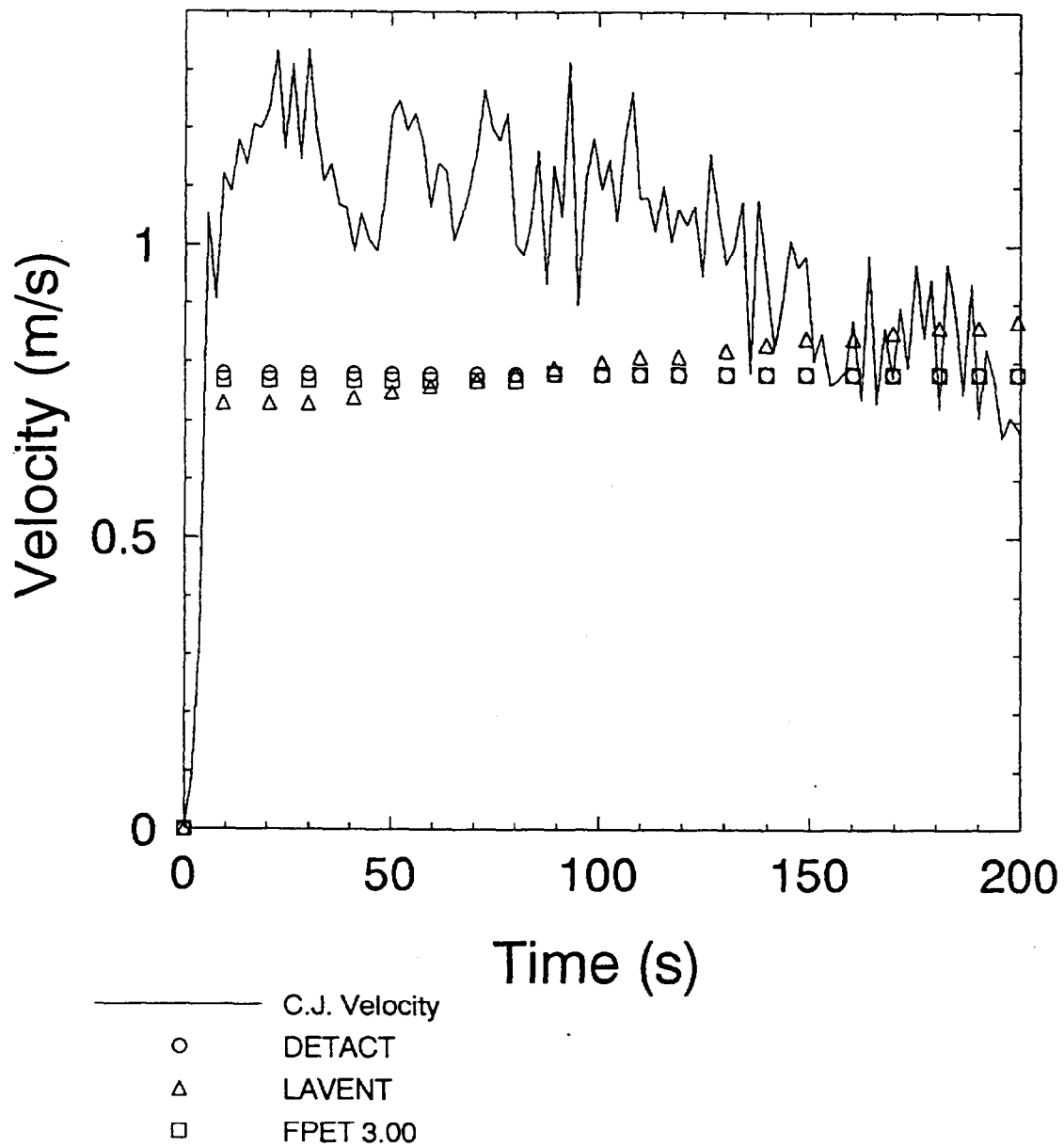


Figure 46. Ceiling jet velocity comparison at  $r = 3$  m, 290 kW.



## C. J. Temperature Increase Comparison

290 kW, 1.5 m

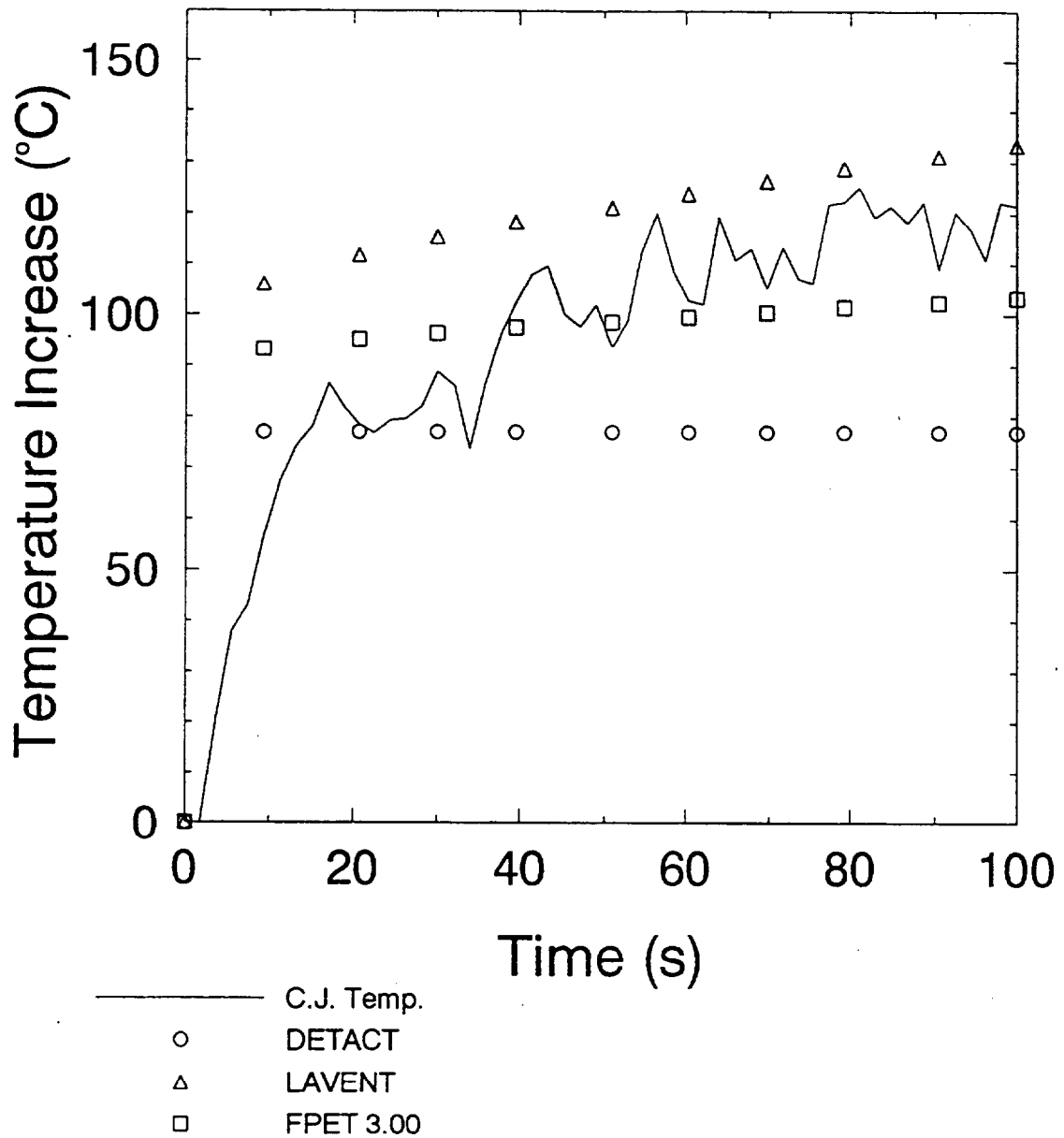


Figure 47. Ceiling jet temperature comparison at  $r = 1.5$  m, 290 kW.

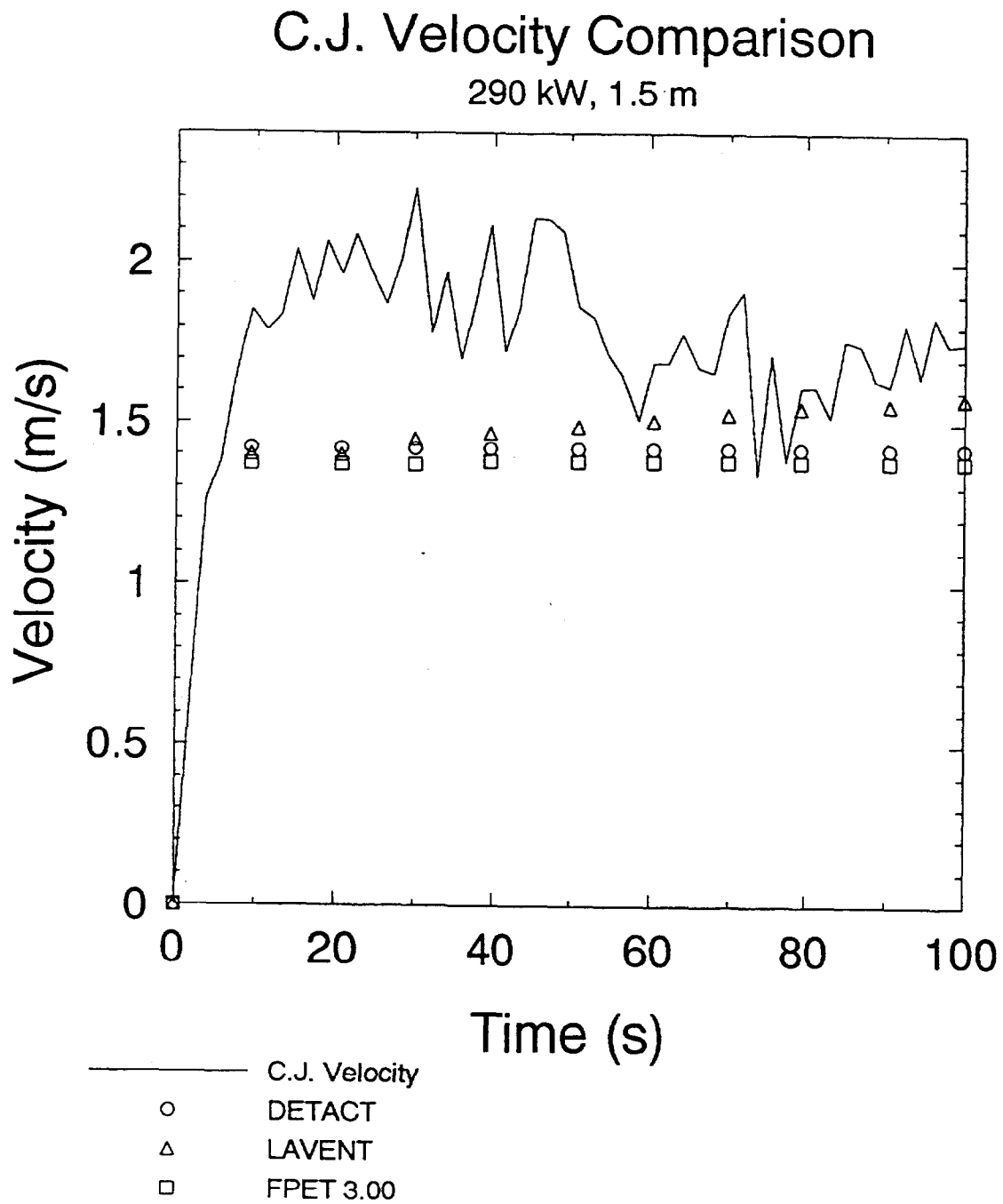


Figure 48. Ceiling jet velocity comparison at  $r = 1.5$  m, 290 kW.

## C. J. Temperature Increase Comparison

215 kW, 1.5 m

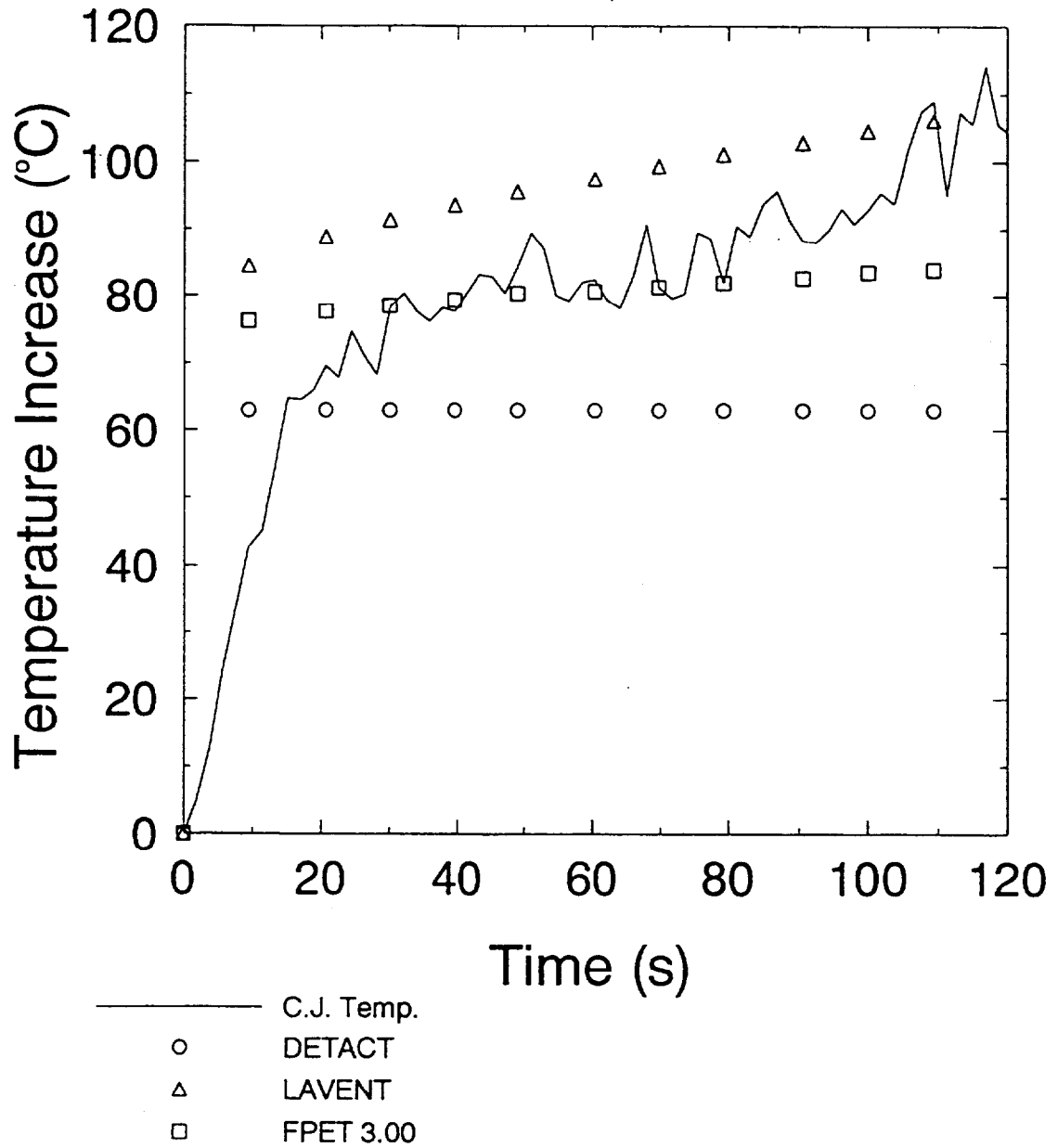


Figure 49. Ceiling jet temperature comparison at  $r = 1.5$  m, 215 kW.

## C.J. Velocity Comparison

215 kW, 1.5 m

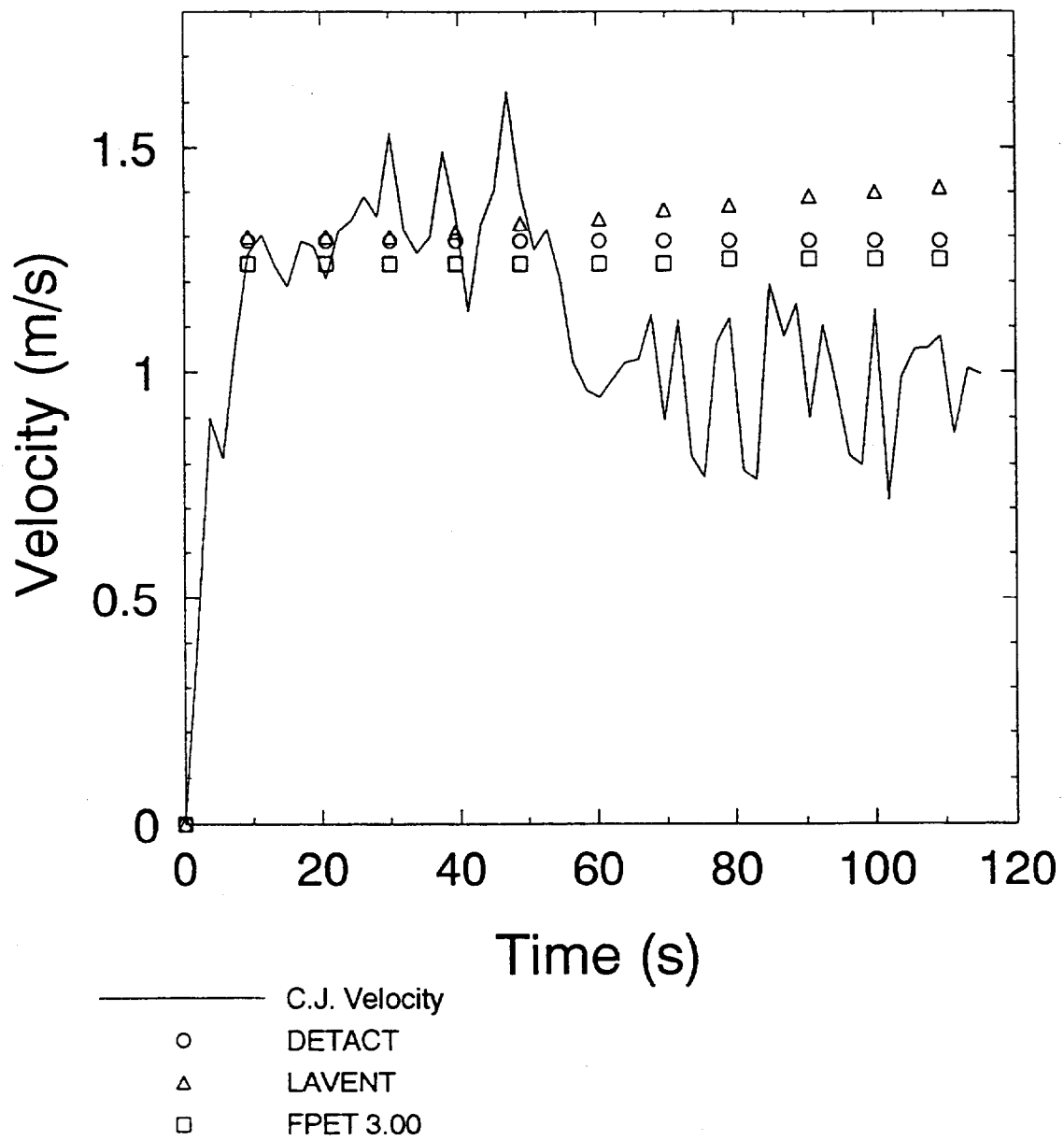


Figure 50. Ceiling jet velocity comparison at  $r = 1.5$  m, 215 kW.

# C. J. Temperature Increase Comparison

155 kW, 1.5 m

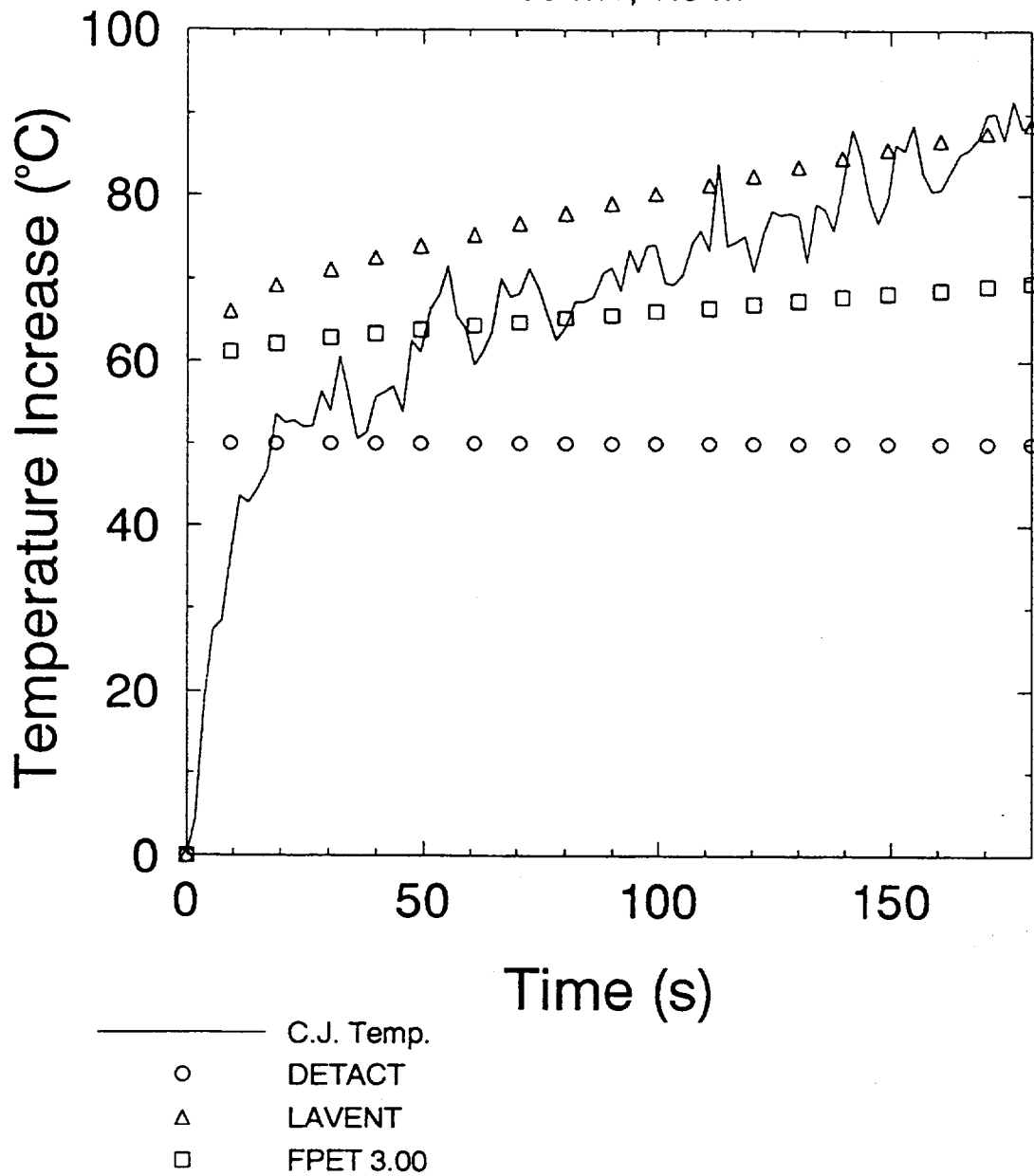


Figure 51. Ceiling jet temperature comparison at  $r = 1.5$  m, 155 kW.

# C.J. Velocity Comparison

155 kW, 1.5 m

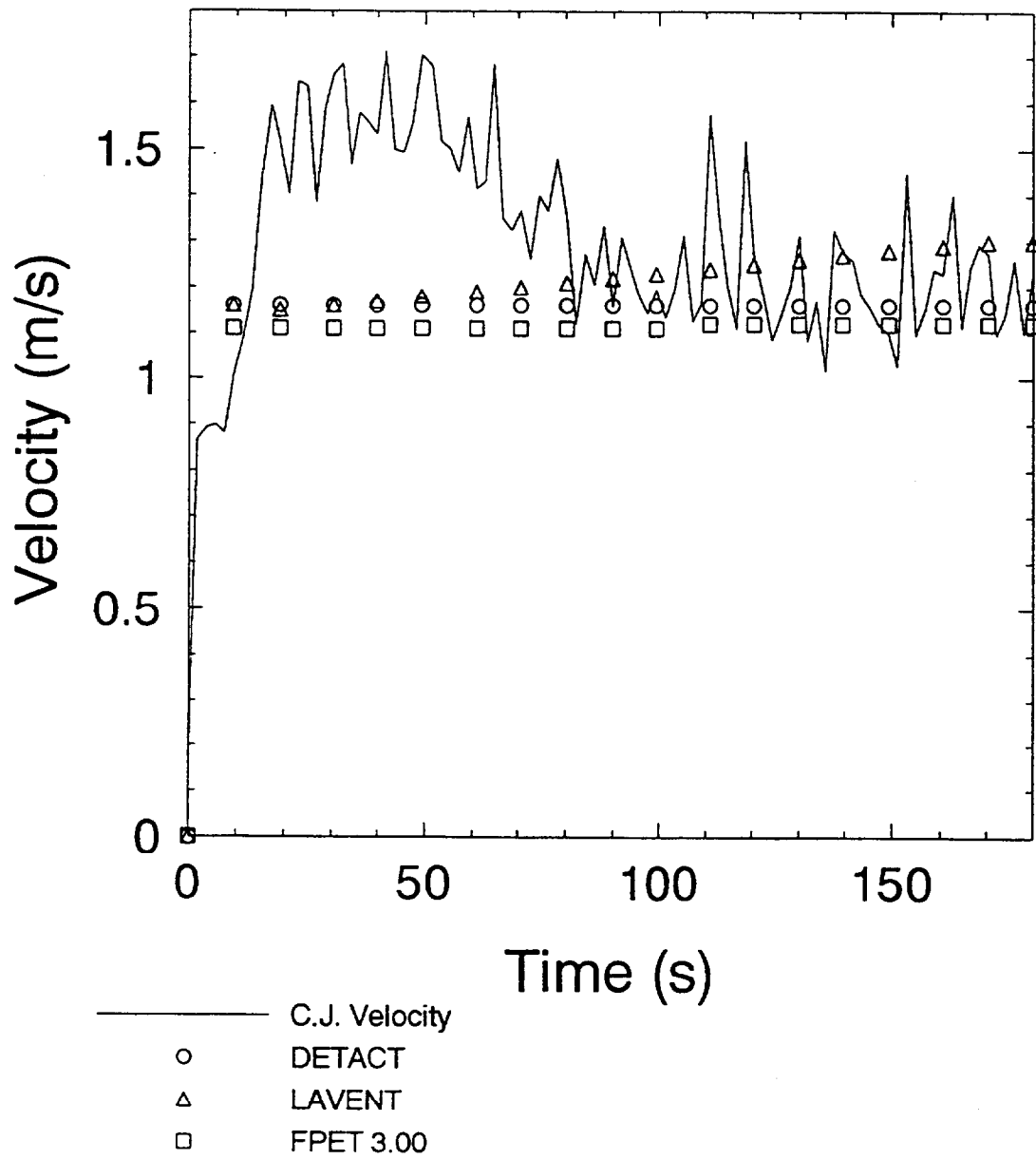


Figure 52. Ceiling jet velocity comparison at  $r = 1.5$  m, 155 kW.

## C. J. Temperature Increase Comparison

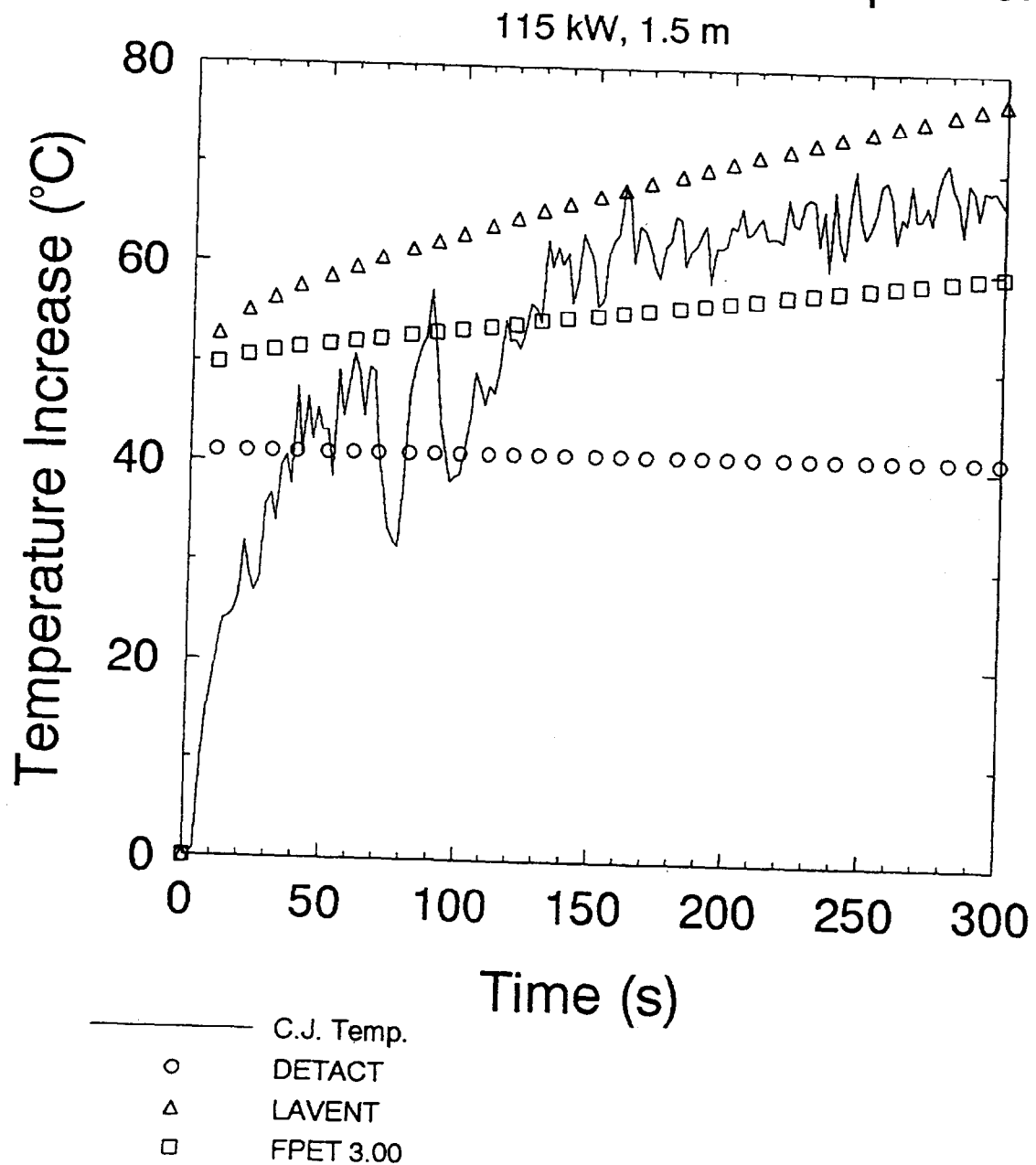


Figure 53. Ceiling jet temperature comparison at  $r = 1.5$  m, 115 kW.

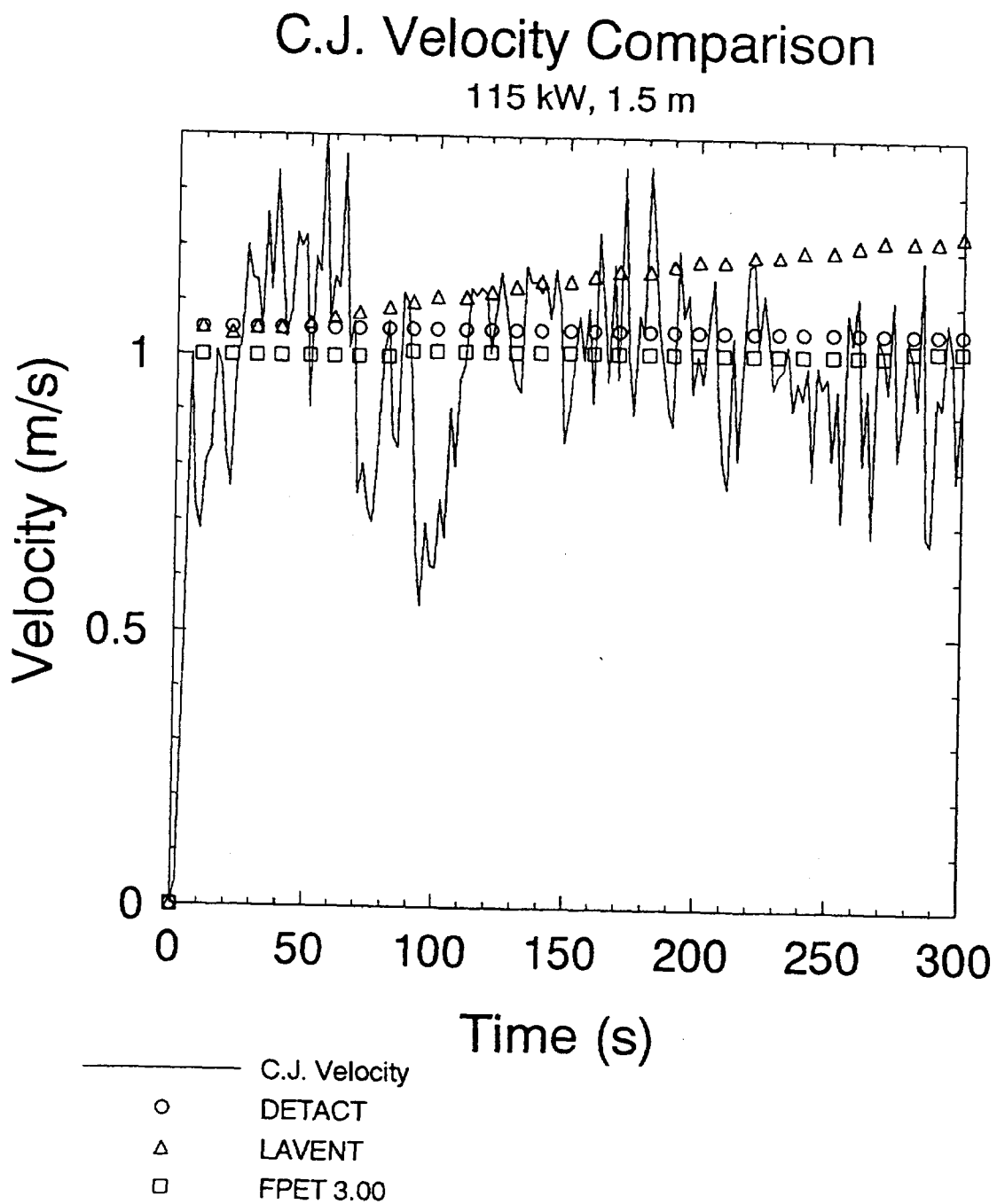


Figure 54. Ceiling jet velocity comparison at  $r = 1.5$  m, 115 kW.



## C. J. Temperature Increase Comparison

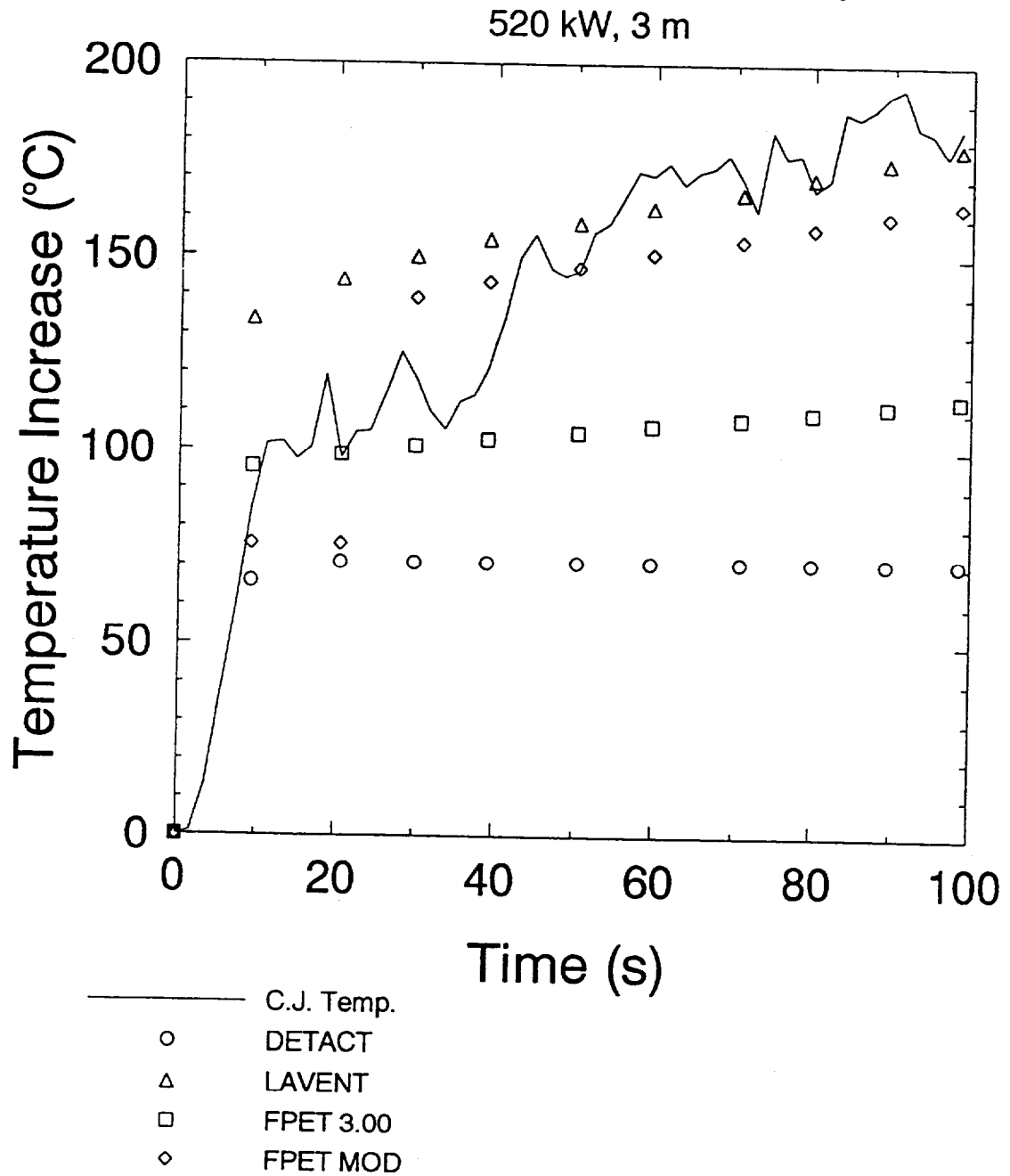


Figure 55. FPEtool Ceiling jet temperature comparison at  $r = 3$  m, 520 kW.

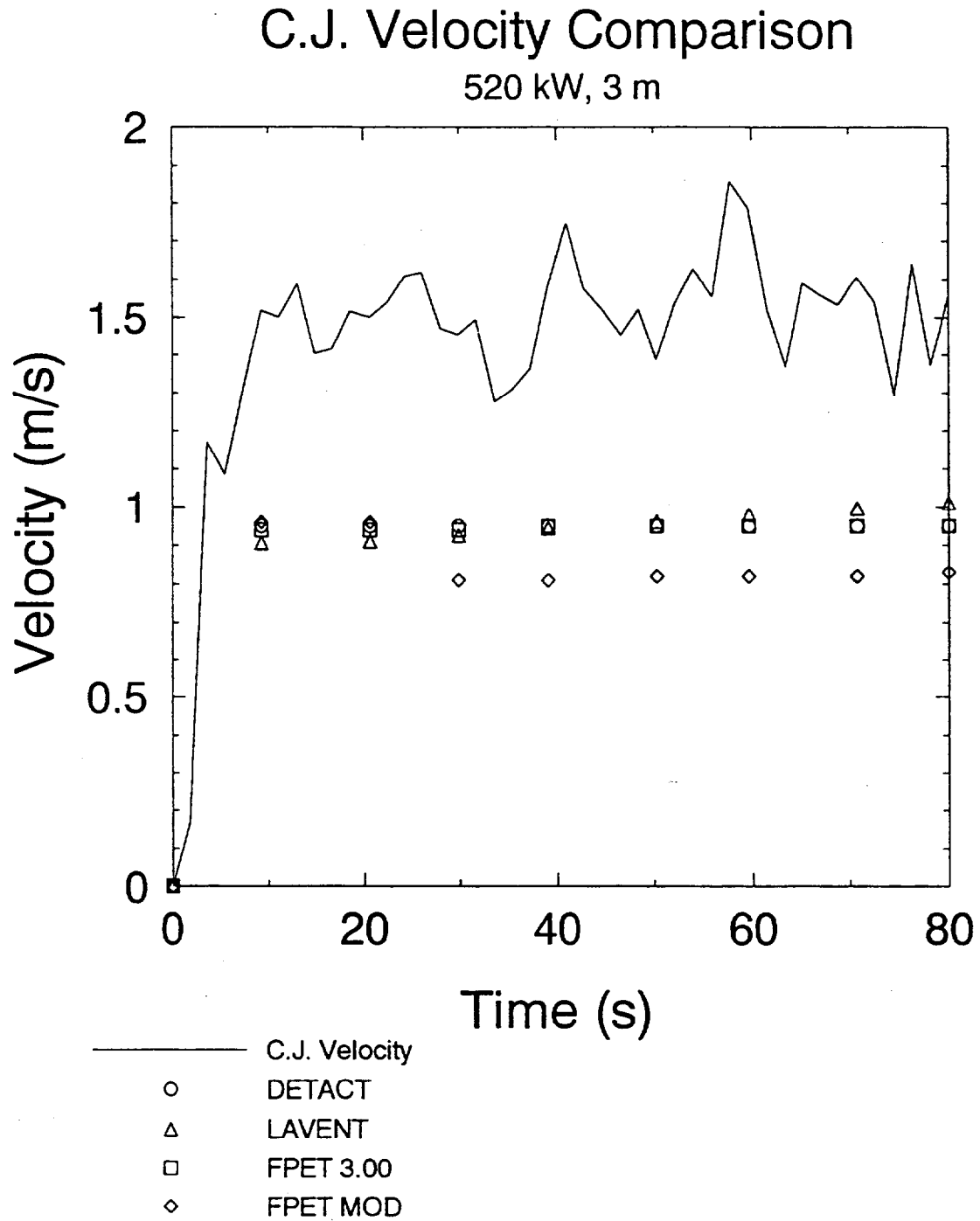


Figure 56. FPEtool Ceiling jet velocity comparison at  $r = 3$  m, 520 kW.

## C. J. Temperature Increase Comparison

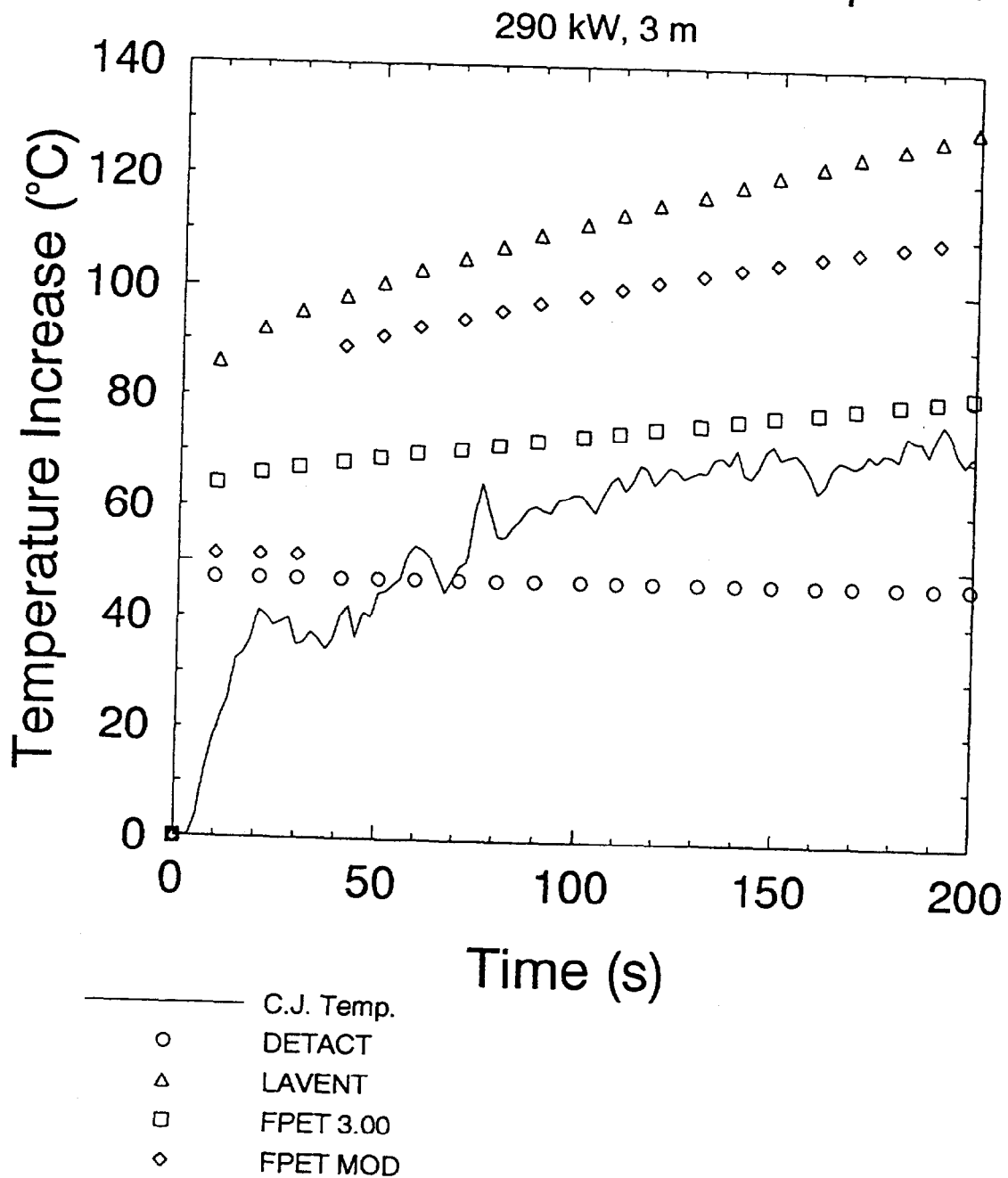


Figure 57. FPEtool Ceiling jet temperature comparison at  $r = 3$  m, 290 kW.

# C.J. Velocity Comparison

290 kW, 3 m

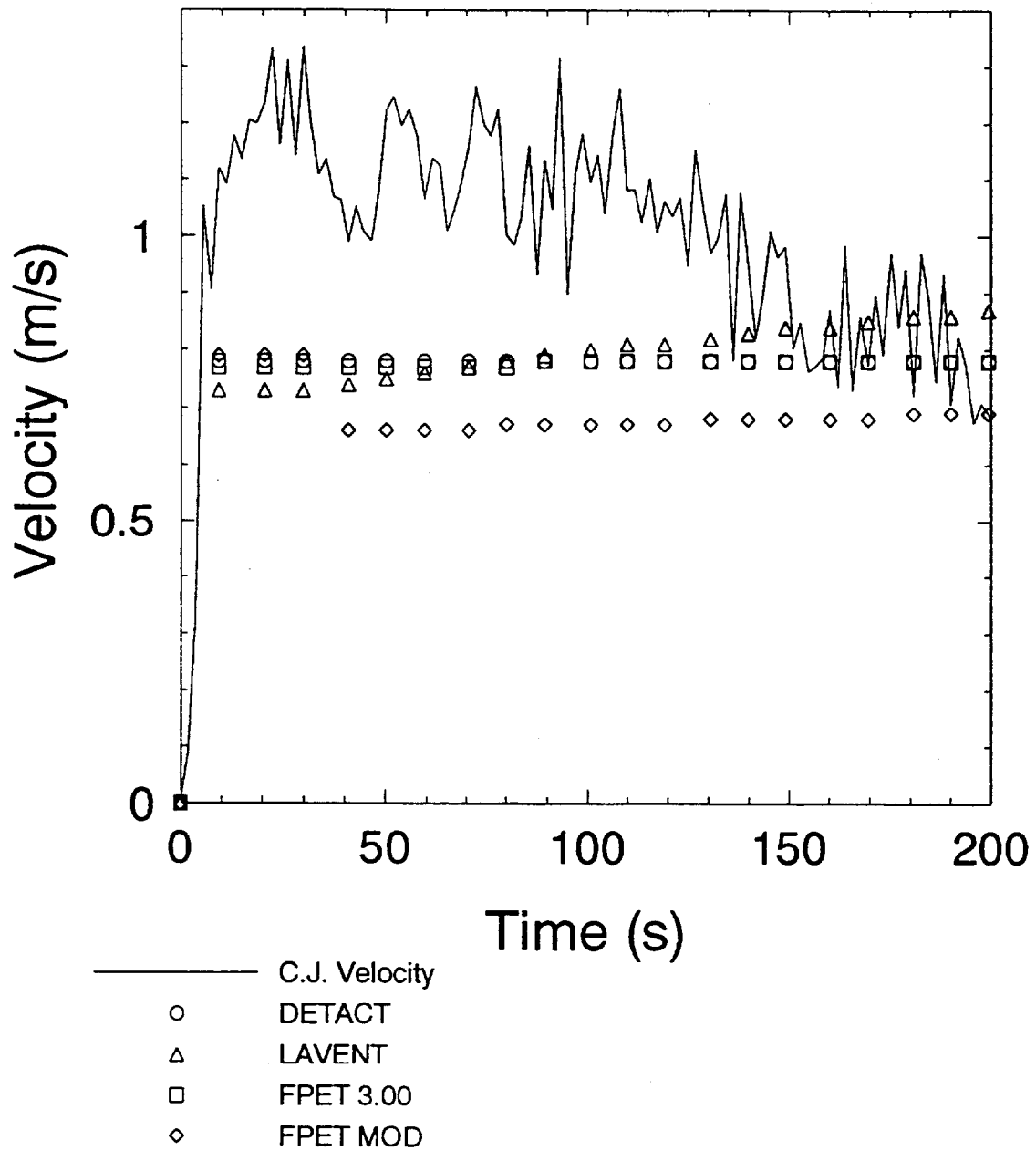


Figure 58. FPEtool Ceiling jet velocity comparison at  $r = 3$  m, 290 kW.

## C. J. Temperature Increase Comparison

290 kW, 1.5 m

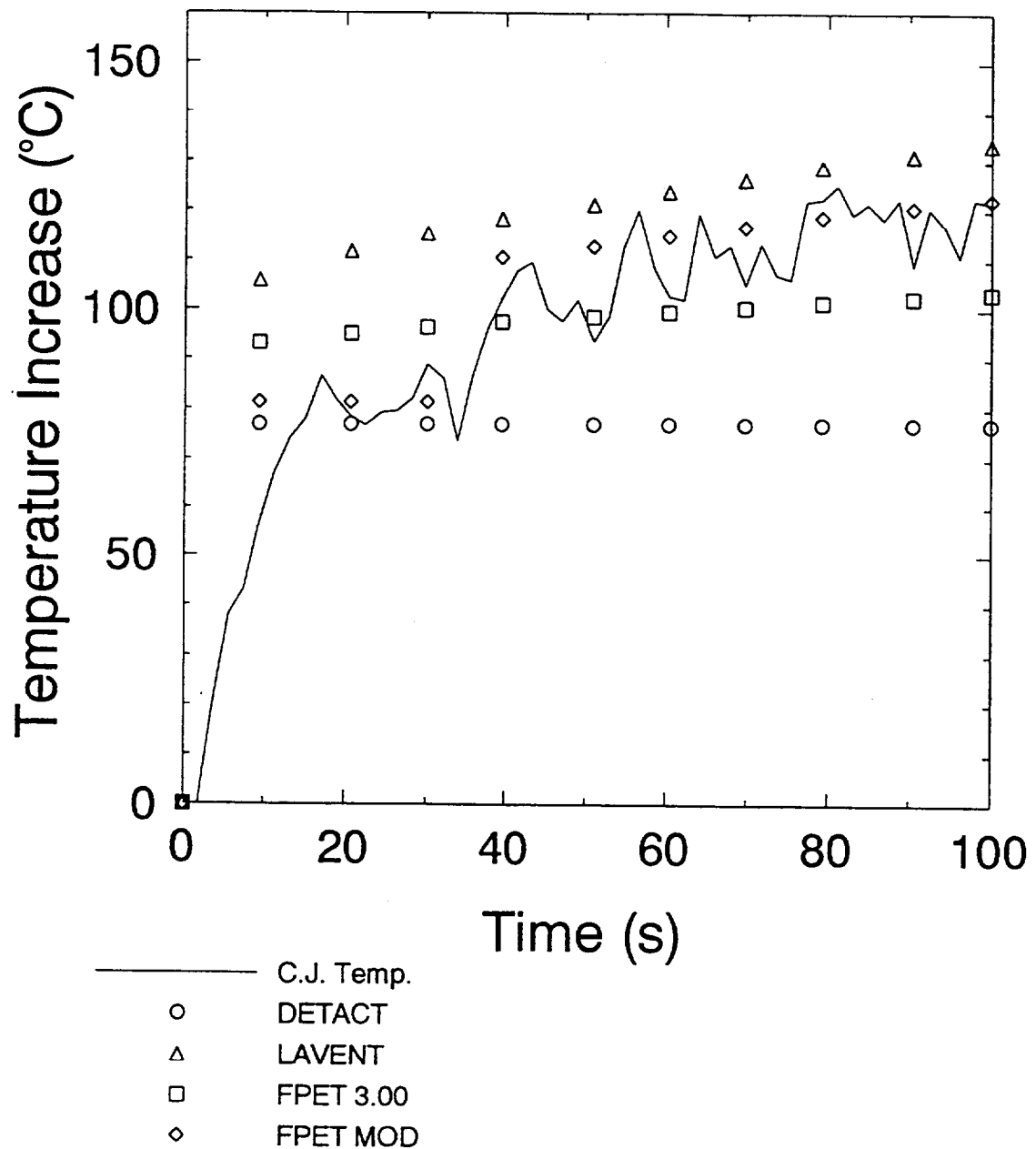


Figure 59. FPEtool Ceiling jet temperature comparison at  $r = 1.5$  m, 290 kW

# C.J. Velocity Comparison

290 kW, 1.5 m

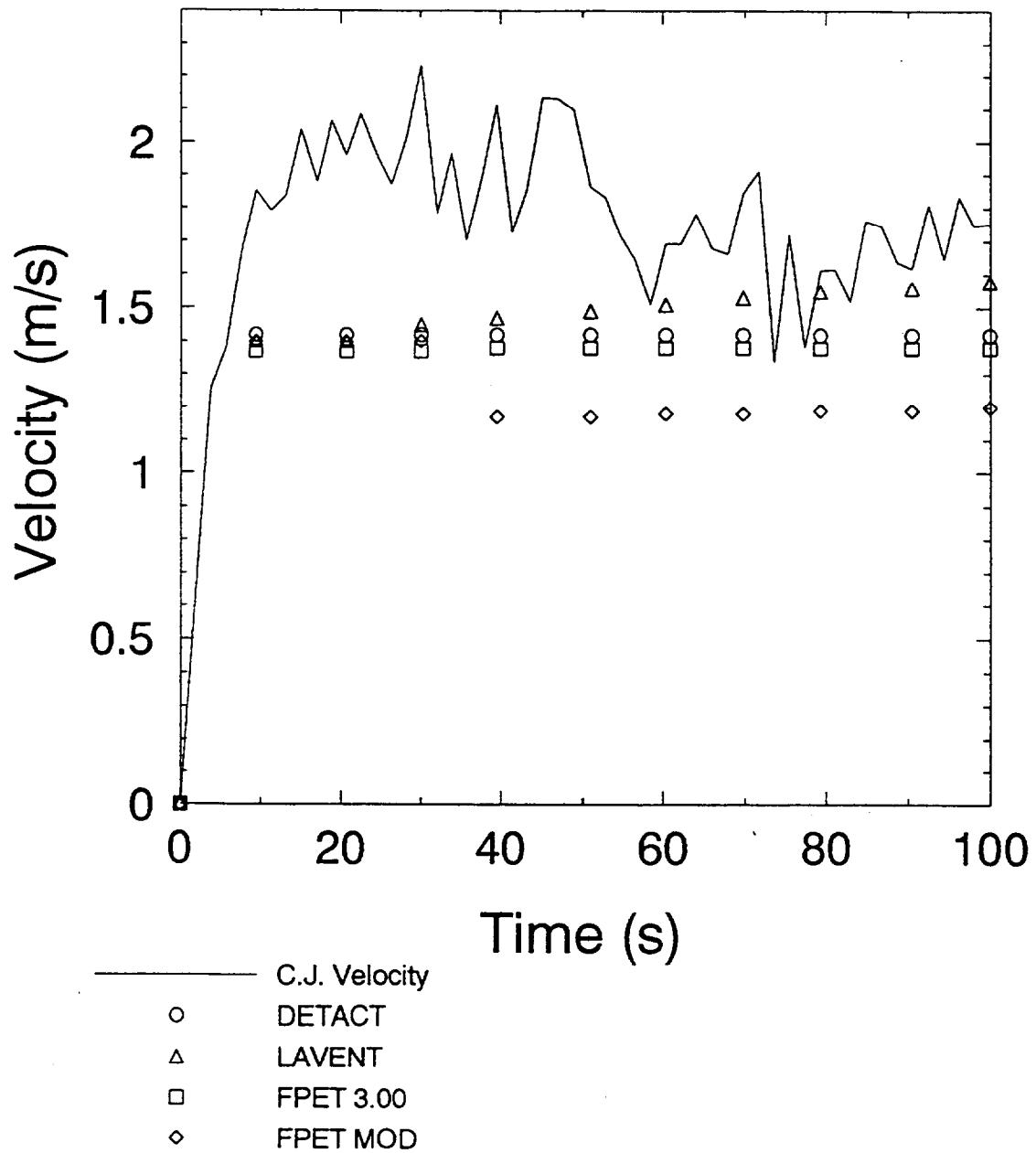


Figure 60. FPEtool Ceiling jet velocity comparison at  $r = 1.5$  m, 290 kW.

## C. J. Temperature Increase Comparison

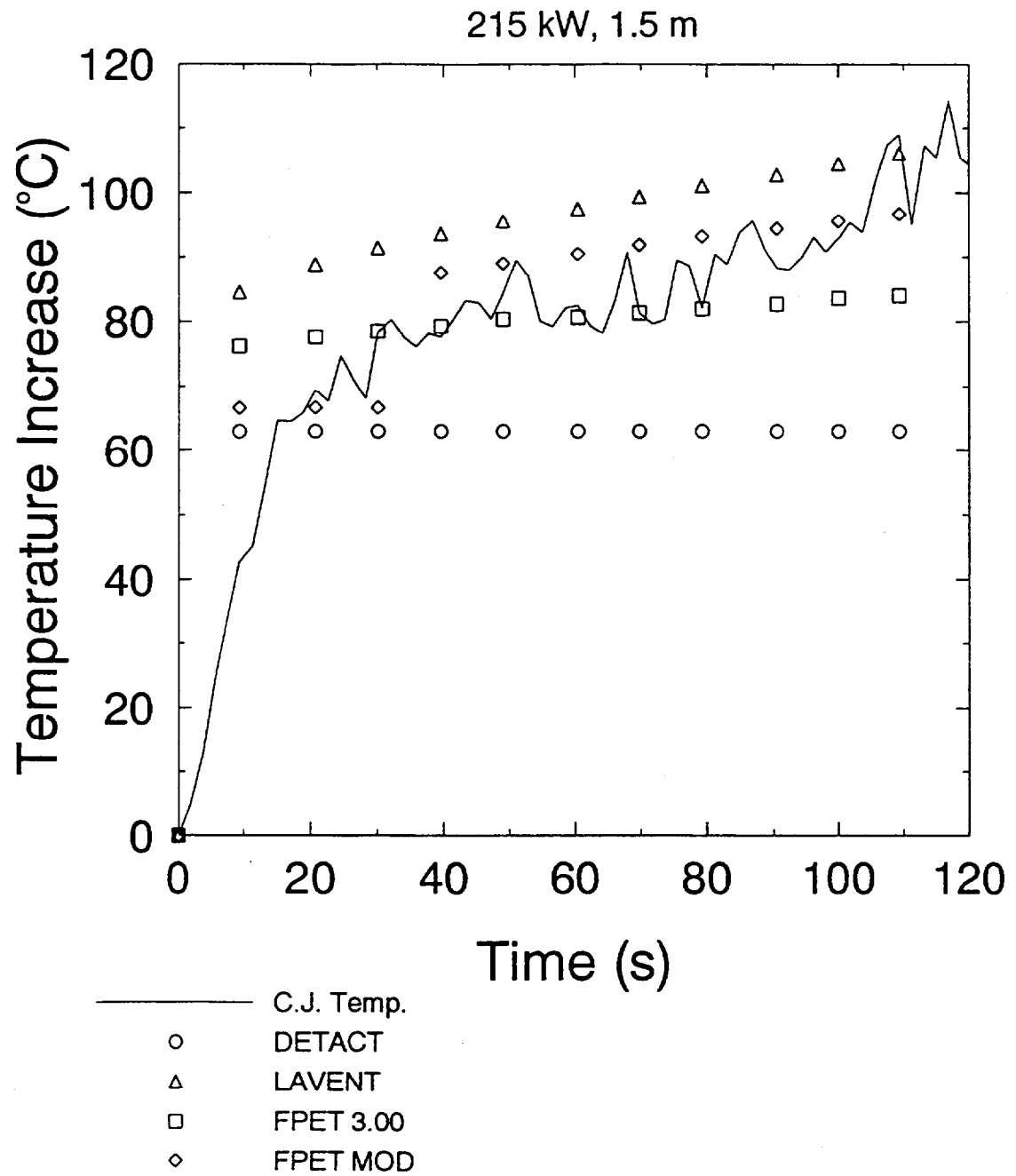


Figure 61. FPEtool Ceiling jet temperature comparison at  $r = 1.5$  m, 215 kW.

## C.J. Velocity Comparison

215 kW, 1.5 m

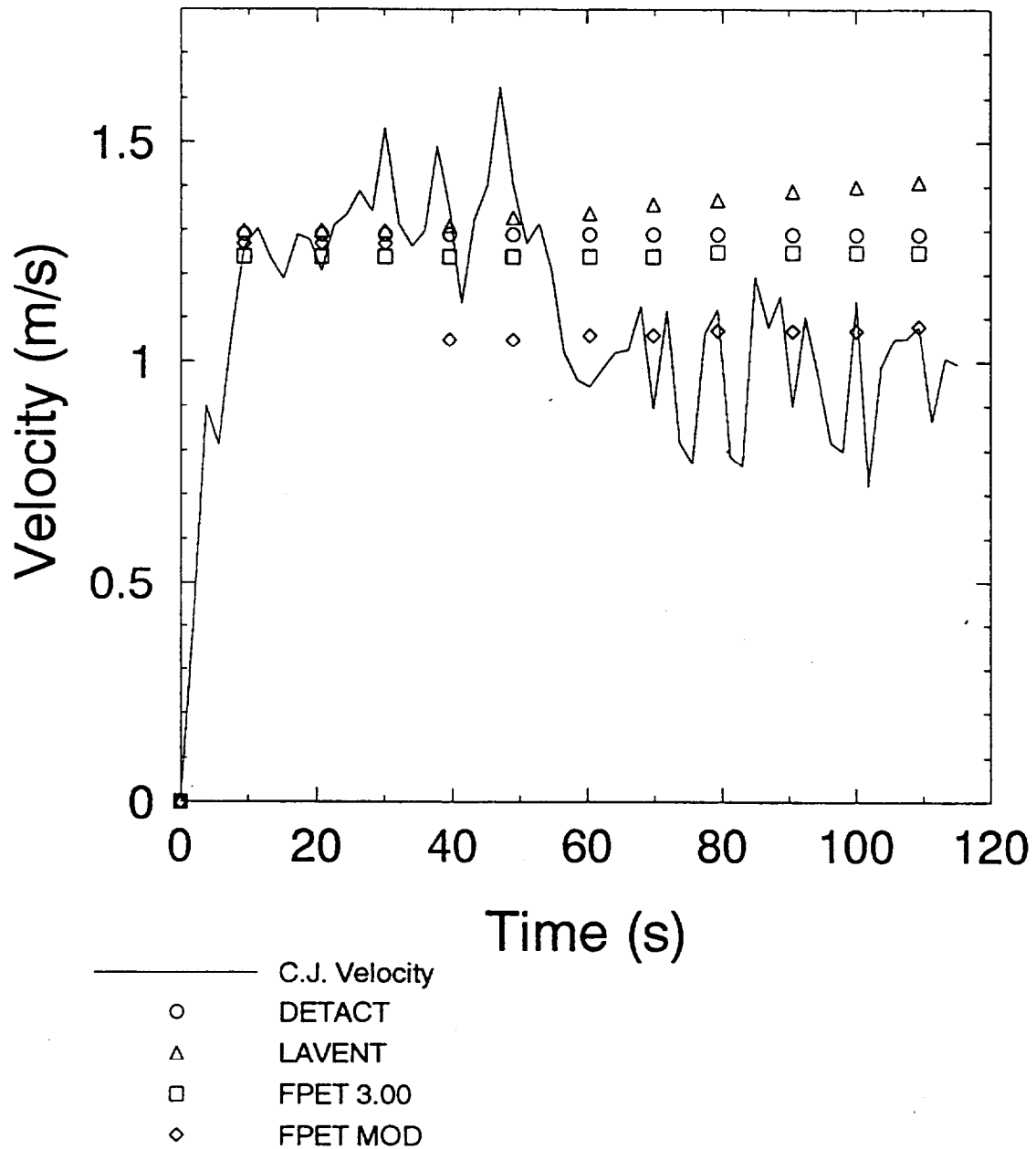


Figure 62. FPEtool Ceiling jet velocity comparison at  $r = 1.5$  m, 215 kW.



## C. J. Temperature Increase Comparison

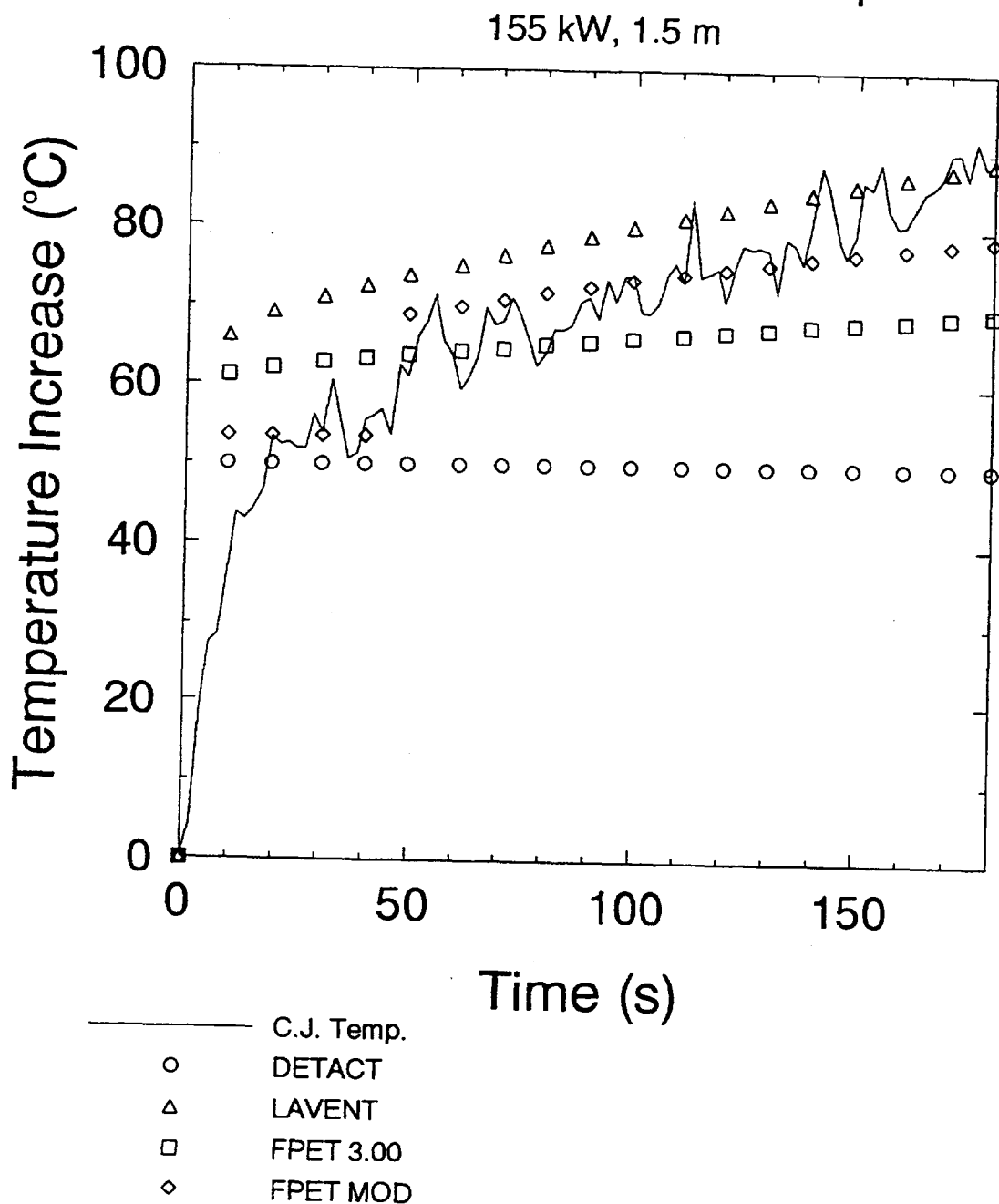


Figure 63. FPEtool Ceiling jet temperature comparison at  $r = 1.5$  m, 155 kW.

# C.J. Velocity Comparison

155 kW, 1.5 m

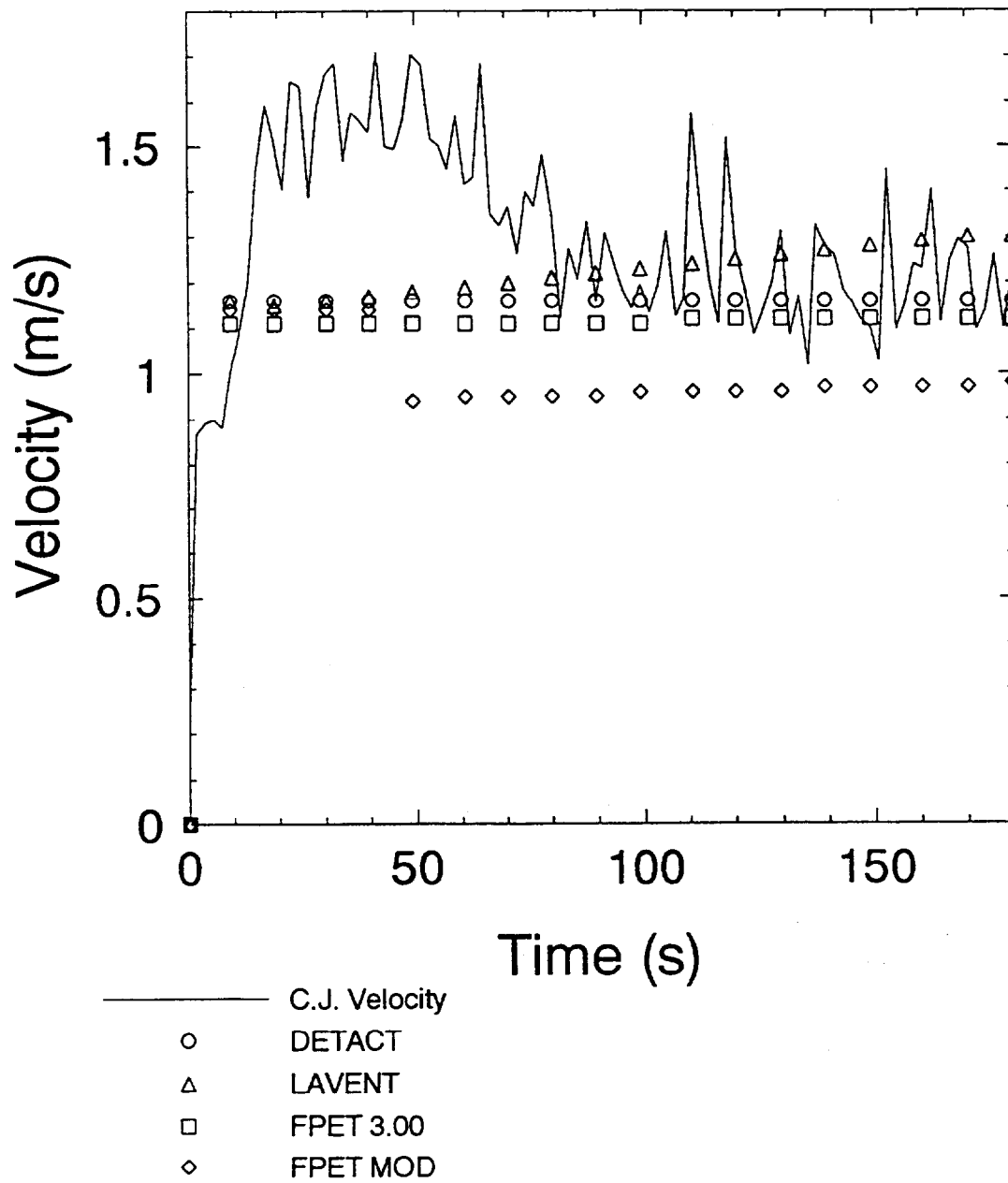


Figure 64. FPEtool Ceiling jet velocity comparison at  $r = 1.5$  m, 155 kW.

## C. J. Temperature Increase Comparison

115 kW, 1.5 m

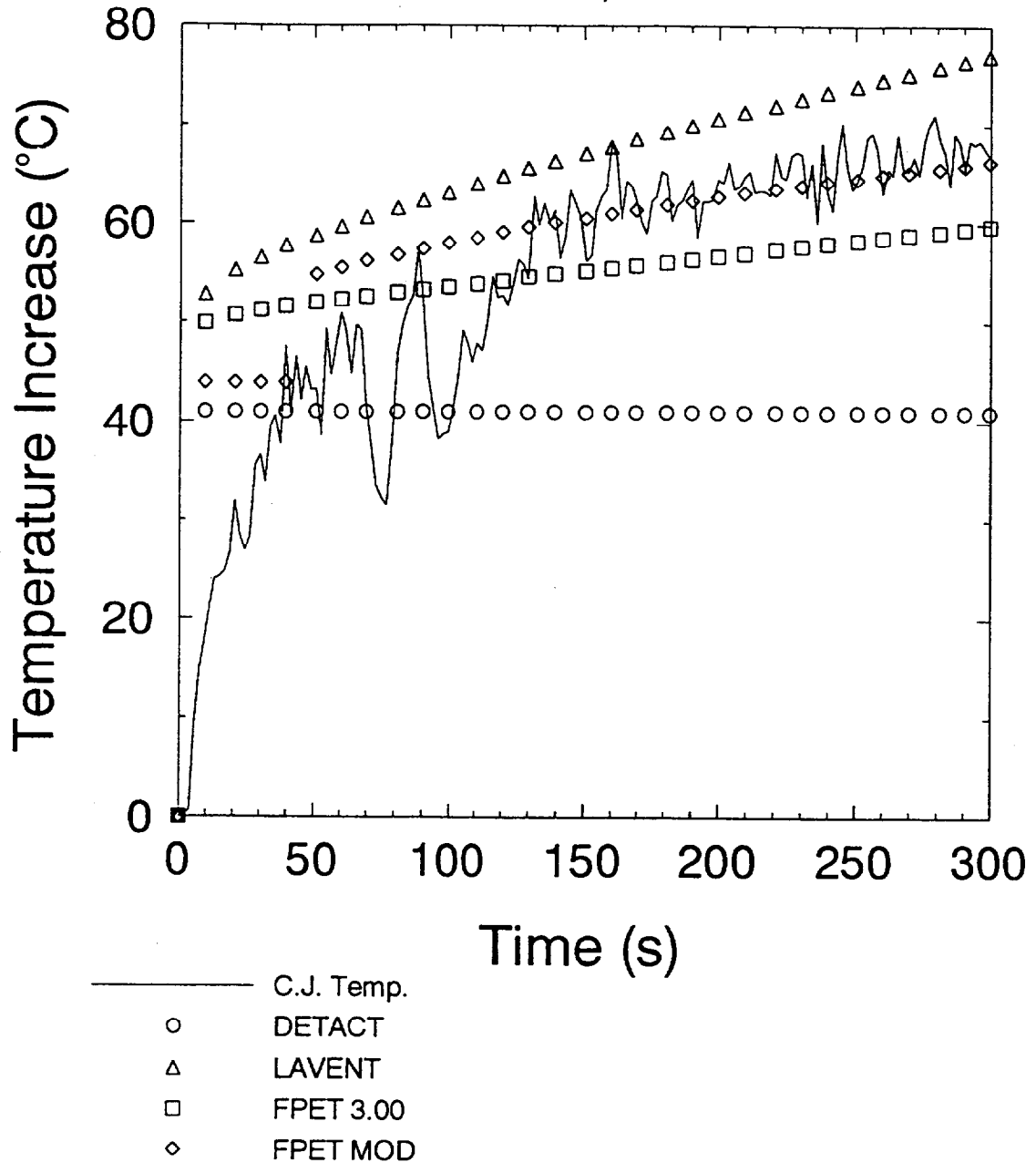


Figure 65. FPEtool Ceiling jet temperature comparison at  $r = 1.5$  m, 115 kW.

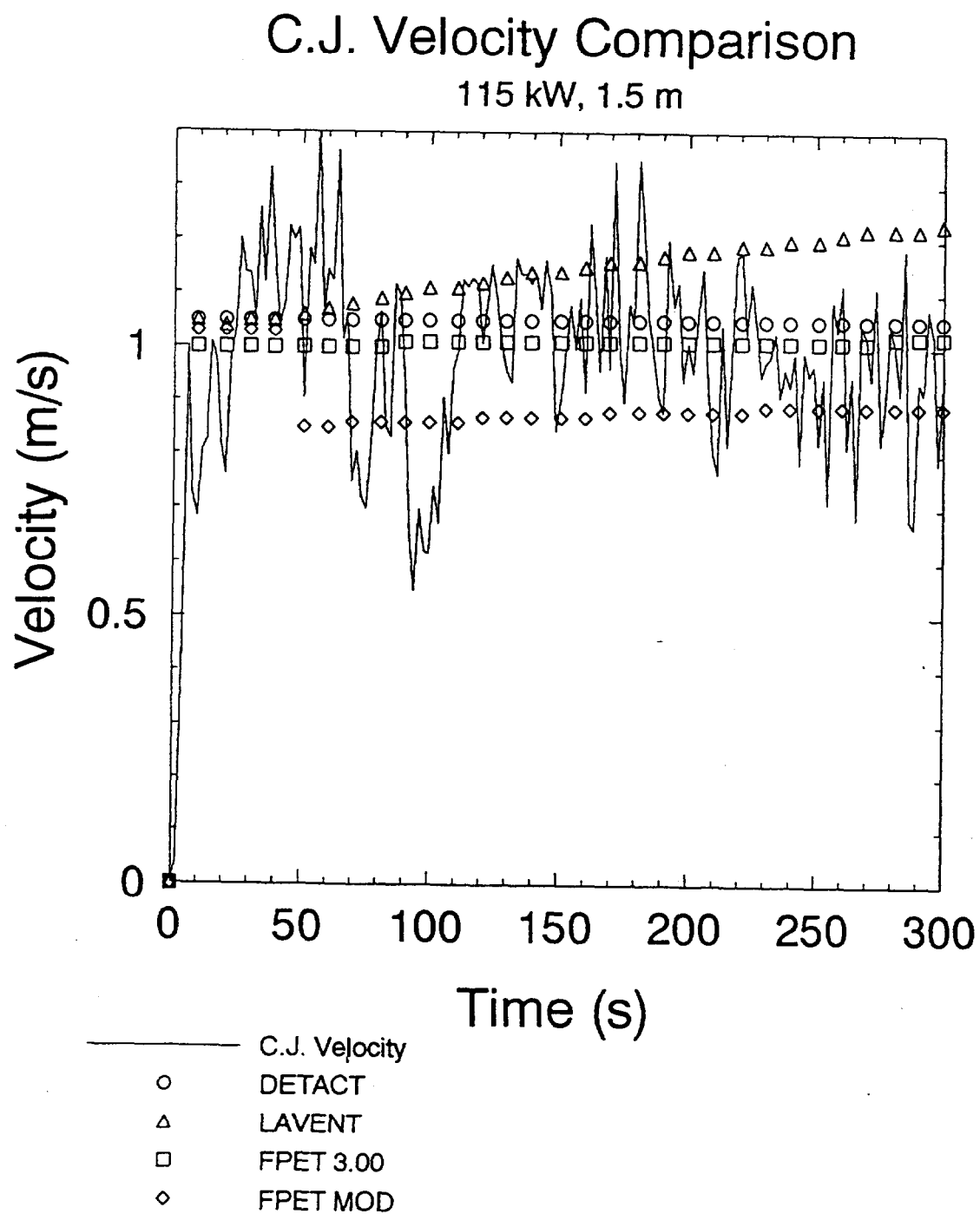


Figure 66. FPEtool Ceiling jet velocity comparison at  $r = 1.5$  m, 115 kW.

# First-Order Response Model

Sensitivity to Gas Temperature

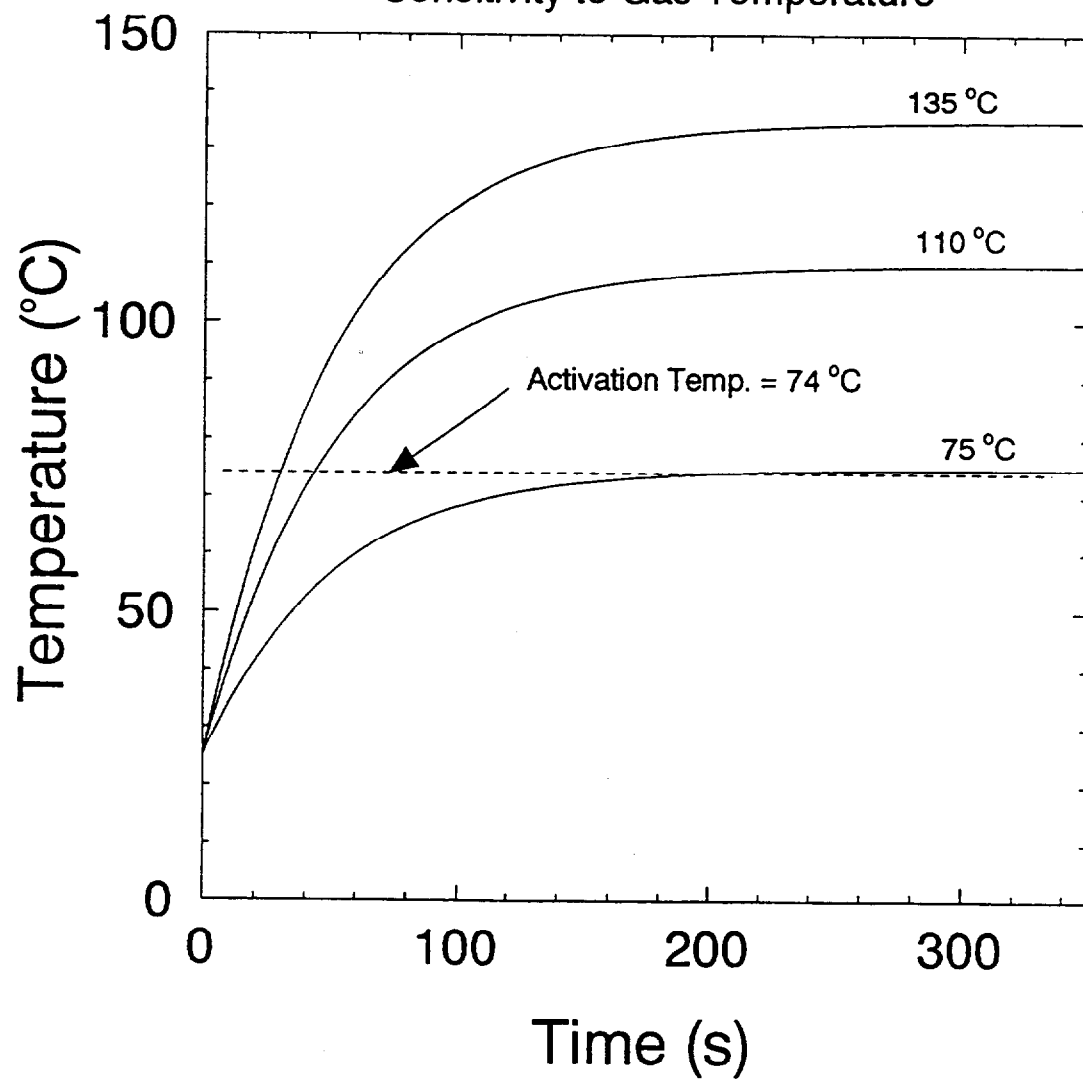


Figure 67. First-order response model sensitivity to gas temperature.

## References

1. Friedman, R., "Survey of Computer Models for Smoke and Fire", 2nd Ed. FORUM for International Cooperation on Fire Research, December 1991.
2. Evans, D.D., Stroup, D.W., "Methods to Calculate the Response Time of Heat and Smoke Detectors Installed Below Large Unobstructed Ceilings," *Fire Technology*, vol. 22, 54-65, 1986.
3. Evans, D.D., Stroup, D.W., and Martin, P., "Evaluating Thermal Fire Detection Systems (SI Units)," NBSSP 713, National Institute of Standards and Technology, April 1986.
4. Davis, William D., and Cooper, Leonard Y., "Estimating the Environment and the Response of Sprinkler Links in Compartment Fires with Draft Curtains and Fusible Link-Actuated Ceiling Vents-Part II: User Guide for the Computer Code LAVENT," NBSIR 89-4122, U.S. National Institute of Standards and Technology.
5. Yu, H-Z, "A Sprinkler-Response-Prediction Computer Program for Warehouse Applications," FMRC Technical Report, J.I. OR2E1.RA, 1991.
6. Björkman, J., Huttunen, O. and Kokkala, M., Calculation models for fire detectors, Research Notes 1036, Technical Research Centre of Finland.
7. Nelson, H.E., FPEtool: Fire Protection Engineering Tools for Hazard Estimation, NISTIR Report 4380, National Institute of Standards and Technology; August 1990.
8. Peacock, R.D., Jones, W.W., Bukowski, R.W. and Forney, C.L., HAZARD I Fire Assessment Method Version 1.1, Nat. Inst. Stand. Tech. (U.S.) NIST Handbook 146; June 1991.
9. Hinckley, P.L., *Fire Safety Journal* 11(3) 1987, 211-225, *Fire Safety Journal* 14(4) 1989, 221-240.
10. Gardiner, A.J., The mathematical modeling of the interaction between sprinkler sprays and the thermally buoyant layers of gases from fires, Ph.D. (CNAA) South Bank Polytechnic, 1988.
11. Heskestad, G. and Smith, H.F., "Plunge Test for Determination of Sprinkler Sensitivity," FMRC J.I. 3A1E2.RR, Factory Mutual Research Corporation, Norwood, Massachusetts, December 1980.
12. UL 199, Standard for Automatic Sprinklers for Fire-Protection Service, 8th ed., Underwriters Laboratories Inc. Northbrook, IL., 1990.

13. Automatic Sprinkler Systems Handbook, 5th ed., Robert E. Solomon, Ed. National Fire Protection Association, Quincy, MA, 1991.
14. Cote, Arthur E., "Final Report on Field Test of a Retrofit Sprinkler System," National Fire Protection Research Foundation, February, 1983.
15. Benjamin/Clarke Associates, "Operation San Francisco Smoke/Sprinkler Test Technical Report," International Association of Fire Chiefs, Washington, April 1984.
16. Walton, W.D., and Budnick, E.K., Quick Response Sprinklers in Office Configurations: Fire Test Results. Nat. Bur. Stand. (U.S.) NBSIR 88-3695, January 1988.
17. Walton, W.D., Quick Response Sprinklers in Chemical Laboratories: Fire Test Results. Nat. Inst. Stand. Tech. (U.S.) NISTIR 89-4200, November 1989.
18. Madrzykowski, D., The Reduction in Fire Hazard in Corridors and Areas Adjoining Corridors Provided by Sprinklers. Nat. Inst. Stand. Tech. (U.S.) NISTIR 4631, July 1991.
19. Life Safety Code Handbook, 5th ed., edited by James K. Lathrop, National Fire Protection Association, Quincy, MA, 1991. pp XII.
20. Mowrer, Frederick W., Lag Times Associated with Fire Detection and Suppression., *Fire Technology*, August 1990.
21. Benedict, Robert P., "Fundamentals of Temperature, Pressure, and Flow Measurements," New York, John Wiley & Sons, Inc., 1969, 142-149.
22. Theobald, C.R., Ramp Test for the Thermal Sensitivity of Sprinklers, *Journal of Fire Protection Engineers*, 1989, pp 23-24.
23. Heskestad, G. and Smith, H.F., "Investigation of a New Sprinkler Sensitivity Approval Test: The Plunge Test," FMRC No.22485, Factory Mutual Research Corporation, Norwood, Massachusetts, December 1976.
24. Cote, A.E. and Fleming, R.P., "Fast Response Sprinkler Technology," Fire Protection Handbook, 17th ed., Section 5/Chapter 13, National Fire Protection Association, Quincy, MA, 1991.
25. Bryan, J.L., Automatic Sprinkler and Standpipe Systems, 2nd ed. National Fire Protection Association, Quincy, MA., 1990.
26. Alpert, R.L., "Calculation of Response Time of Ceiling-Mounted Fire Detectors," *Fire Technology*, Vol 8, No.3, August 1972, 181-195.

27. NFPA 13, Standard for the Installation of Sprinkler Systems, 1992 Edition National Fire Protection Association Quincy, MA.
28. Walton, W.D., ASET-B: A Room Fire Program for Personal Computers, Nat. Bur. Stand. (U.S.), NBSIR 85-3144-1, December 1985.
29. Nelson, H.E., National Institute of Standards and Technology, "History of Fire Technology," presentation for the "Conference on Fire Safety Design in the 21st Century," Worcester Polytechnic Institute, MA, May 8-10, 1991.
30. Heskestad, G. and Delichatsios, M.A., The Initial Convective Flow in Fire, Seventeenth Symposium (International) on Combustion, The Combustion Institute, Pittsburgh, PA, 1978, pp. 1113-1123.
31. Cooper, L.Y., "Estimating the Environment and the Response of Sprinkler Links in Compartment Fires with Draft Curtains and Fusible-Link-Actuated Ceiling Vents-Part I: Theory," Nat. Inst. Stand. Tech. (U.S.), NISTIR 88-3734, April 1988.
32. Evans, D.D., "Calculating Fire Plume Characteristics in a Two-Layer Environment," *Fire Technology*, Vol 20, No. 3, August 1984, 39-63.
33. Beckwith, T.G., Buck, N.L., Marangoni, R.D., "Mechanical Measurements," 3rd ed. Addison-Wesley Publishing Co., Reading, MA 19 .
34. Natrella, M.G., "Experimental Statistics," National Bureau of Standards Handbook 91, National Bureau of Standards (U.S.), October 1966.
35. Morton, B.R., Taylor, Sir Geoffrey, F.R.S., Turner, J.S., Proceedings of the Royal Society of London. Series A. Mathematical and Physical Sciences, Vol 234, Publ. The Royal Society, Burlington House, Piccadilly, London, March 6, 1956.